Immune regulation of superantigenic *Staphylococcus aureus*-driven pro-inflammatory T cell responses in human nasopharynx-associated lymphoid tissue

Thesis submitted in accordance with the requirements of the University of Liverpool for the degree of Doctor in Philosophy by Rong Xu

AUGUST 1, 2019

UNIVERSITY OF LIVERPOOL

Immune regulation of superantigenic *Staphylococcus aureus*-driven pro-inflammatory T cell responses in human nasopharynx-associated lymphoid tissue

Rong Xu, Institute of Infection and Global Health, University of Liverpool

Staphylococcus aureus (*Sau*) is frequently identified to colonize the mucosa and skin compartments in humans. Invasive *Sau* infection induces acute episodes of inflammatory diseases, such as pneumonia, bacteremia and skin abscesses. In asymptomatic *Sau* carriers, superantigenic *Sau* (SAg-*Sau*) infection has been closely associated with several autoimmune diseases, including Wegner's granulomatosis (WG), multiple sclerosis (MS) and rheumatoid arthritis (RS).

SAg-*Sau* induces polyclonal T cell activation and activates pro-inflammatory responses leading to inflammatory pathologies. IL-17A-producing $CD4^+$ T cells (Th17) are identified as a major pro-inflammatory T cell subset causing autoimmune pathogenesis, which can also be activated by SAg-*Sau* stimulation. T cell-mediated immune tolerance is well appreciated for controlling inflammations and avoiding inappropriate activation of pathogenic T cells. How SAg-*Sau* modulates T cell-mediated immune regulation, and whether these modulations are contributing to SAg-*Sau*-activated pro-inflammatory T cell responses remains unclarified.

In this study, I examined the $CD4^+$ T cell activation in human nasopharynx-associated lymphoid tissue (NALT) in response to extracted *Sau* antigens, and how SAg-*Sau*-activated Th17 responses are regulated by $CD4^+$ T cell-mediated immune controls, including $Foxp3^+CD4^+$ T cells (Tregs), IL-10 and IL-35.

SAg-*Sau* activated a potent Th17 response which was markedly higher than *Streptococcus pneumoniae* (*Spn*) and other commonly identified bacterial colonizers in human nasopharynx. The $Foxp3^+$ Treg population was largely expanded by SAg-*Sau*, although it failed to suppress the Th17 activation. The cell surface expression of CD39 on expanded Tregs was downregulated which may account for their lack of suppression on Th17 activation.

SAg-*Sau* also enhanced IL-10 expression, primarily in $Foxp3^-CD4^+$ T cells. Interestingly, the Th17 responses were not altered by neutralizing IL-10 in SAg-*Sau* stimulated tonsillar mononuclear cells (MNCs), although a significantly enhanced Th1 activation was observed. Furthermore, addition of recombinant IL-10 suppressed the Th1 activation but promoted SAg-*Sau*-activated Th17 responses.

In contrast to upregulated IL-10, the expression of IL-35 in tonsillar $CD4^+$ T cells was significantly downregulated by SAg-*Sau*. Treating MNCs with recombinant IL-35 was able to suppress SAg-*Sau*-activated high Th17 responses without affecting those low Th17 responders. In SAg-*Sau*-induced Th17 differentiation, IL-35 downregulated $ROR\gamma t$ expression in $CD4^+$ T cells and inhibited IL-17A production. Further, it was confirmed in an *in vivo* murine model that nasopharyngeal infection of SAg-*Sau* markedly enhanced Th17 response in the cervical lymph nodes (CLNs), which was accompanied with reduced expression of IL-35 in the $CD4^+$ T cells.

The results suggest SAg-*Sau* downregulates $CD4^+$ T cell-mediated immune controls in the nasopharynx, thus allowing activation of over-reactive Th17 responses. Immune suppressive cytokines IL-10 and IL-35 play differential role in SAg-*Sau*-activated inflammatory Th1 and Th17 responses which should be further evaluated to inform cytokine-based immune therapies for inflammatory/autoimmune conditions. The results also suggest that IL-35 has therapeutic potential for the treatment of Th17-mediated inflammatory pathologies.

Acknowledgements

Firstly, I would like to thank my supervisor, Dr. Qibo Zhang, for his endless support and guidance, without which this work would not have been possible. I would also like to thank my co-supervisor, Professor Aras Kadioglu, for all his advice, support and encouragement during my PhD study.

I would like to express my sincere appreciation to Dr. Xiao-Qing Wei in the Cardiff University for his tremendous support throughout my PhD, as well as his expert advice on the IL-35 work. Thanks also to Richard Ali in the Cardiff University for his help with generating the IL-35-expressing CHO cell line.

A special thank you goes to Dr. Suttida Puksuriwong and Dr. Shamsher Ahmed for their full support and advice during my PhD and true friendship that will last forever. I would like to thank Rebecca K. Shears for her help with the animal work and input in the paper writing. I would also like to thank Ziqi Lin, Jingjing Xing, Marion Pouget, Shadia Khandaker and Charlene Adaken for their love and support.

I would like to acknowledge the patients who took part in my PhD study and the theatre staff in Liverpool Children's Hospital and Royal Liverpool & Broadgreen University Hospitals for helping the collection of samples.

Big thanks go to all members, past and present, of the IGH lab! Thanks to the technical team for the help and support during my PhD.

Finally, I would like to acknowledge the University of Liverpool and China Scholarship Council for funding my PhD study.

Table of Contents

List of Tables

List of Figures

List of Abbreviations

APC	Antigen-presenting cells
AHR	Airway hyperresponsiveness
AIG	Autoimmune gastritis
ATP	Adenosine triphosphate
Aire	Autoimmune regulator
BAB	Blood agar base
BSA	Bovine serum albumin
β-ME	β-mecaptoethanol
CIA	Collagen-induced arthritis
CTLA4	Cytotoxic T-lymphocyte-associated protein 4
CCS	Concentrated culture supernatant
CFU	Colony forming units
CNS	Coagulase-Negative *Staphylococcus*
CFSE	Carboxyfluorescein succinimidyl ester
C of A	Certificate of Analysis
CBA	Cytometric Beads Array
Cq	Quantitative cycle
CLB	Clear lysis buffer
Co-IP	Co-Immunoprecipitation
CLNs	Cervical lymph nodes
CHO	Chinese hamster ovary
CSIF	Cytokine synthesis inhibitory factor
CMC	Chronic mucocutaneous candidiasis
dsDNA	Double-stranded deoxyribonucleic acid
DCs	Dendritic cells
DPBS	Dulbecco's phosphate-buffered saline
ddCt	Delta-Delta-Cycle threshold

DMEM	Dulbecco's Modified Eagle Meidum
DP	Double-positive
EAE	Experimental autoimmune encephalomyelitis
ETA	Exfoliative toxin A
ELISA	Enzyme-linked immunosorbent assay
EAM	Experimental autoimmune myocarditis
EDTA	Ethylenediaminetetraacetic acid
EBI3	Epstein-Barr virus-induced gene 3
Foxp3	Forkhead box P3
FBS	Fetal bovine serum
FITC	Fluorescein isothiocyanate
FACS	Fluorescence-activated cell sorting
FSC	Forward scatter
GM-CSF	Granulocyte-macrophage colony-stimulating factor
gp130	Glycoprotein 130
HP	Hypersensitivity pneumonitis
HBSS	Hank's balanced salt solution
HRP	Horseradish peroxidase
i.v.	Intravenous
i.p.	Intraperitoneally
IRBP	Interphotoreceptor retinoid binding protein
IFNγ	Interferon gamma
IL	Interleukin
IL-17A	Interleukin-17A
IL-35	Interleukin-35
IL-10	Interleukin-10
IBD	Inflammatory bowel disease
IL-10R	Interleukin-10 receptor
iT_R35	Inducible interleukin-35-producing regulatory T cells
IP-10	Interferon gamma-induced protein 10

IL-2Rα	Interleukin-2 receptor alpha
IL-23R	Interleukin-23 receptor
IL-12Rβ2	Interleukin-12 receptor subunit beta 2
ICOS	Inducible co-stimulator
ICOSL	Inducible co-stimulator ligand
Ig	Immunoglobin
iTregs	Induced Tregs
IL-27R	Interleukin-27 receptor
IFNGR	Interferon-gamma receptor
JAK	Janus kinase
LTi	Lymphoid-tissue-inducer
MBP	Myelin basic protein
MS	Multiple sclerosis
MNCs	Mononuclear cells
M-MLV RT	Moloney Murine Leukemia Virus Reverse Transcriptase
MW	Molecular weight
m-IgGκ BP	Mouse IgG kappa binding protein
MHC	Major histocompatibility complex
MALT	mucosa-associated lymphoid tissue
MC	Media control
MAPKs	Mitogen-activated protein kinases
MCP	Monocyte chemoattractant protein
MFI	Median fluorescent intensity
Mis	Minor lymphocyte stimulating antigens
MOG	Myelin oligodendrocyte glycoprotein
mTECs	Medullary thymic epithelial cells
M. arthritidis	*Mycoplasma arthritidis*
mAb	Monoclonal antibody
NonSAg-*Sau*	Non-superantigenic *Staphylococcus aureus*
NALT	Nasopharynx-associated lymphoid tissue

nTregs	Natural Tregs
NCBI	National Centre for Biotechnology Information
NC	Negative control
NO	Nitric oxide
NF-κB	Nuclear factor kappa-chain-enhancer of activated B cells
OD	Optical density
PLP	Proteolipid protein
PBMCs	Peripheral blood mononuclear cells
PHA	Phytohemagglutinin
PBS	Phosphate buffered saline
P/S	Penicillin-streptomycin
PMA	Phorbol 12-myristate 13-acetate
PAGE	Polyacrylamide gel electrophoresis
PAI-1	Plasminogen activator inhibitor-1
PC	Positive control
PD-1	Programmed cell death protein 1
PI3K	Phosphoinositide 3-kinase
pSTAT	Phosphorylated STAT
qPCR	Quantitative polymerase chain reaction
RNP	Ribonucleoprotein
RA	Rheumatoid arthritis
RT	Room temperature
RT-qPCR	Quantitative reverse transcription PCR
RNase	Ribonuclease
RLU	Relative light units
ROS	Reactive oxygen species
RORγt	Retinoic acid receptor-related orphan receptor gamma
Sau	*Staphylococcus aureus*
SAg	Superantigen
SAg-*Sau*	Superantigenic *Staphylococcus aureus*

SE	Staphylococcal enterotoxin
SEA	Staphylococcal enterotoxin A
SEB	Staphylococcal enterotoxin B
s.c.	Subcutaneously
SLE	Systemic lupus erythematosus
SFB	Segmented filamentous bacteria
STAT	Signal transducer and activator of transcription
Sm	Smith
Spn	*Streptococcus pneumoniae*
SSC	Side scatter
SEM	Standard error of the mean
TSST-1	Toxic shock syndrome toxin-1
Tregs	Foxp3$^+$ Regulatory T cells
TCR	T cell receptor
Tr1	Type 1 regulatory T cells
TGF-β	Transforming growth factor beta
TNFα	Tumor necrosis factor alpha
TNFR	Tumor necrosis factor receptor
Tconvs	Conventional T cells
THB	Todd Hewitt Broth
TMB	3,3',5,5'-Tetramethylbenzidine
TBS	Tris buffered saline
TMLCs	Transformed mink lung cells
Th cells	Helper T cells
Tc cells	Cytotoxic T cells
TGF-βRII	Transforming growth factor beta receptor type II
tTregs	Thymic derived Tregs
Vα	Variable alpha
Vβ	Variable beta
WG	Wegener's granulomatosis

CHAPTER 1

General Introduction

1.1 Nasopharyngeal colonisation of *Staphylococcus aureus*

The nasopharynx is part of the upper respiratory tract, which hosts a diverse community of microbes. *Streptococcus pneumoniae* (*Spn*) and *Staphylococcus aureus* (*Sau*) are both frequent colonisers of the human nasopharyngeal niche and occasionally cause infectious diseases. Whilst *Spn* carriage is more common in children, the frequency of *Sau* colonisation increases with age and *Sau* rarely co-colonises with *Spn*[1-3]. Interestingly, this negative correlation of *Spn* and *Sau* carriage is not found in HIV-positive individuals, which suggests that host immunity, especially $CD4^+$ T cells, could play an important role in regulating bacterial colonization in nasopharynx[4,5].

The spectrum of diseases caused by *Sau* overlaps with *Spn*, including pneumonia, sinusitis and bacteremia. Apart from upper respiratory tract, *Sau* is also frequently found on the skin and contributes to skin infection. Some *Sau*-related diseases, such as food poisoning and toxic shock syndrome[6], are not caused by direct infection but through the toxins produced and released by *Sau*.

In human nasopharynx, *Sau* has an overall carriage rate of 30%[7,8]. Whilst a large proportion of the population (± 60%) harbours *Sau* intermittently, only a minority of people (± 20%) almost never carry it[7]. *Sau* carriage may lead to an invasive infection contributing to inflammatory diseases e.g. pneumonia, and in rare conditions, causing bacteremia and sepsis. Some *Sau* isolates are known to be superantigenic due to their ability to produce various superantigens (SAgs), including toxic shock syndrome toxin (TSST) and staphylococcal enterotoxins (SEA, SEB, SEC, SED and SEE)[9,10]. SAgs are mostly encoded by mobile genetic elements, such as prophages and staphylococcal pathogenicity islands, and the distribution of SAg genes is strain-dependent[11,12].

Although most of *Sau* carriers are asymptomatic, carriage of enterotoxin-producing *Sau* induces activation of Th17 cells, a $CD4^+$ T cell subset, and relates to a higher relapse rate in patients with Wegener's granulomatosis (WG), an autoimmune vasculitis, which has raised concerns that it may present as a major risk factor for genetically predisposed individuals developing autoimmune diseases[10,13-15].

1.2 Mechanisms of infection-induced autoimmunity

Autoimmune diseases are characterised by aberrant immune responses in the host that attack and damage self-tissues. In healthy subjects, most auto-reactive T cells are deleted through negative selection in the thymus, those that escape are tightly controlled by peripheral tolerance mechanisms. Genetic and environmental factors that break the immune tolerance may lead to the activation of self-antigen specific T and B cells and cause autoimmune pathogenesis either organ-specifically or systemically. The immune responses are commonly triggered by the invasion of exogeneous pathogens, and these infection-induced inflammatory responses could sometimes override tolerogenic signals on auto-reactive immune cells. Infection is therefore considered as a major causative factor for autoimmune development[16-18]. Proposed mechanisms of infection-induced autoimmunity include molecular mimicry (cross-reactivity), epitope spreading and bystander activation[19].

The molecular mimicry theory is based on the possibility of sequence similarity between self-peptides and pathogen-derived foreign peptides, thereby enabling those pathogen-activated immune cells to cross-react with self-tissues. Pharyngeal carriage of group C and G streptococci may cause rheumatic fever with evidence showing that antibodies against group C and G streptococci isolated from throat swabs of asymptomatic Aboriginal children cross-react with human heart myosin[20].

Epitope spreading has been seen in a murine model of experimental autoimmune encephalomyelitis (EAE) induced by proteolipid protein (PLP) epitopes. In this model, the immunodominant PLP epitope, $PLP_{139-151}$, was used to prime the SJL mice. $PLP_{139-151}$-specific $CD4^+$ T cells were initially induced and maintained throughout the disease course, however $PLP_{178-191}$ and myelin basic protein (MBP_{84-104})-specific $CD4^+$ T cells were identified during the first and second relapses respectively[21]. Tissue damage allows the sequestered auto-antigens to be exposed and presented to antigen-presenting cells (APC), and subsequently activates adaptive immune responses[19,22]. In infection caused tissue damage, the invading pathogens induce potent inflammatory responses that enhance the antigen presentation and T cell

priming not only for microbe-derived antigens but also for those previously concealed auto-antigens via mechanisms of bystander activation.

1.3 The link between SAg-*Sau* infection and autoimmune conditions

Up to half of the *Sau* isolates were shown to produce various enterotoxins[9,10], which are highly virulent and function as superantigens that stimulate poly-clonal T cell activation via cross-linking the major histocompatibility complex (MHC) Class II of APC and T cell receptor (TCR) Vβ chain[23,24]. Thus, most studies addressing the relationship between *Sau* and autoimmune disorders focus on the role of enterotoxins. It has also been demonstrated that memory Th17 cells, a $CD4^+$ T cell subset that contributes greatly to autoimmunity, can be activated by superantigenic *Sau* (SAg-*Sau*) (*Sau* strain that produces these enterotoxins)[14]. With evidence showing that staphylococcal superantigens have the ability to induce autoimmune pathologies, as well as its potential in activating pro-inflammatory Th17 cells, it is plausible to suggest that SAg-*Sau* infection may contribute to autoimmune development. Here, I reviewed studies revealing the link between *Sau* infection and chronic inflammatory/autoimmune diseases and explored how it may associate with a potential pathological Th17 activation.

It was first reported in a rat arthritis model demonstrating the capability of staphylococcal superantigens to promote inflammatory pathologies[25]. The joint inflammation was induced by peptidoglycan-polysaccharide, and intravenous (i.v.) injection of staphylococcal TSST-1 was able to reactivate it repeatedly following each injection. The limitation of this study was that the arthritis was induced by complexes isolated from streptococci cell wall, but not self-antigens, thus the inflammatory responses and tissue pathologies presented may be different from an autoimmune arthritis. Nevertheless, it demonstrated that systemic administration of staphylococcal TSST-1 could reactivate T cells in the joint that have been primed by other antigens, resulting in arthritis flare-ups.

Shortly following the arthritis study, 2 parallel studies were carried out to investigate the effects of staphylococcal enterotoxins (SEs) on the development of multiple sclerosis (MS) using a

murine model of EAE[26,27]. In one study, (PL/J × SJL) F1, PL/J and SJL/J mice were immunized with MBP peptide AC1-11 or spinal cord homogenate, and then treated with staphylococcal enterotoxin B (SEB) or enterotoxin A (SEA) intraperitoneally (i.p.). SEB treatment significantly increased relapses and was able to exacerbate sub-clinical EAE. SEA-treated mice showed an increase in relapses, although it was not statistically significant[26]. Both SEA and SEB were demonstrated to be effective in inducing relapses in another study. Furthermore, it was shown that the EAE could be re-induced multiple times with each incident occurring after an SEB injection, which was similar to the effect of TSST-1 shown in the arthritis model mentioned above[27]. However, both studies failed to show EAE induction by SEs without prior antigen challenge. Therefore, SAg-*Sau*/SEs appears to affect EAE development when auto-antigens or auto-reactive T cells are presented. It is notable that pre-treating mice with SEB has been shown to reduce T cell activation and ameliorate Ac1-11-induced EAE, which can be explained by SEB-induced anergy in naïve T cells bearing Vβ8 receptors[28,29]. This contradicted observation could be explained by the timing of SEs administration. While SEB stimulation is able to cause clonal deletion and unresponsiveness in naïve T cells, antigen-experienced T cells are protected from the induction of anergy and could be further activated[27,30]. Hence, SAg-*Sau* infection that happens at different stages of an autoimmune disease may have differential effects on disease development.

Although SEB pre-treatment protected the PL/J mice from EAE induction by rat MBP, administration of SEA was able to overcome the T cell anergy and induced an initial episode of EAE[31]. This indicates that encephalitogenic MBP-specific T cells are not restricted to the $V\beta8^+$ T cells that specifically reactivates with SEB, and those non-$V\beta8^+$ T cells primed by MBP could be activated by other superantigens leading to accelerated onset of disease. Further, SEA pre-treated mice developed EAE and were susceptible to relapse induced by SEB[31]. It is common that a SAg-*Sau* strain can be positive in more than one enterotoxin, and different SAg-*Sau* strains produce various enterotoxins[32,33], SAg-*Sau* colonization/infection is therefore a major risk factor for the development of multiple sclerosis which should not be underestimated.

The effects of SEs for promoting autoimmune pathogenesis have also been reported in other autoimmune disease models[34,35]. In an experimental model of autoimmune uveoretinitis, mice were immunized with human interphotoreceptor retinoid binding protein (IRBP) peptide, and SEB was given on day 10 or day 24 post immunization. While SEB treatment during disease progression enhanced the severity of clinical symptoms, administrating SEB after resolution of clinical signs was able to induce a disease relapse. The promoted proliferation of IRBP-specific T cells by SEB was accompanied with enhanced production of IFNγ and IL-17A[34]. This study further confirms that SEs are able to reactivate auto-reactive T cells via initiating poly-clonal T cell activation regardless of antigen-specificity.

In above described studies, a prior auto-antigen challenge to prime a population of auto-reactive T cells is essential for SAg-*Sau*/SEs to play a role in later autoimmune development. It is well documented that auto-reactive T and B cells exist even in healthy individuals[36]. Therefore, is it possible for SAg-*Sau*/SEs to initiate autoimmunity with naturally occurred auto-reactive T cells? One study addressed this question using HLA-DQ8 transgenic mice that were chronically exposed to SEB[35]. The HLA-DQ8 transgenic mice express human MHC class II, thus the activation of auto-reactive T cells by the SEs resembles the autoimmune events which may happen in humans. Extremely small non-lethal amounts of SEB were administrated subcutaneously (s.c.) with mini-osmotic pumps for 4 weeks without any exogenous antigen challenge. Interestingly, the SEB-treated mice developed systemic inflammatory disease manifested by elevated levels of anti-nuclear antibodies, mononuclear cell infiltration in kidney, lung and liver, accompanied with pathological changes in these organs, which were very similar to human systemic lupus erythematosus (SLE). It further demonstrated that this SEB-induced multi-system autoimmune pathologies were $CD4^+$ T cell/CD28-dependent and IFNγ-producing Th1 cell-mediated. While the importance of Th1 cells in an autoimmune disease mimicking human lupus was shown in this study, it only compared the STAT4- and STAT6-deficient mice to demonstrate Th1, rather than Th2, was involved in disease development. The role of STAT3-dependent pathway and IL-17A-producing Th17 cells in this autoimmune disease model was not investigated. Recent studies have provided a large body of evidence demonstrating a more critical role of Th17 cells in the aetiology and pathology of autoimmune diseases[37].

To establish the role of SAg-*Sau*/SEs in autoimmune disease development, only experimental evidence from murine studies is not sufficient. By identifying bacterial species isolated from the nasopharynx in patients with autoimmune diseases, the association between SAg-*Sau* nasal colonization and certain autoimmune diseases has been established[10,15,32,38-42]. Wegener's granulomatosis is an autoimmune vasculitis that has been consistently found to be closely related to SAg-*Sau* colonization[10,15,43]. In an observational cohort study for patients with biopsy-proven WG, chronic nasal carriage of *Sau* was identified as an independent risk factor (relative risk, 7.16) for disease relapse, and the carriage rate was about three times higher than it was in healthy subjects[15]. Further investigations revealed that *Sau* stains that produce SEA, TSST-1, SEC and exfoliative toxin A (ETA) were most frequently found in WG patients, and carriage of TSST-1-positive *Sau* correlated with the occurrence of relapses (relative risk, 13.3)[10,44].

Significantly higher carriage rate of *Sau* has also been reported in patients with MS[32]. However, another study examining the association between MS patients and colonization of *Sau* that harbour superantigens did not find increased *Sau* carriage in those patients. Nevertheless, they did show that SEA-producing *Sau* was more prevalent in patients who suffered a relapse within 30 days of study recruitment for those individuals carrying *Sau*[39]. SLE is a systemic autoimmune disease that affects multi-organs. Although *Sau* carriage rate in patients with SLE was similar to that reported in healthy subjects, investigation into the organ involvement of these patients showed a higher frequency of renal and skin manifestations in *Sau*-positive patients[45]. These *Sau*-positive patients also had an increased production of auto-antibodies, such as anti-double stranded DNA (dsDNA), anti-Smith (Sm) and anti-ribonucleoprotein (RNP). It suggests that *Sau* colonization is associated with a specific phenotype of SLE. It is possible that certain organs may be more susceptible to *Sau*-induced bystander activation of auto-reactive T cells. Rheumatoid arthritis (RA) is another commonly seen autoimmune disorder that primarily affects joints. A study compared staphylococci carriage rates between patients with RA, healthy adults and elderly volunteers, and reported that RA patients had the highest carriage rate of *Sau* whereas the carriage of staphylococcus epidermidis was comparable among three groups[38]. Report from another study also demonstrated that patients with RA more often carried *Sau* in their nasal vestibule, and had increased antibody titres to

TSST-1, suggesting a distinct subpopulation of *Sau* that produces TSST-1 superantigen is involved in the pathogenesis of rheumatoid arthritis[42]. However, an increased *Sau* carriage rate in RA patients is not consistently found[46], and the association between *Sau* carriage and RA development remains inconclusive.

It has been proved difficult though to track down a particular infectious agent that induces or promotes autoimmune diseases, as the responsible microbe could have been cleared at the time the disease is diagnosed. *Sau* carriage appears to be intermittent in most individuals and can be affected if patients are treated with antibiotics or immune-suppressive drugs. Thus, to establish SAg-*Sau* infection as an initiative event for the patient to develop autoimmune disorder would require a regular check-up of nasal carriage status in longitudinal studies that follow up the patients from disease onset to remissions and relapses. In addition, future epidemiological studies should also consider divergent individual responses to *Sau* infection when evaluating the resulting impact of *Sau* carriage on autoimmune development.

Approaches to identify individuals who are genetically susceptible to autoimmunity are yet to be established. It is likely multiple infectious events are contributing to the aetiology of autoimmune disease, thus making it extremely difficult to establish causative relationship of a particular pathogen infection and an on-going autoimmune condition in clinical patients. Previous evidence from murine models of autoimmune diseases strongly suggest SAg-*Sau*/SEs is a key player in the development of autoimmune pathogenesis. However, the impact of chronic or intermittent colonization of SAg-*Sau* in disease onset and progression has not been clarified. It is equally important to elucidate how *Sau* infection shapes the immune environment to favour the activation of auto-reactive immune responses in order to better understand the relationship between infections and autoimmune disorders and provide new strategies for clinical treatment.

1.4 Th17 cells as key pro-inflammatory T cell subset for autoimmunity

It is plausible that superantigen-activated non-specific T cell responses are the principal mechanism for SAg-*Sau*-related autoimmunity. I propose two possible ways by which SAg-*Sau* nasal colonization may induce potential autoimmune responses. First, SAg-*Sau* infection happens in the presence of auto-reactive T cells and is able to activate these cells via polyclonal T cell activation. Activated auto-reactive T cells escape peripheral immune surveillance and approach the target organ to attack self-tissue. Second, SAg-*Sau* colonization activates a population of pro-inflammatory T cells that cannot be suppressed by regulatory networks. These pro-inflammatory T cells then travel to susceptible organs to cause an initial tissue damage, followed by the exposure of sequestered auto-antigens to prime auto-reactive immune cells. In the inflammatory microenvironment created by SAg-*Sau*-activated T cells, these auto-reactive immune cells are polarised to pro-inflammatory phenotypes leading to self-destruction. The gut-residing segmented filamentous bacteria (SFB), which induce IL-17A-producing Th17 cells, are able to drive autoimmune arthritis and encephalomyelitis, suggesting that locally activated Th17 cells could enter the circulation and cause autoimmune pathogenesis at a distal site[47,48]. In light of these intriguing findings, it will be interesting to know whether SAg-*Sau* colonization can activate Th17 cells that are resistant to regulations and have the potential to initiate autoimmunity. Before this, how have Th17 cells come to the centre of autoimmunity?

$CD4^+$ T cells can differentiate into either pro-inflammatory subsets, Th1 and Th17 cells, or anti-inflammatory subsets e.g. $Foxp3^+$ regulatory T cells (Tregs) in response to various microbial infections. Th1 cell activation was deemed as a key contributor for the development of autoimmune diseases until it was found that Th1 related gene mutations, such as *ifng*, *ifngr* and *T-bet*, led to more severe disease manifestations in murine models of EAE and experimental autoimmune myocarditis (EAM). From these experiments, it was concluded that IL-17-producing Th17 cells rather than IFNγ-producing Th1 cells were the major players in autoimmune disease development[49-51]. It is now known that although Th17 cells are important in host immune defence against bacterial and fungal infections[52,53], they are critically involved

in the development of autoimmune diseases including MS, RA, psoriasis and inflammatory bowel disease (IBD)[37,50,54].

The initial study suggesting that IL-17 drives pathological changes was described in collagen-induced arthritis (CIA), which showed blocking endogenous IL-17 with soluble IL-17 receptor protein dose-dependently suppressed the incidence of arthritis, whereas systemically increased expression of IL-17 enhanced CIA[55]. The effect of IL-17 in promoting CIA development was later confirmed by Nakae et al. using IL-17-deficient mice[56]. They further demonstrated that mice with IL-17 deficiency were also more resistant to the induction of EAE, exhibiting delayed disease onset and improved clinical scores associated with significantly reduced mononuclear cell infiltration within the spinal cords[57].

Another line of evidence delineating the role of IL-17-producing $CD4^+$ T cells in autoimmunity came from studies using *IL23*$^{-/-}$ and *Ror*$\gamma^{-/-}$ mice[58-60]. IL-23 is a heterodimeric cytokine belonging to IL-12 family. IL-23 is shown both *in vitro* and *in vivo* to drive Th17 cell activation, while IL-12 is known to activate IFNγ-producing Th1 cells. IL-23-deficient mice were EAE resistant, although the number of immune cells including IFNγ^+ cells that invaded the central nervous system in *IL23*$^{-/-}$ mice were comparable to wild type mice. However, a lack of IL-17 expression was observed in these infiltrating T cells indicating Th17 deficiency abrogated autoantigen-induced neural inflammation. Indeed, primed with PLP autoantigens, it was the IL-23-expanded Th17 cells but not IL-12-expanded Th1 cells that induced EAE pathology following adoptive transfer in the recipient mice[58]. Th17 cells as a distinct Th cell lineage are induced via signalling pathways independent of those required for the development of Th1 and Th2 cells. The orphan nuclear receptor, RORγt, is the key transcription factor to induce Th17-related gene expression. Mice lacking RORγt were deficient in generating Th17 cells, and in turn they had attenuated autoimmune disease[59].

Besides autoimmune diseases, Th17 cells are also implicated in a wide range of inflammatory conditions, such as contact hypersensitivity, asthma and atopic dermatitis[61-64]. Hypersensitivity pneumonitis (HP) is an allergic pulmonary disorder mediated by inflammatory T cell responses. In the experimental model of HP induced by repeated intranasal

administration of *S. rectivirgula*, depleting IL-17 via genetic deletion or immunoneutralization resulted in less inflammation along with a significantly lower count of mononuclear cells that infiltrated the lungs[65]. Asthma, characterised by airway hyperresponsiveness (AHR), was largely thought to be Th2-driven chronic inflammatory disease. However, the aetiology of asthma is heterogeneous which involves Th17-mediated pathologies[61,66]. Asthma patients with a Th17-dominant inflammatory response have been found by assessing the gene expression profile of endobronchial biopsies[62]. Neutralizing Th2-type cytokines, IL-4 and IL-13, in murine model of allergic asthma induced Th17 responses and neutrophilic inflammation, suggesting that targeting Th2 cytokines in clinical treatment may promote Th17-dependent airway inflammation[62,67].

Several signature molecules, such as IL-23R, GM-CSF and CCR6, are suggested to contribute to the pathogenicity of Th17 cells from murine studies[68-70]. However, IL-17A, the hallmark cytokine of Th17 cells, has been shown to be a highly effective target in clinical studies treating autoimmune diseases including psoriasis, MS and RA[37]. Th17 cells also produce IL-17F and IL-22, but clinical studies targeting these cytokines have provided evidence suggesting that IL-17A is the primary effector cytokine leading to the clinical manifestation of most autoimmune diseases associated with Th17 activation[37]. It has been reported that IL-17A contributes to autoimmunity by inducing chemokine expression, recruiting neutrophils, macrophages and auto-reactive T cells, and promoting germinal centre formation to produce auto-antibodies[47,48]. Given the critical role of IL-17A-producing Th17 cells in mediating inflammatory pathologies, pathogens that are able to activate a strong Th17/IL-17A responses would therefore pose potential risk to the development of inflammatory and autoimmune diseases.

Staphylococcal superantigens activate $CD4^+$ T cell dominant-inflammatory responses, and it has been shown that they mainly trigger Th1 and Th17 responses characterised by a massive production of pro-inflammatory cytokines, such as IFNγ, IL-17A and TNF-α[71]. In humans, the capacity of SAg-*Sau* in activating Th17 responses is associated with the abundance of memory T cell repertoire[14]. Sitting at the entrance of upper respiratory tract, the nasopharynx-associated lymphoid tissue (NALT) is constantly exposed to inhaled foreign antigens and

thereby containing a substantial proportion of antigen-experienced effector and memory cells. Hence, it could be postulated that nasopharyngeal infection of SAg-*Sau* could lead to a potent Th17 activation in the nasopharynx and NALT. It has been reviewed above that SAg-*Sau* infection is related to the pathogenesis of various autoimmune diseases, including MS, WG and RA, and in all these diseases Th17 has been shown to play an indispensable role as demonstrated in both animal disease models and clinical studies[37,56,57,72]. However, how superantigenic Th17 responses may affect the disease development is yet to be illustrated. It is also unknown as to how SAg-*Sau*-activated Th17 responses are regulated, which may well underlie the aetiology of autoimmunity.

1.5 T cell-mediated regulation of Th17 responses

In the periphery, Foxp3$^+$ Tregs are a major cell population to regulate over-activated inflammatory responses and maintain immune tolerance. Tregs regulate effector T cell responses through cell contact and by producing immune suppressive cytokines, such as TGF-β1 and IL-10. Animal studies have demonstrated the importance of Tregs for protecting the host from developing autoimmune disorders by suppressing effector T cell responses[73,74]. Th1-type responses are effectively controlled by Tregs, but Th17 responses appear to be less susceptible to Treg-mediated suppression. In a spontaneous autoimmune gastritis (AIG) model, transfer of polyclonal Tregs markedly suppressed the induction and progression of AIG mediated by Th1 effectors, whereas the Th17-driven inflammation was more aggressive but could only be modestly suppressed at the initial stage[75]. Interestingly however, Tregs with TCRs recognizing the specific autoantigen exhibited higher suppressive activity against the pathological Th17 cells than natural Tregs (nTregs) and TGF-β-induced polyclonal Tregs. By transferring the autoantigen-specific Tregs, the mice were protected from the Th17 cell-mediated tissue destruction[76]. This suggests that Tregs may suppress Th1 and Th17 effectors through divergent pathways, and Treg-mediated suppression of Th17 cells may to some extent depend on TCR specificity.

Another interesting study dissecting the intracellular signalling pathways that endow Tregs with the ability to suppress pathological Th17 cells suggests that Tregs require the activation of signal transducer and activator of transcription 3 (STAT3) to induce a subset of suppressor molecules specialized for Th17 suppression. Treg-specific deletion of STAT3 resulted in the development of Th17-driven colitis, despite these *Stat3*$^{-/-}$ Tregs had unaffected *in vitro* suppressor capacity with regard to controlling effector T cell proliferation[77]. Both IL-6 and IL-10 are known to activate STAT3 signalling but give rise to distinct outcomes. In Tregs, the activation of STAT3-mediated suppressor program against Th17 responses is dependent on IL-10 signalling. Ablation of IL-10 receptor (IL-10R) in Tregs led to the dysregulation of pathological Th17 activation similarly as it was shown by Tregs harbouring STAT3 deficiency[78]. Collectively in mice, Tregs may be less efficient in suppressing Th17 activation, they are capable of restraining overreactive Th17 responses via pathways differentiated from those commonly used to suppress cell proliferation and Th1-type responses.

In humans, IL-17 expression and proliferation of Th17 clones are poorly suppressed by Foxp3^{+} Tregs[79,80]. However, a subpopulation of human Tregs that express CD39 has been shown to inhibit IL-17 production via cell contact[81]. CD39 is an ectonucleotidase expressed by B cell, dendritic cells (DCs) and Tregs. It mediates immune suppression through catalysing extracellular ATP, which has multiple pro-inflammatory effects, to suppressive adenosine[82,83]. Notably, the number of CD39^{+} Tregs were markedly reduced in patients with MS, suggesting this Treg subset may have specific role in the control of the disease and its reduction was likely concerning an impaired suppression of pathological Th17 responses[81,84]. Whilst the suppression mechanism of CD39^{+} Treg requires further investigation, it remains controversial whether human Th17 cells can be controlled by the Tregs. It is therefore of interest to examine the role of Tregs in the control of SAg-*Sau*-activated Th17 responses and how it may relate to the specific CD39^{+} Treg subset.

Unlike Tregs, immune suppressive cytokine IL-10 has a well-defined role in regulating Th17 responses. IL-10 activates STAT3 signalling in the Tregs to mediate their suppression against Th17 cells as has been mentioned above[78]. Besides, it has been reported by Huber et al. that IL-17A-producing CD4^{+} T cells expressed IL-10R and their proliferation was controlled by IL-

10 signalling. T cell-specific deletion of IL-10R disrupted the IL-10 signalling in $CD4^+$ T cells and thereby abrogated the suppression of pathological Th17 cells by $Foxp3^+$ Tregs and $Foxp3^-$ $CD4^+$ IL-10-producing regulatory T cells (Type 1 regulatory T cells, Tr1)[85]. Moreover, some Th17 cells were shown to co-express IL-10 and these IL-10^+ Th17 cells upregulated an array of immunoregulatory molecules, such as TGF-β and CTLA4, as well as molecules involved in the suppressive function of Tregs, thereby directing the Th17 cells towards a non-pathogenic phenotype. When co-cultured with monocytes, the IL-10^+ Th17 cells drove anti-inflammatory M2 macrophages leading to tissue repair, rather than the pro-inflammatory M1 macrophages which could be polarised by IL-10^- Th17 cells [86].

By suppressing pathological Th17 responses, as well as other inflammatory immune responses, IL-10 and IL-10-producing T cells are of significant importance in the control of autoimmunity. IL-10 or IL-10 receptor (IL-10R) knockout mice are prone to the development of autoimmune disorders, such as IBD and EAE[87]. Loss of function mutations in IL-10 and IL-10R in humans has been linked to an early-onset of IBD[88-90]. Nevertheless, attempts to utilise recombinant IL-10 clinically for treating autoimmune diseases have been unsuccessful[91]. It is therefore intriguing to explore whether IL-10 is able to regulate the pro-inflammatory T cell responses, especially the Th17 responses, in all immunological settings, including that in the context of SAg-*Sau*-infected nasopharynx. IL-10 has been shown to suppress Th17 induction in mice with systemic infection of *Sau*, but the superantigenicity of the *Sau* strain used in the study was not indicated, nor whether the *Sau*-activated effector and memory Th17 responses were affected by the increased level of IL-10 in the system[92].

IL-35 is a recently identified immune regulatory cytokine, which may play a protective role in the development of autoimmune disorders[93]. IL-35 belongs to the IL-12 cytokine family, and is made of two shared subunits, IL-12A and EBI3. Unlike most of the other pro-inflammatory cytokines in the IL-12 family, IL-35 has been shown to suppress Th17 cell activation in autoimmune diseases and inflammatory disorders in animal models[94-96]. Treatment with soluble tumor necrosis factor receptor (TNFR) has been proven to be highly effective for patients with RA. CIA is an animal model of RA, in which IL-35 exhibited comparable therapeutic effects to TNFR in protecting the mice from developing severe joint inflammation,

and this protection was associated with IL-35-mediated suppression of Th17 responses[95]. The suppressive effect of IL-35 on Th1 responses was not consistent though which was dependent of the stimulation conditions[95]. In mice, IL-35 is primarily produced by Foxp3$^+$ Tregs and acts as an indispensable suppressive cytokine contributing to the regulatory activity of Tregs[97]. Another CD4$^+$ T cell subset that has been identified as a major source of IL-35 is the inducible IL-35-produing regulatory T cells (iTr35s)[94]. Derived from conventional T cells (Tconvs), iTr35s had potent regulatory control over effector T cells and were able to suppress autoimmune development in mice with induced EAE and IBD. Additionally, iTr35s have been reported to promote tumor growth as well, suggesting an overall suppressive role of iTr35s in the host immunity[94].

A recent report demonstrates that the IL-12A subunit of IL-35 ameliorated autoimmune uveitis in mice by antagonizing Th17 responses which was through inducing IL-10- and IL-35-expressing B cells[98]. IL-35$^+$ B cells have been shown by previous studies to control autoimmune pathologies similarly as iTr35s, but the effect of IL-35$^+$ B cells is suggested to be dependent on IL-10 while iTr35s mediate suppression via IL-35 but not IL-10 or TGF-β[94,99,100].

However, whether iTr35s also exist in humans and have similar immune regulatory effects is still debated[94,101]. Expression of the EBI3 subunit in CD4$^+$ T cells isolated from human peripheral blood mononuclear cells (PBMCs) was detectable only after stimulation with anti-CD3/anti-CD28 or phytohemagglutinin (PHA), while the IL-12A subunit was expressed constitutively[101]. It is still unclear if activated human CD4$^+$ T cell produce heterodimeric IL-35 protein. Current data on the role of IL-35 in human diseases is limited, although a reduced level of IL-35 in the circulation has been shown to be associated with several autoimmune disorders[102-104].

Sau carriage in human nasopharynx is common. Considering the potential of *Sau*, and SAg-*Sau* in particular, to induce strong pro-inflammatory T cell responses in human NALT which may contribute to inflammatory/autoimmune conditions, it will be valuable to examine how the pro-inflammatory responses (e.g. Th17 and Th1) are regulated by the regulatory T cells and cytokines. Such information will add to our understanding of *Sau*- and superantigen-related

inflammatory diseases and on new strategies in the management of inflammatory conditions such as autoimmune diseases.

In this PhD study, in order to delineate T cell-mediated regulation of Th17 responses in the context of SAg-*Sau* infection, I propose to study:

1. Whether *Sau* and SAg-*Sau* are able to activate Th17 responses in human NALT, and to what extent.
2. The effect of SAg-*Sau* on the response of $Foxp3^+$ Tregs, and how they may regulate the Th17 activation.
3. Whether IL-10 and IL-10-producing Tr1 cells are activated by SAg-*Sau* in NALT, and the IL-10-mediated regulation of SAg-*Sau*-activated Th1 and Th17 responses.
4. The effect of SAg-*Sau* on IL-35-producing $CD4^+$ T cells, and the role of IL-35 in SAg-*Sau*-activated pro-inflammatory T cell responses in human NALT.
5. Whether *in vivo* nasopharyngeal infection of SAg-*Sau* in mice could elicit T cell responses similar to that seen in the *in vitro* stimulated human NALT.

CHAPTER 2

Materials and Methods

2.1 Prepare bacterial stocks

For the handling of bacterial culture, all operations were performed in a biosafety cabinet or next to a Bunsen burner to avoid contamination.

2.1.1 Blood agar plates (blood agar base + 5% v/v Horse blood)

40 g of blood agar, base (BAB) (Sigma-Aldrich) was suspended in 1 L of distilled water and then autoclaved at 15 psi for 20 min to completely dissolve the BAB and sterilize the media. After autoclaving, the BAB media was allowed to cool to 56°C approximately, followed by adding 50 ml of sterile defibrinated horse blood to the media. The blood was evenly mixed before pouring culture dishes. The dishes were left in the biosafety cabinet to allow the agar to set. The BAB plates can be used straight away once set or stored upside down at 4°C.

2.1.2 Todd Hewitt Broth media (Todd Hewitt Broth + 0.5% w/v yeast extract)

37 g of Todd Hewitt Broth (THB) and 5 g of yeast extract was dissolved in 1 L of distilled water and then autoclaved at 15 psi for 20 min to sterilize the media. The media was stored at 4°C for later use.

2.1.3 BAB plate inoculation

The bacterial stocks were removed from -80°C freezer and left at room temperature (RT) to thaw. All culture dishes were properly labelled before inoculation. 20 µl of stock culture were added onto the BAB plate and streaked using a sterile loop. For bead stocks, a single bead was transferred onto the plate and streaked. The inoculated plates were kept overnight at 37°C for staphylococcus. *Spn* strains were cultured at 37°C with 5% CO_2.

To prepare a bead stock, several single colonies were transferred into cryopreservative fluid using a sterile loop. Bacterial stocks were stored at -80°C freezer.

2.1.4 Bacterial liquid stocks

Several single colonies were picked up from the culture plate and dispersed into 3 ml of THB media. The bacteria were cultured overnight at 37°C. In the next morning, the bacteria cultures were taken out of the warm room and checked for turbidity. The culture appeared cloudy if the bacteria were growing.

To expand the culture, 1-2 ml of the overnight culture was transferred into 20 ml of fresh THB media, followed by culturing in a shaking incubator with the temperature set at 37°C and the shaking speed set at 250 rpm/min. The culture turbidity was checked hourly. Once the culture started to appear cloudy, 1 ml of the culture was transferred to a plastic cuvette for the measurement of optical density (OD) at a wavelength of 600 nm. The OD value of the culture was read every 30 min. The culture was terminated once the OD value reached 0.5, which meant that the bacterial growth had entered exponential phase. The bacterial cultures were then mixed with equal amount of 30% sterile glycerol before aliquoting into 500 µl aliquots. Bacterial liquid stocks were kept in -80°C freezer.

2.2 Preparation of bacterial culture supernatant

All bacterial strains used for producing concentrated culture supernatant (CCS) are listed in ***Table 2.1***.

Bacterial liquid stock was removed from the -80°C freezer and left at RT to defrost. 20 µl of stock bacteria was inoculated to 3 ml of THB in a Bijou container, and cultured overnight at 37°C. The bacterial culture was expanded as describe in ***2.1.4***. 200 µl of the culture was left out for the measurement of colony forming units (CFU) later.

The expanded bacterial culture was transferred to a 50 ml conical centrifuge tube, followed by centrifuging at 3000 g for 30 min with the temperature set at 4°C. For *Spn* strains, the centrifuging speed was set at 3500 g to ensure proper pelleting of the bacteria. After centrifugation, the supernatant was collected and filtered through a 0.45 μm syringe filter using a 20 ml syringe, followed by filtering through a 0.2 μm syringe filter.

The Vivaspin 20 concentrator (5,000 MWCO) was rinsed with 10 ml of phosphate buffered saline (PBS) before used for concentrating the filtered supernatant. The supernatant was transferred to the concentrator and centrifuged at 3000 g for 30 min with a temperature of 4°C. A maximum of 15 ml sample can be loaded to the concentrator. If the sample volume exceeds 15 ml, remaining sample can be loaded later in the same concentrator. The flow-through was discarded after each centrifugation. The aim is to concentrate the supernatant 10 times (10×), thus if starting from 20 ml, the sample should be centrifuged until 2 ml of liquid was left above the membrane of the concentrator. Several centrifugations were usually required to concentrate the culture supernatant to desired amount.

Once the sample was fully concentrated, it was aliquoted into 500 μl aliquots for long-term storage at -80°C. The CCS was further aliquoted to 50 μl aliquots and stored at -20°C for cell stimulation.

Protein concentration of the CCS was measured using Pierce BCA Protein Assay Kit (Thermo Fisher).

Table 2.1 Bacterial strains

Bacteria		Strain information	Source
Staphylococcus aureus	HIP07930 (NonSAg-*Sau*)	Positive for mec (subtype II); negative for PVL, tsst, sea, seb, sec, sed and see.	BEI Resources
	FRI913 (SAg-*Sau*)	Positive for tsst, sea, sec and see; negative for mecA.	BEI Resources
	C1	Carriage strain isolated from nasal swab	Clinical isolates[1]
	C2	Carriage strain isolated from nasal swab	Clinical isolates[1]
	C3	Carriage strain isolated from nasal swab, positive for total SE(A-E)[3]	Clinical isolates[1]
Coagulase-Negative *Staphylococcus* (CNS)	C4	Carriage strain isolated from nasal swab	Clinical isolates[1]
	C5	Carriage strain isolated from nasal swab	Clinical isolates[1]
Streptococcus pneumoniae	D39WT	Standard encapsulated serotype 2	Kindly provided by Prof. James C Paton[4]
	TIGR4	Virulent serotype 4	Kindly provided by Dr. Michelle Barocchi[5]
	C6	Carriage strain isolated from nasal swab	Clinical isolates[2]
	C7	Carriage strain isolated from nasal swab	Clinical isolates[2]
	C8	Carriage strain isolated from nasal swab	Clinical isolates[2]
	C9	Carriage strain isolated from nasal swab	Clinical isolates[2]
Moraxella catarrhalis	C10	Carriage strain isolated from nasal swab	Clinical isolates[2]

[1] These carriage strains were isolated and tested by Lualuaa Zaki

[2] These carriage strains were isolated and tested by Dr. Qibo Zhang

[3] SE level shown in ***Figure 3.3 d***

[4] University of Adelaide, Australia

[5] Novartis, Siena, Italy

2.3 Viable count (The Miles and Misra Methods)

The bacterial suspension was serially diluted in a 96-well round-bottom microplate by adding 20 µl of sample into wells containing 180 µl of sterile PBS. Serial dilutions were made to $1:10^8$. The BAB plates were equally divided into 8 sectors and labelled with dilutions for these sectors. 3 × 20 µl of the appropriate dilution were dropped onto each sector. The inoculated plates were then left open in the biosafety cabinet to allow the drops to dry into the agar. Avoid touching the agar surface with the pipette when inoculating plates. The plates were inverted and cultured at 37°C for 16 to 24 hours.

Each sector was observed for bacterial growth, and colonies were counted in the sector where the highest number of full-size discrete colonies were seen. The number of CFU per ml from the original sample was calculated using the following equation:

$$\text{CFU per ml} = \text{Number of colonies in the sector}/60 \times \text{dilution factor} \times 1000$$

2.4 Detection of staphylococcal enterotoxins (SEs)

To identify if the *Sau* strains isolated from patient nasal swabs are capable of producing SE (A-E), the RIDASCREEN@ SET Total kit (r-biopharm, Germany) was used to detect the SEs in the bacterial culture supernatant.

The 10× wash buffer was incubated in a 37°C to completely dissolve any visible crystals and then diluted with sterile distilled water. Pre-coated wells were inserted into the microwell holder, followed by adding 1:10 diluted CCS samples. The positive and negative controls provided were also added accordingly. The wells were sealed and incubated for 1 hour at 37°C.

Following the incubation, samples were discarded, and liquid residues were removed by blot the wells on tissue towel. The wells were washed with 300 µl of 1× wash buffer for 5 times. Then, 100 µl/well of green-stained conjugate 1 was added, and the wells were incubated for 1 hour at 37°C. The wells were washed again followed by adding 100µl/well of blue-stained conjugate 2 and incubating for 30 min at 37°C. After washing, the wells were incubated with

100 µl/well of red-stained substrate/chromogen at 37°C for a further 15 min. The microwells were gently tapped to make the colour evenly distributed before adding 100 µl/well of stop solution. The wells were read for OD values at 450 and 620 nm using ELISA microplate reader.

The (OD_{450} – OD_{620}) was calculated for each sample. The assay is deemed valid only when the calculated OD value for the positive control is over 1.0 and the negative control is less than 0.2.

2.5 Isolation of mononuclear cells from human tonsils

The adenotonsillar tissues were obtained from immunocompetent patients undergoing adenoidectomy and/or tonsillectomy due to upper-airway obstructions at Alder Hey children's Hospital, and Royal Liverpool and Broadgreen University Hospitals. Patients with known immunodeficiency or who had been prescribed antibiotics within 3 weeks before surgery were excluded. The study was approved by the National Research Ethics Committee and written consent was obtained in all cases.

Isolation procedure was carried out in a biosafety cabinet and guidelines of aseptic technique were followed to ensure sterile handling of clinical samples.

Tonsillar samples were collected in Hank's balanced salt solution (HBSS) (Sigma-Aldrich) supplemented with 1% of penicillin-streptomycin (10,000 U/ml, Thermo Fisher). Tonsillar tissues were washed with HBSS to remove blood attached on the tissue surface and then transferred to a 100 mm petri dish containing 15ml of HBSS. Using a sterile scalpel, the tissues were loosened to release cells to the media, followed by filtering the cell suspension through a 70 µl cell strainer to remove tissue debris and dissociate cells. Filtered single cell suspension was collected in a 50 ml conical centrifuge tube. The tissues were rinsed with 10 ml of HBSS in order to collect remaining cells. Again, cell suspension was filtered and collected in the same tube.

Mononuclear cells (MNCs) were isolated by density gradient centrifugation with Ficoll-Paque (Sigma-Aldrich). 10-15 ml of the single cell suspension was carefully layered onto 10ml of Ficoll-Paque media solution in a 30 ml Universal tube, making sure to not mix the cell suspension with the Ficoll-Paque media. After all cell suspensions were properly layered, centrifuging at 400 g for 30 min with a temperature of 20°C. The brake of the centrifuge was turned off to avoid disturbing the layers during deceleration. Following centrifugation, the upper layer containing plasma and platelets was drawn off using a sterile pipette, leaving the MNC layer undisturbed at the interface. The layer of MNCs were then carefully collected in a 50 ml conical centrifuge tube. The volume of total MNCs collected was estimated and at least 3 volumes of Dulbecco's phosphate-buffered saline (DPBS) was added to the MNCs to ensure a proper washing of the cells. Cells were well-suspended by inverting the tubed for several times before centrifuging at 300 g for 10 min.

After centrifuging, the supernatant was removed and MNCs were resuspended in RPMI 1640 medium (with L-glutamine and phenol red, Thermo Fisher) supplemented with 10% v/v of fetal bovine serum (FBS) (Sigma-Aldrich) and 1% v/v of penicillin-streptomycin (P/S). Cells were kept in an ice box before stimulation.

2.6 Isolation of mononuclear cells from human peripheral blood

Blood was extracted from healthy donors and collected in heparin treated sterile tubes. The study was approved by the National Research Ethics Committee and written consent was obtained in all cases.

Isolation procedure was carried out in a biosafety cabinet and guidelines of aseptic technique were followed to ensure sterile handling of human samples.

Equal volume of HBSS was added to the blood and mixed by inverting the tube several times. 15 ml of diluted blood sample was carefully layered onto 10 ml of Ficoll-Paque. The rest of isolation procedure was carried out as described in ***2.5***.

2.7 Primary tonsillar MNCs culture and stimulation

All procedures were done in a biosafety cabinet and guidelines of aseptic technique were strictly followed.

Complete medium was prepared by supplementing RPMI 1640 medium with 10% v/v of FBS and 1% v/v of P/S and used for *in vitro* culture of primary tonsillar MNCs.

Following MNC isolation, cells were washed with DPBS by centrifuging at 400 g for 5 min. Supernatant was removed, and the cell pellet was loosened by tapping the tube bottom. Cells were then resuspended with appropriate amount of cold complete medium. Cell numbers were counted using a hemocytometer with properly diluted cell suspension. Cell concentration was adjusted to 4×10^6/ml before seeding cells in culture plate. For 48-well plate and 96-well plate, cells were seed at 500 µl/well and 250 µl/well respectively.

The protein concentration of bacterial CCS was adjusted to 0.1 mg/ml by diluting with complete medium. Cells were stimulated by adding 5 µl of 0.1 mg/ml CCS to each well of cells in 48-well plate to make the final concentration of CCS at 1 µg/ml. 10× concentrated THB media was used to treat control cells. The outer wells of the culture plate were not used for cell culture but filled with appropriate amount of sterile water to minimize edge effect.

Cells were cultured at 37°C with 5% of CO_2 for 48 hours to detect memory T cell responses.

In some experiments, cells were treated with 100 ng/ml of recombinant IL-35 (R&D system) and IL-10 (PeproTech) respectively in order to examine the suppressive effects of IL-35 and IL-10 on memory T cell responses. The lyophilized human IL-35 Fc chimera protein was reconstituted at 100 µg/ml in DPBS and then diluted to 10 µg/ml with complete RPMI 1640 medium. The 10 µg/ml of IL-35 solution was aliquoted into 50 µl aliquots and stored in -70°C freezer. To maintain the biological activity of IL-35, it was ensured that all the aliquots used had undergone no more than two freeze-thaw cycles. Recombinant human IL-10 was reconstituted at 100 µg/ml in DPBS and aliquoted into 5 µl aliquots, stored in -70°C freezer.

The 100 μg/ml of IL-10 solution were further diluted to 10 μg/ml with complete medium before use.

Positive control cells were treated with 20 ng/ml of phorbol 12-myristate 13-acetate (PMA) and 1 μg/ml of Ionomycin for 4 hours before terminating the culture. PMA and Ionomycin both were purchased from Sigma-Aldrich.

2.7.1 Treatment of MNCs with IL-35-conditioned medium

Expression plasmids containing genes encoding human EBI3 (pRP-Neo-hEBI3) and IL-12A (pRP-Puro-hIL12A) were constructed by VectorBuilder. Plasmids were introduced into CHO cells using Lipofectamine3000 (Invitrogen) cell transfection kit. Successful transfectants were selected and expanded via G418 and puromycin double selection. Co-expression of human EBI3 and IL-12A in transfected clones was confirmed by Western blotting. The heterodimeric EBI3/IL-12A (IL-35) secretion was detected by co-immunoprecipitation and Western blotting. IL-35-expressing CHO cell clones and control CHO cells were cultured in a comparable cell density. The cell culture medium collected at 48hrs was used as conditioned medium to test the biological function of native IL-35 in this study.

IL-35-conditioned medium was aliquoted into 200 μl aliquots and stored in -70°C freezer. When used to treat cells, 5 μl, 10 μl and 50 μl of IL-35-conditioned medium was supplemented in 500 μl of cells to make the concentration at 1%, 2% and 10% respectively. Equal volume of conditioned medium harvested from control CHO cells were added to another set of cell cultures as media controls. The cells were stimulated with bacterial CCS and cultured for 48 hours.

2.7.2 IL-10 neutralization

In IL-10 neutralization experiment, cells were treated with 1μg/ml of LEAF™ purified anti-human IL-10 or rat IgG1κ isotype ctrl antibody (BioLegend) and stimulated with bacterial CCS for 48 hours.

2.8 Magnetic cell sorting

All antibody-labelled magnetic beads and separation columns were purchased from Miltenyi Biotec.

2.8.1 Direct magnetic labelling (CD25, CD45RO and CD4 microbeads)

The separation buffer was prepared by supplementing DPBS with 0.5% of BSA.

By calculating separated cells required for the experiment, a starting cell number can be estimated taking into account the proportion of intended cell population within total MNCs and cell loss during isolation process. MNCs were washed and resuspended in appropriate amount of buffer (80 µl of buffer was added per 10^7 total cells). Cells were labelled by adding 20 µl of antibody-conjugated magnetic beads per 10^7 total cells, followed by incubation at 4°C for 15 min.

Following labelling, cells were washed by adding 1-2ml of buffer per 10^7 total cells and centrifuging at 400 g for 5 min. During centrifugation, LS column was set up on a magnetic separator and rinsed with 2 ml of buffer. After washing, cells were resuspended in 500 µl of buffer for up to 10^8 cells. For higher cell numbers, the buffer volume was scaled up accordingly. The cell suspension was applied onto the column, and unlabelled cells that passed through were collected in a Universal tube. The column was washed with 2 ml of buffer for 3 times, and the effluent was collected in the same tube. New buffer was added only when the column reservoir was empty.

To elute magnetically labelled cells, the column was removed from the separator and placed in a new Universal tube, followed by pipetting 5 ml of buffer onto the column and pushing the plunger into the column to flush out those cells.

2.8.2 Indirect magnetic labelling (CD69 microbead kit II)

To separated $CD69^+$ cells from the MNCs, cells were first labelled with Biotin-conjugated anti-CD69 antibody by adding 10 µl of CD69-Biotin to 10^7 cells suspended in 40 µl of buffer and incubating at 4°C for 15 min. Then, 20 µl of Anti-Biotin microbeads and 30 µl of buffer were added per 10^7 cells, followed by a further incubation of 15 min at 4°C. Following the two-steps labelling, cells were washed and separated with LS column as described in ***2.8.1***.

2.9 CFSE cell proliferation assay

Carboxyfluorescein succinimidyl ester (CFSE) is a fluorescent dye that can be activated by 488 nm laser and the emissions are detected by the 530/30 filter, the same filter for fluorescein isothiocyanate (FITC). CFSE is cell permeable and able to covalently bind to intracellular amino acids. Following each cell division, CFSE fluorescence is also halved within daughter cells. Thus, each generation of cells is represented by an individual peak on the flow cytometry histogram, as shown in ***Figure 2.1***.

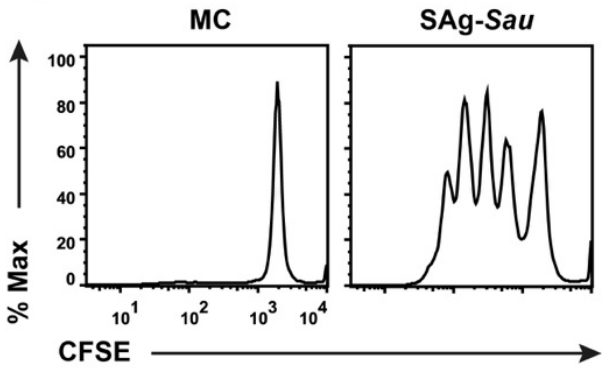

Figure 2.1 The dividing cycles of CFSE-labelled cells

CFSE labelled cells were cultured with or without SAg-*Sau* CCS for 5 days, followed by staining with anti-human CD4 antibody and acquiring data on the flow cytometry machine. The histogram plots are gated on $CD4^+$ T cells, showing the median fluorescent intensity (MFI) of the CFSE signals. The left plot showing one single peak indicates the media control (MC) cells were not proliferated. SAg-*Sau* stimulated $CD4^+$ T cells are shown in the right plot with 4 more separate peaks to the left of the X-axis, representing cells that have undergone 1, 2, 3 and 4 dividing cycles, from right to the left, respectively.

Stock CFSE solution was prepared by reconstituting a vial of lyophilized CellTrace™ CFSE (Life technologies) with 18 µl of DMSO. The stock solution was stored in -20°C and protected from light.

Cells were washed with DPBS before staining with CFSE. To stain 10^8 cells, 2.5 µl of the stock solution was diluted in 5 ml of DPBS, making the CFSE concentration at 2.5 µM. After washing, cells were resuspended in the 5 ml of CFSE solution and incubated at 37°C for 8 min in the dark.

Following incubation, at least 5 volumes of complete RPMI 1640 medium were added to the cells to absorb any unbound dye, followed by centrifuging at 400 g for 5 min. Then, supernatant was removed, and cells were resuspended in appropriate amount of complete medium.

CFSE stained cells were cultured and stimulated with bacterial CCS for 5 days, followed by harvesting cells for cell surface staining before acquiring on the flow cytometry machine.

2.10 Th17 cell induction

$CD45RO^+$ memory T cells were removed from tonsillar MNCs by magnetic cell sorting as described in ***2.8.1***. $CD45RO^+$ T cell-depleted MNCs were resuspended in appropriate amount of complete medium. Cell numbers were adjusted to 4×10^6 cells/ml.

Polarizing cytokines used to assist Th17 cell differentiation were IL-1β, IL-21 and TGF-β1. All three recombinant proteins were purchased from R&D System. Recombinant human IL-1β and IL-21 were reconstituted at 50 µg/ml and 100 µg/ml in DPBS respectively. Recombinant human TGF-β1 was reconstituted at 20 µg/ml in sterile 4mM HCl containing 1 mg/ml of BSA. After reconstitution, recombinant proteins were aliquoted into 5 µl aliquots and stored in -70°C freezer. The reconstituted TGF-β1 was further diluted to 2 µg/ml with DPBS.

1 µl of IL-1β (50 µg/ml), 0.5 µl of IL-21 (100 µg/ml) and 0.5 µl of TGFβ1 (2 µg/ml) were added per ml of cells. Thus, 50 ng/ml of IL-1β and IL-21, plus 2 ng/ml of TGFβ1 were supplemented in $CD45RO^+$ T cell-depleted MNCs. Cells were then seeded to 48-well plate and stimulated with 50 ng/ml of *Sau*-CCS for 7 days. In some experiments, cells were treated with 10 ng/ml of recombinant IL-35 at day 0 and day 3 in order to examine the suppressive effect of IL-35 on SAg-*Sau*-induced Th17 differentiation.

Cell culture supernatant was collected at day 7. 20 ng/ml of PMA, 1 µg/ml of Ionomycin and 1 µl/ml of brefeldin A were added to cells in the last 4 hours if cells were harvested for flow cytometry staining.

2.11 Flow cytometry staining

All antibodies used for flow cytometry staining are listed in ***table 2.2***.

2.11.1 Cell surface staining

The staining buffer was prepared by supplementing PBS with 0.02% of bovine serum albumin (BSA).

Cell culture supernatant was collected before harvesting cells for staining. After removing 400 µl of culture supernatant, 500 µl of staining buffer was added to the cells. Cells were suspended by gently drawing them in and out of a pipette tip, and cell suspensions were collected in a 1.5 ml Eppendorf tube.

Cells were pelleted by centrifuging at 400 g for 5 min. The supernatant was discarded, and the cell pellet was loosened by a brief vortex before resuspending cells with 500 µl of staining buffer and centrifuge again. Supernatant was poured off, followed by briefly blotting the tube on paper towel to remove excess liquid, leaving an approximately 20 µl of buffer in the tube with the cell pellet. Cells were properly suspended in the remaining buffer before adding antibody solutions.

The concentration of antibodies used are either titrated previously or as per manufacturer's instructions. 30 µl of antibody master mix was added to each sample, e.g. 5 µl of BV421-anti-human CD4 (Biolegend), 5 µl of Alexa Fluor 647-anti-human CD3 (BD Biosciences) and 20 µl of staining buffer was mixed for each sample. Thus, up to 2×10^6 cells were stained in 50 µl of staining buffer with antibodies at appropriate concentrations. Cells with antibodies were incubated at 4°C for 30 min.

Following staining, cells were washed with 1ml of staining buffer by centrifuging at 400 g for 5 min. If no further intracellular staining was required, cells were resuspended in 400 µl of staining buffer and filtered through nylon mesh to remove cell clumps. Stained cells were acquired on a flow cytometry machine.

2.11.2 Intracellular cytokine staining

For intracellular cytokine staining, the cells were treated with 1 µl/ml of brefeldin A (eBioscience) for 4 hours before terminating the culture in order to block cytokine secretion.

Cells were harvested and stained with cell surface antibodies as described in ***2.11.1***. After washing cells with staining buffer, cell pellet was properly loosened before resuspended in 100 µl of IC fixation buffer (eBioscience). Cells were fixed by incubating at RT for 30 min, in the dark.

The 10× permeabilization buffer (eBioscience) was diluted with distilled water to make 1× working solution. After fixation, cells were permeabilized by directly adding 1 ml of 1× permeabilization buffer. Permeabilized cells were pelleted by centrifuging at 600 g for 5 min. Cells were washed again with 1× permeabilization buffer before staining with intracellular antibodies. An approximately 20 µl of buffer was remained to suspend cells after removing supernatant.

Intracellular antibody master mix was prepared and added to the cells as it was described for cell surface antibodies. Cells with antibodies were incubated at RT for 30 min, in the dark.

Stained cells were washed by topping up with permeabilization buffer and centrifuging. After washing, cells were resuspended in 400 µl of staining buffer and filtered before acquiring on a flow cytometry machine.

2.11.3 Foxp3/transcription factor staining

Cells were harvested and stained with cell surface antibodies as described in ***2.11.1***.

Fixation/permeabilization buffer was prepared by mixing 1 part concentrate with 3 parts diluent. The Foxp3/transcription factor staining buffer set was purchased from eBioscience.

After washing cells with staining buffer, 350 µl of the fixation/permeabilization buffer was added to the cells to fix and permeabilize cells simultaneously, followed by incubation at RT

for 30 min in the dark. By doing so, both cell membrane and nuclear membrane were properly permeabilized to allow antibodies for transcription factors to enter the nuclear.

Following fixation and permeabilization, cells were washed by directly adding 1 ml of 1× permeabilization buffer and centrifuged at 1000 g for 5 min. Cells were washed again before staining with intracellular antibodies.

Intracellular antibody master mix was prepared and added to the cells the same as it was described for cell surface staining. Cells with antibodies were incubated at RT for 30 min, in the dark.

Stained cells were washed with 1× permeabilization buffer and then resuspended in 400 µl of staining buffer.

If an intracellular cytokine was stained together with Foxp3/transcription factor, the Foxp3/transcription factor staining protocol was followed.

Table 2.2 Fluorescence-activated cell sorting (FACS) antibodies

FACS antibody	Clone	Manufacturer	Isotype control
Alexa Fluor 647 mouse anti-human CD3	UCHT1	BD Biosciences	Alexa Fluor 647 mouse IgG1 κ
PE-Cy5 mouse anti-human CD4	RPA-T4	BD Biosciences	PE-Cy5 mouse IgG1 κ
Alexa Fluor 488 mouse anti-human Foxp3	259D/C7	BD Biosciences	Alexa Fluor 488 mouse IgG1 κ
PE mouse anti-human IL-17A	N49-653	BD Biosciences	PE mouse IgG1 κ
PE rat anti-human IL-10	JES3-19F1	BD Biosciences	PE rat IgG2a κ
Alexa Fluor 647 mouse anti-human IL-17A	SCPL1362	BD Biosciences	Alexa Fluor 647 mouse IgG1 κ

PE-Cy7 mouse anti-human CD4	SK3	BD Biosciences	PE-Cy7 mouse IgG1 κ
Alexa Fluor 647 mouse anti-human Foxp3	259D/C7	BD Biosciences	Alexa Fluor 647 mouse IgG1 κ
BV421 mouse anti-human GARP	7B11	BD Biosciences	BV421 mouse IgG2b κ
PE anti-human CD4	RPA-T4	BioLegend	PE mouse IgG1 κ
BV421 anti-human CD4	RPA-T4	BioLegend	BV421 mouse IgG1 κ
PerCP/Cy5.5 anti-human CD4	RPA-T4	BioLegend	PerCP/Cy5.5 mouse IgG1κ
PE mouse anti-human CD39	TU66	BD Biosciences	PE mouse IgG2b κ
Alexa Fluor 488 mouse anti-human IL-17A	N49-653	BD Biosciences	Alexa Fluor 488 mouse IgG1 κ
PE mouse anti-human IL-17A	SCPL1362	BD Biosciences	PE mouse IgG1 κ
Alexa Fluor 488 anti-human IFNγ	4S.B3	BioLegend	Alexa Fluor 488 mouse IgG1 κ
PE mouse anti-human RORγt	Q21-559	BD Biosciences	PE mouse IgG2b κ
FITC anti-human CD4	RPA-T4	BioLegend	FITC mouse IgG1 κ
Alexa Fluor 488 anti-human Ki-67	Ki-67	BioLegend	Alexa Fluor 488 mouse IgG1 κ
Pacific Blue anti-human CD4	RPA-T4	BioLegend	Pacific Blue mouse IgG1 κ
Pacific Blue 488 anti-human IFNγ	4S.B3	BioLegend	Pacific Blue mouse IgG1 κ
Alexa Fluor 488 anti-human CD3	OKT3	BioLegend	Alexa Fluor 488 mouse IgG2a κ
BV421 rat anti-human GM-CSF	BVD2-21C11	BD Biosciences	BV421 rat IgG2a κ
BV421 rat anti-human CD210a (IL-10RA)	3F9	BD Biosciences	BV421 rat IgG2a κ
Human IL-23R APC-conjugated	218213	R&D Systems	APC mouse IgG2b

2.12 Flow cytometry machine setup

Stained cell samples were acquired using BD FACSCanto II or BD FACSCelesta.

2.12.1 Isotype controls and compensation setup

To exclude nonspecific staining and justify the gate for the positive cell population, cells were stained with the specific antibodies and corresponding isotype control antibodies respectively at the first time of staining.

For a staining panel that contains antibodies conjugating with fluorochromes that have overlapped emission spectra, a spillover could occur if the fluorescence emission of one fluorochrome is detected by a detector that is designed to detect the signal of another fluorochrome. In this circumstance, compensations were set up to correct the spillover and ensure accurate interpretation of the data.

Unstained cells and single colour stained cells were prepared for compensation setup. For the staining panel containing antibodies conjugating with FITC, PE, PerCP and APC, compensation controls were prepared as listed in ***Table 2.3***.

Table 2.3 Staining for compensation controls

Tube 1	Unstained cells
Tube 2	Cells stained with FITC conjugated antibody
Tube 3	Cells stained with PE conjugated antibody
Tube 4	Cells stained with PerCP conjugated antibody
Tube 5	Cells stained with APC conjugated antibody

To ensure a proper positive population being presented, antibodies targeting highly expressed proteins by the cells were used for the compensation setup.

To set up compensations in BD FACSDiva software, *Create Compensation Controls* was chosen, and samples were acquired accordingly. The unstained cells were firstly acquired to gate out the desired cell population. The gate was then applied to all following compensation controls. Forward scatter (FSC) and side scatter (SSC) voltages were adjusted to display the cell population properly. Single colour stained cells were acquired accordingly, and voltages of all fluorescent parameters were optimized in order to place the negative and positive population appropriately in the plot. After recording all compensation control tubes, *Calculate Compensation* was chosen, followed by naming the compensation setup and linking it to the experiment's cytometer settings.

2.12.2 Running samples with BD FACSDiva software

A new experiment was created and named after logging into the software. In the cytometer settings of the experiment, fluorochromes that were not included in the staining panel were deleted. A new specimen was created under the named experiment, and tubes were added under the specimen. In the *Global Work Sheet*, appropriate plots were created for previewing the data when acquiring samples.

The *flow rate* was set to *low* or *medium* speed when adjusting settings. The unstained sample was first loaded and acquired for a few seconds, followed by adjusting voltages for FSC and SSC to make sure cell populations are in scale and displayed appropriately in the plot. The desired cell population, e.g. P1, was gated out, followed by setting the *stopping gate* on P1 and changing the *events to record* to a number you desired in the acquisition setup. Then, by acquiring a stained sample, voltages for fluorochrome parameters were adjusted to ensure that the negative and positive populations were in scale and separated properly.

After optimizing voltages for all parameters, samples were recorded accordingly. All recorded data was exported and analysed using Flowjo software.

2.13 Enzyme-linked immunosorbent assay (ELISA)

Cell culture supernatant was collected in 1.5-ml Eppendorf tubes and stored in -20°C before measurement of cytokine concentrations by ELISA.

Capture antibody was diluted in 5 ml of 1× coating buffer as noted on the Certificate of Analysis (C of A) or as labelled on the antibody vial, followed by coating a Corning ELISA plate (Appleton Woods) with 50 µl/well of diluted capture antibody using a multichannel pipette. The plate was sealed and incubated overnight at 4°C.

The 5× ELISA/ELISPOT Diluent was diluted with distilled water to make 1× working solution. The ELISA washing buffer was prepared by supplementing PBS with 0.05% v/v of Tween 20 (Sigma-Aldrich).

The capture antibody solution was discarded before washing the plate on a plate washer equipped with ELISA washing buffer. The plate was washed for 3 times, followed by adding 100 µl/well of the 1× ELISA/ELISPOT Diluent to block unspecific protein bindings in later steps. The plate was sealed and incubated for 2 hours at RT.

Protein standard was reconstituted and diluted as noted on C of A. Cell culture supernatant was diluted with 1× ELISA/ELISPOT Diluent to make the concentration of analyte that by estimation is within the range of the standard curve.

After blocking, the plate was washed for 3 times, and residual buffer was removed by tapping the plate on paper towels. 50 µl/well of the standard was added to appropriated wells, and 2-fold serial dilutions of the top standards was performed to make the standard curve, followed by adding 50 µl/well of diluted samples. Both standard and samples were added in duplicate. The plate was incubated with samples overnight at 4°C for maximal sensitivity.

Detection antibody was diluted in 5 ml of 1× ELISA/ELISPOT Diluent as noted on C of A. After discarding samples, the plate was washed for 5 times before adding 50 µl/well of diluted detection antibody using a multichannel pipette. Again, the plate was sealed and incubated for 1 hour at RT.

The plate was washed for 5 times after incubating with detection antibody. The detection antibody is biotin conjugated, thus properly diluted Avidin-HRP was added to wells (50 µl/well) in order to link horseradish peroxidase (HRP) to specifically captured proteins for later detection. The plate was incubated with Avidin-HRP for 30 min at RT.

Following Avidin-HRP incubation, the plate was washed for at least 5 times to ensure complete removing of the reagent. Then, 50 µl/well of 1× TMB solution was added to each well. 3,3',5,5'-Tetramethylbenzidine (TMB) is chromogenic substrate for HRP, which causes the solution to take on a blue colour. The plate was incubated in the dark for an approximately 15 min to allow colour development.

50 µl of Stop Solution (2N H_2SO_4) was added to each well to end colour development, which turned TMB to yellow. Plate was then read at 450 nm using ELISA microplate reader. The concentrations of the analyte in samples were determined by the standard curve constructed from 2-fold serial diluted protein standards.

2.14 Cytometric Beads Array (CBA)

CBA is a fluorescent bead-based multiplex assay which allows simultaneous quantification of multiple target analytes using flow cytometry. The Human Th Cytokine Panel (13-plex) kit was purchased from BioLegend. Beads of this kit can be distinguished by size and internal fluorescence (Allophycocyanin, APC), thus different bead set can be identified based on FSC, SSC and APC. Each set of beads are conjugated with a specific antibody to capture the target analyte in samples. By further labelling the captured analyte with biotin-conjugated detection antibody and streptavidin-PE, the amount of the analyte can be reflected by the intensity of

PE signal. This assay was used to measure cytokine concentrations in the culture supernatant of tonsillar MNCs.

2.14.1 Assay procedure

All reagents were removed from the fridge and allowed to warm to RT before use. The 20× stock solution was diluted in distilled water to make 1× Wash Buffer. The top standard C7 (10,000 pg/ml) was defrosted, and 4-fold serial dilution was performed with Assay Buffer provided to obtain standards C6 (2500 pg/ml), C5 (625 pg/ml), C4 (156.3 pg/ml), C3 (39.1 pg/ml), C2 (9.8 pg/ml), C1 (2.4 pg/ml). Assay Buffer only was used as C0 (0 pg/ml).

The pre-mixed beads were well suspended by vortexing for 1 min. 25 µl of Assay Buffer was added into each tube, followed by adding 25 µl/tube of standards or samples respectively. 25 µl/tube of pre-mixed beads and detection antibodies were added subsequently. The beads bottle was shaken intermittently to avoid bead settling. The tubes were then covered with foil and incubated on a shaker with the shaking speed set at 1000rpm for 2 hours at RT. Then, 25 µl/tube of streptavidin-PE was added directly, and tubes were incubated for a further 30 min at RT.

Following incubation, tubes were centrifuged at 1000 g for 5 min to pellet beads. Supernatants were removed completely, followed by washing the beads with 200 µl of 1× Wash Buffer. After washing, beads were resuspended in 200 µl of 1× Wash Buffer and acquired on the flow cytometry.

2.14.2 Flow cytometry setup on BD FACSCanto II

After logging into FACSDiva software, a new experiment was created and parameter FSC, SSC, FITC, PE and APC was kept in the cytometer setting. The Raw Beads provided in the kit were used to set up the PMT settings.

The Raw Beads were properly suspended by vortexing for 30 seconds, followed by transferring 400 µl of the beads to a FACS tube. The *flow rate* was set to *low*, and the Raw Beads were acquired. The voltages of FSC and SSC were adjusted to display populations of Beads A and Beads B appropriately in the plot as shown in ***Figure 2.2 a***. The voltage for FITC parameter was also adjusted to place the majority of beads between 1×10^1 to 1×10^2 for FITC signal (***Figure 2.2 b***). Then Beads A and Beads B populations were gated out, and two dot plots were created with PE for X-axis, APC for Y-axis, and gated on Beads A and Beads B respectively. By adjusting voltages for APC and PE, majority of beads were displayed between 1×10^1 to 1×10^2 for PE signal, and 1×10^2 to 5×10^4 for APC signal (***Figure 2.2 c, d***). After optimizing voltages for all parameters, samples were then recorded accordingly. The number of beads recorded was set to about 300 per analyte.

All recorded data was exported and analysed using LEGENDplex™ Data Analysis Software.

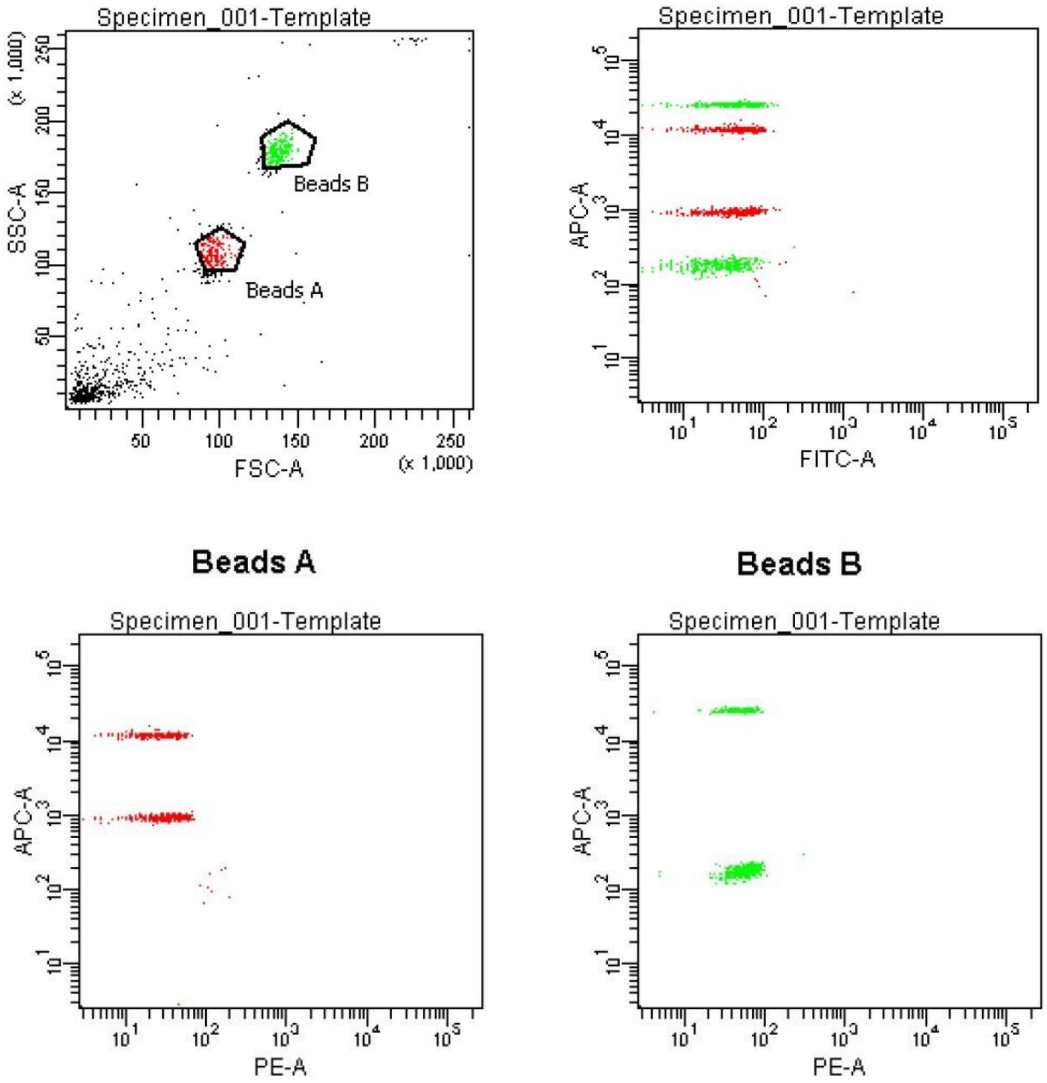

Figure 2.2 Cytometric settings on Canto II FACSDiva for CBA detection

The Raw Beads were acquired on the flow cytometry machine. The voltage of parameter FSC-A, SSC-A, FITC-A, PE-A and APC-A were adjusted as indicated in the above paragraph to put the Beads A and Beads B population in the position shown in the dot plots. This figure is cited from the Manual of LEGENDplex™ Human Th Cytokine Panel.

2.15 Quantitative reverse transcription PCR (RT-qPCR)

2.15.1 mRNA extraction

The RNeasy Mini Kit was purchased from Qiagen for mRNA extraction.

1×10^6 to 5×10^6 of Tonsillar MNCs or isolated $CD4^+$ T cells was pelleted by centrifuging at 400 g for 5 min, followed by completely removing the supernatant. The RLT lysis buffer was freshly supplemented with 1% v/v β-mercaptoethanol (β-ME) to eliminate ribonuclease released during cell lysis. Cell pellet was loosened by flicking the tube before adding 350 µl of RLT lysis buffer to the cells. Cell lysate was frozen in -70°C before the mRNA extraction.

Ribonuclease (RNase) can be found in air, most surfaces and dust. To avoid exposing isolated RNA to surrounding RNase during isolation and the following reverse transcription procedures, the benchtop and surroundings were carefully cleaned with 1% distel, and special precautions were taken when processing samples.

Cell lysates were removed from -70°C freezer and defrosted in 37°C water bath. Once defrosted, cell lysates were immediately removed from the water bath and kept in an ice box. Cell lysate was homogenized by transferring into a QIAShredder spin column and centrifuging at full speed of the microcentrifuge for 2 min. The volume of lysate after homogenization was measured, and then 1 volume of 70% ethanol was added to the homogenized lysate and mixed well by pipetting. Up to 700 µl of sample was transferred to an RNeasy spin column, and centrifuged at ≥ 8000 g for 15 seconds. The flow-through was discarded, followed by adding 700 µl of RW1 buffer to the column and centrifuging again at ≥ 8000 g for 15 seconds. The RPE buffer was prepared by adding appropriate amount of ethanol before use. The column was then washed twice with 500 µl of RPE buffer and the flow-through was discarded following each wash. After washing steps, the column was carefully removed from the old collection tube and placed in a new 2 ml collection tube. The column in the new collection tube was centrifuged at full speed for 1 min to eliminate any possible carry-over of the RPE buffer. Then, the RNeasy spin column was placed in a new 1.5 ml collection tube, and 30 µl of RNase-free water was added directly to the spin column membrane. The column was centrifuged at

≥ 8000 g for 1 min to elute the RNA bound to the column membrane. Isolated RNA samples were kept in an ice box.

The concentration and purity of isolated RNA was measured using NanoDrop spectrophotometer by dropping 2 µl of the RNA sample onto the pedestal. The OD at 260 nm equals 1.0 for a 40 µg/ml RNA solution, thus the RNA concentration in the solution was determined by the reading at OD_{260}. Pure RNA has an OD_{260}/OD_{280} ratio of approximately 2.0.

2.15.2 Reverse transcription

First-strand cDNA was synthesized from the isolated RNA by reverse transcription using Moloney Murine Leukemia Virus Reverse Transcriptase (M-MLV RT) (Promega). All other reagents required for the synthesis were also from Promega. RNA samples and all reagents were placed on ice throughout the procedure. RNase-free water was used for dilution of reagents.

10 mM dNTPs was prepared by mixing and diluting 50 µl of dATP, dCTP, dGTP and dTTP (100 mM) in 300 µl of RNase-free water. 40 u/µl of Recombinant RNasin Ribonuclease Inhibitor was diluted to 25 u/µl, and 500 ng/µl of Random Primers was diluted to 50 ng/µl.

A total 1 µg of RNA was used for the first-strand cDNA synthesis. 1 µl of Random Primers (50 ng/µl) was added to 1 µg of RNA in a total volume of 15 µl RNase-free water in a PCR microtube, followed by heating at 70°C for 5min using a PCR machine. Following the heating, samples were cooled down immediately on ice to prevent reforming of secondary structure.

Volumes of reagents required for a 25 µl reaction was listed in ***Table 2.4***. The reaction master mix was prepared by mixing these reagents with volumes required for total reactions intended. 10 µl of the master mix was added to 15 µl of the pre-heated RNA sample, followed by incubating the reaction tube at 37°C for 1 hour in a PCR machine. Synthesized cDNA sample was kept in -20°C freezer before used for qPCR reaction later.

Table 2.4 Reagents for RT master mix

Reagents	Volume for one reaction (µl)
5× M-MLV Reaction Buffer	5
dNTPs (10 mM)	1
RNasin Ribonuclease Inhibitor (25 u/µl)	1
M-MLV RT (200 u/µl)	1
RNase-free water	2
Total	**10**

2.15.3 Quantitative polymerase chain reaction (qPCR)

The mRNA expressions of targeted genes were detected by SYBR-based quantitative PCR using SYBR® Green JumpStart™ *Taq* ReadyMix™ (Sigma-Aldrich). This 2× qPCR ReadyMix contains *Taq* polymerase, SYBR Green I and dNTPs in $MgCl_2$ buffer. The SYBR Green I stain preferentially binds to double-strand DNA enabling the detection of DNA copies amplified by the thermostable *Taq* polymerase.

Gene-specific primers were designed using the '*Primer-Blast*' tool provided on the website of National Centre for Biotechnology Information (NCBI) and then synthesized by Sigma-Aldrich. All primers used were listed in ***Table 2.5***. The lyophilized primers were reconstituted at 100 µM in nuclease-free water, and then further diluted to 10 µM. The cDNA samples were 1:10 diluted in nuclease-free water and used as template in the qPCR reaction. Other components for a 20µl qPCR reaction were mixed as listed in ***Table 2.6***.

Table 2.5 qPCR Primers

Gene	Primers		T_m (°C)	Product size (bp)
Human *il12a* NM_000882	Forward	5'-TGCCTTCACCACTCCCAAAACCTGCTGA-3'	70.0	154
	Reverse	5'-ATGGTAAACAGGCCTCCACTGTGCTGGT-3'	69.6	
Human *ebi3* NM_005755.2	Forward	5'-AAACTCCACCAGCCCCGTGTCCTTCATT-3'	69.9	161
	Reverse	5'-CGGTGACATTGAGCACGTAGGGAGCCAT-3'	70.1	
Human *il23r* NM_144701.2	Forward	5'-GGTGGCAGCCTGGCTCTGAAGTGGAATTA-3'	70.0	193
	Reverse	5'-GGTTCTACCCAGATGTGGCCAGAGCAGTT-3'	69.6	
Human *il17ra* NM_014339.6	Forward	5'-ACCTTAAAGGGTGCTGTCGCCACCAAGT-3'	70.0	181
	Reverse	5'-AGCAGGATGGAGATGCCCGTGATGAACC-3'	70.0	
Human *b-actin* NM_001101.5	Forward	5'-GCTCACCATGGATGATGATATCGCCGC-3'	67.7	199
	Reverse	5'-GATGCCTCTCTTGCTCTGGGCCTCGTC-3'	70.2	
Mouse *il17a* NM_010552.3	Forward	5'-CCAGCTGATCAGGACGCGCAAACATGAG-3'	69.7	115
	Reverse	5'-TGAGGGATGATCGCTGCTGCCTTCACTG-3'	70.1	
Mouse *il12a* NM_001159424.2	Forward	5'-TTCCAGGCCATCAACGCAGCACTTCAGA-3'	70.2	196
	Reverse	5'-TGAAGGCGTGAAGCAGGATGCAGAGCTT-3'	70.3	
Mouse *ebi3* NM_015766.2	Forward	5'-GCCTCCTAGCCTTTGTGGCTGAGCGAAT-3'	70.3	133
	Reverse	5'-GAGAAGATGTCCGGGAAGGGCCAGGAAG-3'	69.8	
Mouse *b-actin* NM_007393.5	Forward	5'-TTCTTTGCAGCTCCTTCGTTGCCGGTC-3'	69.5	199
	Reverse	5'-CCTTCTGACCCATTCCCACCATCACACC-3'	68.6	

Table 2.6 Components for qPCR reaction

Components	Volume for one reaction (µl)
2× SYBR® Green JumpStart™ *Taq* ReadyMix™	10
Forward primer (10 µM)	0.4
Reverse primer (10 µM)	0.4
Nuclease-free water	5.2
Total	**16**

Depending on total reactions intended for each target gene, volumes of these components were calculated and then mixed to make the master mix for qPCR reactions. 16 µl of the master mix was added to a 96-well PCR plate. Without touching the master mix down in the bottom, 4 µl of 1:10 diluted cDNA sample was added on the inner wall of the well. The plate was sealed and briefly centrifuged to mix the cDNA sample with the master mix. All reactions were made in duplicate. The PCR plate was run in Bio-Rad CFX Connect™ Real-Time PCR machine with cycling parameters set as following (***Table 2.7***).

If only target gene was specifically amplified, a single sharp peak at the melting temperature (T_m) of the amplified gene fragments would be shown in the Melting Curve (***Appendix 1***). The quantitative cycle (Cq) is the number of cycle when the accumulated fluorescence from SYBR Green bound DNA copies is detected above the base level. The Cq value of the target gene was normalized to the Cq of *b-actin* housekeeping gene and translated into fold changes of mRNA expression levels against control samples using Delta-Delta-Ct (ddCt) Algorithm.

Table 2.7 qPCR step protocol

Step 1	94°C for 2:00 min
Step 2	94°C for 0:15 min
Step 3	63°C for 0:20 min
Step 4	72°C for 0:20 min + Plate read
Step 5	GOTO Step 2, 39 more times
Step 6	Melt Curve 75°C to 95°C, increment 0.5°C
	0:05 min + Plate read
Step 7	4°C Hold

2.16 DNA gel electrophoresis

Amplified DNA fragments from the qPCR reaction were examined by agarose gel electrophoresis to ensure the qPCR products are the same size as the predicted gene fragment.

To make a 1.5% agarose gel, 1.05 g of agarose was suspended in 70 ml of TBE buffer in a flask followed by microwaving for 1-3 min until the agarose was completely dissolved. The agarose solution was cooled to 55°C approximately before adding 7 µl of SYBR® Safe DNA gel stain (10,000× concentrated in DMSO) and mixing well by swirling the flask. The SYBR safe binds to the DNA and allows it to be visualized using an imager. The agarose solution was then poured into a gel tray, and a well comb was inserted immediately. The new poured gel was left at room temperature for 20-30 min until it was completely solidified.

The agarose gel was placed into the gel box (electrophoresis unit), followed by filling the box with TBE buffer until the gel was covered. The well comb was removed to expose loading

wells. The 100 bp DNA ladder (New England BioLabs) was loaded into the first and last lanes of the gel. The rest of wells were loaded with qPCR products mixed with the Loading Buffer. By connecting the electrodes of the gel box to a power pack, the gel loaded with DNA samples was run at 100 V for 45-60 min. The DNA is negatively charged and runs towards the positive electrode. The Loading buffer added to the DNA samples contains visible dye showing the migration of DNA in the gel during electrophoresis. It also has a high percentage of glycerol that increases the density of the DNA sample, making it settle down to the bottom of the gel well.

The agarose gel could be equally divided into 2 sections by inserting 2 parallel combs. Once the DNA samples had run nearly half way through the gel, the power was turned off, and the agarose gel was carefully removed from the gel box for DNA imaging using Bio-Rad ChemiDoc^{TM} XRS+ System.

The DNA fragments of human *Il12a*, *Ebi3*, *Il23r*, *Il17ra*, *b-actin* and mouse *Il12a*, *Ebi3*, *Il17a*, *b-actin* following qPCR are shown in ***Appendix 1***.

2.17 Western Blotting

2.17.1 Sample preparation

Tonsillar MNCs with or without stimulation were separated into $CD4^+$ T cells and $CD4^-$ MNCs by magnetic cell sorting as described in ***2.8***. The purity of isolated $CD4^+$ T cells (>96%) was confirmed by FACS staining with anti-CD3 and anti-CD4 antibodies (***Appendix 2***). To ensure enough amount of protein for later detection, at least 2×10^6 of isolated cells were resuspended in 50-100 µl of clear lysis buffer (CLB) which was kindly provided by Dr. Ziqi Lin, and lysed on ice for 20 min. To prevent protein degradation, the CLB was freshly supplemented with protease inhibitor cocktail (Sigma-Aldrich) before use, and lysate samples were kept in cold condition for the subsequent processing. The cell lysate was sonicated for 3×5 seconds and then centrifuged at 10,000 g for 30 min with a temperature of 4°C to pellet cell debris and DNA fragments. Following centrifuging, the supernatant was carefully

transferred to a new Eppendorf tube. Samples were stored in -70°C freezer if not used on the same day.

2.5 µl of the protein sample was diluted 10 times in distilled water for the measurement of protein concentration using Pierce BCA Protein Assay Kit. 40 µg of each protein sample was mixed with 1/3 sample volume of 4× Laemmli sample buffer (Bio-Rad) before heating at 95°C for 5 min. The 4× Laemmli sample buffer was freshly supplemented with 10% v/v of β-ME which helps to break the disulfate bonds in the protein. Following heating, the samples were centrifuged at 10,000 g for 1 min.

2.17.2 Polyacrylamide gel electrophoresis (PAGE) and Blotting

The 4-15% Mini-PROTEAN® TGX™ Precast Protein Gels and 10× Tris/Glycine/SDS running buffer were purchased from Bio-Rad.

The precast gel was placed into a gel tank filled with 1× running buffer, and the well comb was removed carefully. Equal amount of protein samples (40 µg) were loaded into the wells. By connecting the tank to a power pack, the gel was run at 100 V constantly for 90 min approximately. The CLB and running buffer both contain SDS that denatures protein and coats the protein with a uniform negative charge. Thus, proteins in the sample run towards the positive electrode and separated based on their molecular weight (MW).

The proteins were transferred from the gel to a PVDF membrane using Trans-Blot Turbo Transfer System with Trans-Blot® Turbo™ Mini PVDF Transfer Pack (Bio-Rad). Once completing the electrophoresis, the gel was trimmed appropriately and carefully transferred onto the PVDF membrane which is layered on top of the anode stack, followed by placing the cathode stack on the gel. Any air bubble in the assembled transfer pack was removed using a blot roller. The stack with the gel and membrane was then lifted from the tray and placed in the centre of the cassette withdrawn from a Trans-Blot Turbo instrument. The cassette was closed firmly before slid back to the instrument. The transfer pack was run under a pre-programmed '*Mixed MW*' protocol.

2.17.3 Antibody labelling and protein imaging

The 10× Tris buffered saline (TBS) was diluted with distilled water and supplemented with 0.1% v/v of Tween 20 to make TBST washing buffer.

Following blotting, the membrane was instantly immersed in 5% w/v skim milk in TBST and incubated on an orbital shake (110 revs/min) at RT for 2 hours to block unspecific protein bindings in later steps. Then, the membrane was briefly rinsed and incubated in the primary antibody solution against target protein on the shake (110 revs/min) at 4°C, overnight. The primary antibody was diluted in antibody diluent (Life technologies) accordingly (Table 8).

On the following day, the membrane was washed with TBST for 5 × 5 min with the shaking speed set to 150-200 revs/min before incubating with HRP-conjugated secondary antibody solution for 1 hour at RT, also on the shaker (110 revs/min). Anti-Rabbit IgG secondary antibody or Mouse IgG kappa binding protein (m-IgGκ BP) was used depending on the host species used to generate the primary antibody. The secondary antibody was diluted accordingly using 5% w/v skim milk in TBST (***Table 2.8***). After incubation with secondary antibody, the membrane was washed again with TBST for 5 × 5 min with the shaking speed set to 150-200 revs/min. The Clarity Western ECL Substrate (Bio-Rad) was prepared as per manufacturer's instruction and then applied to the membrane, followed by capturing the chemiluminescent signals using the Bio-Rad ChemiDoc™ XRS+ System.

Table 2.8 Western Blot antibodies

Antibodies		Manufacturer	Stock concentration	Dilution
Primary antibody	Anti-IL-12/IL-35 p35 antibody (Clone 27537)	R&D	0.5 mg/ml	1:500
	Anti-IL-27/IL-35 EBI3 antibody (Clone A15058A)	BioLegend	0.5 mg/ml	1:500
	β-Actin antibody (C4)	Santa Cruz	200 µg/ml	1:1000
Secondary antibody	m-IgGκ BP-HRP	Santa Cruz	400 µg/ml	1:5000
	Mouse anti-rabbit IgG-HRP	Santa Cruz	400 µg/ml	1:5000

2.18 Co-Immunoprecipitation (Co-IP)

IL-35 is a heterodimer protein consisting of IL-12p35 and EBI3 subunits. To detect IL-35 heterodimer, the M-280 sheep anti-mouse IgG Dynabeads (Thermo Fisher) was incubated with the protein sample and anti-IL12p35 antibody to capture the target heterodimer protein, followed by eluting the target protein from the beads and immunoblotting with anti-EBI3 antibody.

2.18.1 Co-IP in cell culture supernatant

The cell culture supernatant was collected and centrifuged at 400 g for 5 min to remove residual cells. 1.5 µg of anti-IL-12/IL-35 p35 (Clone 27537) antibody was added to 1 ml of culture supernatant and incubated with gentle rotation at 4°C for 1-2 hours.

Dynabeads in the vial were suspended properly by vortex for 1 min. 50 µl of Dynabeads was used for each sample, which contains approximately 3×10^7 beads. Appropriate amount of Dynabeads were transferred to a 5 ml FACS tube and washed twice with 1 ml RPMI 1640 medium using EasySep™ Magnet (STEMCELL). The beads were resuspended in the same

volume of medium as the initial volume of beads. Then, 50 µl of beads were added to the culture supernatant pre-incubated with anti-IL-12/IL-35 p35 antibody and incubated overnight with gentle rotation at 4°C.

On the following day, the culture supernatant with Dynabeads was transferred to a 5 ml FACS tube, followed by washing the beads twice with 1 ml of cold DPBS. The beads were then resuspended with 30 µl of cold RIPA buffer (Sigma-Aldrich) and transferred to an Eppendorf tube. Appropriate amount of 4× Laemmli sample buffer supplemented with 10% v/v β-ME was added to the beads, followed by heating the beads at 100°C for 10 min to elute the target protein from the beads. The beads were pelleted by centrifuging at 10,000 g for 5 min with a temperature of 4°C, and the supernatant containing eluted protein was carefully collected for detection of EBI3 subunit by Western Blot as described in ***2.17.2*** **and** ***2.17.3***.

2.18.2 Co-IP in cell lysate

The tonsillar MNCs were stimulated with SAg-*Sau* CCS for 48 hours, and the Brefeldin A was added to the cells 4 hours before harvesting cells. 1×10^8 cells were harvested for $CD4^+$ T cell isolation by magnetic cell sorting as described in ***2.8.1***. The number of isolated $CD4^+$ T cells was counted, and 1×10^7 cells were transferred to a new Universal tube and centrifuged at 400 g for 5 min. The supernatant was removed completely, and cell pellet was loosened by flicking the tube. 1 ml of RIPA buffer without SDS and supplemented with protease inhibitors was added to the cells, followed by incubating on ice for 30 min to lyse the cells completely. The cell lysates were sonicated for 3 × 5 seconds on ice before centrifuging at 10,000 g for 30 min with a temperature of 4°C to remove cell debris and DNA fragments. Following centrifuging, the supernatant was carefully collected for Co-IP.

The Co-IP procedure described in ***2.18.1*** was followed for the detection of IL-35 heterodimer in the $CD4^+$ T cell lysis. However, RIPA buffer instead of RPMI 1640 medium and DPBS was used for Dynabeads calibration and washing.

2.19 Luciferase assay for the detection of active TGF-β

2.19.1 Transformed Mink Lung Cells (TMLCs)

TMLC is a luciferase-fused TGF-β reporter cell line, which was kindly provided by Dr Mark Travis from the University of Manchester. TGF-β is secreted in a latent form which requires further processing to release active TGF-β. The TMLCs were transfected with an expression construct containing a truncated plasminogen activator inhibitor-1 (PAI-1) promoter fused to the firefly luciferase reporter gene. Active TGF-β is able to induce the expression of PAI-1 in TMLCs, resulting in dose-dependently enhanced luciferase activity in the cell lysates which can be detected as increased relative light units (RLU) in the luciferase assay.

The TMLCs were revived and cultured with high-glucose Dulbecco's Modified Eagle Medium (DMEM) supplemented with 10% v/v of FBS, 1% v/v of P/S and L-glutamine in a T-75 flask. TMLC are adherent cells and requires digestion by trypsin when passaging cells. Cells were passaged when reaching 80-90% confluency. The cell culture supernatant was discarded, and the cells were washed with DPBS. 2 ml of trypsin-EDTA solution (Sigma-Aldrich) was added to the cells, gently tilting the flask to ensure cells were evenly covered with the solution. The flask was kept in the incubator at 37°C for 2-10 min until over 90% of cells were detached. 10 volumes of complete medium was added to the cell to inhibit trypsin activity, and cells were pelleted by centrifuging at 400 g for 5 min. Cells were then resuspended in complete medium and split 1:10 into new flasks. 1 mg/ml of Geneticin, also known as G418, was supplemented to the cell cultures to remove cells that have lost the transfected expression construct. The tonsillar MNCs were cultured in RPMI 1640 medium, thus the TMLCs were adapted to this culture medium before used for luciferase assay.

2.19.2 Luciferase assay

Cell culture supernatant was collected from tonsillar MNCs stimulated with bacterial CCS at different time points (Day 2, 3, 4, 5, 6) for the detection of active TGF-β produced by MNCs.

Culture medium supplemented with 2-fold serial diluted recombinant TGF-β1 (1000, 500, 250, 125, 62.5, 0 pg/ml) was used to test the functionality of the TMLCs and a standard curve correlating the level of TGF-β and luciferase activity (RLU) was produced as shown in ***Figure 2.3***.

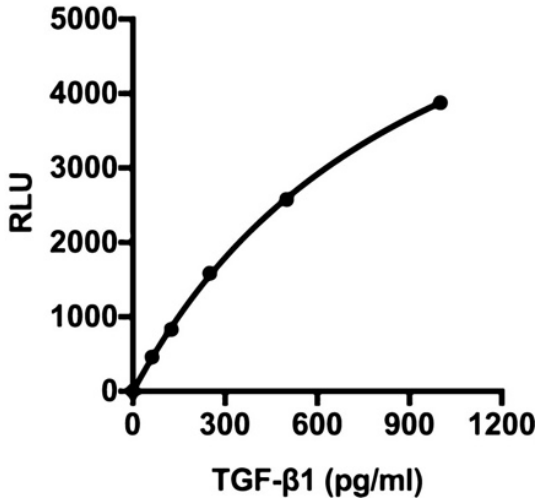

Figure 2.3 Standard curve for the correlation of luciferase activity (RLU) in the TMLCs and the concentration of active TGF-β1 in the media

TMLCs were suspended in complete DMEM, and the cell number was adjusted to 1×10^5 cells/ml. In a 96-well white plate (Thermo Fisher), 2.5×10^4 cells/well (250 µl) of TMLCs were seeded and cultured at 37°C with 5% of CO_2 in the incubator for 3 hours to allow the cells to attach. Once the cells were attached properly, the culture medium was carefully removed and replaced with the MNCs' culture supernatant mixed with equal volume of fresh culture medium. Cells were placed back to the incubator and cultured for 24 hours.

The Luciferase assay kit was purchased from Promega. Before detecting luciferase activity in TMLCs, the cell culture supernatant was completely removed, and the cells were carefully washed with DPBS in the culture plate. Then, 20 µl/well of 1 × lysis buffer (included in the kit)

was added to the cells and the cell culture plate was put into the FLUO STAR Omega Luminometer. A bottle containing Luciferase assay reagent was placed into the Luminometer, and the injector was set to add 100 µl/well of the reagent when reading the plate.

In some experiments, pre-attached TMLCs (4×10^4) were co-cultured with 5×10^5 of tonsillar MNCs and stimulated with bacterial CCS. At 48 hours, the MNCs were resuspended by gentle pipetting and then removed, followed by detecting Luciferase activity of the TMLC as described above.

2.20 Mouse nasal colonization model

2.20.1 Preparation of fresh *Sau* culture

An aliquot of *Sau* liquid stocks was removed from the -80°C freezer and defrosted at RT. The bacterial stock was prepared with bacterial suspension having an OD_{600} of 0.5 that equals to 1×10^8 CFU/ml approximately for the bacterial concentration.

For HIP07930 strain (NonSAg-*Sau*), the bacteria (1×10^8 CFU/ml) was diluted 1:10^6 in 10 ml of fresh THB media and cultured on an orbital shaker with a shaking speed of 230 revs/min for 12 hours at 37°C. 1×10^8 CFU/ml of FRI913 strain (SAg-*Sau*) was diluted 1:10^{10} in 10 ml of THB and cultured at the same conditions as HIP07930 strain.

Following culture, OD_{600} of the bacterial growth was measured to estimate the bacterial concentration. An approximately 1×10^9 CFU of bacteria was resuspended in 1 ml of sterile PBS for the intranasal infection in mice.

2.20.2 Mouse infection and tissue dissection

Female C57BL/6 mice aged 6-8 weeks were purchased from Charles River, UK. Mice were maintained in individually ventilated cages at 22 ± 1°C and 65% humidity with a 12hr light-dark cycle. Prior to use, mice were acclimatised for one week with free access to food and

water. Mice were lightly anaesthetised with O_2/isoflurane and were infected intranasally with 10^7 CFU of *Sau* in 10µl PBS or PBS only for control group mice. 3 infected mice were sacrificed at day 12 post infection to confirm clearance of primary infection, following which mice were re-infected with *Sau* at the same dose at day 14 post primary infection. Mice were then culled at 24hrs post secondary infection to assess the nasopharyngeal bacteria load and $CD4^+$ T cell responses in the cervical lymph nodes (CLNs). All experimental protocols were approved and performed in accordance with the regulations of the Home Office Scientific Procedures Act (1986), project licence P86De83DA and the University of Liverpool Ethical and Animal Welfare Committee.

The nasopharyngeal tissue was removed and homogenised in 3ml of sterile PBS before plating out on blood agar for assessment of tissue CFU. The CLNs were dissected for the isolation of lymphocyte.

2.21 Isolation of MNCs from murine cervical lymph nodes

Lymph nodes dissected from 3 mice were pooled together for MNC isolation. The lymph nodes were collected in HBSS and kept on the ice before the isolation procedure. A 70 µm cell strainer was inserted into the well of a 6-well plate filled with 8 ml of HBSS which should be sufficient to cover the mesh of the cell strainer. The lymph nodes were transferred onto the mesh and ground using the plunger of a 5 ml syringe to release MNCs. The cell strainer was then moved to an adjacent well, and the cell suspension was filtered again through the cell strainer and transferred to a Universal tube. Cell number of the isolated MNCs were determined, followed by centrifuging cells at 400 g for 5 min and resuspending in appropriate amount of separation buffer for magnetic cell sorting.

$CD4^+$ T cells were isolated from the MNCs as described in ***2.8.1*** and per manufacturer's instructions (Mouse CD4 (L3T4) Microbeads, Miltenyi). The purity of isolated $CD4^+$ T cells (>96%) was confirmed by FACS staining with anti-CD3 and anti-CD4 antibodies (***Appendix 2***).

2.22 Statistical analysis

Data distribution was tested using D'Agostino-Pearson or Shapiro-Wilk normality tests and results were then analysed accordingly with paired *t*-test (two-tailed) or unpaired *t*-test (two-tailed). Data that were not normally distributed was log-transformed before performing parametric *t*-tests or analysed using Wilcoxon matched-pairs signed rank test (two-tailed). The association between fold increase in Th17 and Th17 inhibition by IL-35 was analysed using linear regression. All data were analysed in Prism 7 software. Data displayed are mean ± SEM for column bar graphs and grouped line plots. For data shown as box and whiskers, median (centre line), upper and lower quartile (box limits) and minimum to maximum range (whiskers) are displayed. Asterisks denote *p*-value ($^{*}p$ <0.05, $^{**}p$ <0.01, $^{***}p$ <0.001, $^{****}p$ <0.0001). *p*-value < 0.05 were considered significant. n.s. means not significant.

CHAPTER 3

Staphylococcus aureus activates Th17 and Treg responses in human nasopharynx-associated lymphoid tissue

3.1 Abstract

Staphylococcus aureus (*Sau*) is a frequently identified colonizer in human nasopharynx, and its colonization has been associated with relapse/exacerbation of inflammatory and autoimmune diseases. However, little is known about the site-specific T cell-mediated immunity in response to nasal colonization of *Sau*. Pro-inflammatory Th17 cells and anti-inflammatory Foxp3$^+$ Tregs are two critical CD4$^+$ T cell subsets that are involved in the aetiology and pathogenesis of inflammatory/autoimmune conditions. By evaluating the local Th17 and Treg responses to *Sau* in nasopharynx-associated lymphoid tissue (NALT) in humans, it may help to identify underlying mechanisms for infection-induced autoimmunity.

In this study, *Sau*, especially superantigenic *Sau* (SAg-*Sau*), was shown to activate a potent Th17 response in tonsillar MNCs which was substantially higher than *Streptococcus pneumoniae* (*Spn*) and other commonly identified bacteria in the nasopharynx. An inverse correlation between Th17 and Treg responses was observed in *Spn*-stimulated tonsillar MNCs, indicating Treg-mediated suppression on Th17 responses. However, this inverse correlation was not found in the context of *Sau* stimulation even though the Treg population was largely expanded. Interestingly, *Sau* stimulation promoted IL-17A expression in Foxp3$^+$ Tregs which partially explained why *Sau*-activated Th17 and Tregs were not negatively associated. Further investigation on Treg-related suppression pathways demonstrated that despite increased production of active TGF-β and IL-10, the expression of CD39 on the Tregs was markedly downregulated by *Sau*. Human Tregs have been shown to require CD39 for their suppressive function against Th17 cells. This reduced proportion of CD39$^+$ Tregs following *Sau* stimulation may result in a deficient regulation of Th17 activation.

The results suggest *Sau* infection may impair Treg-mediated suppression on Th17 responses in the NALT, thus contributing to inflammatory/autoimmune pathogenesis through uncontrolled Th17 activation.

3.2 Introduction

The tonsils (palatine tonsils) are secondary lymphoid tissues located at the rear of the pharynx. As a major component of the mucosa-associated lymphoid tissue (MALT), tonsil sits at the entrance of upper respiratory tract and helps to protect the host from exogenous pathogens inhaled through the nasopharynx[105]. Frequently exposed to foreign antigens, tonsils are important induction sites for adaptive immune responses and contain a substantial repertoire of memory T cells, including both central memory and effector memory cells[106]. A markedly higher proportion of $CD4^+$ T cells (CD4/CD8 ratio > 5) is found in tonsils compared to the average CD4/CD8 ratio of around 2 in the peripheral blood and spleen[107]. The activation and regulation of $CD4^+$ T cell responses are of significant importance in fighting against pathogen infection but also in mediating inflammatory pathologies in the nasopharynx.

It has been shown that local immune responses have systemic effects and are able to influence specific organs at distal sites[108]. The gut segmented filamentous bacteria (SFB) induced Th17 cells are able to migrate into central nervous system, spleen and lung and provoke autoimmune pathogenesis in these organs as shown in animal models[47,48,108]. A clinical case report describing a patient of autoimmune Tourette syndrome with intermittent *Sau* nasopharyngeal carriage demonstrated that the local *Sau* colonization-induced immune activation cleared the bacterial infection but also induced a systemic autoimmune reactivation[109].

Sau-activated Th17 and Treg responses have been studied using human peripheral blood mononuclear cells (PBMCs)[14,110]. It is reported that SAg-*Sau* activates IL-17A production from memory T cells in PBMCs[14]. *Sau*-derived superantigen SEA is shown to induce $CD25^+Foxp3^+$ Tregs from $CD25^-$ cells in PBMCs, and these induced Tregs are capable of suppressing anti-CD3 activated T cell proliferation[111]. Compared to the peripheral blood, the NALT (refers to palatine tonsils in this study) has a different composition of immune cells and contains significantly higher frequency of antigen-experienced T cells, which has shaped the distinct immune environment of nasopharynx. Understanding of host-microbe interaction in the nasopharynx can shed light on the pathogenesis of infection-related diseases and provide new strategies for vaccine design. In this study, I explored the impact of *Sau*-derived antigens

on nasopharyngeal T cell responses, which could help to understand the underlying mechanisms of how nasal colonization of *Sau* contributes to the development of inflammatory diseases.

3.3 Aims

- To examine the capacity of *Sau* in activating Th17 responses in human NALT comparing to other common bacterial colonizers.
- To assess whether *Sau* stimulation affects the $Foxp3^+$ Treg population in human NALT.
- To evaluate Treg associated suppression pathways in *Sau* stimulated tonsillar MNCs.

3.4 Results and Discussion

T cell co-receptor CD3 is the cell surface marker to distinguish thymus-derived T cells from other lymphocytes. The helper T (Th) cells express anther co-receptor CD4 and can thereby be separated from the $CD8^+$ cytotoxic T (Tc) cells. Monocytes and macrophages also express low level of CD4, but they are generally excluded from the typical lymphocyte gate due to larger size and more granulated cell surface. Within the lymphocyte gate, a single $CD4^+$ cell population was identified in tonsillar MNCs, and this cell population also expressed CD3 indicating these cells were Th cells (***Figure 3.1 a***). Thus, CD4 staining only is sufficient to separate $CD4^+$ Th cells from tonsillar MNCs.

IL-17A is the signature cytokine expressed by Th17 cells, and Foxp3 is the transcription factor that governs the suppressive function of $Foxp3^+$ T regulatory cells (Tregs). In accordance with current knowledge, IL-17A and Foxp3 were primarily expressed by $CD4^+$ T cells in human tonsillar MNCs (***Figure 3.1 b, c***). The Th17 cells and Tregs in this study were gated as IL-$17A^+CD4^+$ and $Foxp3^+CD4^+$ cells respectively (***Figure 3.1 d***). The proportion of Th17 cells shown in this study indicates all IL-$17A^+CD4^+$ cells, including IL-$17A^+$ $Foxp3^+CD4^+$ cells, unless otherwise stated.

Concentrated culture supernatant (CCS) was prepared from bacterial cultures as described in ***2.2*** and used to stimulate MNCs isolated from human tonsillar tissue. The bacterial culture media, Todd Hewitt Broth (THB) supplemented with 0.5% w/v of yeast extract, was concentrated the same way as bacterial culture supernatant and used to treat cells as media control (MC).

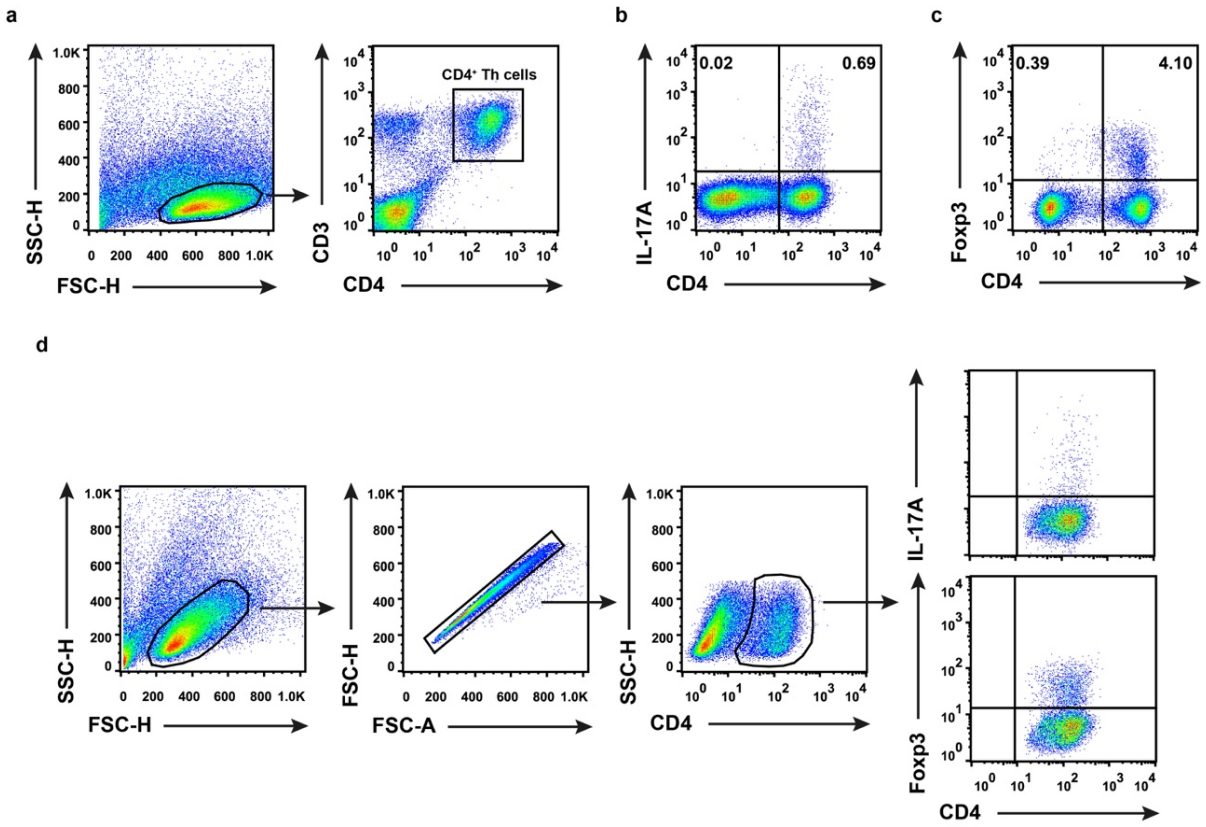

Figure 3.1 Gating strategies for Th17 cells and Foxp3⁺ Tregs

a) CD3 and CD4 double staining for tonsillar MNCs. Lymphocytes were gated out to show the Th cells which are $CD3^+CD4^+$ cells as indicated in the rectangular gate. **b)** IL-17A intracellular cytokine staining showing $CD4^+$ T cells are the primary source of IL-17A. Numbers in top left and right quadrants indicate the percentages of $IL\text{-}17A^+CD4^-$ cells and $IL\text{-}17A^+CD4^+$ cells (Th17 cells) in SAg-*Sau* stimulated tonsillar MNCs. **c)** Foxp3 intracellular nuclear transcription factor staining to identify $Foxp3^+CD4^+$ Treg population. Numbers in top left and right quadrants indicate the percentages of $Foxp3^+CD4^-$ cells and $Foxp3^+CD4^+$ cells (Tregs) in tonsillar MNCs. **d)** Lymphocytes were gated by FSC and SSC. After excluding doublets from the lymphocytes, $CD4^+$ T cells were gated to show $IL\text{-}17A^+CD4^+$ Th17 cells and $Foxp3^+CD4^+$ Tregs.

3.4.1 *Sau* activates a potent Th17 response in human NALT

Th17 cells are pro-inflammatory $CD4^+$ T cells that play a pivotal role in host defence against external microbes but also in the development of inflammatory disorders[37]. *Spn* and *Sau* are two commonly identified colonizers of human nasopharynx that drive inflammatory diseases, such as pneumonia and septicaemia. Extracted pneumococcal antigens from wild type D39 strain were able to activate memory Th17 cells in tonsillar MNCs shown by colleagues in our group[112]. Consistent with their finding, a modest increase in Th17 cells was detected in *Spn*-D39 stimulated MNCs, accompanied with enhanced production of IL-17A in the culture supernatant (***Figure 3.2 a, b***). I then examined whether pneumococcal carriage strains isolated from the nasal swabs were also capable of activating Th17 responses in tonsillar MNCs. As shown in ***Figure 3.2 c***, 3 out of 4 pneumococcal carriages strains (C6, C7, C8, C9) were capable of stimulating a Th17 response.

It has been reported that superantigen-producing *Staphylococcus aureus* (SAg-*Sau*) promotes IL-17 production from memory $CD4^+$ T cell in human PBMCs[14]. Located at the entry of the upper airway, tonsils are exposed to a large number of foreign antigens, and therefore contains a substantial amount of effector and memory T cells[106]. As expected, SAg-*Sau* (positive for *tsst*, *sea*, *sec* and *see*) stimulation produced a potent Th17 response in tonsillar MNCs. Interestingly, the NonSAg-*Sau* (negative for *tsst*, *sea*, *seb*, *sec*, *sed* and *see*) also activated a Th17 response, although it was significantly less than SAg-*Sau* stimulation (***Figure 3.3 a***). In line with the markedly increased proportion of Th17 cells, a high concentration of IL-17A in the cell culture supernatant was detected by ELISA upon SAg-*Sau* stimulation (***Figure 3.3 b***). To further assess the Th17 activation by clinical *Sau* strains, CCS prepared from 3 carriage strains (C1, C2, C3) isolated from the nasal swabs was used to stimulate tonsillar MNCs. Strong Th17 responses were detected for all three strains (***Figure 3.3 c***).

I have shown that superantigen-positive *Sau* strain activated a remarkably higher Th17 response compared to superantigen-negative strain. To examine whether this also applies to isolated carriage strains, the total SE (A-E) level in culture supernatant of the 3 carriage strains were measured. As expected, the C3 strain, which activated stronger Th17 responses than the other 2 carriage strains (C1 and C2), and NonSAg-*Sau* also produced higher level of SE

(A-E) (***Figure 3.3 d***). The results indicate a strong promoting effect by staphylococcal superantigens in Th17 activation.

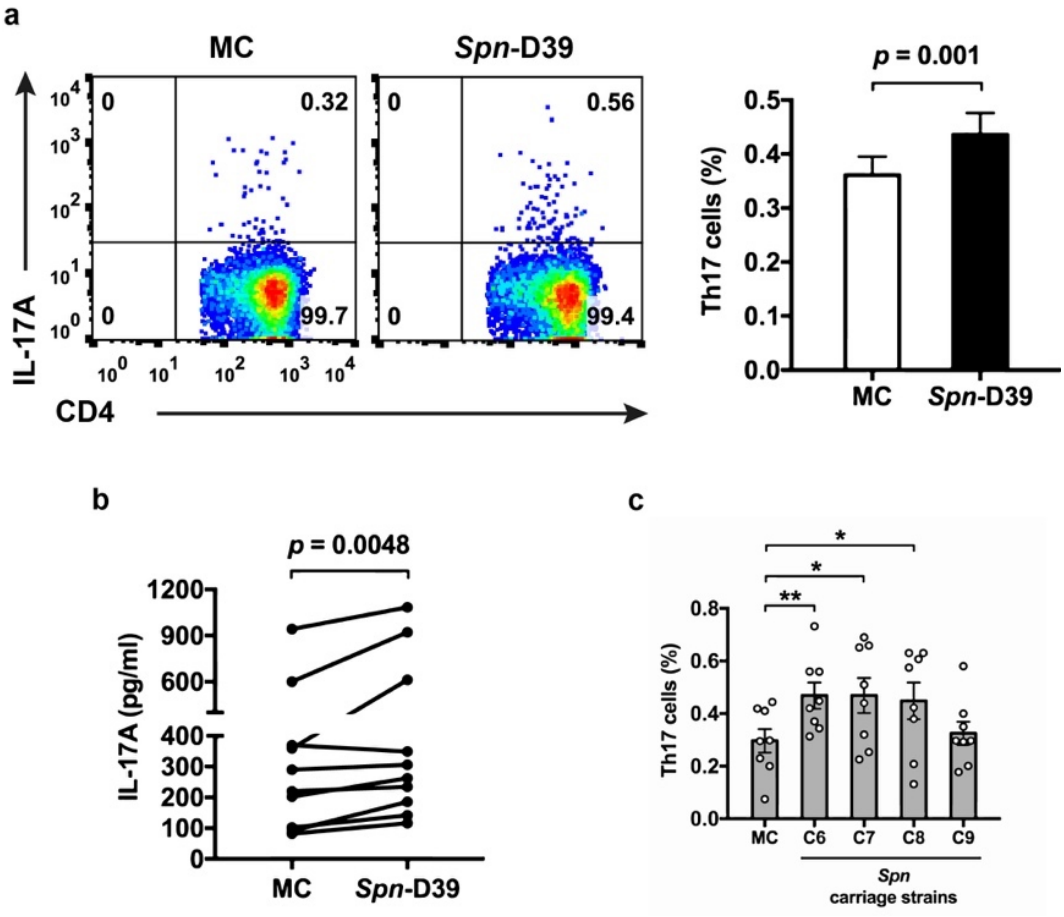

Figure 3.2 *Spn*-activated Th17 responses in tonsillar MNCs

Tonsillar MNCs were stimulated with 1 μg/ml of concentrated culture supernatant (CCS) from wild type D39 (serotype 2 *Spn* strain) for 48hrs, and the Th17 responses were analysed comparing to the media control (MC) cells. **a)** Dot plots were gated on $CD4^+$ T cells, and numbers in top right quadrants indicate the percentage of Th17 cells. Data displayed in the bar graph is mean ± SEM, n = 29. **b)** IL-17A concentration in the culture supernatant of MNCs measured by ELISA, n = 10. **c)** The Th17 responses activated by 4 carriage *Spn* strains isolated from nasal swabs. Mean ± SEM with individual data points are shown in the bar graph, n = 8. All data was analysed using paired *t*-test (*$p < 0.05$, **$p < 0.01$).

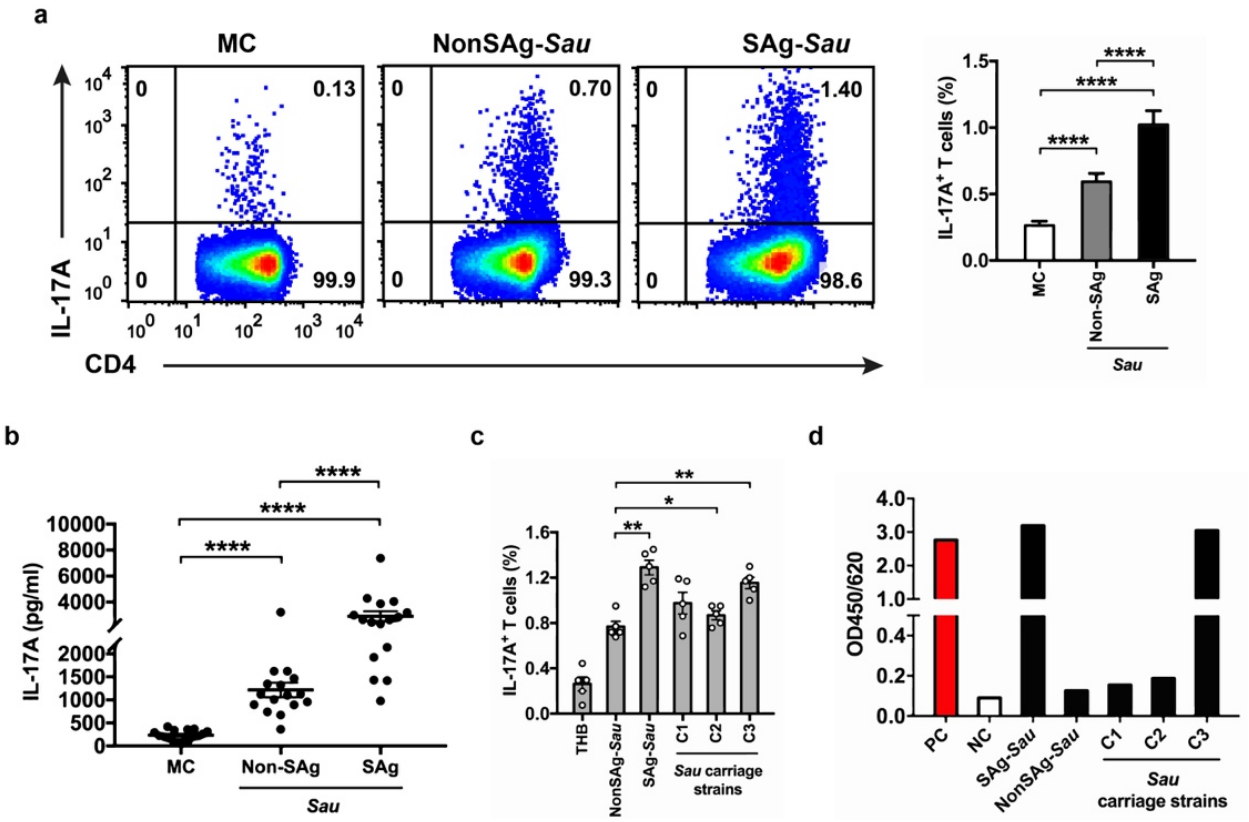

Figure 3.3 SAg-*Sau* activates a potent Th17 response in tonsillar MNCs

Tonsillar MNCs were stimulated with 1 µg/ml of CCS from NonSAg-*Sau* and SAg-*Sau* respectively for 48hrs, and Th17 responses were analysed. **a)** Dot plots were gated on $CD4^+$ T cells, and the percentage of Th17 cells is shown in top right quadrants. Mean ± SEM is displayed in the bar graph, n = 30. **b)** IL-17A concentration in the culture supernatant of CCS stimulated MNCs. Individual data points with mean ± SEM are shown in the scatter plot, n = 16. **c)** The Th17 responses activated by 3 carriage *Sau* strains were compared to NonSAg-*Sau* stimulated tonsillar MNCs. The percentages of Th17 cells (mean ± SEM) from different stimulation groups are shown in the scatter plot with bars, n = 5. **d)** Staphylococcal enterotoxin A-E levels in the culture supernatant of *Sau* strains. PC, positive control; NC, negative control. All data was analysed using paired *t*-test (*$p < 0.05$, **$p < 0.01$, ****$p < 0.0001$).

The Th17 activation by SAg-*Sau* was then compared with pneumococcal strains (D39, TIGR4) and other commensal colonizers, *M. catarrhalis* and coagulase-negative *Staphylococcus* (CNS-C4, C5), in individual MNCs. SAg-*Sau* stimulation consistently activated a remarkably higher Th17 response than the *Spn* strains, and no significant Th17 response was elicited by the other commensal bacteria tested (***Figure 3.4***).

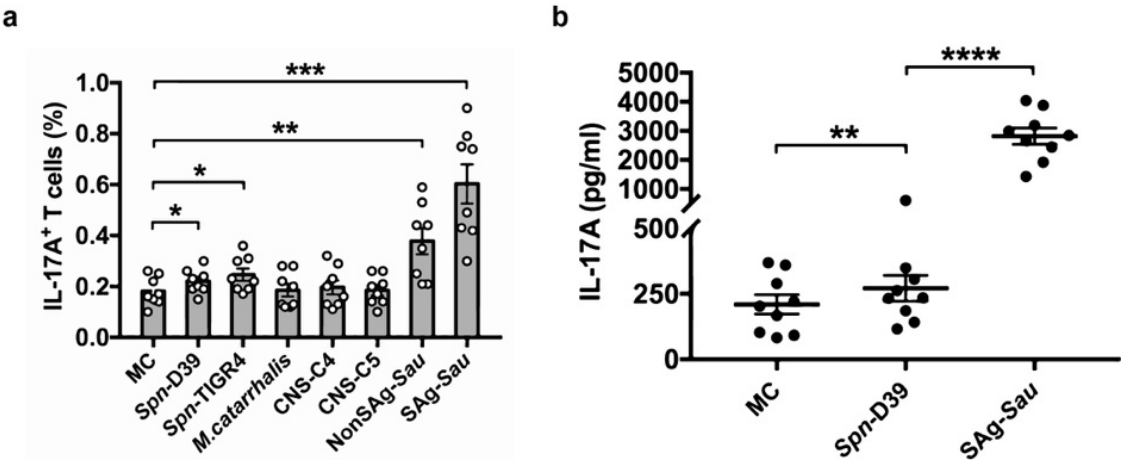

Figure 3.4 SAg-*Sau* activates a markedly higher Th17 responses than *Spn*

a) Tonsillar MNCs were stimulated with 1 μg/ml of CCS from *Spn*, *Sau*, coagulase negative *staphylococcus* (CNS) and *M. catarrhalis* respectively for 48hrs. The percentages of Th17 cells following stimulation were determined and shown as mean ± SEM in the scatter plot with bars, n = 8. **b)** IL-17A concentration in the culture supernatant of MNCs stimulated by *Spn*-D39 and SAg-*Sau* respectively. Mean ± SEM is displayed in the scatter plot, n = 9. All data was analysed using paired *t*-test (**p* < 0.05, ***p* < 0.01, ****p* < 0.001, *****p* < 0.0001).

The results demonstrate SAg-*Sau* is the major activator of Th17 responses in human NALT. Superantigen activates T cells through cross-linking MHC class II of the antigen-presenting cells with T cell receptor (TCR) V_β chains which is not restricted to antigen specificity[24]. The NonSAg-*Sau* strain used in this study also had the ability in activating effector and memory Th17 cells, suggesting the presence of staphylococcal antigen-specific memory Th17 cells in the NALT. However, it cannot be excluded that this NonSAg-*Sau* strain may produce some unknown toxins that have superantigenic properties.

Simultaneous colonization of *Spn* and *Sau* in the nasopharynx is uncommon, and one of the suggested underlying mechanisms is competing growth of these two bacteria. Interestingly, this exclusive colonization was not observed in HIV-infected individuals indicating host immunity also plays a role. Th17 activation-induced neutrophil influx is critical for the clearance

of pneumococcal colonization in the nasopharynx[53]. Although *Spn* itself is able to activate a mild Th17 response, it may not be sufficient for an efficient clearance. While SAg-*Sau* is introduced, the potent Th17 activation could help to remove the pneumococcal carriage in the nasopharynx.

SAg-*Sau*-activated Th17 responses in the host may also promote its own clearance. How strong the Th17 responses are activated can be individual-dependent, which may determine the duration of bacterial carriage. Notably, superantigen-activated T cell responses are shown to assist superantigenic *Streptococcus pyogenes* in the establishment of nasopharyngeal colonization at earliest stages by a recent study[113]. It is possible that SAg-*Sau*-activated Th17 responses can also be used by the bacteria to initiate its own colonization.

The biological effect of Th17 cells is largely attributed to its signature cytokine, IL-17A. IL-17A acts on structural cells, such as epithelia cells, fibroblasts and keratinocytes, to activate the NF-κB signalling pathway resulting in the production of inflammatory cytokines (e.g. IL-6 and G-CSF) and chemokines by these cells. Macrophages and neutrophils are recruited by the chemokines and further developed into pro-inflammatory phenotypes with enhanced ability in phagocytosis and generating highly active molecules including nitric oxide (NO) and reactive oxygen species (ROS), thereby clearing the invading pathogens and also initiating inflammatory pathologies.

In the presence of SAg-*Sau*, the NALT elicits a potent Th17 response which may promote bacterial clearance thereby protecting host against infection. Whether this defensive immunity is manipulated by the bacteria to facilitate its initial infection is yet to be elucidated. However, it is likely that this strong Th17 activation, if not controlled, may cause inflammatory tissue damage and present as a major risk for the development of inflammatory diseases.

3.4.2 *Sau* expands the Foxp3$^+$ Treg population in human NALT

Foxp3$^+$ Tregs have been intensively studied for their central role in maintaining immune tolerance to auto-reactive immune responses and resolving inflammations[114]. By sharing the

common TGF-β-mediated signalling pathway during differentiation, the development of Th17 cells and Foxp3$^+$ Tregs are reciprocally regulated and their phenotypes remain interchangeable in effector stage. Disturbed balance between these two cell populations has been implicated in various inflammatory/autoimmune diseases[115,116]. The Th17 activation was elicited by both *Spn* and *Sau* in tonsillar MNCs (***Figure 3.2, 3.3***), it was therefore of interest to examine whether Foxp3$^+$ Tregs in the NALT were responding to these colonizers.

Following stimulation, a significantly increased Treg population was detected in *Spn*-D39 treated tonsillar MNCs, as well as the other 4 carriage *Spn* strains (***Figure 3.5***). This result confirmed that *Spn* promotes Treg activation in order to persistently colonize the nasopharynx shown by previous studies[112,117].

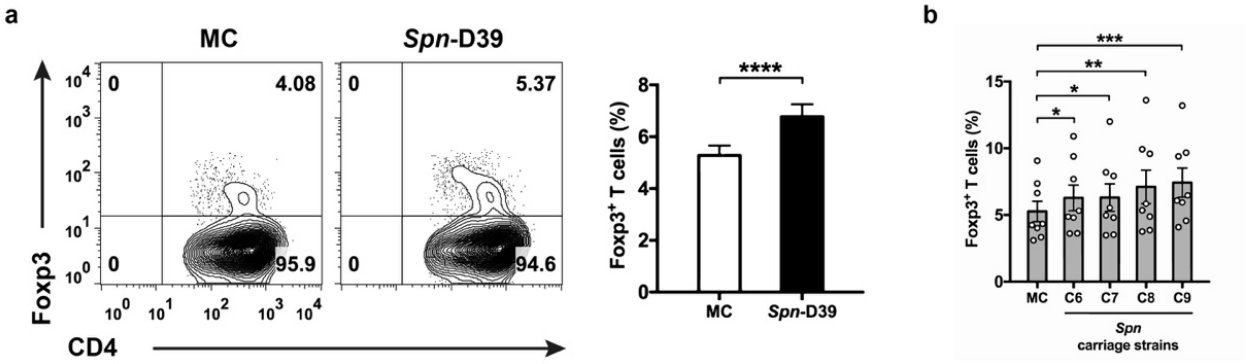

Figure 3.5 *Spn* promotes Foxp3$^+$ Treg population

Tonsillar MNCs were stimulated with *Spn* CCS (1 µg/ml) for 48hrs, and the Treg population was analysed. **a)** The contour plots were gated on CD4$^+$ T cells, and numbers in top right quadrants indicate the percentage of Foxp3$^+$CD4$^+$ cells. Treg proportions were summarised in the bar graph, n = 29. **b)** Bar graph with individual data points showing percentages of Tregs within CD4$^+$ T cells for tonsillar MNCs stimulated by 4 carriage *Spn* strains, n = 8. Data displayed is mean ± SEM.

Interestingly, the Foxp3$^+$ Treg cell population was largely expanded following *Sau* stimulation, and SAg-*Sau* was again more potent than NonSAg-*Sau* in expanding Tregs (***Figure 3.6 a***). This Treg expansion was also observed in MNCs activated by the 3 carriage strains. However, the superantigen-producing C3 strain was not the strongest one in stimulating Treg expansion

as it was shown for Th17 activation compared to the other 2 carriage strains that produced barely detectable enterotoxin A-E (***Figure 3.6 b***).

The Treg expansion stimulated by SAg-*Sau* was markedly higher than *Spn* which may be a negative regulation to counteract the potent Th17 activation by the host (Figure 6c). The commensal colonizers, *M. catarrhalis* and CNS, were not able to activate either Th17 or Tregs in the NALT (***Figure 3.4 a*** and ***Figure 3.6 c***).

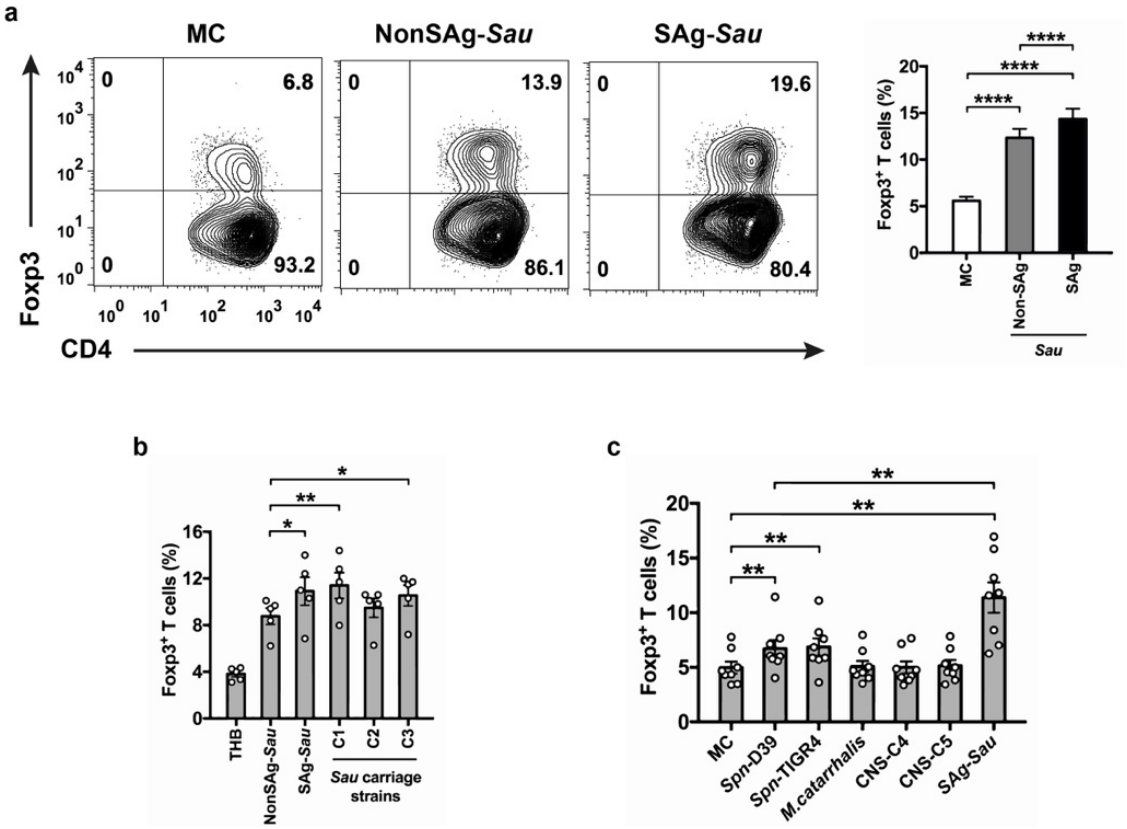

Figure 3.6 The Treg population is largely expanded by SAg-*Sau*

a) Tonsillar MNCs were stimulated with 1 µg/ml of NonSAg-*Sau* and SAg-*Sau* CCS respectively for 48hrs. Contour plots showing Foxp3$^+$ cells within CD4$^+$ T cells with percentages of the Treg population displayed in top right quadrants. The Treg percentages were summarised in the bar graph with mean ± SEM, n = 29. **b)** Percentages of Tregs within CD4$^+$ T cells in tonsillar MNCs stimulated by NonSAg-*Sau*, SAg-*Sau* and 3 carriage *Sau* strains. Mean ± SEM is displayed in the scatter plot with bars, n = 5. **c)** The Treg expansion in tonsillar MNCs stimulated with *Spn*, SAg-*Sau*, CNS and *M. catarrhalis* respectively. Percentages of Tregs (mean ± SEM) are shown in the scatter plot with bars, n = 8.

It has been reported that Foxp3$^+$ Tregs derived from human PBMCs are anergic to anti-CD3 stimulation but able to proliferate in response to staphylococcal superantigen[110]. Another study demonstrates that bacterial superantigens are able to induce Foxp3 expression in CD25$^-$CD4$^+$ T cells[111]. Therefore, the expanded Treg population following SAg-*Sau* stimulation is likely to contain both proliferated Tregs and freshly induced Tregs. Whether this expanded Treg population has retained suppressive functions requires further investigation.

3.4.3 The correlation of Th17 and Treg responses stimulated by *Spn* and *Sau* strains

An intriguing finding was revealed when I looked into the correlation of Th17 and Treg proportions stimulated by 5 *Spn* and 5 *Sau* strains respectively in two individual samples (S1 and S2). As shown in the ***Figure 3.7***, the MNCs stimulated by 5 *Spn* strains showed an inverse correlation between activated Th17 and Tregs which meant a *Spn* strain that was more potent in activating Tregs would have a lower Th17 response. This inverse correlation indicates suppression of Th17 responses by activated Tregs in *Spn* stimulated MNCs. In contrast to *Spn* stimulation, Th17 and Treg responses stimulated by 5 *Sau* strains were not negatively correlated but more towards a positive correlation, suggesting *Sau*-expanded Tregs were not able to suppress the highly activated Th17 responses.

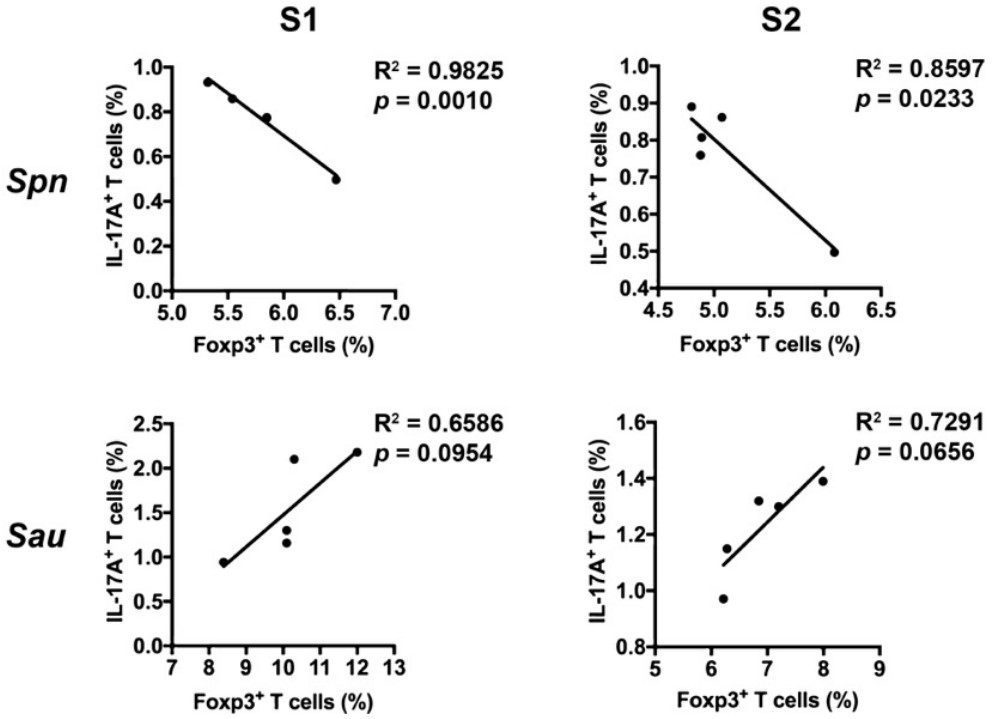

Figure 3.7 The correlation of Th17 and Treg responses in tonsillar MNCs stimulated by *Spn* or *Sau*

The tonsillar MNCs isolated from 2 individuals (S1 and S2) were stimulated with 5 *Spn* strains (D39WT, C6, C7, C8, C9) and 5 *Sau* strains (NonSAg-*Sau*, SAg-*Sau*, C1, C2, C3) respectively. At 48hrs, percentages of Tregs and Th17 cells within $CD4^+$ T cells were determined, and associations between these two cell populations activated by different *Spn* or *Sau* strains was analysed using linear regression. Each dot represents a bacteria strain. R^2 and *p* values are displayed.

3.4.4 SAg-*Sau* promotes IL-17A expression in Foxp3⁺ Tregs

In addition, an increased IL-17A expression was detected in the expanded Tregs following *Sau* stimulation, and this was more evident in SAg-*Sau* stimulated MNCs (***Figure 3.8***). Th17 cells and Tregs share the common TGF-β signalling for their initial differentiation which results in the interchangeable phenotype between these two $CD4^+$ T cell subsets at effector phase[116]. The existence of IL-17A-producing Tregs in human PBMCs and tonsillar MNCs has been reported by stimulating cells with PMA/ionomycin. However, it requires extra addition of certain cytokines, such as IL-2, IL-6 and IL-21, to induce IL-17A expression in these Tregs if

stimulated via TCR signalling (anti-CD3 and anti-CD28)[118]. Here, I show that SAg-*Sau* stimulation only was able to induce a substantial expression of IL-17A in Foxp3$^+$ Tregs. SAg-*Sau* stimulation enhanced the production of IL-6 and IL-2 in tonsillar MNCs (***Figure 3.9***), which may help to convert Tregs into Th17 cells and thereby promoting inflammations.

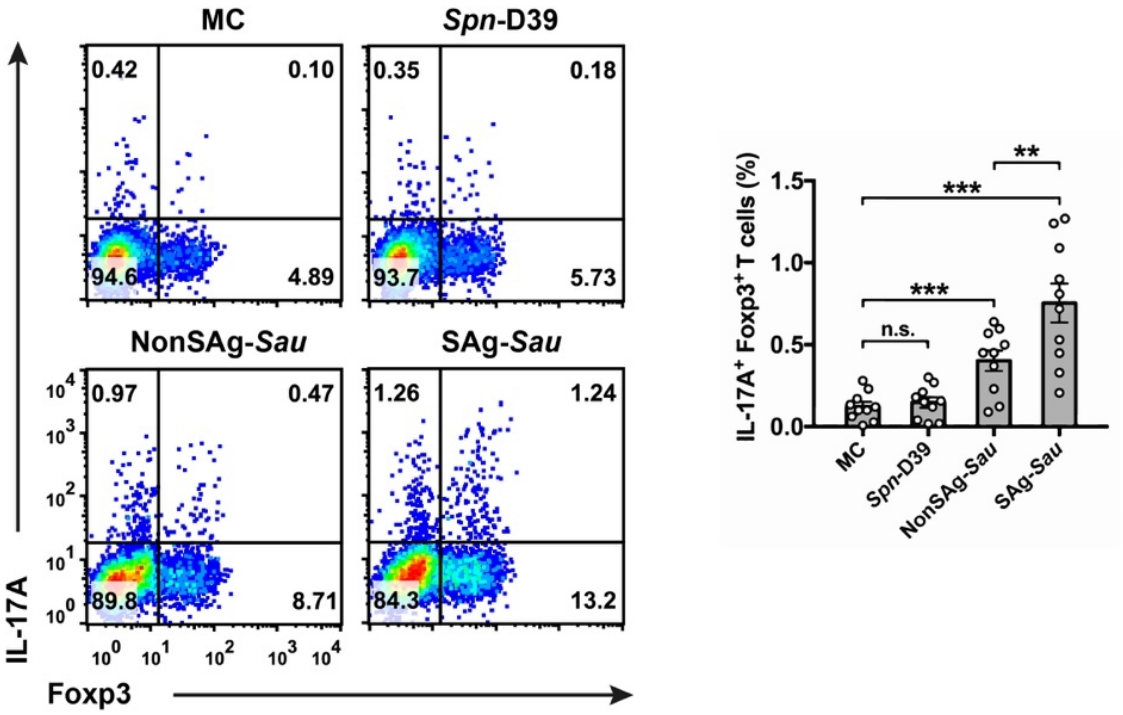

Figure 3.8 SAg-*Sau* promotes IL-17A expression in Foxp3$^+$ Tregs

Tonsillar MNCs were stimulated for 48hrs by *Spn* and *Sau* CCS respectively. The dot plots were gated on CD4$^+$ T cells showing IL-17A expression in Foxp3$^-$ and Foxp3$^+$ cells with numbers in top right quadrants indicating the percentage of IL-17A$^+$Foxp3$^+$ cells. Data was summarised (mean ± SEM) in the scatter plot with bars and analysed using paired *t*-test, n = 10.

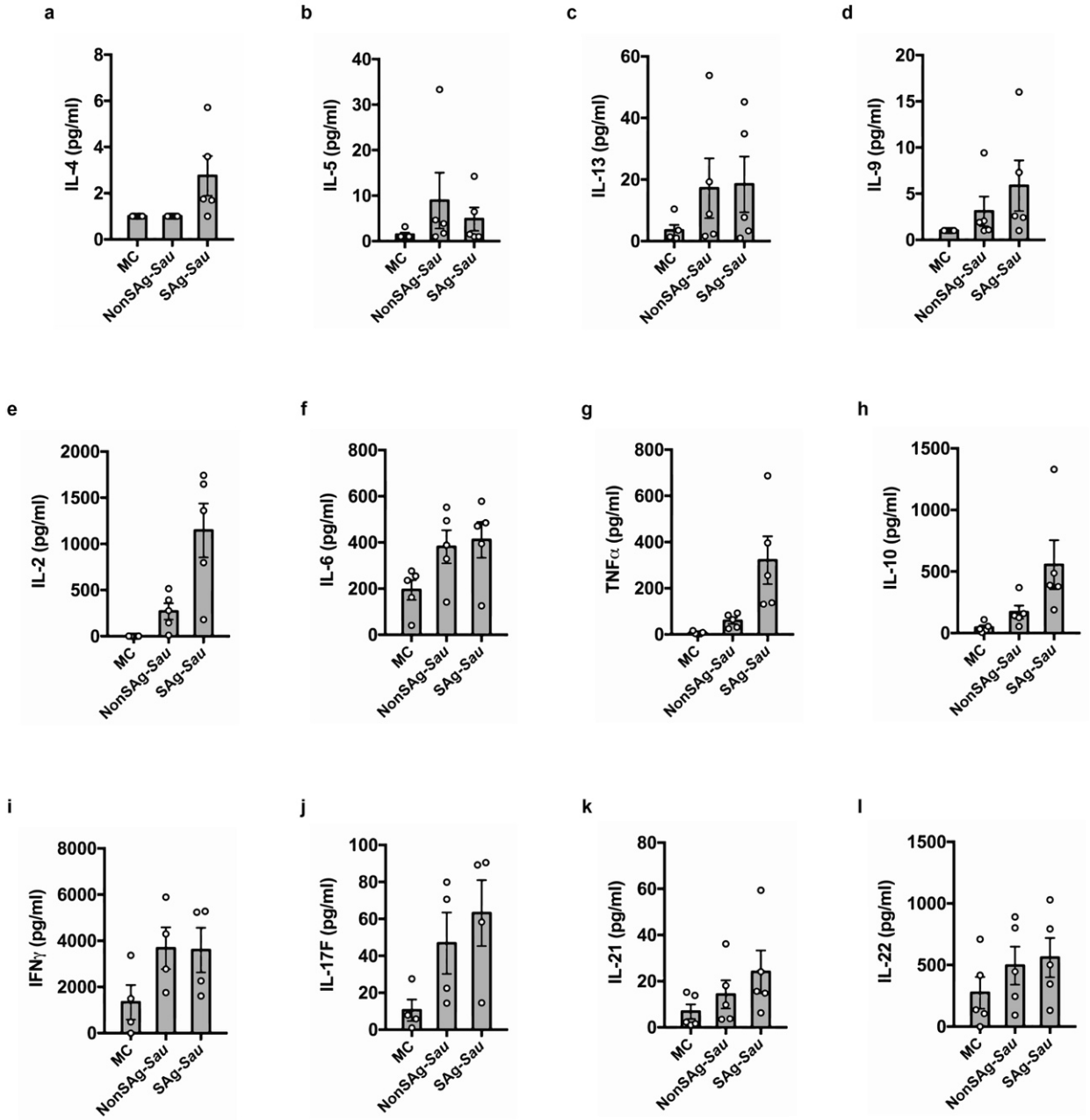

Figure 3.9 Cytokine production in the tonsillar MNCs stimulated by NonSAg-*Sau* or SAg-*Sau*

Tonsillar MNCs were stimulated by 1 μg/ml of NonSAg-*Sau* and SAg-*Sau* respectively for 48 hours. Cell culture supernatants were collected, and the cytokine production were detected by CBA. n=5.

The plasticity of Tregs which enabling them to convert to Th17 cells is correlated with the development of inflammatory/autoimmune conditions[119,120]. In a murine model of collagen-

induced-arthritis (CIA), the arthritogenic and autoreactive Th17 cells are shown to derive from $Foxp3^+CD4^+$ T cells, indicating the autoimmune potential of $Foxp3^+$ Tregs should they convert to Th17 cells[119]. Our results suggest that certain tonsillar $Foxp3^+$ Tregs may also acquire an autoimmune potential in the context of SAg-*Sau* stimulation. However, it is technically difficult to track a Th17 conversion from $Foxp3^+$ Treg in experimental human studies.

3.4.5 SAg-*Sau* induces production of active TGF-β and IL-10

Sau-expanded Tregs seemed unable to suppress the Th17 activation and contributed to IL-17A production in tonsillar MNCs. It is plausible that *Sau* may downregulate Treg-mediated suppression pathways. To evaluate the suppressive activity of *Sau*-expanded Tregs, I first examined the production of active TGF-β and IL-10, two signature cytokines that mediate Treg-dependent suppressions.

TGF-β is secreted as latent precursor protein which requires further activation to exert its biological functions. The latent TGF-β is produced by many cell types, including immune cells. The activation of TGF-β is tightly controlled and can be mediated by activated Tregs[121-123]. In this study, transformed mink lung cells (TMLCs), which produce luciferase in response to TGF-β signalling (as described in ***2.19***), were used to examine the production of active TGF-β in bacterial antigen stimulated tonsillar MNCs.

By co-culturing tonsillar MNCs with TMLCs in the presence of *Spn* or *Sau* CCS, an enhanced luciferase activity was detected at 48hrs following *Sau* stimulation, indicating an increased production of active TGF-β in *Sau*-activated MNCs (***Figure 3.10 a***). The TMLCs were then cultured with MNC culture supernatant collected at day 2, 3, 4, 5 and 6 following stimulation. *Sau* stimulation promoted TGF-β activation, and this increased level of active TGF-β was maintained throughout the 6-day culture. In accordance with the higher proportion of Tregs, SAg-*Sau* also activated more TGF-β than NonSAg-*Sau* and *Spn* (***Figure 3.10 b***).

The active TGF-β was not increased by *Spn* stimulation, nor was IL-10 (***Figure 3.10 a*** and ***Figure 3.11 a, b***). In contrast, both active TGF-β and IL-10 production were enhanced by *Sau*, especially in SAg-*Sau* stimulated MNCs (***Figure 3.10*** and ***Figure 3.11 c***).

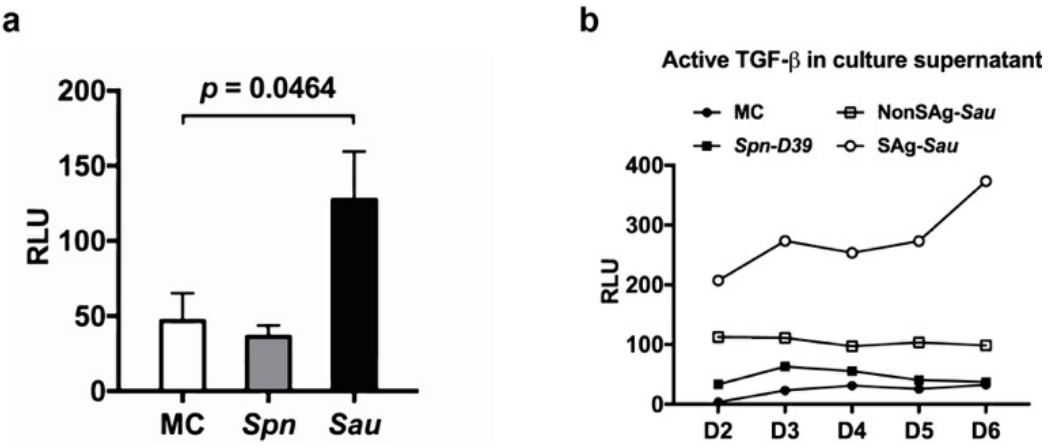

Figure 3.10 Production of active TGF-β is enhanced by *Sau* stimulation

a) Tonsillar MNCs (5×10^5) were co-cultured with TMLCs (4×10^4) and stimulated with *Spn* and *Sau* respectively for 48hrs. The TMLCs were washed and lysed for the detection of luciferase signal (RLU, relative light unit). Data was analysed using paired *t*-test, n = 3. **b)** The cell culture supernatant was collected from *Spn* or *Sau* stimulated MNCs at different time points (D2, D3, D4, D5 and D6), and the level of active TGF-β in the culture supernatant was detected by TMLCs.

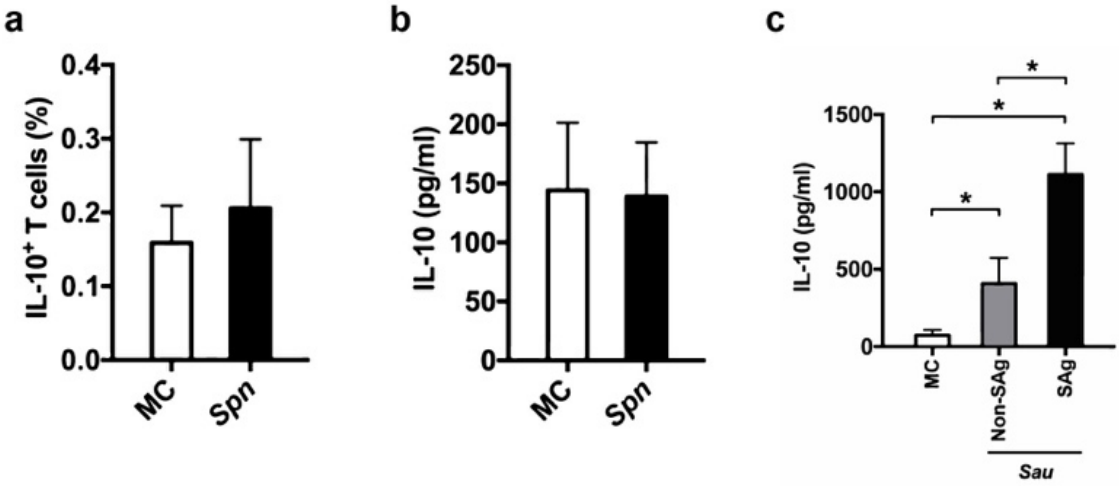

Figure 3.11 SAg-*Sau* stimulation promotes IL-10 production in tonsillar MNCs

Tonsillar MNCs were cultured in the presence of 1 μg/ml of *Spn* or *Sau* CCS for 48hrs. **a)** The percentage of IL-10$^+$ cells within CD4$^+$ T cells following *Spn* stimulation was summarised in the bar graph, n = 4. **b)** IL-10 concentration in the culture supernatant of *Spn* stimulated MNCs, n = 5. **c)** IL-10 concentration in the culture supernatant of MNCs stimulated by NonSAg-*Sau* and SAg-*Sau* respectively, n = 4. Data was analysed using paired *t*-test.

IL-10 can be expressed by monocytes, B cells and T cells. Hence, intracellular cytokine staining was performed to determine whether SAg-*Sau* activated IL-10 production was from the Foxp3$^+$ Tregs. As shown in ***Figure 3.12***, Foxp3$^-$CD4$^+$ T cells were the primary source of IL-10 in SAg-*Sau* stimulated tonsillar MNCs, although an increase in IL-10 expression was detected in Foxp3$^+$CD4$^+$ T cells.

IL-10-producing $CD4^+$ T cells that do not express Foxp3 have been described by previous studies and termed as type 1 regulatory T cells (Tr1). Tr1 cells are critical in controlling the activation of effector T cells during tissue inflammation, autoimmunity and graft-versus-host disease. The effect of IL-10 on SAg-*Sau*-activated Th1 and Th17 responses was examined in the next chapter.

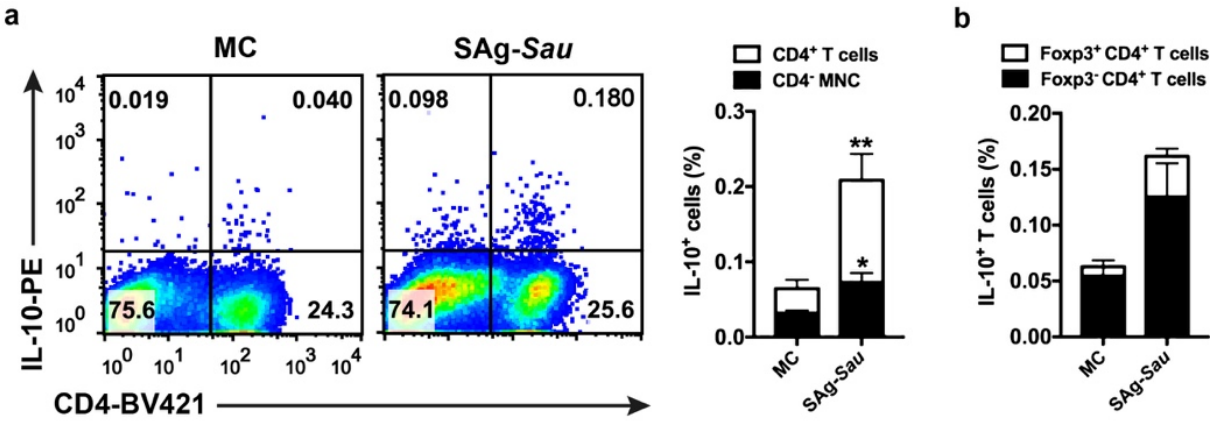

Figure 3.12 SAg-*Sau* induces IL-10 expression primarily in $Foxp3^-CD4^+$ T cells

IL-10 expression in different immune cell populations was examined in SAg-*Sau* stimulated tonsillar MNCs. **a)** Dot plots showing IL-10 expression in $CD4^-$ lymphocytes and $CD4^+$ T cells. Numbers in top left and right quadrants indicate percentages of $IL\text{-}10^+CD4^-$and $IL\text{-}10^+CD4^+$ cells respectively. Mean ± SEM is shown for both cell populations (%) in the stacked bar graph, n = 8. **b)** Percentages of $IL\text{-}10^+$ cells in $Foxp3^+CD4^+$ and $Foxp3^-CD4^+$ T cell populations were summarised in the stacked bar graph, n = 3.

3.4.6 SAg-*Sau* upregulates CTLA4 but downregulates CD39 expression in $Foxp3^+$ Tregs

Cytotoxic T lymphocyte-associated protein 4 (CTLA4) and its structure relative CD28 are both expressed by T cells and interact with the same shared ligands CD80 and CD86 on antigen-presenting cells (APC) but have opposing functions[124]. While CD28 binds to the ligands to provide co-stimulatory signal for T cell activation, CTLA4 signalling inhibits T cell responses. CTLA4 is constitutively expressed in $Foxp3^+$ Tregs and induced in conventional T cells following activation. With higher affinity and avidity to both ligands, CTLA4 contributes to Treg-

dependent suppression via outcompeting CD28 for ligand binding and thereby abrogating the co-stimulatory signal delivered by CD28[125].

The CTLA4 expression in $CD4^+$ T cells was increased in *Spn* stimulated tonsillar MNCs. Matched with the potent activation of T cells, SAg-*Sau* induced CTLA4 expression in over 80% of $CD4^+$ T cells (***Figure 3.13 a***). SAg-*Sau*-expanded Tregs also exhibited enhanced CTLA4 expression comparing to *Spn* and NonSAg-*Sau* stimulation (***Figure 3.13 b***). Thus, SAg-*Sau* stimulation did not appear to affect Treg-mediated suppressions through CTLA4 route.

CTLA4 is a well-recognized immune checkpoint that limits immune responses to self-tissues. CTLA4 deficiency caused by genetic mutation and immune checkpoint blockade therapy in cancer patients both lead to autoimmune reactions[126,127]. In $Foxp3^+$ Tregs, CTLA4 signalling represents a critical suppressive pathway in containing effector T cell responses. However, Treg-specific CTLA4 deficiency is shown to enhance both Th1 and Th2 activation but not affect the Th17 frequency in the splenocytes of mice[128]. Further, it has been reported that the colon inflammation induced by adoptive transfer of *in vitro* differentiated Th17 cells can be augmented by co-transfer of induced Tregs, which is dependent on the CTLA4-mediated signalling of the Tregs[129]. Hence, the enhanced CTLA4 expression in SAg-*Sau*-expanded Tregs is less likely to confer effective suppression on the Th17 activation.

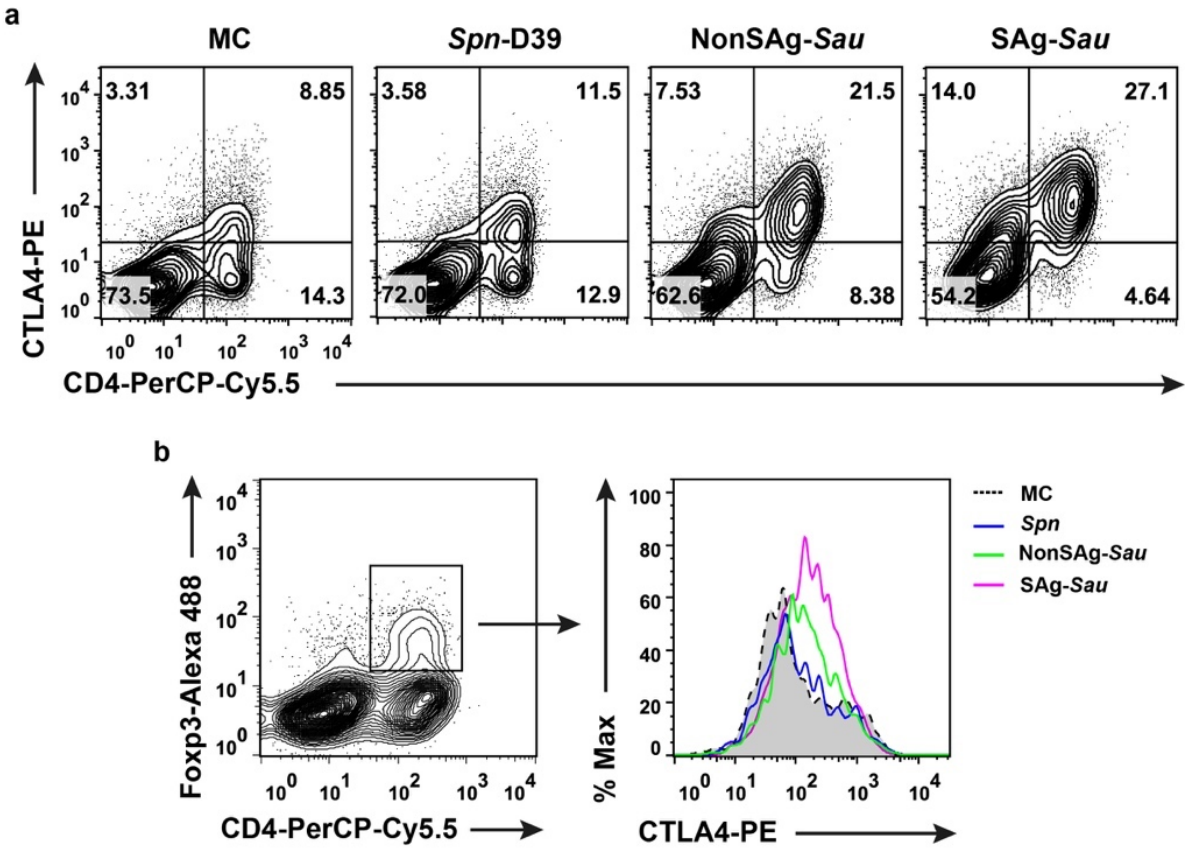

Figure 3.13 Increased CTLA4 expression in CD4⁺ T cells and Foxp3⁺ Tregs by *Sau*

Tonsillar MNCs were stimulated with *Spn* and *Sau* CCS respectively for 48hrs, and the expression of CTLA4 was examined by intracellular staining. **a)** The percentage of $CTLA4^+$ and $CTLA4^-$ cells within $CD4^+$ T cells are shown in top and bottom right quadrants of the contour plots. **b)** $Foxp3^+CD4^+$ T cells were gated out to show CTLA4 expression in $Foxp3^+$ Tregs. Results represent 3 independent experiments.

CD39 is an ectonucleotidase that works with CD73 to convert extracellular ATP into immunosuppressive adenosine[83,130]. By engaging with the A_{2A} receptor on effector T cells, adenosine downregulates NF-κB activation, thereby reducing the release of proinflammatory cytokines and chemokines[83].

In human PBMCs, both $CD39^+$ and $CD39^-$ Tregs suppressed IFNγ production and effector T cell proliferation but only $CD39^+$ Tregs were capable of suppressing IL-17 production[81,131]. The

frequency of CD39$^+$ Tregs was lower in patients with multiple sclerosis which may have led to Th17-driven autoimmune pathology in these patients[81]. In light of this study, I examined CD39 expression on tonsillar Foxp3$^+$ Tregs stimulated by *Spn* and *Sau* respectively. The results showed that *Spn* induced upregulation of CD39 on activated Tregs which was in contrast to the remarkably downregulated CD39 expression by NonSAg-*Sau* and SAg-*Sau* stimulation (***Figure 3.14***).

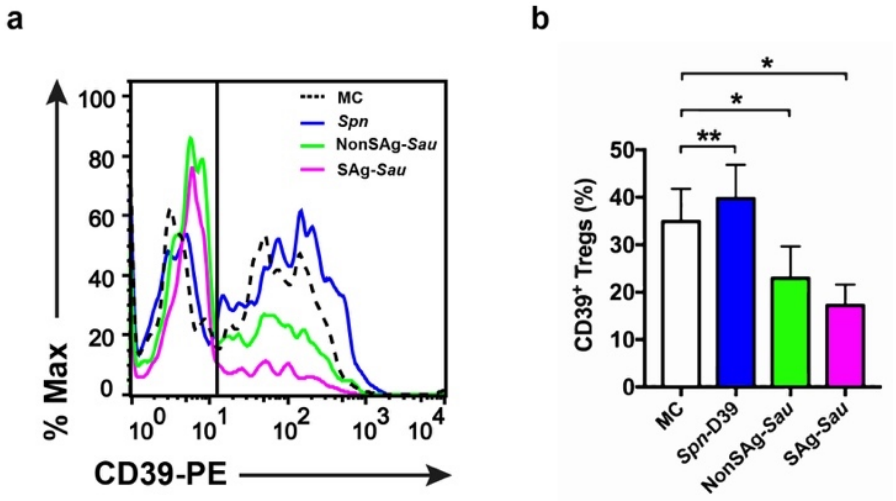

Figure 3.14 SAg-*Sau* downregulates cell surface expression of CD39 on Foxp3$^+$ Tregs

Tonsillar MNCs were stimulated with *Spn*, NonSAg-*Sau* and SAg-*Sau* CCS respectively for 48hrs. Expression of CD39 was detected by cell surface staining and compared to media control (MC). **a)** Histogram plots were gated on Foxp3$^+$CD4$^+$ T cells, and the percentage of CD39$^+$ cells in Tregs were summarised in the bar graphs (**b**), n = 6. Data displayed is mean ± SEM.

Following SAg-*Sau* stimulation, the Foxp3$^+$ population was expanded which was accompanied with increased level of active TGF-β and IL-10. The expanded Tregs also had enhanced expression of CTLA4. However, CD39 expression on SAg-*Sau*-activated Tregs was significantly downregulated which could lead to inefficient clearance of extracellular ATP and impaired suppression through adenosine/A_{2A} signalling pathway.

ATP is released from CD4$^+$ T cells upon stimulation and acts in an autocrine manner through P2X receptors to further augment TCR-initiated activation of mitogen-activated protein

kinases (MAPKs) and IL-2 secretion[132]. It is demonstrated that accumulated ATP inhibits the suppressive potential of Tregs and induces their conversion to IL-17-producing Th17 cells[133]. SAg-*Sau*-expanded Tregs could therefore fail to suppress Th17 activation and further contribute to IL-17A production due to increased ATP level which was associated with low proportion of $CD39^+$ Tregs.

3.4.7 The association of SAg-*Sau*-activated T cell responses with age

With PMA/ionomycin stimulation, an age-dependent increase in the tonsillar Th17 frequency was shown by our colleagues previously[112]. I examined whether SAg-*Sau*-activated Th17 and Treg responses in the NALT were associated with age. The age of patients recruited in this study ranges from 2 to 50 yrs old. SAg-*Sau* activated Th17 responses in tonsillar MNCs were observed from all age groups. The proportion of Th17 cells following SAg-*Sau* stimulation was increasing with age in children but not further increased in adults (> 16 yrs) (***Figure 3.15 a***). A trend of decline in the Th17 response was observed in individuals over 30-year-old which may relate to the decreasing of T cell responsiveness to antigen stimulation when grow older. However, the sample size of this age group was too small to make the conclusion. Overall, there was a lack of clear association between age and SAg-*Sau*-activated Th17 responses in the NALT (***Figure 3.15 c***).

Interestingly, the proportion of the Tregs expanded by SAg-*Sau* showed a positive correlation with age (***Figure 3.15 b, d***). However, this expanded Treg population did not appear to possess the ability to suppress the Th17 response activated by SAg-*Sau* as shown above.

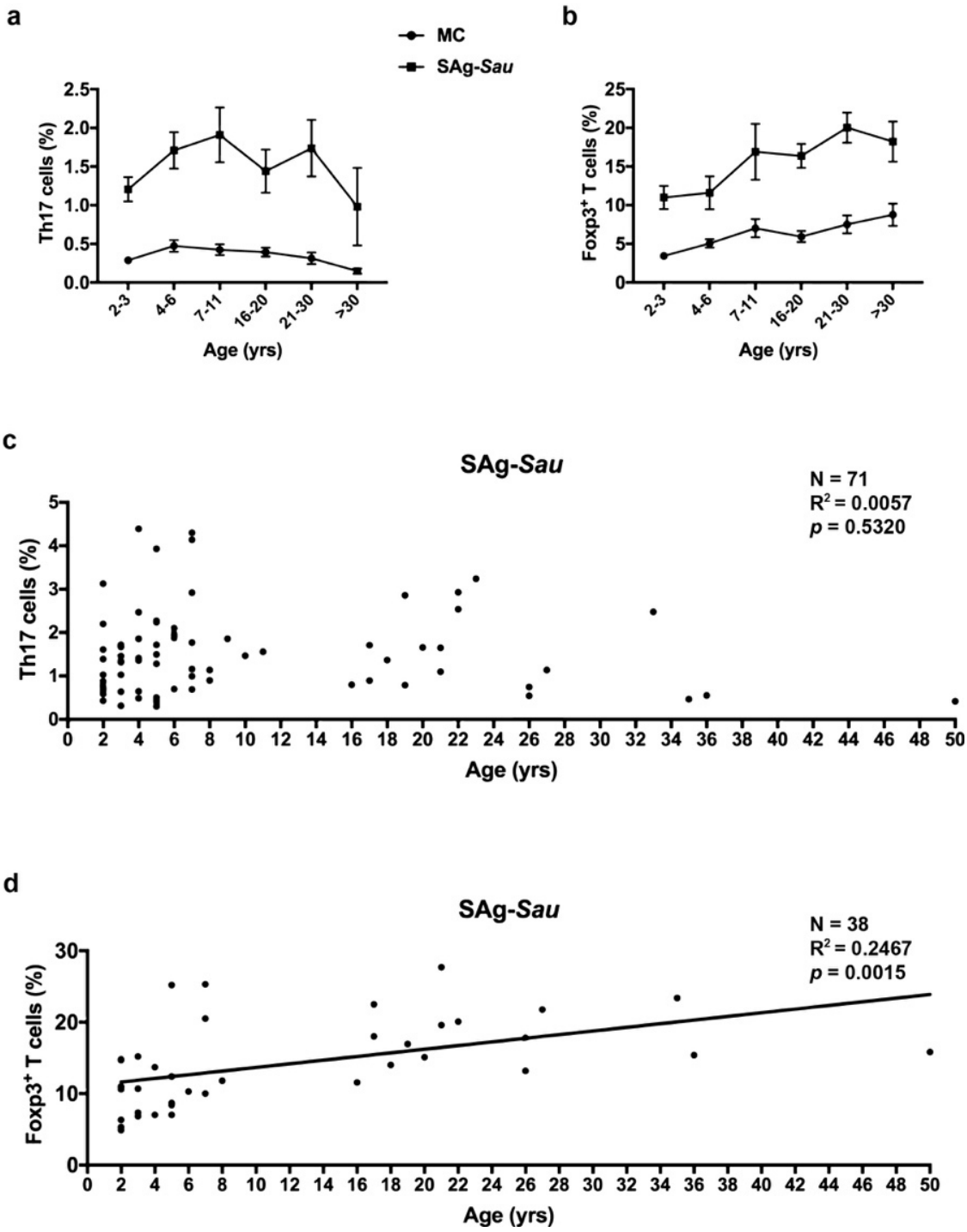

Figure 3.15 The association of SAg-*Sau*-activated T cell responses with age

Tonsillar MNCs were cultured with or without SAg-*Sau* CCS for 48hrs, and Th17 and Treg cell responses were analysed following stimulation. Percentages of Th17 cells (**a**) and Tregs (**b**) within $CD4^+$ T cells are shown in the line plots as mean ± SEM for different age groups. Individual data points are displayed in (**c**) and (**d**) for Th17 and Tregs respectively, and their associations with age were analysed using linear regression. Sample size (n), R square (R^2) and *p* values are indicated.

3.4.8 SAg-*Sau* activates significantly higher Th17 responses in tonsillar MNCs compare to PBMCs

Since the nasopharynx is intensively exposed to foreign antigens, the NALT contains a markedly higher proportion of effector and memory T cells compared to peripheral blood. SAg-*Sau* has been shown to activate IL-17 production from memory $CD4^+$ T cells[14]. Indeed, I show here that SAg-*Sau* elicited a strong Th17 response in tonsillar MNCs, whereas only modest Th17 activation was detected in SAg-*Sau* stimulated PBMCs (***Figure 3.16 a***). In contrast, SAg-*Sau* induced more Tregs in PBMCs than tonsillar MNCs (***Figure 3.16 b***). It is possible that superantigen is more potent to induce naïve T cell proliferation, and this is followed by a phenotype switch to $Foxp3^+$ Tregs[111].

My results suggest a high potency of SAg-*Sau* in activating effector and memory Th17 cells, and the nasopharynx provides a well-suited immune environment for SAg-*Sau* to elicit strong Th17 responses. It is of significant importance to investigate whether this potent Th17 activation can be controlled by local immune regulation to avoid potential Th17-driven pathologies.

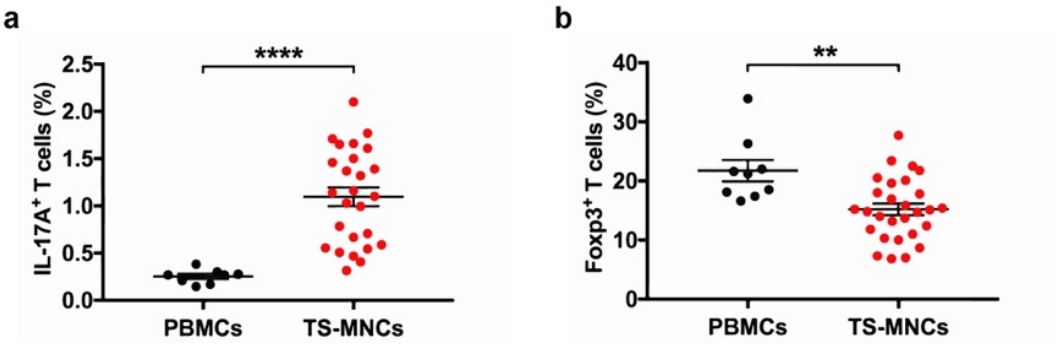

Figure 3.16 Comparison of SAg-*Sau*-activated Th17 and Treg responses in tonsillar MNCs and PBMCs

Tonsillar MNCs or PBMCs were stimulated with 1 μg/ml of SAg-*Sau* CCS, and the Th17 and Treg cells were examined at 48hrs following stimulation. Percentages of IL-17A$^+$ cells (**a**) and Foxp3$^+$ cells (**b**) within CD4$^+$ T cell population are shown in the scatter plots with mean ± SEM. The results represent 8 (**a**, PBMCs group), 26 (**a**, TS-MNCs group), 9 (**b**, PBMCs group) and 28 (**b**, TS-MNCs group) independent samples. Data was analysed using unpaired *t*-test.

3.5 Conclusions

In this chapter, I have shown the activation of Th17 cells and Foxp3$^+$ Tregs by *Sau* and *Spn* in human NALT. Treg-associated suppression pathways were also investigated to inform potential functional defects in *Sau*-activated Tregs.

Sau-derived antigens activated a remarkably higher Th17 responses than *Spn*, and this strong Th17 activation was associated with high level of staphylococcal superantigens. Along with elevated Th17 responses, *Sau* also expanded the Foxp3$^+$ Treg population. However, the proportion of Tregs and Th17 cells activated by *Sau* strains was not negatively associated as it was observed in *Spn*-stimulated tonsillar MNCs, indicating *Sau*-expanded Tregs were not able to suppress the potent Th17 responses.

An increased level of active TGF-β and IL-10 was detected in MNC culture supernatant following SAg-*Sau* stimulation, although the enhanced IL-10 production was primarily derived from Foxp3$^-$CD4$^+$ T cells. SAg-*Sau*-expanded Tregs exhibited enhanced expression of CTLA4, suggesting these Tregs were able to efficiently antagonize CD28-mediated co-stimulatory

signal, hereby suppressing T cell activation. However, the proportion of $CD39^+$ cells within the $Foxp3^+$ Treg population expanded by SAg-*Sau* was markedly reduced. It has been demonstrated that only $CD39^+$ Tregs were capable of suppressing IL-17 production in human PBMCs, and a significantly lower frequency of $CD39^+$ Tregs was found in the circulation of patients with multiple sclerosis which may contribute to the Th17-driven pathologies in these patients[81]. Thereby, SAg-*Sau*-expanded Tregs may be unable to suppress the Th17 activation due to downregulated CD39 expression.

Further, SAg-*Sau* activated a remarkably stronger Th17 response in the nasopharynx compared to the peripheral blood, suggesting that the capacity of SAg-*Sau* in activating Th17 responses is associated with high proportion of effector and memory T cells. Also, memory Th17 cells are more enriched at the mucosal site. This potent Th17 activation in SAg-*Sau*-infected human nasopharynx is a potential risk for the development of inflammatory/autoimmune conditions. Hence, $CD4^+$ T cell-mediated immune controls on SAg-*Sau*-activated proinflammatory T cell responses were further investigated and demonstrated in the following chapters.

CHAPTER 4

Superantigenic *Staphylococcus aureus*-activated Th17 cells are resistant to Treg- and IL-10-medatied suppressions

4.1 Abstract

Foxp3$^+$ Tregs and IL-10 play critical roles in suppressing pathological Th17 activation in murine models of autoimmune diseases. Staphylococcal superantigens have been shown to induce CD4$^+$ T cell-mediated autoimmune pathologies. I have demonstrated that SAg-*Sau* was able to activate a potent Th17 response accompanied with largely expanded Treg population and significantly upregulated IL-10 production in tonsillar MNCs. It was therefore of interest to examine whether Tregs and IL-10 were able to suppress SAg-*Sau*-activated Th17 responses in human NALT.

By depleting Foxp3$^+$ Tregs, an enhanced proliferation of CD4$^+$ T cells was detected in *Spn* stimulated tonsillar MNCs, whereas *Sau*-activated cell proliferation was not altered. Treg-mediated suppression of IFNγ-producing Th1 and IL-17A-producing Th17 responses was further evaluated in SAg-*Sau* stimulated MNCs. Interestingly, Treg removal enhanced the Th1, but not the Th17 activation, indicating that Foxp3$^+$ Tregs were not competent in suppressing SAg-*Sau*-activated T cell responses, especially for Th17 cells. IL-10-mediated suppression of Th1 and Th17 activation in SAg-*Sau* stimulated MNCs was examined by neutralizing IL-10. Again, IL-10 depletion did not affect the strong Th17 responses, although it significantly augmented Th1 activation. Further, I found that addition of recombinant IL-10 enhanced the IL-17A expression in CD4$^+$ T cells upon SAg-*Sau* stimulation and promoted GM-CSF expression in the activated Th17 cells, suggesting a potential pathogenic role of IL-10 in SAg-*Sau*-infected nasopharynx.

The results demonstrate that SAg-*Sau*-activated Th17 cells in the NALT are resistant to Tregs- and IL-10-mediated suppression. This aberrant immune regulation on proinflammatory Th17 responses may underlie SAg-*Sau*-driven inflammatory and autoimmune conditions.

4.2 Introduction

From suppressor T cells to regulatory T cells, the discovery and delineation of $Foxp3^+CD25^+CD4^+$ regulatory T cell subset (Tregs) has gone through its own history of renaissance[134-136]. The existence of a specific suppressive T cell subpopulation was initially proposed in the early 1970s[134]. However, it was followed by decades of chaos in the field of suppression until this self-tolerance maintaining Treg cell population was characterised as $CD25^+CD4^+$ T cells by Sakaguchi in 1995[137]. Later in 2003, transcription factor Foxp3 was found to be a unique marker for $CD25^+CD4^+$ regulatory T cells. Foxp3 is specifically required for the thymic development of Tregs, and forced expression of Foxp3 in $CD25^-CD4^+$ cells confers suppressor activity on these cells[138-140].

It has been well described that $Foxp3^+$ Treg depletion and *Foxp3* gene mutations lead to the development of autoimmune and inflammatory diseases as a result of uncontrolled activation of $CD4^+$ T cells[139-144]. $Foxp3^+$ Tregs suppress effector T cell proliferation and Th1 activation. However, the suppression has been questioned when it comes to Th17 cells. Tregs and Th17 cells share the common TGF-β signal for their initial differentiation, and Tregs can convert into IL-17-producing cells when they are exposed to certain cytokines, such as IL-6 and IL-23[116,118].

IL-10 is a well-established immune suppressive cytokine produced by a number of immune cells including $Foxp3^+$ Tregs and $Foxp3^-$ type 1 regulatory cells (Tr1)[145,146]. IL-10 was originally termed as cytokine synthesis inhibitory factor (CSIF) that expressed by Th2 cells to inhibit proinflammatory cytokine production in Th1 cells[147]. Later studies demonstrate that IL-10 inhibits production of a broad spectrum of inflammatory cytokines (IL-1, IL-6, GM-CSF, TNFα, IL-12, etc.) and chemokines (MCP1, MCP5, IL-8, IP-10, etc.) by macrophages/monocytes and subsequently suppresses the recruitment and activation of T cells and monocytes[145].

There is a large body of evidence to support the potent suppressive activity of IL-10 on both Th1 and Th17 activation in mice and humans[78,85,148,149]. IL-10 or IL-10 receptor knockout mice have significantly increased risk of developing autoimmune disorders, such as IBD and EAE[87,150]. Loss of function mutations in IL-10 and IL-10 receptor (IL-10R) in humans has also been linked to an early-onset of IBD[88-90]. Despite these findings, attempts to utilise

recombinant IL-10 clinically for treating autoimmune diseases have been unsuccessful[91]. Further studies to elucidate IL-10-mediated suppression in a wide range of immunological settings, including SAg-*Sau*-driven inflammations, are required to demystify the IL-10 paradox.

4.3 Aims

- To examine Treg-mediated suppression on SAg-*Sau*-activated $CD4^+$ T cell responses, including cell proliferation and inflammatory cytokine production by Th1 and Th17 cells.
- To evaluate the role of IL-10 in suppressing SAg-*Sau*-activated Th1 and Th17 responses in human NALT.
- To test whether IL-10 affects the effector phenotype of SAg-*Sau*-activated Th17 cells.

4.4 Results and Discussion

4.4.1 SAg-*Sau*-activated $CD4^+$ T cell proliferation is not inhibited by $Foxp3^+$ Tregs

It is shown in the previous chapter that activation of Th17 cells and Tregs upon SAg-*Sau* stimulation were not inversely correlated, and the expanded Tregs exhibited significantly reduced expression of CD39, suggesting the suppressive capacity of these Tregs may be compromised in terms of SAg-*Sau* stimulation. To characterise the function of Tregs in this specific inflammatory setting, I first examined their suppression against the T cell proliferation activated by *Spn* and *Sau* respectively.

The proliferative response of $CD4^+$ T cells following bacterial antigen stimulation was detected in the tonsillar MNCs with or without Tregs. $Foxp3^+$ Tregs express high level of CD25 on the cell surface, making them distinguishable from other conventional $CD4^+$ T cells. Magnetic cell sorting was used to deplete $CD25^+$ cell from tonsillar MNCs which removed over 95% of $Foxp3^+$ Tregs (***Figure 4.1***). The Treg-depleted MNCs and unfractionated MNCs were stained

with CFSE, a fluorescent cell staining dye that is halved with cell division and can thereby be used to indicate dividing cycles of proliferated cells. CFSE-labelled cells were stimulated with *Spn* and *Sau* CCS respectively for 5 days, and $CD4^+$ T cell proliferation was assessed by flow cytometry.

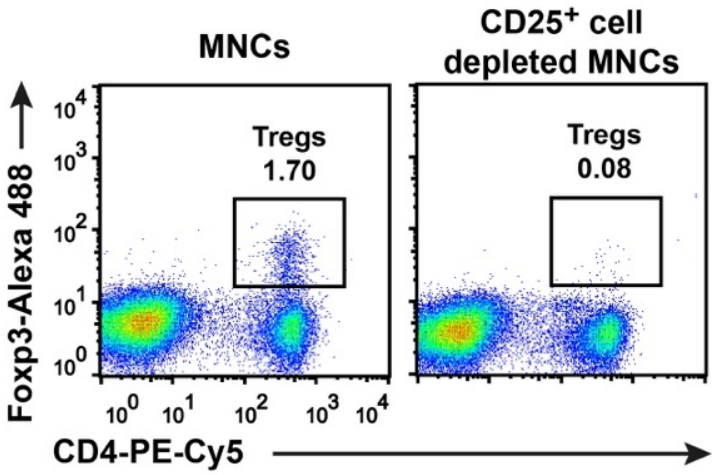

Figure 4.1 $CD25^+$ cell depletion removes Tregs in tonsillar MNCs

$Foxp3^+$ $CD4^+$ cells (Tregs) were gated out in the rectangular boxes with numbers on top showing the percentage of Tregs within lymphocytes before and after $CD25^+$ cell depletion.

The CFSE fluorescence is halved within daughter cells following each cell division. As shown in the histogram of ***Figure 4.2***, proliferated cells exhibited decreased fluorescent intensity, and peaks in the left compartment of the histogram represent cells undergone different dividing cycles. Following *Spn* stimulation, the proportion of proliferated $CD4^+$ T cells was significantly increased in Treg-depleted MNCs, indicating suppression of *Spn*-activated T cell proliferation by the Tregs (***Figure 4.2***).

Sau-derived antigens were extremely potent in inducing T cell proliferation with 70-80% of $CD4^+$ T cells undergone at least one dividing cycle following stimulation. Different from pneumococcal stimulation, the $CD4^+$ T cell proliferation following *Sau* stimulation was not changed by removing Tregs (***Figure 4.3***). The results indicate that *Sau*-activated proliferation of $CD4^+$ T cells were not suppressed by $Foxp3^+$ Tregs.

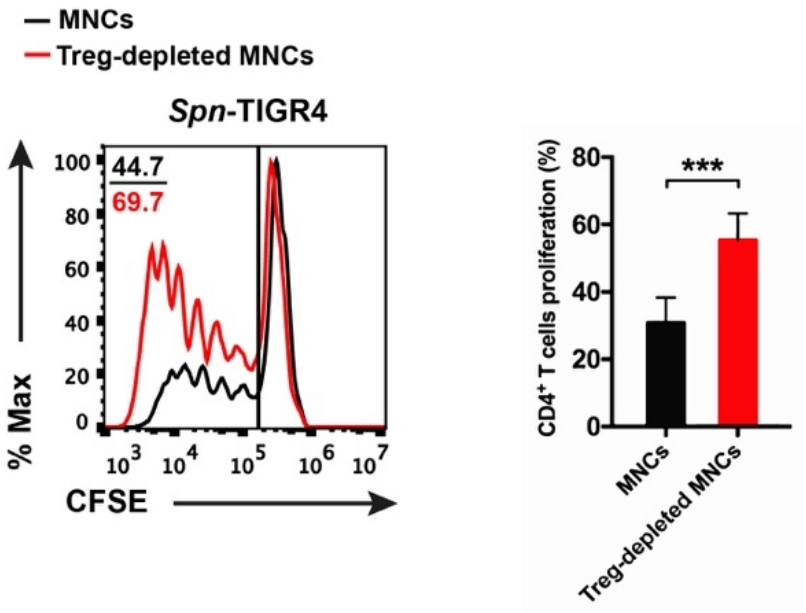

Figure 4.2 *Spn*-activated CD4$^+$ T cell proliferation is enhanced by removing Tregs

CFSE stained tonsillar MNCs were stimulated with 1 µg/ml of *Spn*-TIGR4 CCS for 5 days, and CD4$^+$ T cell proliferation was analysed by flow cytometry. The histogram plot was gated on CD4$^+$ T cells showing median fluorescence intensity (MFI) of CFSE signals, and numbers in the top left corner indicate percentages of proliferated CD4$^+$ T cells in unfractionated MNCs (black font) and Treg-depleted MNCs (red font). Data was summarised in the bar graph and analysed using paired *t*-test, ***$p < 0.001$. Mean ± SEM is displayed, n = 3.

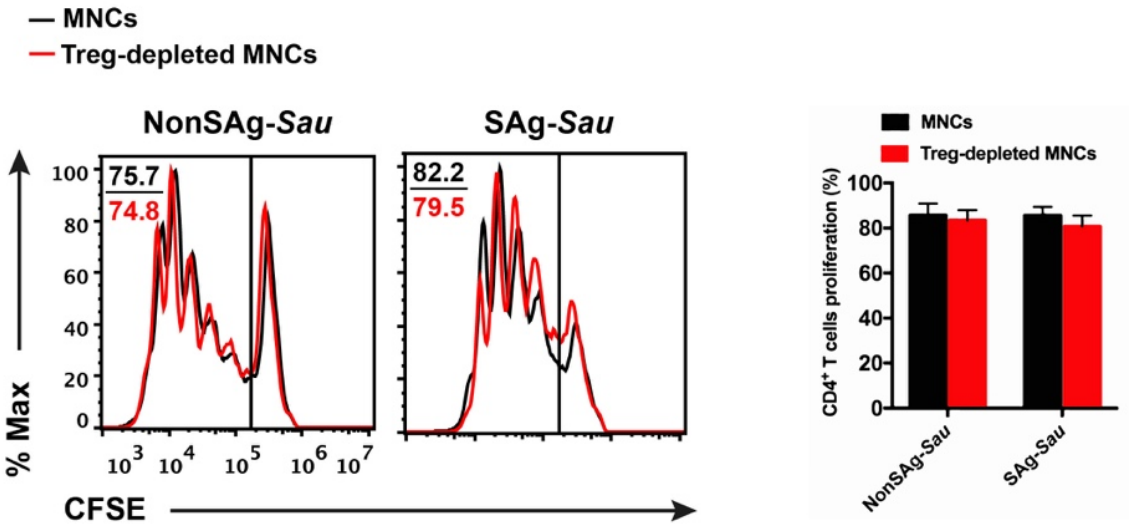

Figure 4.3 *Sau*-activated CD4⁺ T cell proliferation is not altered by Treg removal

CFSE labelled tonsillar MNCs were stimulated with 1 μg/ml of NonSAg-*Sau* and SAg-*Sau* CCS respectively, and cell proliferation was assessed at day 5. The histogram plots were gated on CD4⁺ T cells, and numbers in top left corner indicate percentages of CD4⁺ T cells that had undergone at least one dividing cycle in unfractionated MNCs (black font) and Treg-removed MNCs (red font) respectively. The percentages of proliferated CD4⁺ T cells were summarised in the grouped bar graph, n = 3.

Ou et al. show that Foxp3⁺ Tregs derived from human PBMC were not able to suppress T cell proliferation following staphylococcal enterotoxin B (SEB) stimulation[110]. My results further demonstrate that human NALT-derived Tregs also lack suppressive activity for SAg-*Sau*-stimulated proliferation of CD4⁺ T cells. Interestingly, this lack of suppression was also seen in NonSAg-*Sau* stimulated tonsillar MNCs. It is possible that the NonSAg-*Sau* strain may produce some unknown proteins that resemble the effects of superantigens.

Another study demonstrates that staphylococcal enterotoxin A (SEA) and streptococcal pyrogenic enterotoxin K/L could induced Foxp3 expression in proliferated CD25⁻ T cells, and these superantigen-induced Tregs exhibited suppressive activity comparable to naturally occurred Tregs for anti-CD3 stimulated T cell proliferation[111]. Since Foxp3⁺ Tregs were depleted before stimulation in my study, the effect of SAg-*Sau*-induced Tregs cannot be excluded. I showed in the previous chapter that SAg-*Sau*-expanded Tregs had enhanced

expression of CTLA4 but downregulated CD39, suggesting these Tregs may have retained certain suppressive activity. However, the potent proliferation of $CD4^+$ T cells stimulated by SAg-*Sau* suggests limited suppressive effect, if there is any, by induced Tregs.

It is notable that the suppression of T cell proliferation shown by previous studies was concluded from a single staphylococcal superantigen which cannot actually reflect the effects exerted by combined SAg-*Sau* antigens. The T cell responses and regulation examined using CCS containing secreted antigens from SAg-*Sau* are more likely to represent the host responses in SAg-*Sau*-infected nasopharynx.

4.4.2 $Foxp3^+$ Tregs suppress SAg-*Sau*-activated Th1, but not the Th17 responses

Having shown the $Foxp3^+$ Tregs exhibited no suppression on SAg-*Sau* stimulated $CD4^+$ T cell proliferation, I then examined the suppressive activity of Tregs for SAg-*Sau*-activated IFNγ and IL-17A expression. In the tonsillar MNCs without Tregs, a significantly increased IFNγ expression was seen in both $CD4^-$ and $CD4^+$ cells indicating enhanced cytotoxic T cell responses (IFNγ-producing $CD8^+$ T cells) and Th1 responses (IFNγ-producing $CD4^+$ T cells) (***Figure 4.4***). The results suggest that SAg-*Sau* stimulated Th1 activation can be efficiently inhibited by $Foxp3^+$ Tregs in the NALT.

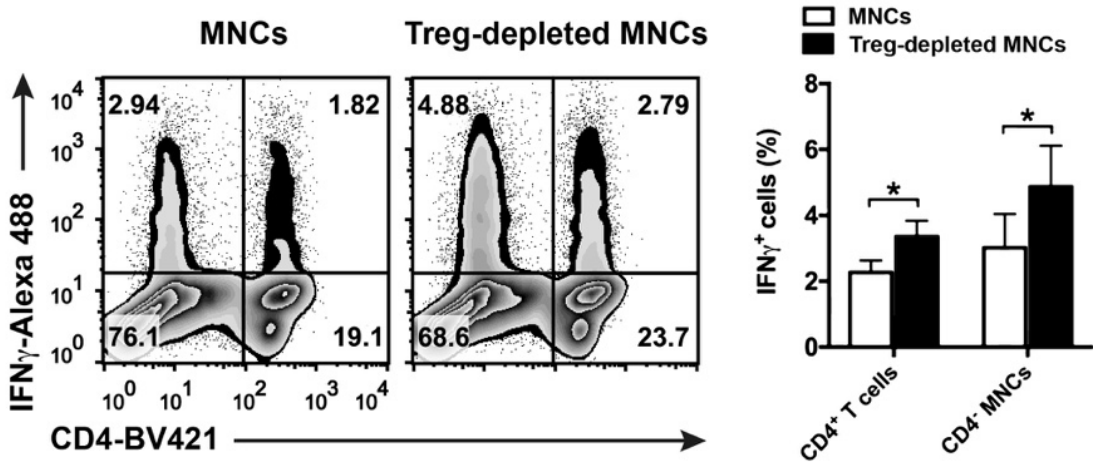

Figure 4.4 Treg removal enhances IFNγ expression in SAg-*Sau* stimulated tonsillar MNCs

Unfractionated MNCs and Treg-depleted MNCs were stimulated with SAg-*Sau* CCS respectively. The expression of IFNγ was examined at 48hrs following stimulation by intracellular staining. The zebra plots showing IFNγ expression in $CD4^-$ lymphocytes and $CD4^+$ T cells. Percentages of $IFN\gamma^+$ cells in these cell populations are shown in top left and right quadrants respectively and summarised in the grouped bar graph with mean ± SEM, n = 3. Data was analysed using paired *t*-test, $*p < 0.05$.

In contrast to an enhanced IFNγ expression, the expression of IL-17A in $CD4^+$ T cells showed a trend to decrease although it did not reach significance in Treg-depleted MNCs (***Figure 4.5***). The results clearly demonstrate that NALT-derived Tregs have the ability to suppress Th1 response but fail to control the potent T cell proliferation and Th17 response following SAg-*Sau* stimulation.

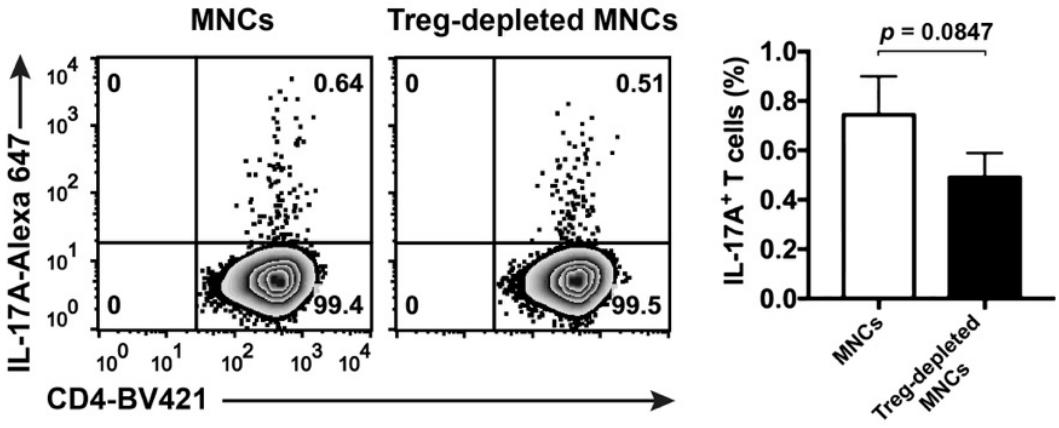

Figure 4.5 SAg-*Sau*-activated Th17 responses are not altered by removing Tregs

Unfractionated tonsillar MNCs and Treg-depleted MNCs were stimulated with SAg-*Sau* for 48hrs, and IL-17A expression in $CD4^+$ T cells was determined following stimulation. The zebra plots were gated on $CD4^+$ T cells, and numbers in top right quadrants indicate percentages of Th17 cells. Data was summarised in the bar graph and analysed using paired *t*-test, n = 3.

In order to determine whether this observation was distinct to the immune microenvironment of nasopharynx, I further examined the regulatory role of $Foxp3^+$ Tregs in peripheral blood mononuclear cells (PBMCs). Consistent with the findings obtained from tonsillar MNCs, the Treg-depleted PBMCs also had an enhanced Th1, but reduced Th17 response upon SAg-*Sau* stimulation (***Figure 4.6***). Thus, despite its critical role in maintaining immune tolerance, the $Foxp3^+$ Tregs are unable to inhibit SAg-*Sau*-activated Th17 response in humans.

The removal of Tregs resulted in decreased IL-17A expression provided further evidence to support that SAg-*Sau* was able to induce IL-17A expression in $Foxp3^+$ Tregs shown in the previous chapter. The Treg depletion also removed those Tregs that had the potential to convert into Th17 cells upon SAg-*Sau* stimulation.

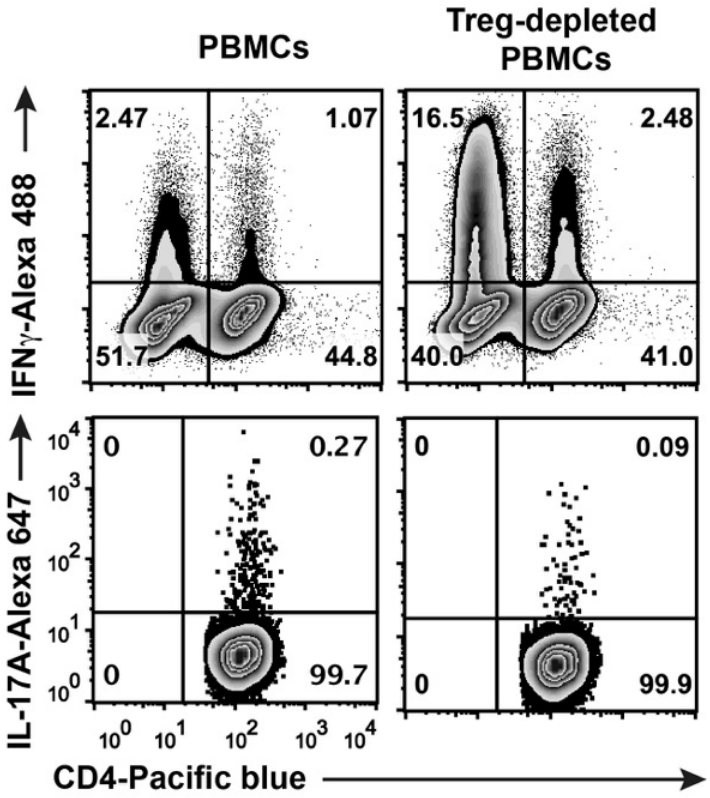

Figure 4.6 Treg depletion upregulates IFNγ but not IL-17A expression in SAg-*Sau* stimulated PBMCs

Unfractionated and Treg-depleted PBMCs were treated with 1 μg/ml of SAg-*Sau* CCS for 48hrs, and expression of IFNγ and IL-17A was examined by intracellular staining. The top zebra plots are showing the percentages of $IFN\gamma^{+}CD4^{-}$ (numbers in top left quadrants) and $IFN\gamma^{+}CD4^{+}$ cells (numbers in top right quadrants). The bottom zebra plots were gated on $CD4^{+}$ T cells, and numbers in top right quadrant indicate the percentage of $IL\text{-}17A^{+}$ cells. Results are representative of 3 individual samples.

Annunziato et al. show that human Th17 cells have significantly lower susceptibility to autologous Tregs compared to Th1 and general proliferative response when stimulated with irradiated allogeneic PBMCs[79]. My results agree with their finding by showing SAg-*Sau*-activated Th17 cells are highly resistant to Treg-mediated suppression, while the Th1 cells remained sensitive. However, it was shown in my study that the Tregs were also incapable of suppressing the T cell proliferation in response to SAg-*Sau* stimulation (***Figure 4.3***).

The differential regulation of the Th1 and Th17 responses by Tregs may be explained by the insensitivity of Th17 cells to Treg-mediated suppression pathways. Foxp3$^+$ Tregs express high level of IL-2 receptor α (IL-2Rα), CD25, and IL-2 signalling is required for the induction and survival of Tregs[151]. By consuming large amount of IL-2, Tregs could suppress T cell responses through IL-2 deprivation[152]. However, Th17 differentiation is inhibited by IL-2, and activation of memory Th17 cells is shown to be independent of IL-2[153,154]. Further, it has been reported that CTLA4 expression in Tregs is required for the suppression of Th1 and Th2 responses, whereas peripheral induced Tregs are shown to promote proinflammatory Th17 response in CTLA4-dependent manner, suggesting increased CTLA4 expression in Tregs may results in enhanced Th17 responses[128,129].

Tregs also mediates suppression via producing inhibitory cytokines, such as TGF-β and IL-10. It is known that TGF-β promotes Th17 development and activated/memory T cells are shown to be resistant to TGF-β-mediated suppression due to the downregulation of TGF-β receptor type II (TGF-βRII)[155], thereby the TGF-β produced and activated by Tregs is unlikely to restrict SAg-*Sau*-activated Th17 responses. I have shown that SAg-*Sau* stimulation significantly enhanced IL-10 production primarily from Foxp3$^-$CD4$^+$ T cells, the Foxp3$^+$ Tregs also exhibited increased IL-10 expression. Whether SAg-*Sau*-activated Th17 responses could be controlled by IL-10 was further examined.

4.4.3 SAg-*Sau*-activated Th17 responses are not enhanced by IL-10 neutralization

Tonsillar MNCs were stimulated with SAg-*Sau* CCS and treated with anti-human IL-10 monoclonal antibody to neutralise the biological effects of secreted IL-10. The stimulation control MNCs were treated with the corresponding isotype control antibody. The activation of IFNγ-producing Th1 cells and IL-17A-producing Th17 cells were examined using intracellular cytokine staining at 48hrs following stimulation.

It is well known that IL-10 potently suppresses T cell activation in various inflammatory settings. Consistently, IL-10 neutralization resulted in significantly increased proportion of Th1 cells in

tonsillar MNCs upon SAg-*Sau* stimulation, indicating efficient suppression of SAg-*Sau*-activated Th1 response by endogenous IL-10 (***Figure 4.7***).

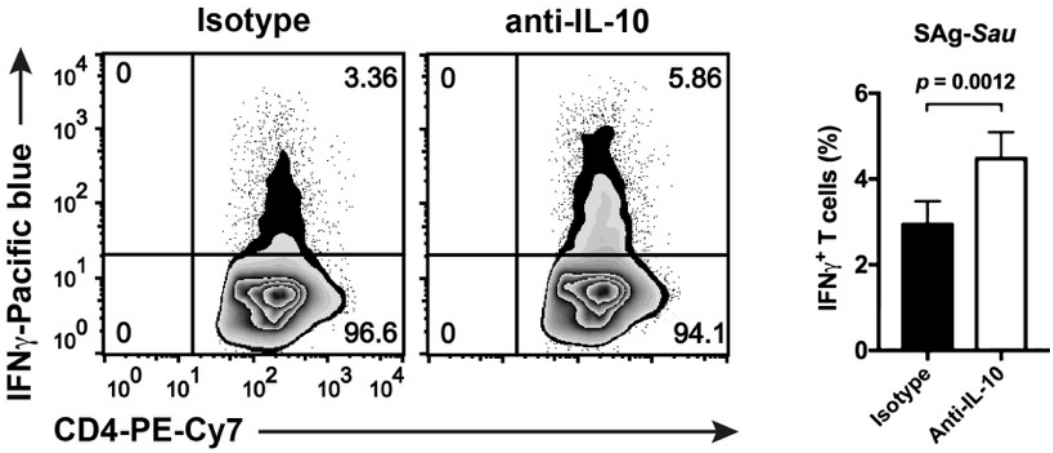

Figure 4.7 IL-10 neutralization enhances Th1 responses in SAg-*Sau* stimulated tonsillar MNCs

Tonsillar MNCs were stimulated with SAg-*Sau* CCS in the presence of 1 μg/ml of anti-IL-10 or isotype control antibody. The IFNγ expression in $CD4^+$ T cells was determined at 48hrs. The zebra plots were gated on $CD4^+$ T cells, and percentages of Th1 cells are shown in top right quadrants. Data was summarised in the bar graph, n = 7. Data was analysed using paired *t*-test and displayed in mean ± SEM with *p* value.

However, when assessing the Th17 cell population following SAg-*Sau* stimulation, it was surprising to show that the proportion of Th17 cells were not altered by IL-10 neutralization (***Figure 4.8***). The results suggest that SAg-*Sau*-activated Th17 responses were not controlled by endogenous IL-10 despite that its expression was markedly upregulated by SAg-*Sau*.

IL-10 suppresses T cell activation mainly through downregulating antigen presentation and cytokine production by accessory cells[145]. Superantigen elicited effector and memory Th17 cell activation may require only minimum signals from accessory cells. Chaudhry et al. demonstrate that IL-10 activates the STAT3 signalling in $Foxp3^+$ Tregs enabling them to suppress pathological Th17 responses which are responsible for the development of colitis[78]. Since I have shown that NALT-derived $Foxp3^+$ Tregs are unable to suppress SAg-*Sau*-

activated Th17 responses, it is possible that this IL-10/STAT3 signalling in the Tregs may be defective following SAg-*Sau* stimulation.

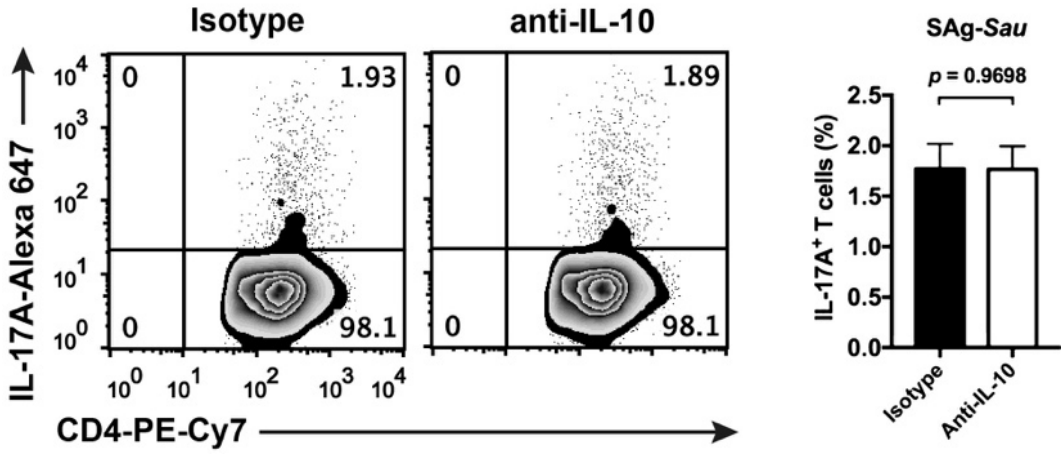

Figure 4.8 SAg-*Sau*-activated Th17 responses are not changed by neutralizing IL-10

Tonsillar MNCs were stimulated with SAg-*Sau* CCS in the presence of 1 μg/ml of anti-IL-10 or isotype antibody, and the Th17 responses were analysed at 48hrs. Percentages of IL-17A$^+$ cells within CD4$^+$ T cells are shown in top right quadrants of the zebra plots and summarised in the bar graph (mean ± SEM) on the right, n = 7.

4.4.4 Addition of IL-10 promotes Th17 activation by SAg-*Sau*

The endogenous IL-10 showed no suppression on SAg-*Sau* elicited Th17 activation. To further examine the suppressive activity of IL-10, SAg-*Sau* stimulated tonsillar MNCs were treated with recombinant IL-10 and followed by detecting the Th1 and Th17 responses.

As shown in ***Figure 4.9***, IL-10-treated MNCs had markedly decreased proportion of activated Th1 cells which again proved that IL-10 could potently suppress the Th1 responses stimulated by SAg-*Sau*.

Although it was anticipated that treatment of exogenous IL-10 may not affect the Th17 responses, the following results were still striking to show that addition of IL-10 actually promoted SAg-*Sau*-stimulated Th17 responses (***Figure 4.10***).

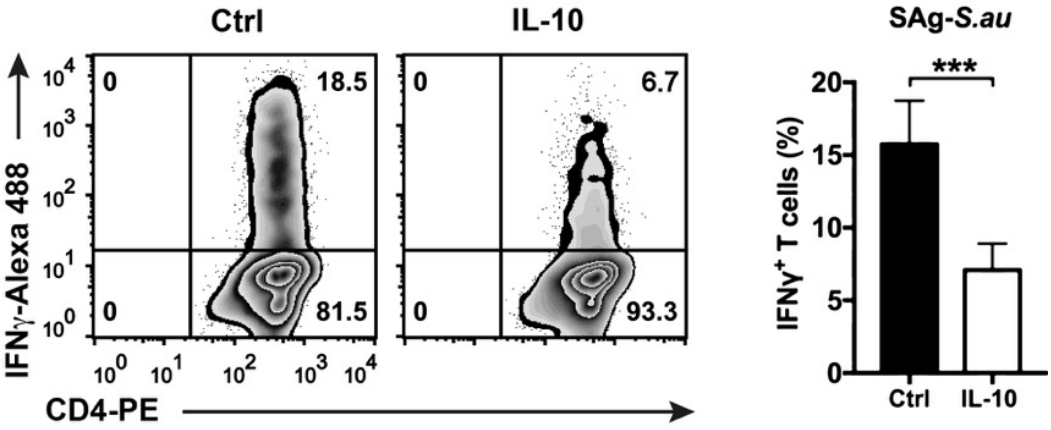

Figure 4.9 Addition of IL-10 inhibits Th1 responses in SAg-*Sau* stimulated tonsillar MNCs

Tonsillar MNCs were stimulated by SAg-*Sau* with or without 10 ng/ml of recombinant IL-10, and the Th1 responses were analysed at 48hrs following stimulation. Percentages of IFNγ$^+$ cells within CD4$^+$ T cells are indicated in top right quadrants of the zebra plots and summarised in the bar graph (mean ± SEM), n = 9. Ctrl, stimulation control without IL-10.

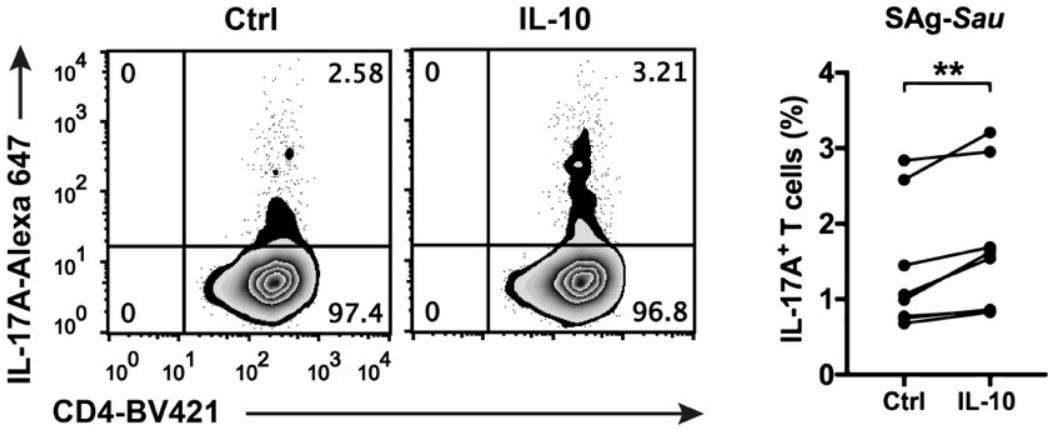

Figure 4.10 Exogenous IL-10 promotes SAg-*Sau*-activated Th17 responses

SAg-*Sau* stimulated tonsillar MNCs were treated with or without 10 ng/ml of recombinant IL-10 for 48hrs. The Th17 activation was analysed following stimulation. The zebra plots were gated on CD4$^+$ T cells, and numbers in top right quadrants indicate the percentage of IL-17A$^+$ cells. The symbols and lines plot on the right shows changes of Th17 proportions for each individual sample in the absence (Ctrl) and presence of IL-10, n = 8. Data was analysed using paired *t*-test, $^{**}p < 0.01$.

The Th1 and Th17 cell populations were then divided into IL-17A$^+$IFNγ^-, IL-17A$^+$IFNγ^+, and IL-17A$^-$IFNγ^+ subpopulations to further define the opposing roles of IL-10 in the regulation of IFNγ and IL-17A expression in SAg-*Sau*-activated tonsillar CD4$^+$ T cells. IL-17A$^-$IFNγ^+ cells were significantly reduced, and IL-17A$^+$IFNγ^+ cells were also decreased although this did not reach significance. However, a marked increase in IL-17A$^+$IFNγ^- cell population was observed in IL-10 treated cells, providing further evidence that IL-10 could promote IL-17A expression in SAg-*Sau*-activated tonsillar CD4$^+$ T cells (***Figure 4.11***).

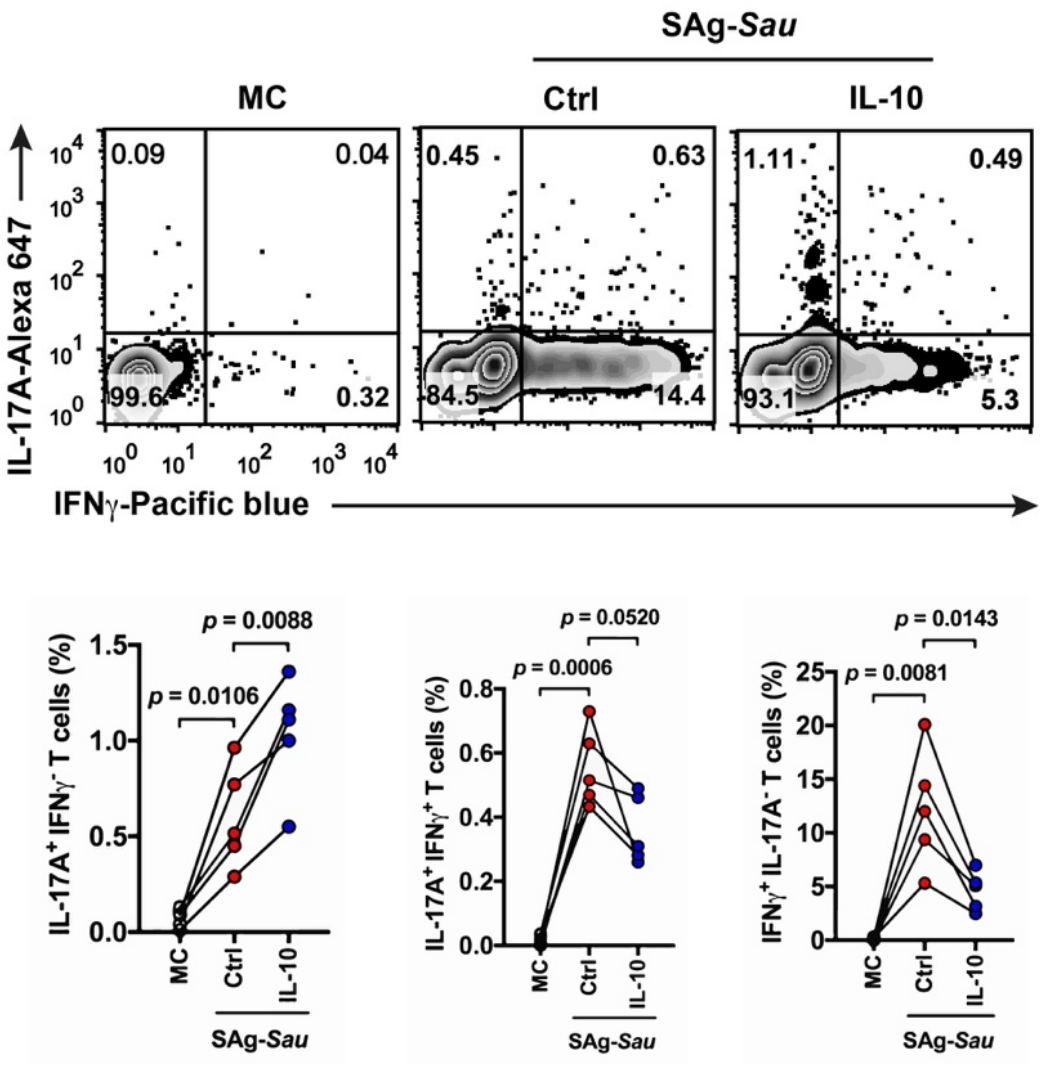

Figure 4.11 IL-10 promotes IL-17A and suppresses IFNγ expression in SAg-*Sau*-activated CD4⁺ T cells

SAg-*Sau* stimulated tonsillar MNCs were treated with or without recombinant IL-10, and expression of IL-17A and IFNγ in CD4⁺ T cells were determined at 48hrs. The zebra plots were gated on CD4⁺ T cells. Percentages of IL-17A⁺IFNγ⁻, IL-17A⁺IFNγ⁺ and IL-17A⁻IFNγ⁺ cells are shown in top left, top right and bottom right quadrants. The dots and lines plots showing percentage changes of these 3 cell populations for individual samples, n=5. Data was analysed using paired *t*-test, and *p* values were indicated.

Th17 cells are able to acquire phenotypes of other Th cell subsets in response to different environmental cues[156]. It is possible that human NALT may contain Th1 cells originating from Th17 cells (ex-Th17), which is supported by the presence of IL-17A⁺IFNγ⁺ (Th17/Th1) cells.

IL-10 mediated Th1 suppression may downregulate T-bet expression in these ex-Th17 cells which removes the antagonizing effect of T-bet on RORγt function, thus reactivating the Th17 phenotype[79]. Combined with the resistance to endogenous IL-10-mediated suppression in SAg-*Sau*-activated Th17 cells, this may provide a plausible explanation for the promoting effect of exogenous IL-10 on SAg-*Sau* stimulated Th17 activation. Further investigation to elucidate mechanisms involved in this unexpected effect of IL-10 for human Th17 activation is required to inform future development and optimization of IL-10-based therapy in clinical inflammatory/autoimmune conditions.

4.4.5 IL-10 promotes GM-CSF expression in SAg-*Sau*-activated Th17 cells

While IL-10 promoted IL-17A expression in SAg-*Sau* stimulated tonsillar $CD4^+$ T cells, it appeared to reduce the cell population that co-expresses IL-17A and IFNγ (***Figure 4.11***). It has been shown that IL-17A and IFNγ double positive $CD4^+$ T cells are a subset of pathological Th17 cells associated with autoimmune pathologies[156]. Therefore, it can be argued that if IL-10 was able to suppress this specific Th17 cell subset, it remains a promising candidate to control autoimmune conditions. However, studies also reveal that granulocyte-macrophage colony-stimulating factor (GM-CSF)-producing Th17 cells are highly pathogenic, and autoreactive Th cells lacking GM-CSF fail to induce neuroinflammation despite expression of IL-17A and IFNγ[157,158]. To further evaluate the influence of IL-10 on SAg-*Sau*-activated Th17 cells, I next examined the effector phenotype of the activated Th17 cells with or without IL-10.

SAg-*Sau*-stimulated MNCs were treated with recombinant IL-10 and the expression of GM-CSF and IFNγ in the activated Th17 cells was assessed. It was surprising to find that IL-10 reduced IFNγ expression in SAg-*Sau*-activated Th17 cells, but instead significantly enhanced the expression of GM-CSF. The proportion of Th17 cell subset that co-expresses GM-CSF and IFNγ was not altered by exogenous IL-10 (***Figure 4.12 a***).

To test whether the endogenously produced IL-10 also promoted GM-CSF-producing Th17 cell, tonsillar MNCs were stimulated with SAg-*Sau* in the presence of anti-IL10 neutralizing antibody. As shown in ***Figure 4.12 b***, IL-10 depletion resulted in a significant decrease in GM-

CSF expression by SAg-*Sau*-activated Th17 cells, consistent with the positive effect of IL-10 in inducing GM-CSF$^+$ Th17 cells.

GM-CSF was originally discovered as a growth factor capable of generating granulocytes and macrophages from myeloid precursor cells. However, it was later identified that GM-CSF is not essential for myelopoiesis in steady state and circulates at low and even undetectable levels[159,160]. Instead, increased concentration of GM-CSF is found at sites of inflammation and has been shown to drive autoimmune pathologies in murine models of arthritis and EAE[160]. In tissue inflammation, GM-CSF is prominently produced by Th cells. It has been reported that GM-CSF expression in the Th cells can be induced by RORγt, the dominant transcription factor of Th17 cells, and confers pathogenicity to Th17 cells[157]. Here, I show that IL-10 not only promoted SAg-*Sau*-activated Th17 responses, but also enhanced GM-CSF expression in these Th17 cells, which challenges the well-recognized anti-inflammatory role of IL-10 and provides new insights into pleiotropic effects of cytokines.

Codarri et al. show that expression of GM-CSF in CD4$^+$ T cells can be potently inhibited by blocking Th1 cytokines, IFNγ and IL-12[157]. In my stimulating model, IL-10 effectively suppressed IFNγ expression in the Th17 cells which may be associated with the upregulated GM-CSF in these cells. It is plausible to propose that IL-10 may promote GM-CSF-producing Th17 cells via downregulating IFNγ/STAT1 signalling in the responding cells.

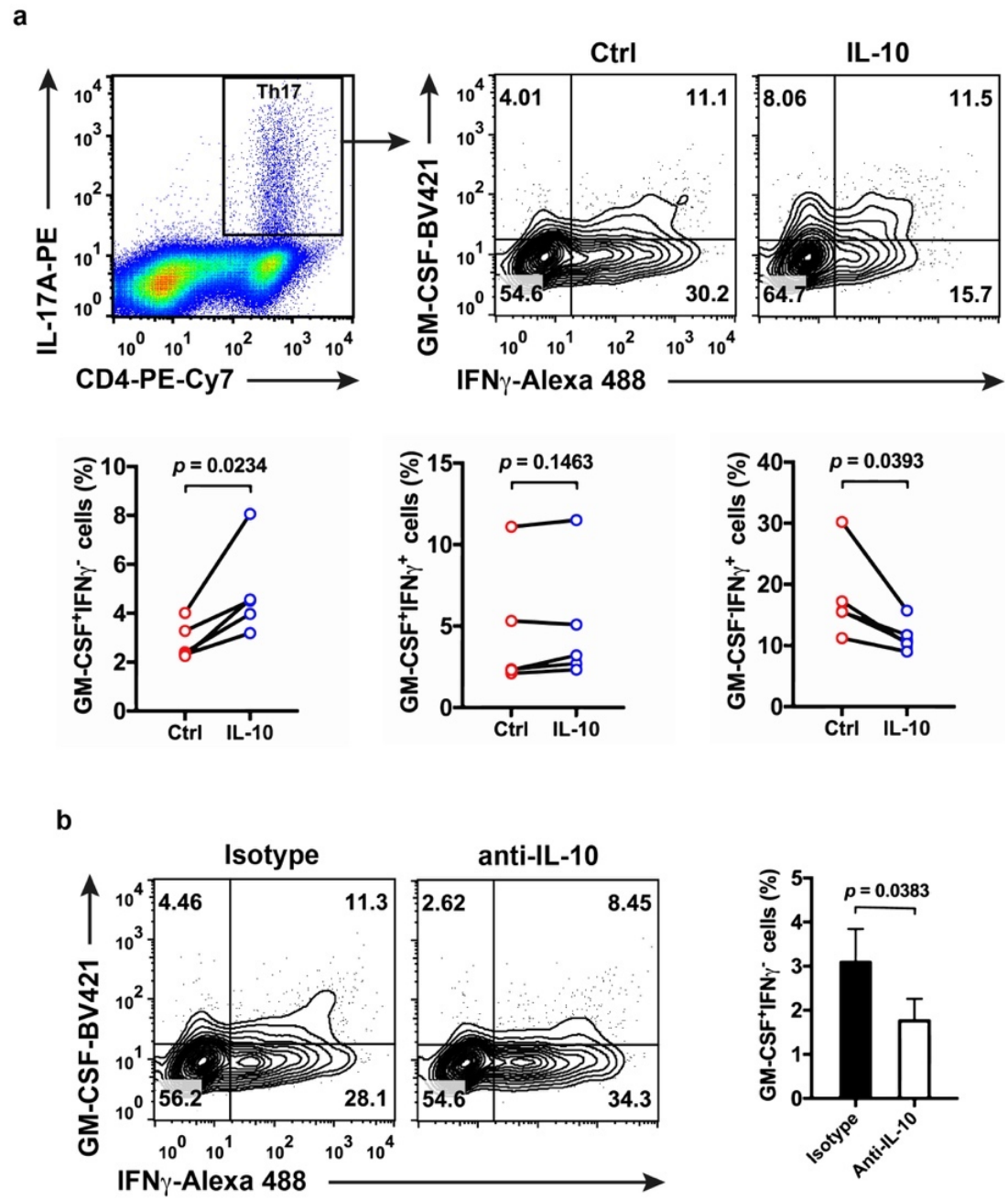

Figure 4.12 IL-10 promotes GM-CSF expression in SAg-*Sau*-activated Th17 cells

Intracellular cytokine staining was performed to detect the expression of GM-CSF and IFNγ in Th17 cells activated by SAg-*Sau* (1 μg/ml) in the presence of recombinant IL-10 (100 ng/ml) (**a**) or anti-IL-10 neutralizing antibody (1 μg/ml) (**b**). Th17 ($IL\text{-}17A^+CD4^+$) cells were gated out. The contour plots show percentages of $GM\text{-}CSF^+IFN\gamma^-$, $GM\text{-}CSF^+IFN\gamma^+$ and $GM\text{-}CSF^-IFN\gamma^+$ cells within the activated Th17 cells in the top left, top right and bottom right quadrants respectively. Individual data was plotted in the dots and lines graphs. **a)** IL-10-treated MNCs were compared to stimulation control (Ctrl), n = 5. **b)** SAg-*Sau*-stimulated MNCs were treated with anti-IL-10 and isotype control antibody respectively, n = 3. Data was analysed using paired *t*-test with *p* values indicated.

4.4.6 GM-CSF-producing CD4$^+$ T cells express high level of IL-23R

IL-23 signalling is shown to be crucial for the stabilization of Th17 cells and their ability to induce autoimmune tissue inflammation[161]. In SAg-*Sau*-stimulated tonsillar CD4$^+$ T cells, the expression of IL-23 receptor (IL-23R) was upregulated at both mRNA and protein levels (***Figure 4.13 a-c***), which is in line with the highly activated Th17 responses.

By examining the IL-23R expression in effector CD4$^+$ T cell subsets, it was revealed that GM-CSF-producing CD4$^+$ T cells expressed higher level of IL-23R than Th1 and Th17 cells (***Figure 4.13 d***). SAg-*Sau*-activated CD4$^+$ T cells were then further divided into 8 effector phenotypes depending on the expression of IL-17A, IFNγ and GM-CSF in different combinations. Notably, the IL-17A$^+$GM-CSF$^+$IFNγ^- cell population (indicated by red-outlined rectangle in ***Figure 4.13 e***), which can be promoted by IL-10 as shown above, exhibited prominent expression of IL-23R compared to other CD4$^+$ T cell phenotypes. The lowest expression of IL-23R was seen in the CD4$^+$ T cells expressing IFNγ only (***Figure 4.13 e***). The results suggest that enhanced GM-CSF expression in human tonsillar Th17 cells is associated with upregulated expression of IL-23R. This is supported by a previous study showing expression of GM-CSF in the Th17 cells is induced via IL-23 signalling in mice[158].

Using transgenic mice that express a TCR specific for myelin basic protein (MBP), it was demonstrated that GM-CSF-deficient Th17 cells had remarkably lowered ability to drive autoimmune neuroinflammation[158]. Other studies also show that both GM-CSF and IL-23R deficiency render resistance to autoimmune pathologies in mice[162,163]. GM-CSF and IL-23R are therefore suggested as molecular signature for pathological Th17 cells. My results suggest that IL-10 may drive the development of inflammatory/autoimmune pathologies in the context of SAg-*Sau* infection via promoting IL-23R^{high}GM-CSF$^+$ Th17 cells.

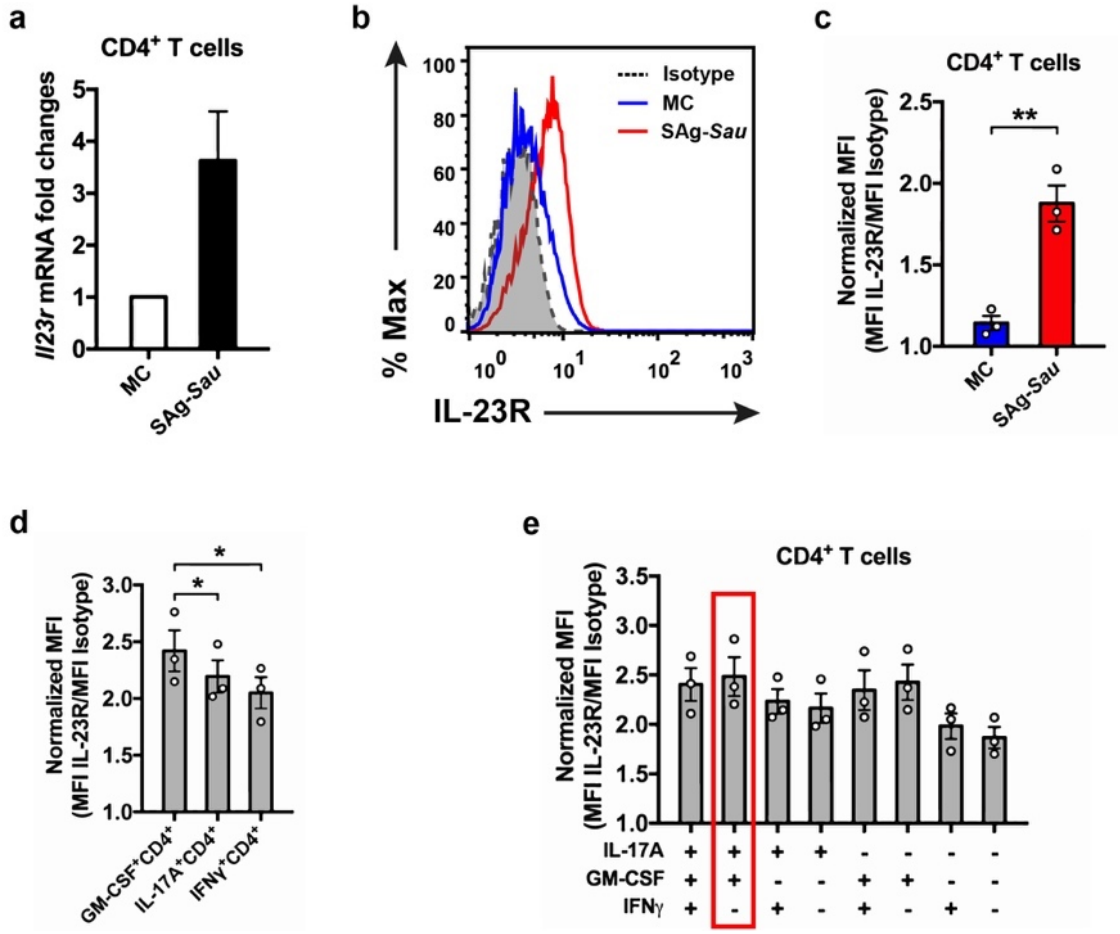

Figure 4.13 GM-CSF-producing CD4⁺ T cells express high level of IL-23R

a) CD4⁺ T cells were isolated from SAg-*Sau*-stimulated tonsillar MNCs for RNA extraction. RT-qPCR was performed to measure the RNA expression of *il23r* in SAg-*Sau*-activated CD4⁺ T cells. The Cq value of *il23r* gene was normalised by housekeeping gene *b-actin* and shown as fold increase against media control (MC) in the bar graph, n = 3. **b-e)** Tonsillar MNCs were stimulated with SAg-*Sau* for 48hrs, and the expression of IL-23R was assessed by flow cytometry. **b)** CD4⁺ T cells were gated out to show the median fluorescent intensity (MFI) of IL-23R with or without SAg-*Sau* stimulation in the histogram plot. **c)** The MFI of IL-23R was normalised by isotype control and displayed in mean ± SEM in the bar graph, n = 3. **d, e)** Expression of IL-23R shown as normalised MFI in CD4⁺ T cell subsets, n =3. Data was analysed by paired *t*-test (**c, d**). **p* < 0.05, ***p* < 0.01.

4.5 Conclusions

Foxp3⁺ Tregs and IL-10 are known to play pivotal roles in suppressing CD4⁺ T cell-mediated pro-inflammatory responses[114,146]. Although SAg-*Sau* stimulation was shown to induce Treg

expansion and enhance IL-10 production, I found that SAg-*Sau*-activated Th17 responses were not affected by increased Treg or IL-10 levels.

It has been reported that human PBMC-derived Foxp3$^+$ Tregs are able to proliferate in response to staphylococcal superantigen but cannot suppress superantigen-activated T cell proliferation[110]. My results support this published finding by showing human NALT-derived Tregs also failed to control the proliferative response of CD4$^+$ T cells stimulated by secreted antigens of SAg-*Sau.* Further, I show that both PBMC- and NALT-derived Tregs were unable to suppress SAg-*Sau*-activated Th17 responses, although they retained the suppressive ability to control Th1 activation. Intriguingly, this differential regulation of Th1 and Th17 responses was also found in IL-10-mediated suppression. Foxp3$^+$ Treg- and IL-10-mediated immune regulation are the centre of peripheral tolerance that keep over-reactive inflammatory responses and auto-reactive T cells in check. These highly resistant Th17 cells activated by SAg-*Sau* infection could lead to an unresolvable inflammation resulting in pathological tissue damage.

Intriguingly, addition of exogenous IL-10 was shown to further promote SAg-*Sau*-activated Th17 response and induce a potential pathological Th17 cell population which is IL-23R^{high}GM-CSF$^+$ in human NALT. To my knowledge, this is the first report to demonstrate that IL-10 may play a pathogenic role in certain inflammatory settings. It is conceivable that this promoting effect on pathological Th17 activation may underlie the failure of IL-10-based therapy for the treatment of clinical autoimmune diseases. Despite IL-10 has been reported to protect against Th17-mediated autoimmunity in mice, it is questioned that to what extent these experimental findings obtained from the murine studies can be translated to humans. Therefore, joint efforts should be made to clarify the potential divergent regulatory mechanisms that control human and mouse Th17 activation and illustrate the signalling pathways IL-10 has engaged with to promote the development of pathological Th17 cells in humans.

Taken together, Foxp3$^+$ Tregs and IL-10 are unable to control the potent Th17 responses activated by SAg-*Sau* in human NALT, suggesting an aberrant immune regulation of

superantigenic Th17 activation may present in the nasopharynx, which may potentially contribute to the initiation and exacerbation of inflammatory/autoimmune conditions.

CHAPTER 5

IL-35 is critical in suppressing superantigenic *Staphylococcus aureus*-activated inflammatory Th17 responses

5.1 Abstract

IL-35 has been identified as a novel suppressive cytokine that has therapeutic effects against autoimmune diseases by suppressing pathological Th17 cells in mice. However, the role of IL-35 in human Th17 activation and autoimmune disorders remains controversial. Whether human $CD4^+$ T cells express IL-35 as their murine counterparts is also disputed.

Here, I examined the expression of IL-35 in human tonsillar $CD4^+$ T cells and its role in regulating SAg-*Sau*-activated Th17 responses. It shows that IL-35 was expressed by tonsillar $CD4^+$ T cells and significantly downregulated upon SAg-*Sau* stimulation. Addition of IL-35 was able to suppress SAg-*Sau* elicited Th17 activation in high responders (fold increase in Th17 response $\geq$ 5-fold), while those low Th17 responders (fold increase in Th17 response $<$ 5-fold) were not affected. The native form of IL-35 also suppressed SAg-*Sau*-activated Th17 responses in a dose-dependent manner. Furthermore, IL-35 downregulated RORγt expression in $CD4^+$ T cells and thereby inhibited SAg-*Sau*-induced Th17 differentiation. Additionally, in mice with nasal infection of SAg-*Sau*, the cervical lymph node (CLN)-derived $CD4^+$ T cells showed markedly increased expression of IL-17A accompanied with downregulated IL-35 which was consistent with the *in vitro* findings from human NALT.

The results suggest IL-35 is a key cytokine to suppress over-reactive Th17 responses while maintaining a proper Th17 activation against bacterial/fungal infections in humans and may therefore has therapeutic potential in the management of Th17-mediated inflammatory/autoimmune diseases.

5.2 Introduction

IL-35 belongs to IL-12 family which is a unique heterodimeric cytokine family consisting of shared subunits. This cytokine family includes IL-12 (IL-12p40:IL-12p35), IL-23 (IL-12p40:IL-23p19), IL-27 (EBI3:IL-27p28) and IL-35 (EBI3:IL-12p35) (***Figure 5.1***). Different from the other family members, IL-35 shows purely suppressive effects on T cell activation, while IL-12 and IL-23 are known to promote Th1 and Th17 development respectively and the effect of IL-27 is environment-dependent[164].

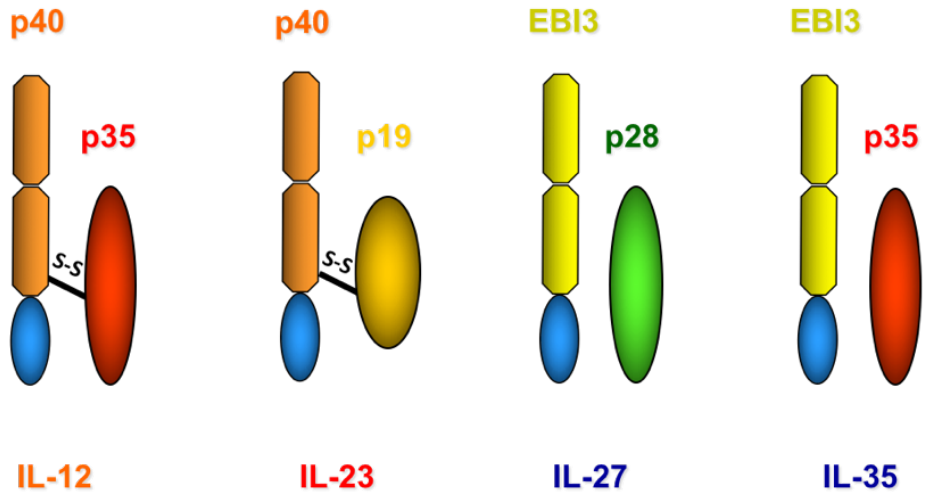

Figure 5.1 The IL-12 family of cytokines

The subunits of IL-12 and IL-23 are linked by disulphide bond (S-S), whereas EBI3 subunit is heterodimerized with p28 or p35 by protein-protein interaction to form IL-27 or IL-35.

Epstein-Barr virus-induced gene 3 (EBI3) is a homologue to IL-12 subunits, IL-12p40, which has led to the discovery of its association with another subunit of IL-12, IL-12p35 (also termed IL12A), in 1997[165]. It was postulated that the EBI3:IL-12p35 heterodimer (later named interleukin-35, IL-35 in 2007) may possess immune suppressive properties due to the following reasons. First, EBI3 is highly expressed in Epstein-Barr virus (EBV) transformed B lymphocytes and placental syncytial trophoblasts, two cell types that must survive in a potential hostile immunological environment with extensively activated NK and T cell

responses[165,166]. Second, due to the shared IL-12p35 subunit with IL-12, IL-35 is likely to antagonise IL-12's biological effects via competing for the receptor binding[165].

Later in 2007, IL-35-mediated suppression on pathological immune responses was reported in murine models of collagen-induced arthritis and inflammatory bowel disease[95,97]. Interestingly, IL-35 was found to be expressed by murine Foxp3$^+$ Tregs and contribute to their suppressive activities[97]. In the follow-up study done by the same group, a novel regulatory CD4$^+$ T cell population that express IL-35 independent of Foxp3 was identified and termed as iT$_R$35. The iT$_R$35 can be induced by treating conventional T cells with IL-35 and exhibit potent suppressive properties by restoring homeostasis and preventing lethal autoimmunity in *Foxp3*-knockout mice[94].

However, it was demonstrated that IL-35 was not constitutively expressed by human Foxp3$^+$ Tregs. Although activated human CD4$^+$ T cells were shown to express both subunits at mRNA level, the protein expression of heterodimeric IL-35 protein was not demonstrated[101]. Seyerl et al. detected enhanced production of heterodimeric IL-35 by human peripheral blood-derived CD3$^+$ T cells (including CD4$^+$ and CD8$^+$ cells) co-cultured with human rhinovirus-treated dendritic cells[167]. Nevertheless, whether IL-35 is expressed in human CD4$^+$ T cells remains inconclusive.

Murine studies have shown that IL-35 controls autoimmune pathogenesis at least partially through suppressing inflammatory Th17 responses[95,96,100,168,169]. In humans, reduced IL-35 serum level was detected in autoimmune patients with rheumatoid arthritis, Sjogren's syndrome and systemic lupus erythematosus (SLE)[102-104,170]. Since the biological activity of recombinant IL-35 is highly unstable, it has been difficult to study IL-35-mediated suppression on human Th17 cells, and further investigations to evaluate the therapeutic potential of IL-35 in human autoimmune disorders are also hindered.

I have shown in the previous chapter that both Foxp3$^+$ Tregs and IL-10 cannot effectively suppress the Th17 responses activated by SAg-*Sau.* As a promising suppressive effect of IL-35 against Th17-driven autoimmune pathologies have been demonstrated in previous studies, the regulatory role of IL-35 in human NALT was examined for SAg-*Sau*-activated Th17

responses which is a common inflammatory setting closely associated with inflammatory/autoimmune conditions.

5.3 Aims

- To detect IL-35 expression in human tonsillar $CD4^+$ T cells and determine whether it is affected by SAg-*Sau* stimulation.
- To examine the role of IL-35 in regulating SAg-*Sau*-activated Th17 responses in human NALT.
- To examine *in vivo* activation of Th17 and IL-35-expressing $CD4^+$ T cells in the cervical lymph nodes of mice infected intranasally with SAg-*Sau*.

5.4 Results and Discussion

5.4.1 SAg-*Sau* downregulates IL-35 in human tonsillar $CD4^+$ T cells

In the previous chapters, it has been demonstrated that SAg-*Sau* stimulation expands the $Foxp3^+$ Tregs and activates IL-10-expressing Tr1 cells, indicating $CD4^+$ T cell-mediated immune regulatory mechanisms were activated by SAg-*Sau*. However, the potent Th17 responses activated by SAg-*Sau* were not suppressed by either of them, suggesting an aberrant immune suppression on SAg-*Sau*-activated Th17 responses. It therefore led to the question of what role IL-35-expressing iT_R35 might play in human nasopharynx infected with SAg-*Sau*. To answer this intriguing question, the first step is to resolve the controversy of whether human $CD4^+$ T cells express heterodimeric IL-35.

In order to detect the expression of IL-35 in human tonsillar $CD4^+$ T cells, $CD4^+$ T cells were separated from tonsillar MNCs either unstimulated or stimulated with *Sau*-derived antigens and both mRNA and protein expression of IL-35 subunits, IL12A and EBI3, were examined. It has been reported that IL-12A was expressed constitutively by human $CD4^+$ T cells but EBI3

was undetectable in any $CD4^+$ T cell subset, including effector and regulatory T cells, without stimulation in peripheral blood[101]. However, I show here that both IL-12A and EBI3 were detected at mRNA and protein levels in unstimulated $CD4^+$ T cells in tonsils (***Figure 5.2 and 5.3 a***). Although the protein expression of EBI3 in unstimulated $CD4^+$ T cells was relatively low, it was able to form heterodimer with IL-12A which can be detected by immunoprecipitation (***Figure 5.3***).

Intriguingly, a significant reduction of both *Il12a* and *Ebi3* mRNA was observed in SAg-*Sau*-stimulated tonsillar $CD4^+$ T cells (***Figure 5.2***). Although a slightly enhanced level of EBI3 protein was detected in SAg-*Sau*-activated $CD4^+$ T cells which may indicate a reduced secretion of EBI3 protein, the protein expression of IL-12A was remarkably decreased, consistent with the mRNA expression (***Figure 5.3 a***).

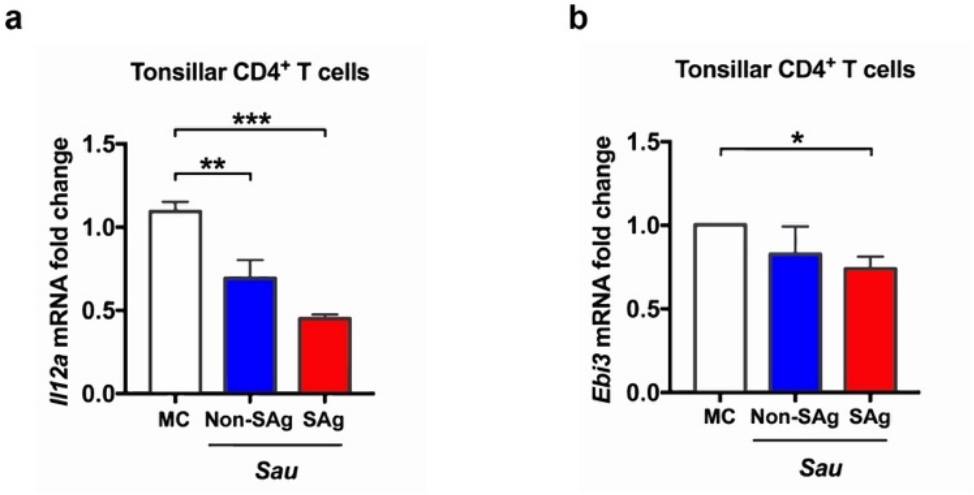

Figure 5.2 SAg-*Sau* downregulates mRNA expression of IL-35 in human tonsillar $CD4^+$ T cells

Tonsillar MNCs were stimulated with 1 µg/ml of *Sau* for 24hrs followed by isolating $CD4^+$ T cells to detect mRNA expression of *il12a* and *ebi3* in the cells. The targeted gene expression was normalized to the expression of *b-actin*. The fold change in *il12a* (**a**) and *ebi3* (**b**) mRNA expression compared to media control (MC) are shown in the bar graphs with mean ± SEM, n = 4. Data was analysed using paired *t*-test, $*p < 0.05$, $**p < 0.01$, $***p < 0.001$.

By performing immunoprecipitation, it was confirmed that SAg-*Sau*-stimulated downregulation of IL12A had resulted in a marked decrease of IL-35 heterodimer in tonsillar CD4$^+$ T cells (***Figure 5.3 b***), and this was in contrast to the upregulated IL-10 expression shown in the previous chapter.

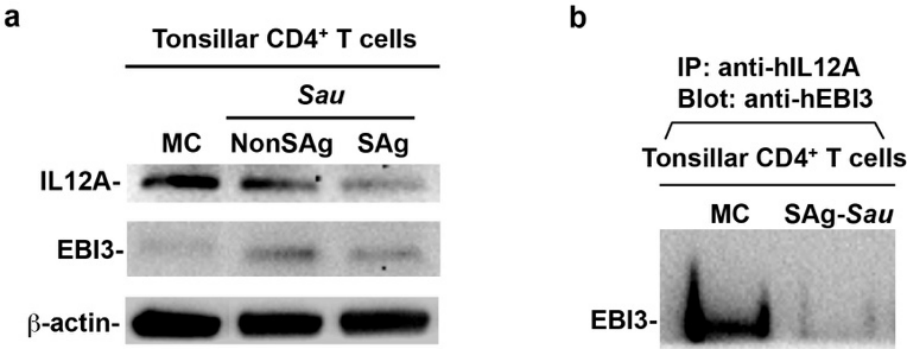

Figure 5.3 Protein expression of IL-35 in human tonsillar CD4$^+$ T cells is inhibited by SAg-*Sau*

Tonsillar CD4$^+$ T cells were isolated from *Sau* stimulated MNCs at 48hrs. **a)** The protein expression of IL-12A and EBI3 subunits in NonSAg-*Sau* and SAg-*Sau* activated CD4$^+$ T cells was detected by Western blot. **b)** CD4$^+$ T cell lysates were immunoprecipitated using anti-human IL12A (anti-hIL12A) and blotted with anti-human EBI3 (anti-hEBI3) to detect heterodimeric IL-35 in the cells. The results represent 3 independent experiments.

Reciprocal expression of IL-35 and IL-10 in Foxp3$^+$ Tregs has been demonstrated in murine studies, defining two separated effector Treg populations[171,172]. In humans, the expression of IL-35 is not dependent on Foxp3, and I have shown that SAg-*Sau* activated IL-10 expression primarily in Foxp3$^-$ Tr1 cells. However, the notion of segregated T cell population that produces IL-35 and IL-10 respectively may also apply and be presented as IL-35-producing iT$_R$35 and IL-10-producing Tr1 cells in humans.

The mRNA expression of *Il12a* was also reduced by NonSAg-*Sau* stimulation, but the reduction was less significant at protein level. It suggests that *Sau*-derived superantigens and other soluble antigens both contribute to the downregulation of IL-35 in tonsillar CD4$^+$ T cells. To the best of my knowledge, this is the first study to show SAg-*Sau*-mediated alteration of

IL-35 expression in $CD4^+$ T cells. With evidence provided by previous studies demonstrating suppression of inflammatory Th17 responses by IL-35, It was hypothesized that marked reduction of IL-35-expressing $CD4^+$ T cells following SAg-*Sau* stimulation may underlie the potent Th17 activation. Further studies to identify specific staphylococcal antigens that modulate IL-35-expressing $CD4^+$ T cell function may inform new strategies for novel vaccines targeting *Sau*-driven inflammatory diseases.

5.4.2 IL-35 suppresses over-reactive Th17 responses in SAg-*Sau* stimulated tonsillar MNCs

I next examined the hypothesis that SAg-*Sau* downregulated IL-35 expression was contributing to the strong Th17 responses by supplementing recombinant IL-35 to SAg-*Sau* stimulated tonsillar MNCs. Tonsillar MNCs were stimulated with SAg-*Sau* in the presence/absence of recombinant IL-35 followed by examining the Th17 responses. To better reflect the individual difference in the level of Th17 response activated by SAg-*Sau*, the activated Th17 responses were normalised and presented as fold increase against unstimulated media controls for each sample. Interestingly, the percentage of IL-35-mediated Th17 suppression was shown to be positively correlated with the level of Th17 activation (***Figure 5.4 a***).

The average fold increase in Th17 cells following NonSAg-*Sau* and SAg-*Sau* stimulation was 2.25 (range: 1.22-5.40) and 4.67 (range: 2.50-9.82) respectively (***Figure 5.4 b***). To further delineate IL-35-mediated Th17 suppression, the tonsillar samples were then divided into high responders ($\geq$ 5-fold increase) and low responders (< 5-fold increase) based on the average fold increase of the Th17 proportion within SAg-*Sau*-activated tonsillar $CD4^+$ T cell population. As shown in ***Figure 5.5 a***, the addition of IL-35 significantly reduced Th17 activation in the high responder group, whereas there was no effect on the low responders. Consistent with this, IL-17A production was also decreased in the culture supernatant of the high responders following IL-35 treatment (***Figure 5.5 b***). These results suggest that IL-35 is able to suppress

over-reactive Th17 responses while maintaining a low level of Th17 activation for the host defence in human NALT.

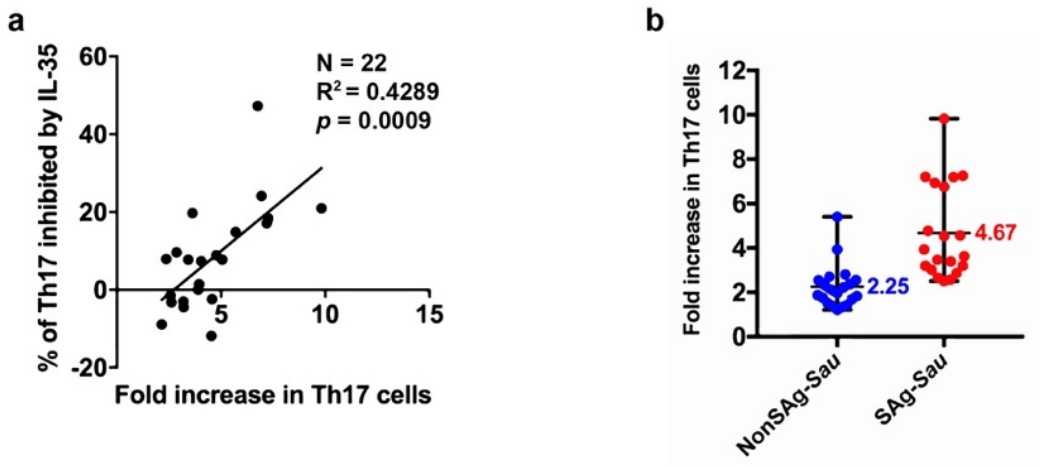

Figure 5.4 Inhibition of SAg-*Sau*-activated Th17 responses by IL-35 is associated with the level of Th17 activation

Tonsillar MNCs were stimulated with *Sau* CCS for 48hrs, and the Th17 responses were analysed as fold increase in percentage of Th17 cells against media control. **a)** The association between fold increase in Th17 proportion and Th17 inhibition by IL-35 (100 ng/ml) was analysed using linear regression. The R^2 and *p* values are displayed, n = 22. **b)** The Th17 fold increase in NonSAg-*Sau* and SAg-*Sau* stimulated MNCs are shown in mean with range, and individual data points are plotted. Mean values are indicated, n = 20 per stimulation group.

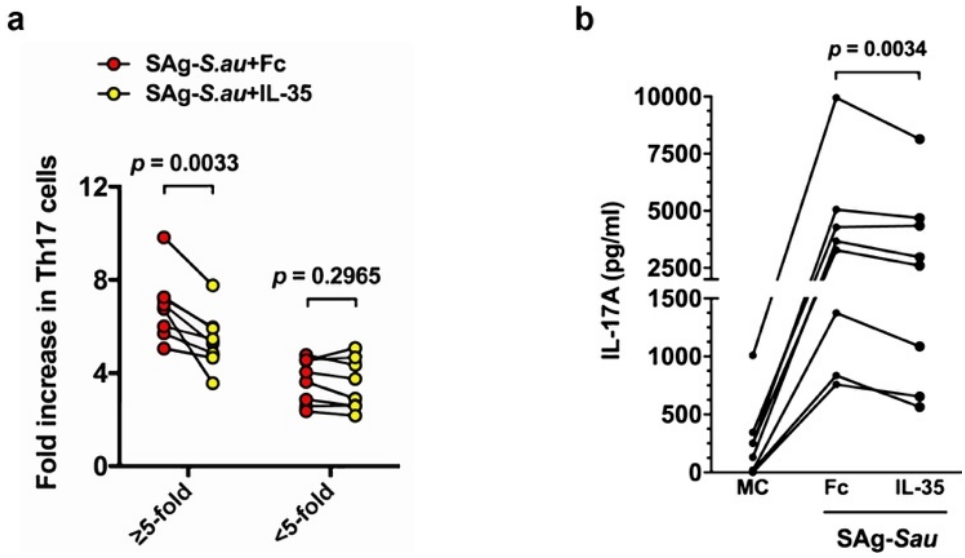

Figure 5.5 IL-35 suppress SAg-*Sau*-activated Th17 responses in the high responders

Tonsillar MNCs were treated with 100 ng/ml of IL-35 or Fc control protein and stimulated with SAg-*Sau* CCS. The Th17 responses were analysed at 48hrs. **a)** Suppression of SAg-*Sau*-activated Th17 responses by IL-35 in high responder group (fold increase ≥ 5-fold) and low responder group (fold increase < 5-fold) are shown, n = 8 per group. **b)** IL-17 concentration in the MNC culture supernatant of the high responders treated with IL-35 and the Fc control protein respectively, n = 8. Data was analysed using paired *t*-test with *p* values indicated.

IL-10 was shown to suppress SAg-*Sau*-activated IFNγ expression and in fact promoted IL-17A expression in tonsillar $CD4^+$ T cells (described in ***4.4.4***). To examine whether IL-10 and IL-35 were playing divergent roles in SAg-*Sau*-activated Th1 and Th17 responses, the suppressive effect of IL-35 was compared to that of IL-10 on the effector $CD4^+$ T cell responses stimulated by SAg-*Sau*. Indeed, IL-35 was shown to suppress the $IL\text{-}17A^+IFN\gamma^-$ cells without affecting the $IL\text{-}17A^-IFN\gamma^+$ $CD4^+$ T cell population which was in contrast to IL-10-mediated suppression (***Figure 5.6***), suggesting a reciprocal regulation of Th1 and Th17 activation by IL-10 and IL-35 in the context of SAg-*Sau* infection.

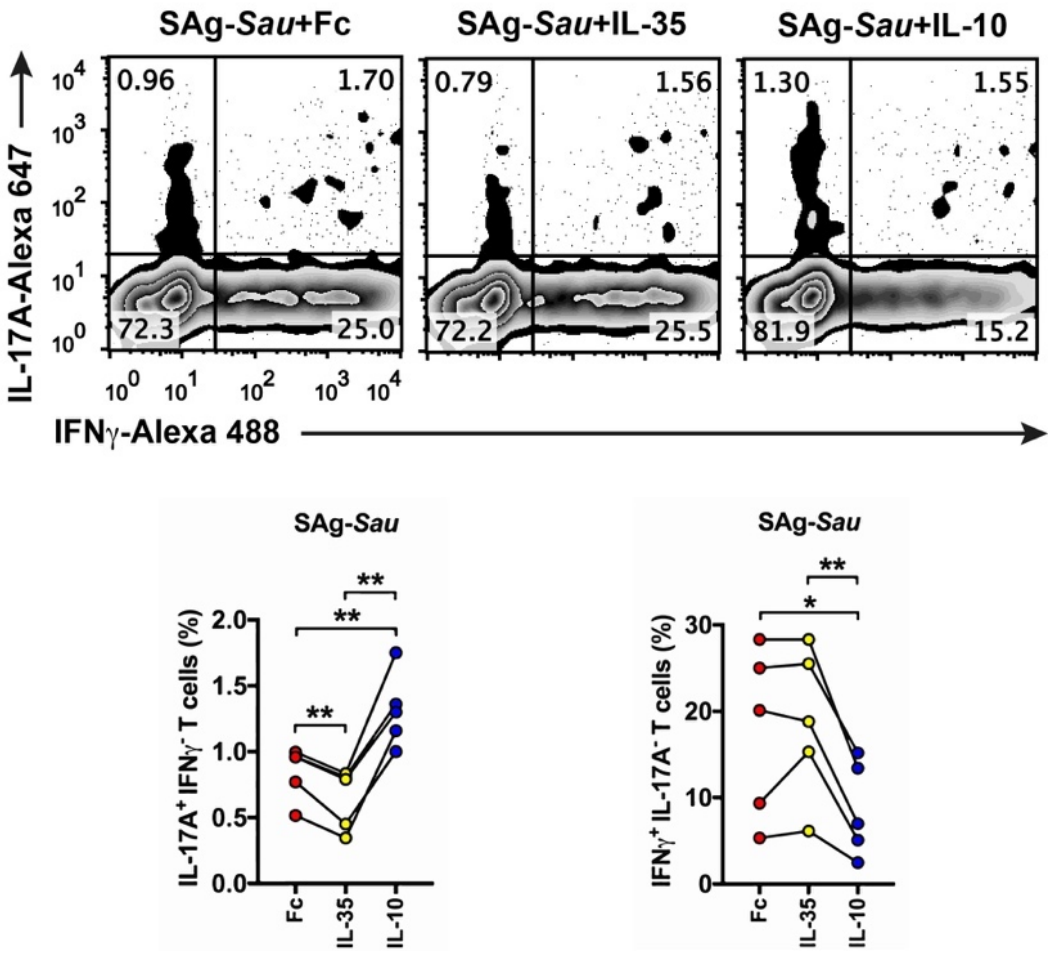

Figure 5.6 IL-35 and IL-10 have opposite effects on SAg-*Sau*-activated Th1 and Th17 responses

Tonsillar MNCs were treated with recombinant IL-35 or IL-10 and stimulated with SAg-*Sau* CCS for 48hrs, and expression of IL-17A and IFNγ in $CD4^+$ T cells were determined by intracellular staining. The zebra plots on the top were gated on $CD4^+$ T cells, and numbers in top left and bottom right quadrants indicate percentages of $IL\text{-}17A^+IFN\gamma^-$ and $IL\text{-}17A^-IFN\gamma^+$ cells respectively. Individual data was plotted in the dots and lines graphs, n = 5. Data was analysed using paired *t*-test, $*p < 0.05$, $**p < 0.01$.

The recombinant IL-35 used for the above experiments was an Fc fusion protein with linked EBI3 and IL-12A, which is widely used to study the biological function of IL-35[95,173,174]. Although an Fc control protein was used at all times to exclude possible biological effects from the human IgG1 Fc protein region included in the recombinant protein, the way that the protein

subunits were fused together may also have impact on the biological activity of the recombinant IL-35. To confirm that the IL-35 mediated suppression of SAg-*Sau* activated Th17 response in tonsillar MNCs was not due to artificial IL-35-Fc fusion protein, a transfected CHO cell line producing the native form of IL-35 was constructed by introducing IL-12A and EBI3 expressing plasmids into CHO cells respectively. As shown in ***Figure 5.7***, both IL-12A and EBI3 proteins were expressed in 4 transfected CHO cell colonies selected (C7, C8, C14 and C15), and the heterodimeric IL-12A/EBI3 protein secretion was confirmed by Co-IP Western Blot. The conditioned medium generated by C7 CHO cells, which produced the highest amount of the IL-35 heterodimer, was used to examine the suppressive activity of native IL-35 on SAg-*Sau* stimulated Th17 response.

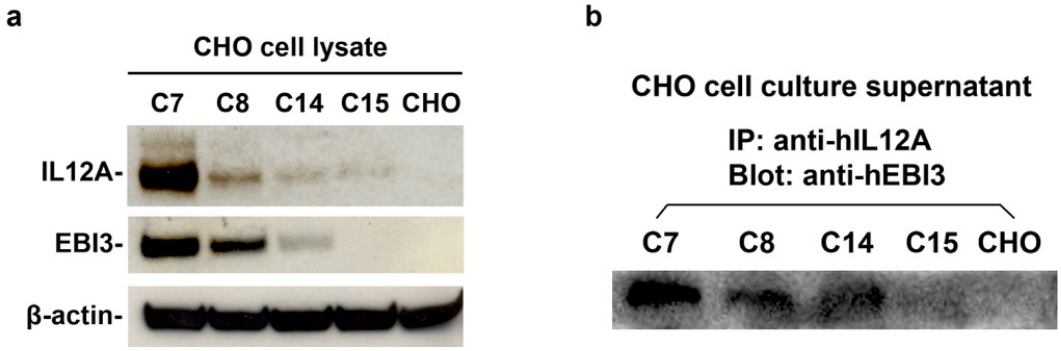

Figure 5.7 Secretion of native form IL-35 by IL-35-expressing CHO cells

The CHO cells were transfected with plasmids encoding human EBI3 (pRP-Neo-hEBI3) and human IL-12A (pRP-Puro-hIL12A). **a)** Protein expression of IL-12A and EBI3 in the transfected CHO cell clones (C7, C8, C14 and C15) and control CHO cells (CHO) were detected by Western blot (this image was kindly provided by Richard Ali and Dr. Xiaoqing Wei from Cardiff University). **b)** Measurement of heterodimeric IL-35 in the culture supernatant of transfected CHO cells by co-immunoprecipitation (Co-IP).

Tonsillar MNCs were cultured in medium containing C7 CHO cell or control CHO cell conditioned medium (either 1, 2 or 10%) and stimulated with SAg-*Sau*. The native IL-35 showed inhibition of SAg-*Sau* activated Th17 proliferation in a dose-dependent manner (***Figure 5.8***). Thus, it was confirmed that both IL-35-Fc and the native form of IL-35 were

functionally capable of regulating SAg-*Sau* activated Th17 response in human tonsillar MNCs. Recombinant IL-35 with Fc fusion was used for all subsequent experiments.

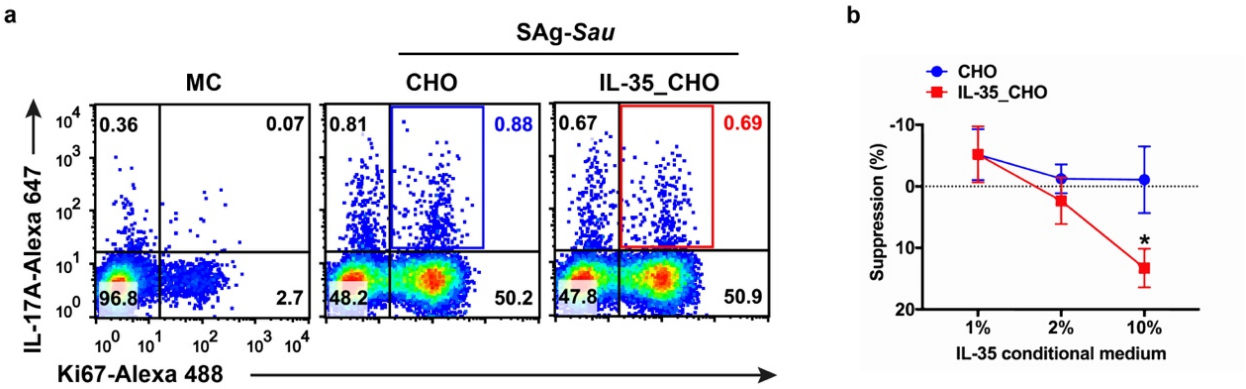

Figure 5.8 Native form IL-35 supresses SAg-*Sau*-activated Th17 proliferation

Tonsillar MNCs were stimulated with SAg-*Sau* CCS (1µg/ml) in the presence of conditioned medium from CHO-C7 or control CHO cells at 1%, 2% and 10% respectively. **a)** Dot plots were gated on $CD4^+$ T cells and numbers in top right quadrants indicate the percentage of $IL\text{-}17A^+$ $Ki67^+$ cells (Proliferating Th17 cells). **b)** Suppression (%) of Th17 proliferation was calculated against stimulated MNCs without conditioned medium. Data displayed is mean ± SEM, n = 5. Data was analysed using paired *t*-test, $*p < 0.05$.

IL-35 signals through interleukin-12 receptor subunit beta 2 (IL-12Rβ2) and glycoprotein 130 (gp130) to activate members of the Janus kinase (Jak) family followed by phosphorylation of signal transducer and activator of transcription (STAT1 and STAT4), thereby suppressing the proliferative responses of effector T cells in mice[175]. However, the downstream signalling pathways involved in IL-35-mediated suppression of Th17 responses are yet to be elucidated. Both IL-12 and IL-35 bind to IL-12Rβ2 but modify downstream gene transcriptions distinctively. IL-12 is well known for its ability to promote Th1 development, while IL-35 acts on IL-12Rβ2/STAT4 pathway to suppress helper T cell responses. gp130 is a common co-receptor for IL-6 family cytokines and mediates phosphorylation of STAT1 and STAT3 upon ligand binding. Collison et al. show that IL-35 interacts with gp130 to activate STAT1 signalling which also leads to the suppression of effector T cells. They further demonstrate that induction of IL-

35 expression in effector CD4$^+$ T cells by IL-35 requires both receptors and through a unique and unconventional STAT1:STAT4 heterodimer[175].

In human tonsillar MNCs, IL-12Rβ2 was primarily expressed in CD4$^+$ T cells and markedly higher expression of gp130 was also detected in CD4$^+$ T cell population compared to the CD4$^+$ cell-depleted lymphocytes (***Figure 5.9***). It suggests that IL-35-mediated suppression of SAg-*Sau*-activated Th17 responses is likely a direct suppression on the activated CD4$^+$ T cells through JAK/STAT signalling.

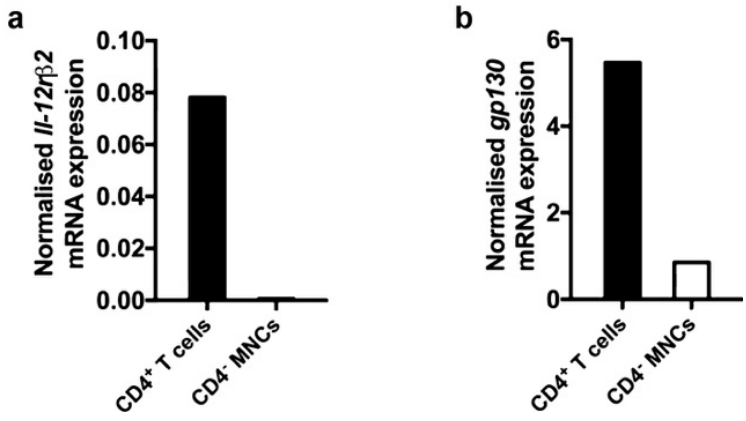

Figure 5.9 IL-35 receptors are primarily expressed in CD4$^+$ T cells in human NALT

mRNA expression of *Il-12rβ2* (**a**) and *gp130* (**b**) was examined in freshly isolated tonsillar CD4$^+$ T cells and CD4$^-$ MNCs. The targeted gene expression was normalized to the expression of *b-actin*.

IL-10- and Treg-dependent mechanisms have been reported to play a role in IL-35-mediated Th17 suppression[98,169]. However, I have demonstrated that IL-10- and Treg-mediated suppression of the Th17 activation stimulated by SAg-*Sau* is impaired, which may explain why IL-35 was not able to suppress SAg-*Sau*-activated Th17 response in tonsillar MNCs from low responders. The mechanism used by IL-35 to suppress the Th17 response in high responders may require expression of the IL-12Rβ2:gp130 heterodimer at high levels in activated Th17 cells, thus allowing IL-35 to signal through an unconventional pathway to induce IL-35 expression in the targeted Th17 cells. Similar to IL-10 expression in Th17 cells, which directs the cell towards a regulatory phenotype[86], IL-35 expression in pathological Th17 cells may

also elicit an anti-inflammatory gene expression profile to reverse the post-activation fate of pathogenicity.

5.4.3 IL-35 downregulates SAg-*Sau*-induced RORγt expression and inhibits Th17 differentiation

IL-35 has been reported to suppress Th17 cell differentiation[164,176]. It is therefore interesting to examine the effect of IL-35 on SAg-*Sau*-induced Th17 differentiation from naïve tonsillar $CD4^+$ T cells. CD45RO is expressed on the cell surface of memory but not naïve T cells. Depleting $CD45RO^+$ cells using magnetic cell sorting can therefore remove the memory $CD4^+$ T cells from the tonsillar MNCs. Over 99% of $CD45RO^+CD4^+$ T cells was removed following magnetic cell sorting (***Figure 5.10***).

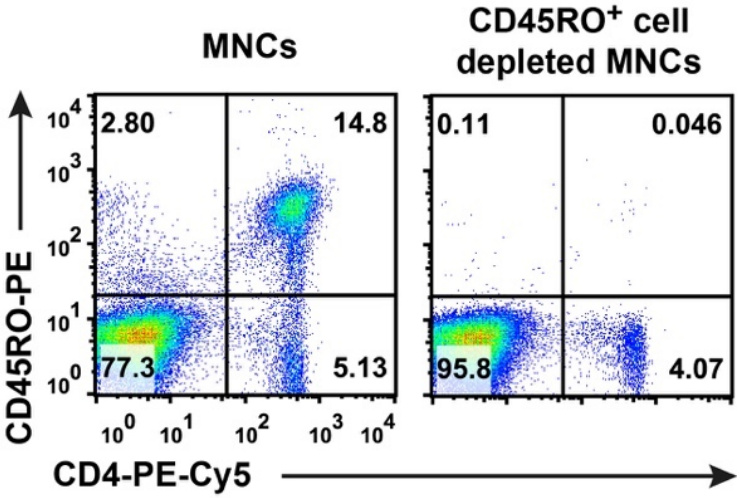

Figure 5.10 The efficiency of depleting $CD45RO^+$ memory T cells using magnetic cell sorting

Dot plots showing percentages of $CD45RO^+CD4^+$ cells (numbers in top right quadrants) in unfractionated tonsillar MNCs and $CD45RO^+$ cell depleted MNCs.

$CD45RO^+$ cell-depleted MNCs were then stimulated with SAg-*Sau* in the presence of Th17 polarizing cytokines (IL-1β, IL-21 and TGFβ1) for 7 days either with or without IL-35. SAg-*Sau*

induced IL-17A production was significantly reduced by the addition of IL-35 (***Figure 5.11 a***). The expression of RORγt, the key transcription factor controlling the differentiation of Th17 cells[59], was also analysed. Along with reduced IL-17A production, SAg-*Sau* induced RORγt expression in $CD4^+$ T cells was downregulated by IL-35 (***Figure 5.11 b***), suggesting that IL-35 could suppress SAg-*Sau*-induced Th17 differentiation via direct inhibition of RORγt expression.

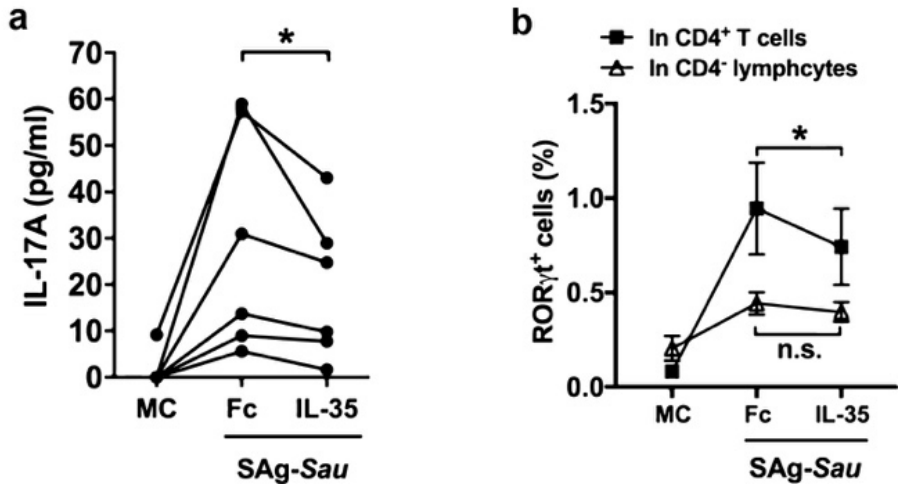

Figure 5.11 IL-35 inhibits SAg-*Sau*-induced RORγt expression and Th17 differentiation

$CD45RO^+$ cell depleted tonsillar MNCs were stimulated with SAg-*Sau* CCS (50ng/ml) for 7 days in the presence of recombinant IL-1β (50ng/ml), IL-21 (50ng/ml) and TGFβ1 (2ng/ml). 10ng/ml of recombinant IL-35 or Fc control protein were added at day 0 and day 3. **a)** IL-17A concentration in the cell culture supernatants as measured by ELISA, n = 6. **b)** Line plot showing the percentage of $ROR\gamma t^+$ $CD4^-$ lymphocytes and $ROR\gamma t^+$ $CD4^+$ T cells in SAg-*Sau* stimulated tonsillar MNCs with or without IL-35. Mean ± SEM are shown, n = 4.

Orphan nuclear receptor RORγt has long been known as a transcription factor expressed by $CD4^+CD8^+$ double-positive (DP) thymocytes and lymphoid-tissue-inducer (LTi) cells, which is required for the regulation of thymic development and lymphoid-tissue genesis[177]. Ivanov et al. discovered that RORγt was also expressed in a subpopulation of lamina propria T cells and directed the differentiation of Th17 cells[59]. Later studies have surged to provide accumulating evidence demonstrating that RORγt is the master transcription factor to drive the gene

transcription profile of Th17 lineage, and RORγt deficiency results in the lack of Th17 cells and thereby confers protection against autoimmune pathologies. Small molecules and proteins that block the activity of RORγt have been developed and show promising effects in clinical trials for autoimmune diseases, such as psoriasis and multiple sclerosis. Here, I show that IL-35 treatment was able to downregulate the expression of RORγt in the $CD4^+$ T cells, thereby hampering the development of Th17 cells in the context of SAg-*Sau* stimulation. This may serve, at least partially, the mechanism of IL-35-mediated suppression of SAg-*Sau*-activated Th17 responses.

5.4.4 SAg-*Sau*-activated IL-23R expression in $CD4^+$ T cells is not altered by IL-35

The differentiation and activation of Th17 cells are facilitated by certain cytokines, such as TGFβ, IL-1β, IL-6 and IL-23. It is shown in Chapter 4 and here that SAg-*Sau* stimulation enhanced the expression of IL-23R in $CD4^+$ T cells (***Figure 5.12***). Although IL-23 signalling is not required for the initial development of Th17 lineage, it is essential for Th17 cells to maintain stable phenotype in the effector phase and contributes to the pathological features of Th17 cells in inflammatory settings. IL-35 has been shown to inhibit the transcription factor RORγt during Th17 differentiation. It was tempting to know whether IL-35 suppressed the effector and memory Th17 cells activated by SAg-*Sau* through downregulating the IL-23 signalling in Th17 cells. To examine this hypothesis, SAg-*Sau* stimulated tonsillar MNCs were treated with recombinant IL-35 and the expression of IL-23R in $CD4^+$ T cells were measured by RT-qPCR and flow cytometry.

Both mRNA and protein expression of IL-23R in SAg-*Sau*-activated $CD4^+$ T cells did not change following addition of IL-35, as shown in ***Figure 5.12***. It indicates IL-35-mediated suppressive signals may not act on the pathway that regulates the expression of IL-23R in Th17 cells. However, If IL-35-mediated suppression of SAg-*Sau*-activated Th17 response was dependent on the cell surface expression of IL-12Rβ2:gp130 heterodimer, it would mean that only a small proportion of Th17 cells are specifically targeted. Changes in IL-23R expression in these cells may be too subtle to be detected in the whole $CD4^+$ T cell population. Further

studies using single-cell RNA sequencing may help to characterise these SAg-*Sau*-activated Th17 cells which could be specifically regulated by IL-35.

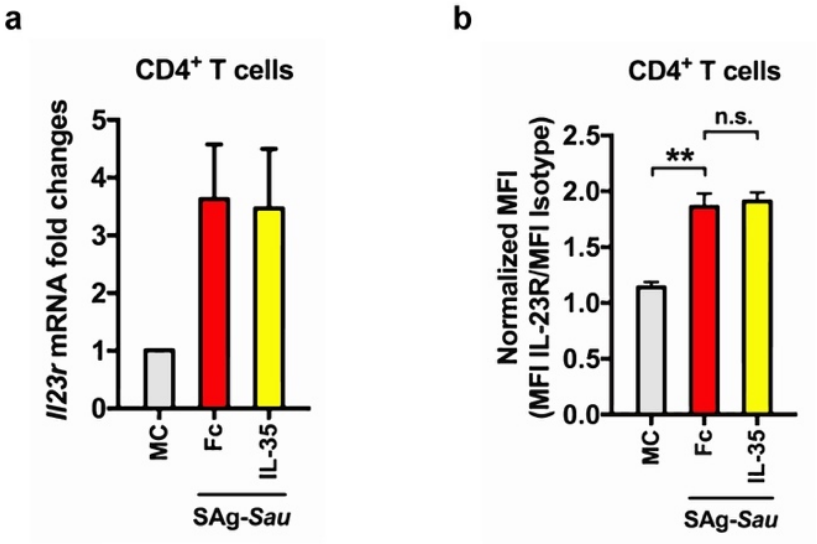

Figure 5.12 Expression of IL-23R in SAg-*Sau*-activated CD4$^+$ T cells is not altered by IL-35

a) Tonsillar MNCs were stimulated with SAg-*Sau* CCS for 24hrs in the presence of IL-35 or Fc control protein and followed by CD4$^+$ T cell isolation. mRNA was extracted from isolated CD4$^+$ T cells for RT-qPCR. *Il23r* mRNA expression is shown as fold change against media control (MC) in the bar graph, n = 3. **b)** SAg-*Sau*-stimulated MNCs were treated with IL-35 for 48hrs and the protein expression of IL-23R was examined by flow cytometry. The median fluorescent intensity (MFI) of the IL-23R-APC in the CD4$^+$ T cells was normalized by the isotype control and shown as mean ± SEM in the bar graph, n=3. Data was analyzed using paired *t*-test, $^{**}p < 0.01$, n.s. means not significant.

5.4.5 IL-35 does not affect CD39 expression in SAg-*Sau*-expanded Tregs

Although previous studies tend to support the notion that IL-35 acts directly on the effector T cells to suppress their activation, Treg-dependent mechanisms has been reported[94,169,175]. It was shown IL-35 suppressed Th17 cells and ameliorated pathological changes in murine models of collagen-induced arthritis (CIA) by promoting CD39$^+$ Tregs, as well as Foxp3$^-$ CD39$^+$CD4$^+$ T cells[169]. The importance of CD39 expression in human Tregs for their suppressive effect against Th17 activation was discussed in chapter 3 and the Foxp3$^+$ Treg

population expanded by SAg-*Sau* had a significantly lower proportion of CD39$^+$ cells has been shown in ***3.4.6***. Hence, it would be interesting to examine whether IL-35 was able to enhance CD39 expression in SAg-*Sau*-expanded Tregs and thereby enabling these Tregs to effectively suppress the Th17 activation.

As shown in ***Figure 5.13***, high frequency of CD39$^+$ cells were detected in the Foxp3$^+$ Treg population without stimulation. However, the frequency of CD39$^+$ cells dropped significantly in SAg-*Sau*-stimulated Tregs, and this downregulation of CD39 cannot be rescued by IL-35 treatment. Therefore, IL-35 seems not to act through Foxp3$^+$ Tregs for its suppression of Th17 responses in human NALT activated with SAg-*Sau*.

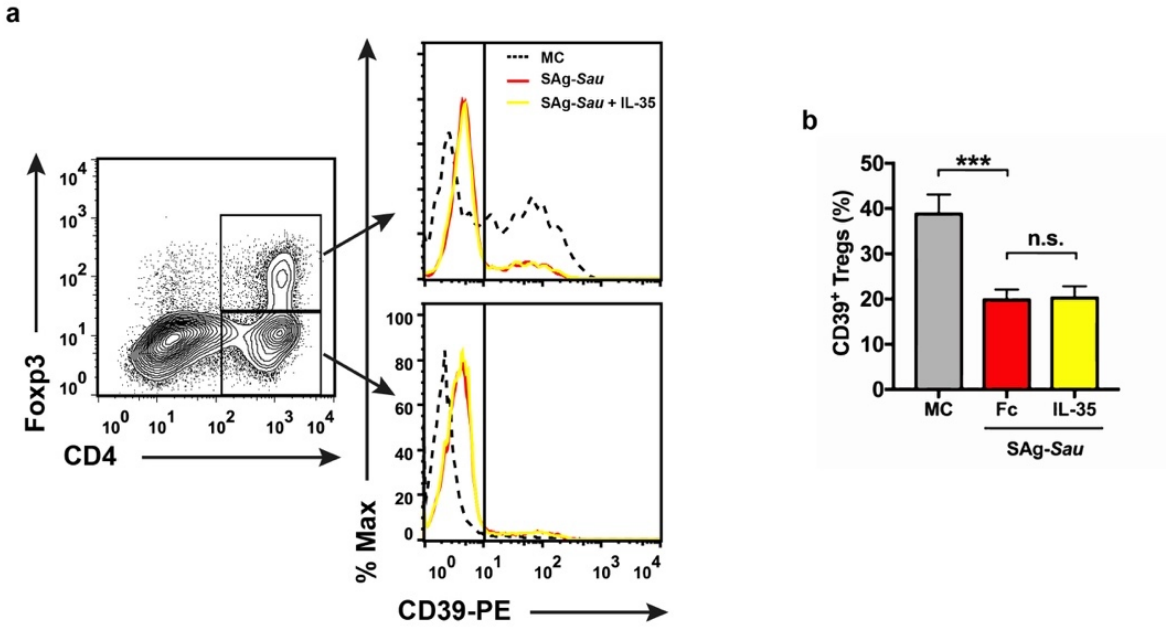

Figure 5.13 IL-35 does not affect CD39 expression in SAg-*Sau*-expanded Tregs

MNCs were stimulated with SAg-*Sau* CCS in the presence of IL-35 or Fc control protein for 48hrs, and cell surface expression of CD39 on Foxp3$^+$ Tregs was examined by flow cytometry. **a)** Histograms showing the MFI of CD39 bound by PE-conjugated antibody in Foxp3$^+$CD4$^+$ (top) and Foxp3$^-$CD4$^+$ (bottom) cells respectively, with CD39$^+$ cells gated in the right compartments. **b)** Percentages of CD39$^+$ cells within Foxp3$^+$ Tregs were summarised in the bar graph, n = 10. Data was analysed using paired *t*-test and Wilcoxon matched-pairs signed rank test, ***$p < 0.001$.

5.4.6 SAg-*Sau* colonization of the mouse nasopharynx induces IL-17A expression and downregulates IL-12A in the cervical lymph node $CD4^+$ T cells

I have demonstrated a highly activated Th17 response in human tonsillar MNCs driven by SAg-*Sau*, which was associated with downregulated IL-35 expression in the $CD4^+$ T cells *in vitro*. A mouse nasal colonization model was used to further examine the *in vivo* activation of NALT $CD4^+$ T cells. C57BL/6 mice were intranasally infected with SAg-*Sau* and the Th17 response in the cervical lymph nodes (CLN) was assessed after secondary infection. All mice infected with SAg-*Sau* carried the bacterium at 24hrs post-secondary infection (***Figure 5.14 a***). Consistent with *in vitro* Th17 activation by SAg-*Sau* in human tonsillar MNCs, mice infected with SAg-*Sau* also had significantly higher *Il17a* mRNA expression in their CLN $CD4^+$ T cells compared to their naïve counterparts (***Figure 5.14 b***). The mRNA expression of *Il12a* and *Ebi3* were also determined. Although less significant than in human tonsillar $CD4^+$ T cells, the expression of *Il12a* in the mouse CLN $CD4^+$ T cells was also reduced by SAg-*Sau* colonization, while *Ebi3* expression remained unchanged (***Figure 5.15***).

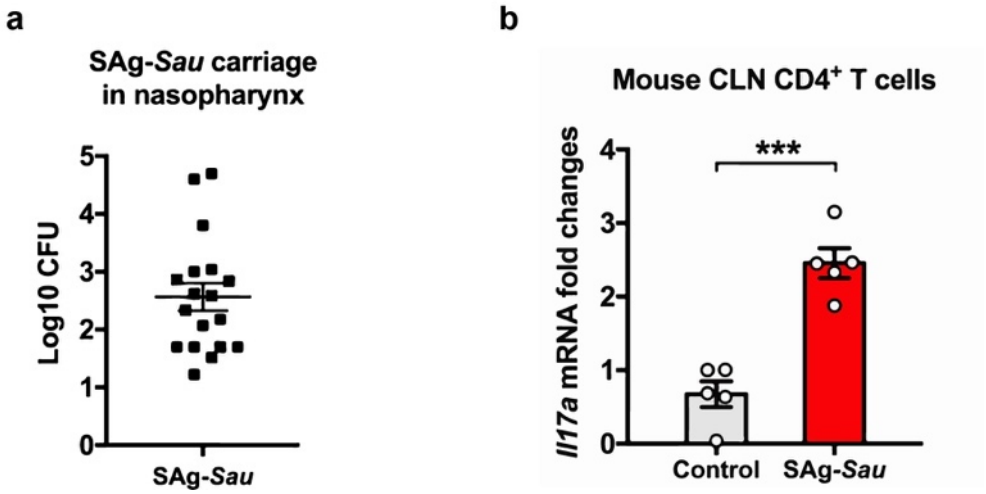

Figure 5.14 Nasal colonization of SAg-*Sau* induces IL-17A expression in mouse cervical lymph node CD4$^+$ T cells

C57BL/6 mice were infected intranasally with 10^7 CFU of SAg-*Sau* at day 0 and day 14 respectively. Nasopharynx and cervical lymph nodes (CLN) were harvested at 24hrs post-secondary infection. **a)** Nasopharyngeal homogenates were plated on blood agar plates and colonies were counted after overnight culture. **b)** CLN from 3 mice were pooled for lymphocyte isolation and CD4$^+$ T cell separation. mRNA was extracted from separated CD4$^+$ T cells for RT-qPCR. The mRNA expression of *Il17a* are shown as fold change against control mice. Results represent 2 independent experiments, 9 mice per group were used in each experiment. Data was analysed using unpaired *t*-test and displayed as mean ± SEM. Mouse intranasal infection and tissue dissection were done by Dr. Rebecca K. Shears.

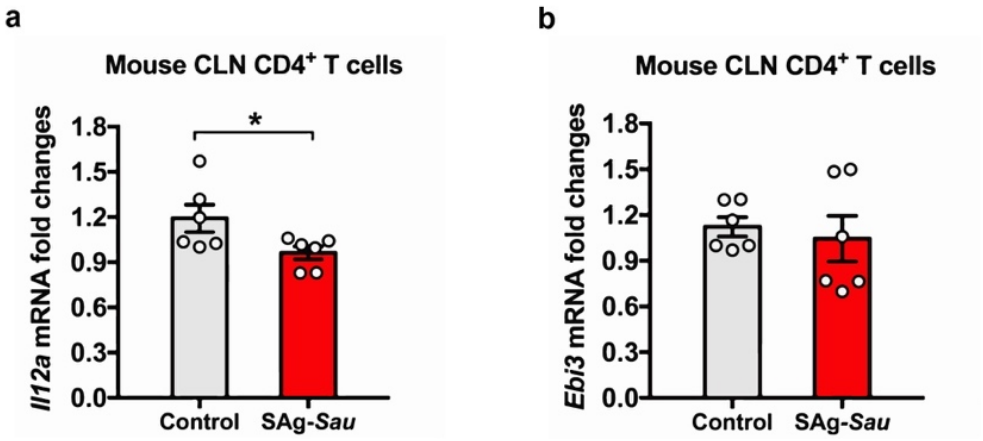

Figure 5.15 *Il12a* expression in mouse CLN CD4$^+$ T cells was downregulated by SAg-*Sau* colonization

C57BL/6 mice were infected intranasally with 10^7 CFU of SAg-*Sau* at day 0 and day 14 respectively, and the CLN were harvested at 24hrs post-secondary infection. mRNA expression of *il12a* (**a**) and *ebi3* (**b**) was detected in the CD4$^+$ T cells isolated from the CLN and shown as fold change against control mice.

In humans, IL-35 is produced primarily by effector CD4$^+$ T cells, however in mice, Foxp3$^+$ Tregs constitutively express IL-35 and are the primary source of this cytokine[97,101]. SAg-*Sau* stimulation led to a more significant decrease in IL-35 expression in human CD4$^+$ T cells, suggesting that it may primarily downregulate IL-35 expression in effector CD4$^+$ T cells. Despite this, both human and mouse carriage models show that SAg-*Sau* downregulates IL-35 expression in CD4$^+$ T cells, which could contribute to an enhanced Th17 response.

5.5 Conclusions

In this chapter, immune suppressive cytokine IL-35 was identified to play a key role in controlling the pro-inflammatory Th17 responses activated by SAg-*Sau* in human NALT.

IL-35 is a heterodimeric protein consisting of IL-12A and EBI3 subunits. In mice, the expression of EBI3 subunit is found to be the downstream target of transcription factor Foxp3, therefore IL-35 is constitutively and primarily expressed by Foxp3$^+$ Tregs[97]. Further study shows that IL-35 can be induced in effector CD4$^+$ T cells and these IL-35-producing CD4$^+$ T cells (iT$_R$35) exhibit potent suppressive function[94]. However, it remains controversial whether IL-35 is expressed in human CD4$^+$ T cells[101]. Here, I show that human tonsillar tissue-derived CD4$^+$ T cells expressed heterodimeric IL-35 and its expression was inhibited by SAg-*Sau*, in contrast to the expanded Foxp3$^+$ Tregs and enhanced IL-10 expression. It indicates that expression of IL-35 in human CD4$^+$ T cells may be independent of Foxp3$^+$ Tregs which is supported by a previous study showing EBI3 subunit is not constitutively expressed in human PBMC-derived Tregs[101]. Despite the potential discrepancy in human and mice CD4$^+$ T cell subsets that express IL-35, mice with nasopharyngeal infection of SAg-*Sau* also showed reduced expression of IL-35 in the CD4$^+$ T cells of cervical lymph nodes.

Not only the expression of IL-35 was regulated by SAg-*Sau* in a way that is opposing to IL-10 and Tregs, IL-35 also showed differential regulatory effects by suppressing the activation of IL-17A-producing Th17 cells but not the IFNγ-producing Th1 cells. Interestingly, IL-35-mediated Th17 suppression was shown to positively correlate with the level of Th17 activation, and IL-35 significantly reduced SAg-*Sau*-activated Th17 responses in those high responders (fold increase in Th17 response $\geq$ 5-fold) only. Since appropriate Th17 activation is required to protect the host from fungal and bacterial infection, patients with autoimmune diseases treated by IL-17A/Th17 antagonists frequently develop chronic mucocutaneous candidiasis (CMC). IL-35 has the ability to suppresses over-reactive Th17 responses while maintaining a "physiological level" of Th17 activity against bacterial infection in human nasopharynx, making it potentially a promising treatment option for Th17-mediated inflammatory/autoimmune diseases.

Further, addition of IL-35 was shown to downregulate RORγt expression in CD4$^+$ T cells and thereby inhibiting SAg-*Sau*-induced Th17 differentiation. However, the IL-23R expression in CD4$^+$ T cells which was enhanced by SAg-*Sau* was not affected by IL-35 treatment. Further studies are required to illustrate the signalling pathways used by IL-35 in suppressing the high

Th17 responses activated by SAg-*Sau* infection, as well as other inflammatory settings mediated by strong Th17 activation in humans.

In summary, SAg-Sau infection is able to inhibit IL-35-expressing CD4+ T cells in human NALT which may contribute substantially to the over-reactive Th17 responses activated by SAg-Sau, thus leading to Th17-mediated inflammatory pathologies.

CHAPTER 6

General Discussion

In this project, the T cell activation and regulation in response to SAg-*Sau* in NALT were examined using human tonsillar tissue and murine nasopharyngeal infection model. The majority of data were acquired from *in vitro* re-stimulation of human tonsillar MNCs. Tonsils are organised lymphoid tissue and interaction between lymphocytes and epithelial cells of the tissue are important for the development of immune responses. *In vitro*-isolated tonsillar MNCs lack organised lymphocyte zones (e.g. germinal centres) and do not include tissue epithelial cells, therefore results obtained from this *in vitro* re-stimulation system require a careful interpretation. However, the simplicity of isolated tonsillar MNCs makes it possible to explore mechanisms by which *Sau*-activated inflammatory T cell responses are regulated and therefore inform new strategies in the management of *Sau*-associated inflammatory conditions. SAg-*Sau* was shown to activate not only pro-inflammatory Th1 and Th17 responses, but also anti-inflammatory Foxp3$^+$ Tregs and IL-10-producing Tr1 cells in human NALT. Interestingly, the expression of IL-35 in the tonsillar CD4$^+$ T cells was markedly downregulated by SAg-*Sau*, indicating the development of iT$_R$35 cells may be inhibited in SAg-*Sau*-infected nasopharynx. The regulation of SAg-*Sau*-activated Th1 and Th17 responses by the Foxp3$^+$ Tregs, IL-10 and IL-35 was demonstrated in the previous chapters and summarised in ***Figure 6.1***.

Based on these results, I would like to discuss a number of questions and hypotheses underlying the findings of this project. 1) SAg-*Sau* showed a potent ability in activating T cell responses. How do staphylococcal superantigens stimulate T cells in a way different from conventional antigen in terms of the three-signal model of T cell activation? 2) SAg-*Sau* activated a strong Th17 response and induced IL-17A expression in the Foxp3$^+$ Tregs. Will this contribute to autoimmunity? 3) SAg-*Sau*-activated Th1 and Th17 responses were divergently regulated by Foxp3$^+$ Tregs and IL-10. Is this related to the opposing role of CD28/B7 co-stimulatory signalling in Th1 and Th17 activation? 4) Exogenous IL-10 was shown to promote SAg-*Sau*-activated Th17 responses. Is this associated with the downregulation of endogenous IFNγ by IL-10 which may act through lifting STAT1-mediated suppression of STAT3 signalling? 5) IL-35 was able to suppress the strong Th17 responses activated by SAg-*Sau*. What are the cellular mechanisms that mediate this suppressive effect? These will be discussed respectively in conjunction with current literatures.

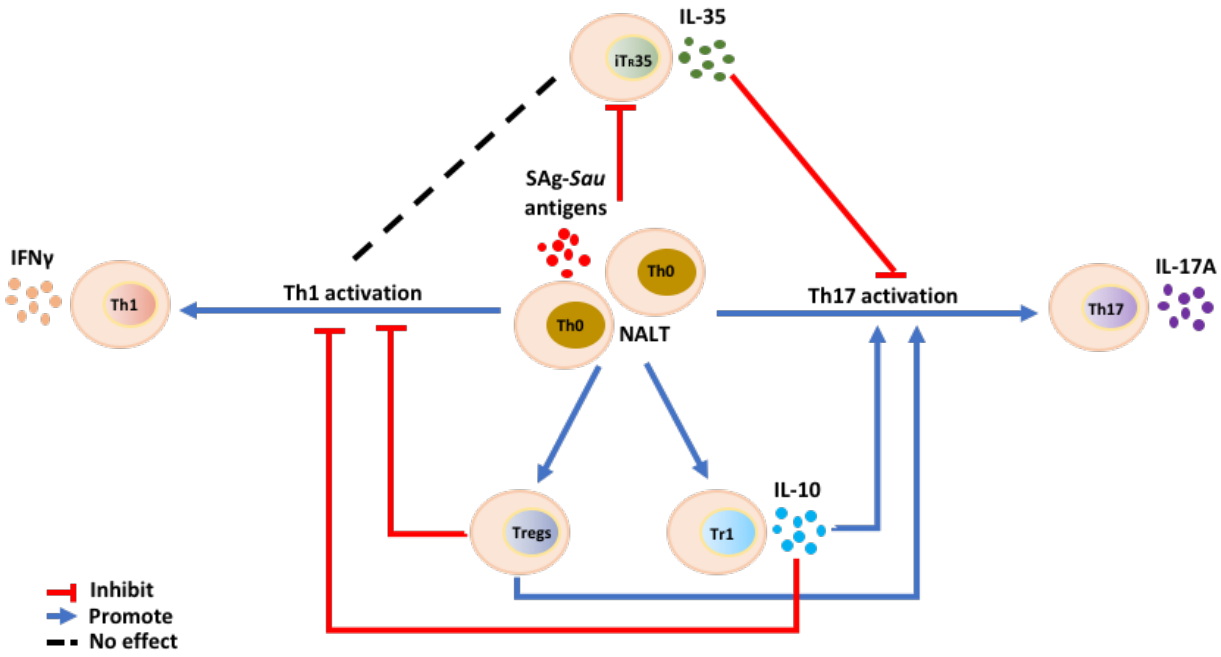

Figure 6.1 Schematic representation of T cell-mediated regulation of SAg-*Sau*-activated Th1 and Th17 responses in NALT

SAg-*Sau*-derived antigens activates IFNγ-producing Th1 cells, IL-17A-producing Th17 cells, Foxp3$^+$ Tregs and IL-10-producing Tr1 cells but suppressed the IL-35-producing iT$_R$35 cells. The Th1 responses are inhibited by the Tregs and IL-10, while IL-35 does not appear to affect the Th1 activation in SAg-*Sau* stimulated tonsillar MNCs. However, IL-35 is shown to inhibit the Th17 responses which in fact are promoted by exogenous IL-10. Some Tregs exhibit expression of IL-17A following SAg-*Sau* stimulation and removal of Tregs reduces the proportion of activated Th17 cells, indicating Tregs may also promote Th17 activation in the context of SAg-*Sau* infection.

6.1 Staphylococcal superantigens activate T cells by circumventing the canonical TCR recognition of peptide/MHC complex

The recorded history of *Sau* causing infection and diseases can be dated back to the 19th century[178]. *Sau* commonly colonizes skin and mucous of the upper respiratory tract and associates with infectious and inflammatory diseases which is mainly due to its capability of producing numerous virulence factors[179,180]. Staphylococcal enterotoxins (SEs) and TSST-1 are an important group of protein toxins produced by *Sau*, and these toxins have attracted a large number of studies aiming to uncover their potent ability in activating antigen-presenting cells (APCs) and T cells and how this activation leads to inflammatory pathologies[181].

Those staphylococcal antigens stimulate T cells in a way that is similar to a group of endogenous antigens expressed by mice, named minor lymphocyte stimulating antigens (MIs), by interacting with a particular variable beta (Vβ) chain of the TCR regardless of the composition of variable alpha (Vα) chain[23,182]. By a process of somatic gene rearrangement, the two separately rearranged Vα and Vβ chains have resulted in the vast diversity of $\alpha\beta$ TCRs, and thereby allowing the T cells to recognize an even larger repertoire of foreign antigenic peptides presented by APCs[183,184]. However, T cells possess limited type of Vβ elements with 54 and 35 TCR Vβ genes expressed in humans and mice respectively[183]. Thus, SEs and the mice MIs are able to activate simultaneously a large proportion of total T cells through recognizing specific Vβ chains, whereas only a very small fraction of T cells can be activated by conventional antigens which have to match the binding epitopes of both Vα and Vβ regions[185] (***Figure 6.2***). Antigens that activate T cells depending on the Vβ specificity only are termed “superantigens”[186].

Superantigen-producing *Sau* is common with up to 50% of *Sau* strains identified are positive for one or multiple superantigens[10,33]. The SAg-*Sau* used in this study produces TSST-1, SEA, SEC and SEE and exhibit potent ability in activating both proliferative response and production of inflammatory cytokines, such as IL-17A and IFNγ, in human tonsillar CD4$^+$ T cells.

TCR recognition by MHC class II loaded with foreign peptide which is presented on the cell surface of APCs is the primary signal required to initialize $CD4^+$ T cell activation[187]. Normally, exogenous antigens can be taken by professional APCs, including dendritic cells (DCs), macrophages and B cells, through phagocytosis or endocytosis and are processed into small peptides. These peptides can then be loaded onto MHC class II molecules and displayed by the APCs[188]. Different from conventional antigens, superantigens are able to directly bind to the MHC class II molecules without prior processing[24]. It is notable that presentation of the conventional antigenic peptide is not inhibited by the association of superantigen with MHC class II because superantigens do not occupy the peptide-binding groove of MHC class II[23] (***Figure 6.2***).

Here, I stimulated tonsillar MNCs with concentrated culture supernatant of SAg-*Sau* which was a mixed antigen pool containing not only superantigens, but also other conventional antigens secreted by the bacteria. Therefore, both superantigenic and antigen-specific T cell responses were activated. By comparing the $CD4^+$ T cell responses activated by SAg-*Sau* with NonSAg-*Sau* and other common colonizers of the nasopharynx, including *Spn*, coagulase-negative *staphylococcus* and *M. catarrhalis*, SAg-*Sau* and/or its superantigens were shown to activate highly pro-inflammatory T cell responses (e.g. Th1 and Th17) in human NALT.

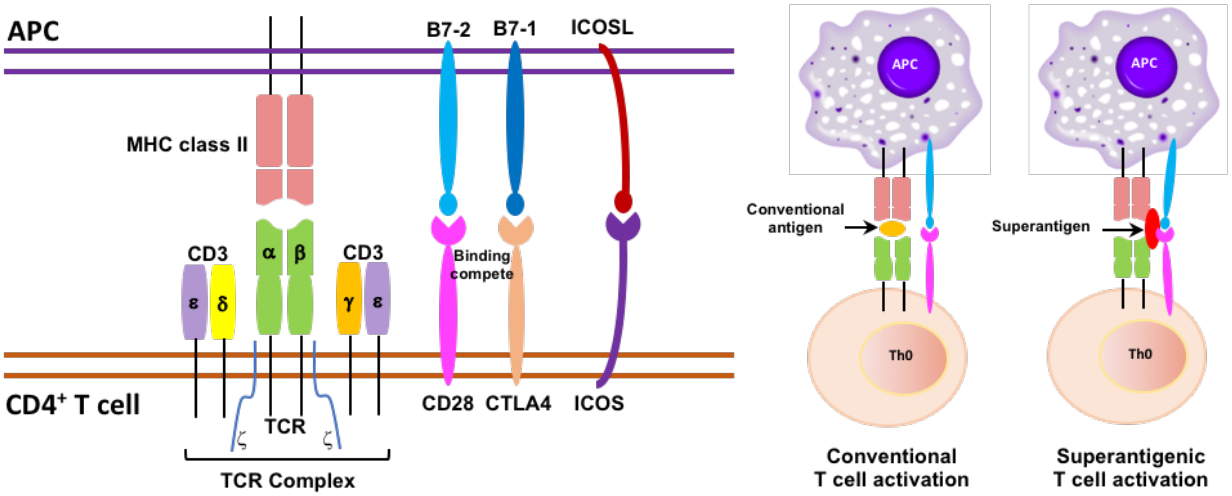

Figure 6.2 Superantigen activates T cells by directly binding to the TCR Vβ, MHC class II and co-stimulatory molecules

Schematic diagram of the two stimulatory signals for T cell activation. Left: The TCR complex of T cells consists of α chain, β chain, CD3 and ζ chain molecules. The TCR α and β chains are composed of two extracellular domains, variable region and constant region. The T cells recognize the peptide/MHC class II complex on the APCs by variable α and β chains which provides the first signal for T cell activation. The co-stimulatory molecules CD28 and ICOS are expressed by T cells which bind to the B7 and ICOS ligand (ICOSL) on the APCs respectively, acting as the secondary signal to assist T cell activation. Activated T cells upregulate the co-inhibitory molecule, CTLA4, which is homologous to CD28 and thereby could compete with CD28 for the binding of B7 proteins. Compare to the B7-2 which is constitutively expressed in APCs, the B7-1 is induced only following T cell activation and it has higher avidity to CTLA4. Thus, CTLA4 binds to the B7-1 more efficiently and transduce inhibitory signals to contain T cell activation. Right: Different from the conventional antigen which needs to be processed by the APCs and then be loaded onto the MHC class II for TCR recognition, superantigen can bind to the MHC class II and TCR Vβ chain directly. Furthermore, superantigen can also bind directly to the co-stimulatory molecules CD28/B7, providing strong co-stimulation signals for the activation of inflammatory cytokine production in the effector T cells.

6.2 Staphylococcal superantigens may contribute to autoimmunity by activating self-reactive T cells

It is worth noting that the random rearrangement of Vα and Vβ chain enables the TCR to recognize various antigens derived from external pathogens, but also generates TCR that

reacts to self-derived antigens which underlies the aetiology of autoimmunity[73,189]. To eliminate those self-reactive T cells, the thymus has developed a central tolerance mechanism described as negative selection by which T cell clones with high avidity to self-antigens are depleted during the selection process[190,191]. In addition to the negative selection, some self-antigen specific T cells can differentiate into suppressive Foxp3$^+$ Tregs via agonist selection and those thymic-derived Tregs (tTregs) are crucial for maintaining peripheral immune tolerance[190]. However, studies have shown that self-reactive Foxp3$^-$ T cells (conventional T cells, Tconvs) can sometime escape the thymic selection and exit to the periphery. This occurs especially when they express TCRs with high affinity for certain tissue-restricted peptides that are not expressed or have limited expression in the thymus[192,193]. These self-reactive T cells are normally ignored in the periphery because tissue-specific antigens are usually concealed behind the anatomical barrier in physiological context[36]. However, infection or other causes of tissue damage could lead to the exposure of sequestered self-antigens and therefore increasing the risk of activating auto-reactive T cells. Peripheral immune suppressive mechanisms, including regulatory T cell subsets (e.g. Foxp3$^+$ Tregs, Tr1 and iT$_R$35) and inhibitory molecules (e.g. CTLA4, PD-1), are important to control those auto-reactive T cells upon encountering autoantigens[36].

With the ability to activate T cells regardless of antigen specificity, staphylococcal superantigens could also activate those escaped autoreactive T cells. Superantigenic activation of naïve T cells are shown to result in clonal deletion and cell anergy which could be a tolerance mechanism to protect the host from massive T cell activation. However, it has been demonstrated that superantigen stimulation in mice pre-challenged by self-antigens could reactivate autoreactive T cells, leading to autoimmune pathologies[26,27,31,34]. Studies linking *Sau* and its superantigens with autoimmunity were reviewed in ***Chapter 1***. In addition, pathogen-primed T cells may also be activated by staphylococcal superantigens and thereby mediating inflammatory tissue damage[25]. In my study, SAg-*Sau* showed potent ability of activating inflammatory Th17 responses which were more resistant to immune suppression than Th1 responses. Although the antigen specificity of these activated Th17 cells were not defined, it was possible that SAg-*Sau*-activated Th17 responses could underlie pathological

changes of certain inflammatory and autoimmune diseases, given the highly pathogenic property of Th17 cells shown by a large number of studies.

6.3 SAg-*Sau* may break down immune tolerance by inducing Treg conversion into pro-inflammatory Th17 cells

Furthermore, I found an aberrant expansion of Foxp3$^+$ Tregs in SAg-*Sau* stimulated tonsillar MNCs and a significant proportion of these Treg showed expression of IL-17A, indicating SAg-*Sau* may alter the anergic state of Tregs and promote their conversion into effector T cells. It is known that Foxp3$^+$ Tregs do not respond to TCR-mediated activation and are capable of suppressing immune responses of effector T cells[194-197]. The unresponsiveness of Tregs is critical for the maintenance of immune tolerance against self-tissue, since natural Tregs (nTregs) developed in the thymus have a TCR repertoire biased towards self-peptides and exhibit greater avidity for self-peptide/MHC class II complexes than Tconvs[198-200]. In a model of autoimmune neuroinflammation induced by myelin oligodendrocyte glycoprotein (MOG), the functional avidity and encephalitogenic capacity of the MOG-specific TCRs derived from Tregs and Tconvs were compared. It shows that poly-clonal Tconvs engineered to express the Treg-derived TCRs show stronger reactivity to the MOG antigen and cause an earlier onset of EAE and more severe disease manifestation upon adoptive transfer in the recipient mice[200]. Another strong evidence to support the proposal of strong self-reactive Tregs comes from the transgenic mice harbouring autoimmune regulator (Aire) deficiency. The Aire is a transcription factor expressed by the medullary thymic epithelial cells (mTECs) controlling the promiscuous expression of tissue-restricted antigens in the thymus, its deficiency results in multi-organ autoimmunity in mice. By characterising TCR specificities of the Tconvs infiltrating the autoimmune lesions in *Aire*$^{-/-}$ mice, it reveals that the predominant TCR clonotypes expressed by these infiltrating Tconvs are primarily expressed by Tregs in *Aire*$^{+/+}$ mice[199]. Thus, the removal of anergy and the subsequent phenotypic changes in Tregs, which has been observed following SAg-*Sau* stimulation, could lead to the expansion of auto-reactive Tconvs which may break down the immune tolerance and initiate autoimmune pathologies.

6.4 The possible role of CD28/B7 co-stimulations for Treg- and IL-10-mediated differential regulation of SAg-*Sau*-activated Th1 and Th17 responses

Upon TCR engaging with the peptide/MHC class II complex, the interaction between co-stimulatory receptors of T cells and the corresponding ligands on the APCs provides the second signal for T cell activation (***Figure 6.2***). The classical co-stimulation signal is represented by the CD28-B7 paradigm[201]. CD28 is the most well-known co-stimulatory receptor which is constitutively expressed on T cells and interacts with both B7 ligands, B7-1 (also known as CD80) and B7-2 (also known as CD86)[201,202]. B7-2 is constitutively expressed on APCs, although at a low level, and rapidly upregulated within 6 hours of stimulation, whereas B7-1 is undetectable on resting APCs and it is not until 24 hours post stimulation that the B7-1 is induced to express[202,203]. The B7 ligands can also bind to CTLA4, a co-inhibitory receptor which is homologous to CD28, with high affinity. In Tconvs, CTLA4 is induced only by stimulation and peaks 48 hours following cell activation and negatively regulate the activated T cells[202,204]. The B7-1 binds 13-fold more strongly to CTLA4 than B7-2, therefore the delayed expression of B7-1 is timed to specifically enhance the co-inhibitory signal mediated by CTLA4[204]. Different from Tconvs, Foxp3$^+$ Tregs constitutively express CTLA4 and the suppression through the CTLA4 pathway plays an important role in Treg-dependent immune regulation and tolerance[128].

T cells activated in the absence of CD28 signalling acquire the state of functional unresponsiveness which means they cannot respond following stimulations for a certain period, and this is thought to be an immune tolerance mechanism against autoimmunity[36]. CD28 signalling is also involved in the T cell activation stimulated by superantigens[205-207]. Superantigens bind directly into the dimer interface of CD28 and B7 coligands (***Figure 6.2***), potently promoting their interaction and thereby eliciting strong production of inflammatory cytokines, including IFNγ, TNF-α and IL-2[208]. Peptide mimetics that block binding sites of superanigens in CD28 and B7 both abrogate the inflammatory cytokine production and protect

mice from superantigen-induced lethal shock[208-210]. Furthermore, CD28-deficient mice are completely resistant to staphylococcal superantigen TSST-1-induced toxic shock syndrome[205]. The T cells derived from $CD28^{-/-}$ mice pre-challenged with SEB exhibit dramatically reduced proliferation and TNF-α production following secondary SEB stimulation, indicating T cell anergy is induced by the superantigen without CD28 signalling[206].

The lack of CD28 co-stimulatory signals inhibits production of IFNγ and Th1 responses in both conventional and superantigenic T cells activation. However, studies have shown the activation of Th17 cells are not affected in the absence of CD28 signals and these activated Th17 cells respond normally to restimulations. Moreover, CD28 co-stimulation in fact suppresses Th17 differentiation in the initial induction period[211,212]. Instead, the accessory co-stimulatory molecule, inducible co-stimulator (ICOS), is shown to mediate the development of Th17 cells[213,214]. Another study demonstrates that CD28-mediated increasing of metabolic activity which supports the proliferation and effector cytokine production of Th1 cells can be replaced by Th17-related cytokines IL-1β and IL-23 for Th17 activation[212]. The negative modulation of Th17 responses by CD28-B7 signalling explains why CTLA4-immunoglobin (CTLA4-Ig), which is supposed to inhibit T cell responses via blocking the interaction of CD28 and B7, actually enhances Th17 responses and exacerbates Th17-mediated intestinal inflammations[129].

The CD28-B7 co-stimulations also play an opposing role in superantigen-activated Th1 and Th17 responses. In a murine model of arthritis induced by superantigen-producing *Mycoplasma arthritidis* (*M. arthritidis*), treatment of anti-B7-1 significantly enhances Th17 responses whereas the Th1 responses are reduced, making mice more susceptible to the arthritogenic effects of *M. arthritidis*[215]. I've shown that $Foxp3^{+}$ Tregs derived from both NALT and peripheral blood suppressed the activation of Th1 but not Th17 cells following SAg-*Sau* stimulation (***Figure 4.4* and *4.5***). In Treg-depleted MNCs, the proportion of activated Th17 cells even showed a trend of decreasing, which was consistent with reduced IL-17A production in the culture supernatant (IL-17A concentration measurement was done after first draft thesis submission). Those SAg-*Sau* stimulated Tregs exhibited upregulated CTLA4 expression indicating an enhanced regulatory pathway through CTLA4 signalling. Therefore,

it is plausible that the divergent regulation of SAg-*Sau*-activated Th1 and Th17 responses by Tregs is correlated with CTLA4-mediated immune modulations which antagonise CD28-mediated costimulatory signals and selectively suppressed Th1 activation.

Similar to Tregs, IL-10 also showed opposing effects in the superantigenic Th1 and Th17 responses which may be explained by a previous study showing IL-10 acts directly on CD28 co-stimulation pathways for its suppression of Th1 and Th2 responses. It demonstrates that IL-10 is able to inhibit the tyrosine phosphorylation of CD28 and its following association with phosphoinositide 3-kinase (PI3K) which is an essential step for the downstream activation of CD28 signalling pathway, and this IL-10-mediated suppression affects Th1/Th2-related cytokine production activated by both conventional antigens and superantigens[148]. However, if IL-10 suppresses superantigenic effector T cell responses through blocking CD28 signalling, it is possible that SAg-*Sau*-activated Th17 responses were not suppressed by IL-10 since CD28-mediated co-stimulations are not required for Th17 activation as discussed above. The differential regulation of Th1 and Th17 responses by co-stimulatory/co-inhibitory signals is summarised in ***Figure 6.3***.

6.5 Inflammatory cytokine milieu may be responsible for the reprogramming of Tregs into Th17 cells

The third signal for T cell activation is the cytokine milieu in which the T cells are activated. It largely affects the T cell lineage commitment during differentiation and phenotypic changes in the effector phase which is described as T cell plasticity (***Figure 6.3***). In general, a pro-inflammatory cytokine environment supports the development and activation of inflammatory T cell subsets, such as Th1 and Th17, whereas immune suppressive Tregs are developed in the absence of pro-inflammatory cytokines[115,216]. Interestingly, the differentiation of $Foxp3^+$ Tregs and Th17 cells both require TGF-β signal[115,120,217]. Although TGF-β may not be necessary for the development of nTregs in the thymus, it is critical for the maintenance of nTregs in the periphery[218]. TGF-β induces the expression of both Foxp3 and RORγt nuclear factors in $CD4^+$ T cells, which transcription factor is dominant depends on the cytokine

environment and determines whether the cells are programmed into Tregs (Foxp3-dominant) or Th17 cells (RORγt-dominant)[116,217]. Without inflammatory cytokines, such as IL-6 and IL-21, the function of RORγt is repressed by the Foxp3 and thereby leading to the suppressive phenotype of Tregs. However, this inhibition of RORγt can be relieved once Foxp3 is downregulated which can be induced by inflammatory cytokine-mediated STAT3 activation[219].

SAg-*Sau* activated IL-17A expression in the Tregs suggesting a potential Treg conversion into Th17 cells, and this could be the results of enhanced inflammatory signals in SAg-*Sau* stimulated tonsillar MNCs, such as increased production of IL-6. IL-6-mediated activation of STAT3 signalling has been shown to induce the redifferentiation of both thymic-derived nTregs and peripheral-induced Tregs (iTregs) into effector Th17 cells. Functionally, Tregs that have been reprogrammed to express IL-17 exhibited markedly reduced suppressive activity[220,221]. This may partially explain why tonsillar Tregs were unable to suppress the proliferation and IL-17A production in $CD4^+$ T cells upon SAg-*Sau* stimulation. Notably, another study demonstrates that IL-17-producing Tregs still have the ability to inhibit the proliferation of $CD4^+$ responder T cells activated by anti-CD3 and anti-CD28[118]. In the context of SAg-*Sau* stimulation, the proliferative responses activated were not suppressed by Tregs. This may be explained by impaired suppressive function of SAg-*Sau*-stimulated Tregs or associate with high resistance of superantigen-activated T cells to Treg-mediated suppression. Whether SAg-*Sau*-activated IL-17A-producing Tregs retained the suppressive capability for conventional T cell activation requires further investigation.

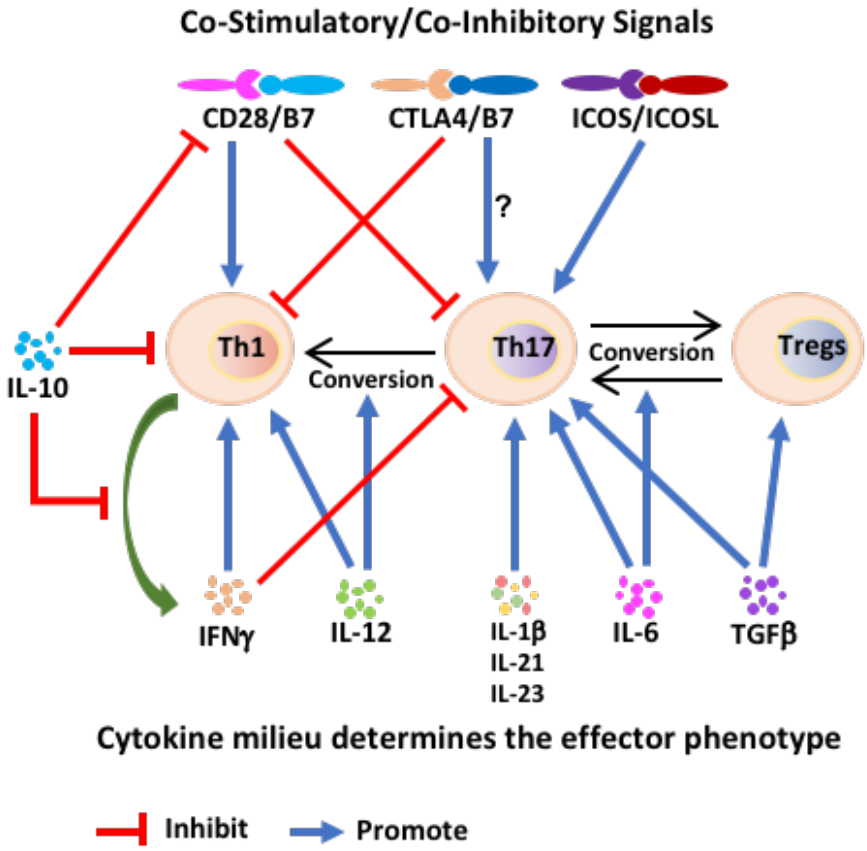

Figure 6.3 Co-stimulatory signals and cytokine milieu that regulate the development of different CD4$^+$ T cell subsets

Schematic representation of how effector T cell subsets are regulated by the co-stimulatory/co-inhibitory signals and cytokine environment. The activation of Th1 cells requires CD28/B7 co-stimulation and the stimulation signals mediated by IFNγ and IL-12 cytokines. IL-10 could thereby suppress the Th1 responses by inhibiting the co-stimulatory signal delivered by CD28 and B7 interaction. IL-10 can also suppress IFNγ production by Th1 cells and thereby blocking the positive feedback of IFNγ signalling for Th1 activation. CTLA4 suppresses Th1 responses by displacing CD28 to bind the B7 proteins and transduce inhibitory signals. However, the co-stimulatory signal CD28/B7 which supports Th1 activation, in fact inhibits the development of Th17 cells. Rather, the co-stimulation that facilitate Th17 activation is provided by the interaction of ICOS and ICOSL. The co-inhibitory CTL4 also appears to assist Th17 activation, in contrast to its general inhibitory role for the proliferative response of T cells and Th1 responses. Cytokines that support Th17 activation include TGFβ, IL-6, IL-1β, IL-21 and IL-23. The Th1 cytokine IL-12 could induce Th17 conversion into Th1 cells. TGFβ is also required for Foxp3$^+$ Treg induction, and the Tregs could be reprogrammed to Th17 cell in the presence of inflammatory cytokines, such as IL-6. IFNγ is the signature cytokine produced by Th1 cells, and its presence can inhibit Th17 development.

It has been mentioned above that the TCR specificity of nTregs is self-antigen biased. The potential of these strong self-reactive Tregs to be reprogrammed into effector Th17 cells may contribute to the high pathogenicity of Th17 cell subset, although it remains controversial regarding the *in vivo* stability of nTregs[222,223]. Compared to nTregs, the iTregs are developed from peripheral naïve T cells and thereby their TCR repertoire is overlapped with conventional T cells, exhibiting low avidity to self-antigens. However, conversion of iTregs into Th17 cells also leads to autoimmunity. Komatsu et al. demonstrates in a murine model of collagen-induced arthritis (CIA) that those arthritogenic IL-17-producing T cells originate from $Foxp3^+$ Tregs which are transdifferentiated into Th17 cells in the inflamed joint containing high level of IL-6. These ex-Tregs have a gene expression profile matched with iTregs, distinguishable from Tconvs and nTregs[119]. Hence, despite the origin of the Tregs, their conversion into Th17 cells could occur in response to environmental cues and this conversion has pathological implications for inflammatory and autoimmune diseases. SAg-*Sau* infection can therefore be a trigger of autoimmunity by promoting the Treg conversion into pathological Th17 cells.

6.6 Dose endogenous IFNγ affect the activation of committed Th17 cells?

For the regulation of SAg-*Sau*-activated Th17 responses in the nasopharynx, both Treg- and IL-10-mediated suppression were shown to be inefficient, in contrasting to their potent effects in controlling Th1 activation. Further, exogenous IL-10 was found to promote Th17 responses stimulated by SAg-*Sau*. This may be partially related to the inhibition of CD28 signalling by IL-10 which removes the negative effects of CD28 co-stimulation on Th17 activation[148]. However, it is notable that CD28-induced suppression on Th17 cells mainly affects Th17 differentiation but does not appear to inhibit memory Th17 activation[212].

Different Th cell lineages are counter-regulated during differentiation but committed Th cells could exhibit heterogenous effector phenotypes. Following SAg-*Sau* stimulation, not only IL-17A and Foxp3 double positive $CD4^+$ T cells were activated, a $CD4^+$ T cell population that co-express IL-17A and IFNγ (Th17/Th1 cells) was also detected. Along with highly activated Th17

responses, SAg-*Sau* also activated strong Th1 responses. It has been reported by two parallel studies that development of Th17 cells from naïve $CD4^+$ T cells is strongly suppressed by IFNγ, whereas committed effector and memory Th17 cells are resistant to exogeneous IFNγ[224,225]. These two studies also examined whether blocking endogenously produced IFNγ could enhance IL-17 expression by committed Th17 cells but generated contradicting results. The principal difference between their stimulations is one study used anti-CD3 stimulation only and the other stimulated the cells with anti-CD3 and anti-CD28. Depletion of endogenous IFNγ enhanced the effector Th17 responses when anti-CD28 stimulation was present. The CD28-mediated suppression of Th17 activation is shown to be dependent on the increased IFNγ and IL-2 production, although this suppression seems to not apply to effector Th17 cells[211]. It is possible that depleting IFNγ enhances the effector Th17 responses by removing certain suppressive effects mediated by CD28 co-stimulations but do not alter the responses activated by anti-CD3 only. Consistent with this notion, IFNγ blockade has been shown to enhance IL-17 expression in human memory $CD4^+$ T cells coming into contact with activated monocytes[80]. Activation signals via TCR and CD28 co-stimulatory molecules both were delivered by tonsillar monocytes and B cells in my stimulation model, exogenous IL-10 significantly reduced IFNγ production following SAg-*Sau* stimulation, this reduction of endogenously produced IFNγ may contribute to the enhanced IL-17A expression in tonsillar $CD4^+$ T cells. How IFNγ-mediated signalling pathway in effector $CD4^+$ T cells may affect the IL-17 expression and Th17 activation is discussed below.

6.7 STAT3 activation by IL-6 and IL-10 could confer distinct effector phenotypes in $CD4^+$ T cells

A wide range of cytokines that regulate T cell responses signal through type I and type II receptors, including IL-2, IL-10, IFNγ, IL-6 and IL-12 family cytokines. These cytokine receptors lack an intrinsic catalytic kinase activity and rely on Janus kinases (JAKs) to phosphorylate downstream signal proteins. The JAK family has 4 members, JAK1, JAK2, JAK3 and tyrosine kinase 2 (TYK2), each associates with the cytoplasmic domain of different

cytokine receptors[226]. Upon cytokine binding, the receptor goes through conformational changes which allows the adjacent JAKs to phosphorylate each other and followed by phosphorylation of the signal transducer and activator of transcription (STATs). Phosphorylated STATs (pSTATs) form homodimer or heterodimer and translocate to the nucleus where they bind DNAs and regulate the transcription of target genes (***Figure 6.4***). There are 7 STAT proteins that have been identified, STAT1, STAT2, STAT3, STAT4, STAT5A, STAT5B and STAT6[227]. The extracellular cytokine milieu shapes the effector responses of T cells through integrated JAK-STAT signalling. Although IL-17 do not signal via JAK-STAT pathway, the development of Th17 cells is dependent on the activation of STAT3 which can be induced by IL-6 and IL-21. Dimerised STAT3 enters the nucleus and induce the transcription of IL-17A, as well as other Th17-related protein targets like IL-23R and IL-21[228]. Staphylococcal superantigen SEA has been shown to activate STAT3 for its promoting effects on Th17 responses[229].

What has to be born in mind is that IL-10 also activates STAT3, although no evidence yet to show IL-10-induced STAT3 activation could lead to enhanced Th17 activation. Rather, studies demonstrate that the STAT3 activation by IL-10 directs the T cell towards a tolerogenic phenotype resembling Tr1[230]. Moreover, $CD4^+$ T cells transfected with active form of STAT3 cannot enhance IL-17 expression without TGF-β signalling, but rather promote the suppressive capacity of T cells, suggesting STAT3 per se induce a dominant suppressive gene expression profile in T cells[228,231]. However, when the master regulator of Th17 cells, RORγt, is induced by TGF-β and IL-6, activated STAT3 could work synergistically with RORγt to potently promote IL-17 expression and Th17 responses[228]. In contrast to IL-6-mediated STAT3 activation which enhance Th17 activation, IL-10/IL-10R-mediated STAT3 activation in T cells are shown to be necessary for the suppression of Th17 responses by $Foxp3^+$ Tregs and IL-10-producing Tr1 cells in murine models of colitis[78,85]. Whether the superantigenic stimulation altered the commonly suppressive IL-10/STAT3 signalling and resulted in the promoting effect of exogenous IL-10 on Th17 activation shown in my study is yet to be elucidated. Here, I would like to discuss another possibility relating to IFNγ-mediated STAT1 activation which may help to decipher this interesting effect from the perspective that emphasise the counter-regulation between STAT proteins.

6.8 IL-10 may promote SAg-*Sau*-activated Th17 responses through inhibiting IFNγ-STAT1 signalling

The STAT proteins were initially thought to be positive transactivating factors until it was found that they also serve as repressors for a considerable number of genes[232]. Different STATs could target the same gene but exert opposing effects and thereby fine-tune the phenotype of the effector T cells activated in a complicated cytokine milieu, with both STAT1 and STAT5 having been demonstrated to negatively regulate Th17 activation via interfering with the function of STAT3[233-235] (***Figure 6.4***). Yang et al. shows IL-2-activated STAT5 bind the promoter and several distal sites of *Il17a* locus, which regions can also be bound by IL-6-activated STAT3. Therefore, the STAT3 binding in the *Il17a* promoter as a strong enhancer can be displaced by STAT5 which results in reduced gene transcription and diminished IL-17A expression[233].

Several mechanisms have been suggested for STAT1-mediated STAT3 inhibition. 1) STAT1 may displace STAT3 binding to *Il17a* promoter like STAT5; 2) STAT1 may bind to distinct regions of *Il17a* locus acting as a repressor for the transcription. Although the mechanism is yet to be clarified, it is clear that enhanced STAT1 activation is able to suppress STAT3-induced IL-17 expression and Th17 activation[234-236]. In patients carrying gain-of-function *STAT1* mutation, a smaller proportion of IL-17-produing cells is found in the circulation compared to normal individuals[236]. The PBMCs derived from these patients express significantly lower Th17-related genes (IL-17A, RORγt and IL-22) following stimulation, and this decreased expression of IL-17A can be fully restored by inhibiting the phosphorylation of STAT1[234].

IFNγ stimulates a predominant STAT1 activation, which can be further enhanced by IL-12-activated STAT4 signalling, together they drive Th1 effector phenotype. Th17 cells are shown to express not only its own master regulator RORγt, but also T-bet, the master regulator of Th1 cell lineage[79,237]. The T-bet is the downstream target of STAT1, and its expression can be upregulated in the Th17 cells in response to IL-12 signalling leading to increased IFNγ and

decreased IL-17A expression[79]. The plasticity of Th17 cells leads to the generation of a heterogenic T cell subset, IL-17A$^+$IFNγ^+ Th17/Th1 cells, which has been observed in SAg-*Sau*-activated tonsillar MNCs. The occurrence of Th17/Th1 phenotype means enhanced STAT1 activation in the cells which limits STAT3 activity and its downstream IL-17 expression. If the STAT1 signalling keeps pushing over and perturbs the delicate balance of STAT1 and STAT3 in the Th17/Th1 cells, these cells may lose the expression of Th17-related genes and become ex-Th17 cells[238]. However, inhibiting the STAT1 activation could remove its suppression over STAT3 and thereby revive the Th17 effector phenotype[234]. Hence, in SAg-*Sau* stimulated tonsillar MNCs, exogenous IL-10 may promote the IL-17A expression in Th17/Th1 and ex-Th17 cells through downregulating IFNγ and the STAT1 activation it mediates, therefore showing positive effects on SAg-*Sau*-activated Th17 responses.

6.9 Possible cellular mechanisms underlie IL-35-mediated Th17 suppression

STAT1-dependent Th17 inhibition has also been demonstrated to play a role in IL-27-mediated suppression of pro-inflammatory Th17 responses[239,240]. Although IL-27 (IL-27p28:EBI3 heterodimer) shares the gp130-STAT3 signalling with IL-6, it has contrasting effects on Th17 responses which is associated with the unique IL-27 receptor (IL-27R)-mediated activation of STAT1. In *STAT1*$^{-/-}$ CD4$^+$ T cells, IL-27-induced substantial inhibition of IL-17 production was abrogated[240]. IL-35 and IL-27 both belong to IL-12 heterodimeric cytokine family and they share the EBI3 subunit[164]. It has been shown that IL-35 could signal through IL-12Rβ2 homodimer, gp130 homodimer and IL-12Rβ2:gp130 heterodimer, activating STAT1, STAT4 and a unique STAT1/STAT4 heterodimer signalling respectively[175] (***Figure 6.4***). The IL-35-mediated suppression of Th17 responses activated by SAg-*Sau* shown in this study may be partially related to the activation of STAT1. However, given the selective suppression of high Th17 responses by IL-35 and the ability of IL-35 to downregulate RORγt expression in CD4$^+$ T cells shown in the context of SAg-*Sau* stimulation, I propose that IL-35-activated STAT1/STAT4 heterodimer may be capable of regulating the transcription of RORγt

directly or indirectly through inducing IL-35 expression. Hence, only Th17 cells that express the IL-12Rβ2/gp130 heterodimer receptor can be specifically regulated by IL-35 in SAg-*Sau*-infected nasopharynx.

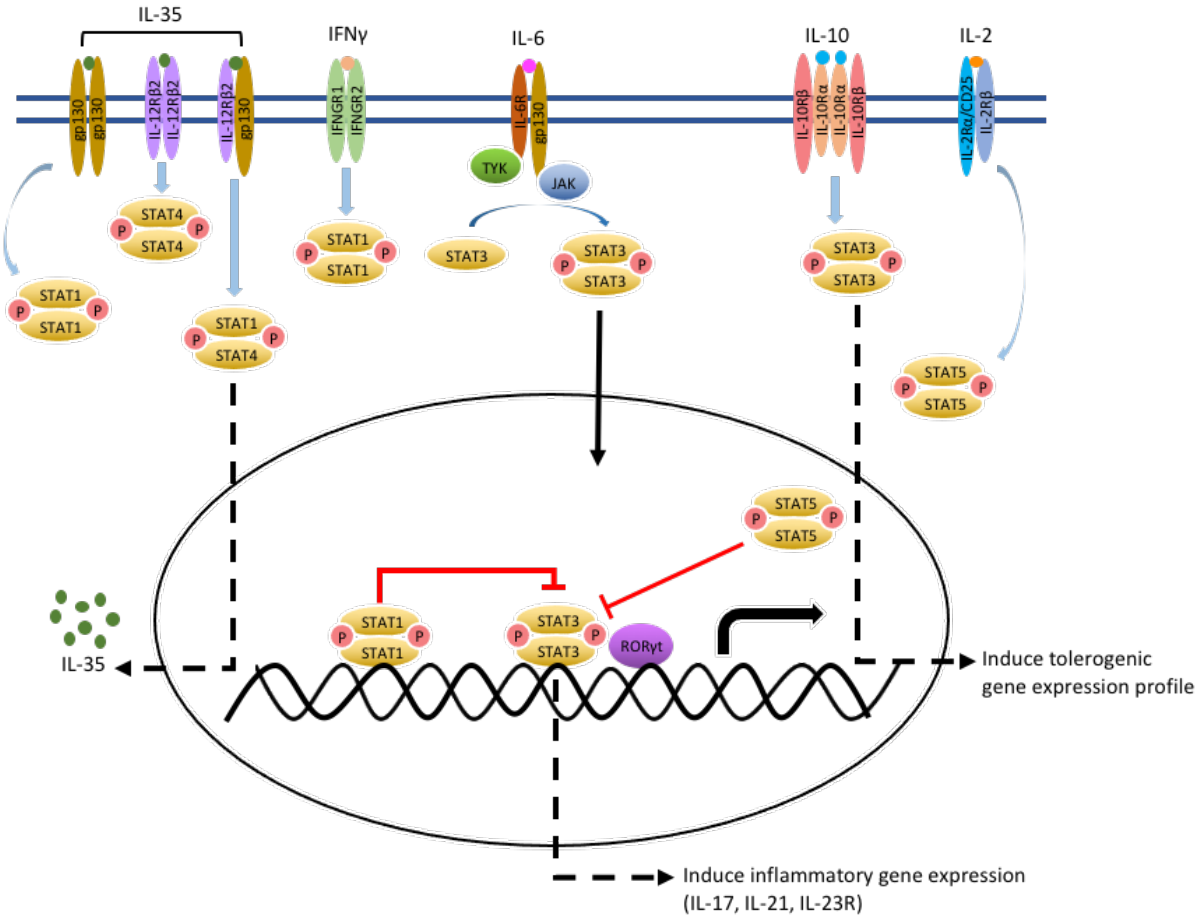

Figure 6.4 Cytokines regulate T cell responses through JAK-STAT signalling

Schematic diagram of the JAK-STAT signalling activated by cytokines through type I and type II receptors in $CD4^+$ T cells. The intracellular domains of type I and type II receptors are associated with JAK proteins (JAK1, JAK2, JAK3 and TYK2). Upon cytokine binding, the STATs are phosphorylated by the JAKs and then form active homodimers (e.g. STAT3/STAT3) or heterodimers (e.g. STAT1/STAT4), these dimerised STATs translocate into the nucleus and modulate gene expression. IL-6 activates STAT3 which together with RORγt induces the expression of Th17-related genes. However, the STAT3 signal activated by IL-10 is shown to induce a tolerogenic gene expression profile. The IL-6-mediated STAT3 activation can be inhibited by IFNγ-activated STAT1 and IL-2-activated STAT5 at transcription level, IFNγ and IL-2 may thereby suppress the activation of Th17 responses. IL-35 could signal through gp130 homodimer and IL-12Rβ2 homodimer to activate STAT1 and STAT4 signalling, but only through the gp130/IL-12RB2 heterodimeric receptor which activates the unique STAT1/STAT4 heterodimer can it induce the expression of IL-35.

In addition to above discussed questions/hypotheses which may explain the potential underlying cellular mechanisms of my findings, the pathogenicity of Th17 cells and the therapeutic potential of IL-35 are also interesting topics closely related to my study. Compared to the Th1 responses, SAg-*Sau*-activated Th17 responses were more resistant to T cell-mediated immune regulation. The highly pathogenic property of Th17 cells is discussed which could provide rationale for the autoimmune potential of SAg-*Sau*-activated Th17 responses. IL-35 may control inflammatory/autoimmune pathologies through suppressing superantigenic Th17 responses. Those milestone IL-35 studies have been reviewed in ***Chapter 1***, here I would like to further discuss what my study has added to the understanding of IL-35 and current challenges for IL-35 research which should be addressed in future studies, in order to develop IL-35-based immune therapy for clinical diseases.

6.10 The culprit of autoimmunity, Th1 or Th17?

In the presence of SAg-*Sau*, both Th1 and Th17 were potently activated but only Th1 responses were effectively controlled by Foxp3$^+$ Treg and IL-10. Although IL-35 was shown to regulate the Th17 responses, the expression of IL-35 in the tonsillar CD4$^+$ T cells were markedly suppressed by SAg-*Sau* stimulation. The Th17 responses in the nasopharynx are certainly important for the host defence against bacterial and fungal infections but they need to be tightly controlled. Th1 and Th17 cells both are implicated in the pathogenesis of inflammatory/autoimmune diseases. Since the development of these two CD4$^+$ T cell subsets is counter-regulated, it has been a dilemma on which subset should be primarily targeted when treating inflammatory conditions. The current opinions tend to suggest that Th17 cells are more pathogenic which is supported by a large number of studies.

Firstly, mice with IL-12p40-deficiency (*Il12p40*$^{-/-}$) are resistant to EAE induced by MOG peptide, whereas *Il12p35*$^{-/-}$ mice are susceptible[241]. IL-12p40 and IL-12p35 can be linked by disulphide bond to form the heterodimeric IL-12 which has been mentioned above for its ability to activate Th1 responses. Interestingly, the IL-12p40 subunit is shared by IL-23 (IL-12p40:IL-23p19

heterodimer) which is known to promote Th17 responses. By depleting IL-12p40, both Th1 and Th17 responses are limited due to IL-12 and IL-23 deficiency. In *Il12p35*$^{-/-}$ mice, only IL-12 is removed resulting in defected Th1 activation but leaving the IL-23-driven Th17 responses unaffected which may underlie the susceptibility of mice in EAE induction. Indeed, later studies have clarified the central role of Th17 cells in the pathology of autoimmune neural inflammation[58,60]. Notably, IL-12p35 can also pair with EBI3 to generate IL-35 heterodimer which means the *Il12p35*$^{-/-}$ mice also lack IL-35 expression leading to impaired suppression of Th17 responses. Though the overall clinical scores of developed EAE are comparable between *Il12p35*$^{-/-}$ and wild type mice, IL-12p35-deficiency has led to a higher production of nitric oxide (NO) in MOG-stimulated MNCs and an increase in TNF-α expression by lesional macrophages, which may correlate with the enhanced Th17 activation[241].

Secondly, genetic deletion of IFNγ cannot prevent the animal from developing EAE and increased mortality is observed in mice with IFN-gamma receptor (IFNGR) deficiency[49,242]. The paradoxical role of IFNγ-producing Th1 cells in autoimmunity is also manifested in collagen-induced arthritis (CIA), a murine model of rheumatoid arthritis, in which IFNGR deficiency has resulted in an accelerated onset of disease and more severe clinical symptoms[243,244]. Moreover, the loss of T-bet, the transcription factor that drives the development of Th1 cells, leads to a severe autoimmune heart disease which is associated with markedly increased Th17 responses[51]. Th17 cells also express T-bet but the Th17-mediated autoimmune inflammation is T-bet-independent, because *T-bet*$^{-/-}$ Th17 cells are still capable of inducing autoimmunity following adoptive transfer[50,245].

Finally, results obtained from clinical trials show biological agents that target IL-17A and IL-17RA have better efficacy than IL-12p40 monoclonal antibody (mAb) which affects both Th1 and Th17 in treating a wide range of autoimmune diseases, such as psoriasis, multiple sclerosis, rheumatoid arthritis and ankylosing spondylitis[37]. This suggests pro-inflammatory Th17 cells are at the centre of autoimmunity and Th1 responses may have certain beneficial effects through counteracting the development of Th17 cells.

Collectively, all these experimental and clinical evidences support that an uncontrolled Th17 response is likely to place the host at high risk of developing inflammatory/autoimmune

conditions. The SAg-*Sau* infection of nasopharynx has been shown in my study to activate potent Th17 responses in the NALT which cannot be effectively controlled by T cell-mediated immune suppression. My results therefore suggest SAg-*Sau*-mediated Th17 activation may underlie the mechanism of those inflammatory and autoimmune diseases associated with *Sau* infection.

6.11 IL-35 may have therapeutic potential for the treatment of autoimmune diseases

In this study, I have demonstrated that IL-35 is able to suppress highly activated Th17 response upon SAg-*Sau* stimulation in human NALT. IL-35-mediated suppression of Th17 activation and its therapeutic effects against CIA, IBD, EAE and uveitis have also been illustrated by previous studies in mice[95,97,99,100]. However, these IL-35-targeted murine studies cannot be fully translated into human studies due to the different expression profile of IL-35 in human T cells. In mice, IL-35 is primarily expressed by Foxp3$^+$ Tregs and can be induced in Tconvs by IL-35 itself[94,97]. However, human Foxp3$^+$ Tregs are not shown to express IL-35 with or without stimulation[101]. To induce IL-35 expression in Tconvs, longer period of stimulation is required by human Tconvs (9-day compared to the 3-day induction period in mice), and the protein expression and secretion of the heterodimeric IL-35 in human PBMC-derived Tconvs are not confirmed following induction[94]. I showed here that human tonsillar CD4$^+$ T cells expressed heterodimeric IL-35 using immunoprecipitation, indicating that IL-12p35 and EBI3 subunits expressed in human CD4$^+$ T cells can be associated to form IL-35. Although the level of IL-35 expression was lower than expected, the efficacy of cytokine was not absolutely determined by its concentration that can be detected by current methods.

The stability of IL-35 heterodimer affects its biological activity. Unlike IL-12 subunits, IL-12p40 and IL-12p35, which are linked by disulphide bond to maintain a stable structure of the heterodimer, the subunits of IL-35, IL-12p35 and EBI3 are dimerised depending on pure protein-protein interactions[164,246]. Detection of IL-35 in human peripheral blood has been repeatedly reported by various studies. The stability of IL-35 may rely on an additional

unidentified protein subunit binding to it. Specific binding proteins and soluble receptors that could affect the biological activity of cytokines, such as IL-18 and IL-15, has been demonstrated previously[247,248]. Currently, the widely used IL-35 recombinant protein is constructed by covalently linking EBI3 with the IL-12p35-Fc fusion protein[95]. This Fc-linked recombinant IL-35 is used in most of the experiments of this study. However, a CHO cell line that express native form of human IL-35 was constructed by our collaborators from Cardiff University and the biological activity of the native IL-35 was tested in my study and confirmed that it suppressed SAg-*Sau*-activated Th17 responses similarly as the Fc-linked IL-35. The native IL-35 used was not in purified form but was applied to the cell cultures as conditioned medium harvested from the IL-35-producing CHO cells. Hence, whether the native IL-35 can be efficiently purified without compromising its biological activity remains unknown. IL-35 is a potential therapeutic cytokine for inflammatory/autoimmune diseases, therefore a more stabilised recombinant protein preparation needs to be developed by future studies through identifying the potential binding protein or a possible chemical cross linking of the two protein subunits.

Studies have demonstrated the promising effects of IL-35 in controlling inflammatory and autoimmune pathologies, but how IL-35 expression is regulated in inflammatory conditions and what cellular and molecular mechanisms, particularly for those involved in IL-35-mediated suppression of Th17 responses need to be studied in detail. My key finding in this study was to show a significantly downregulated IL-35 expression in tonsillar $CD4^+$ T cells by SAg-*Sau* stimulation in human NALT, which was a potential mechanism of the potently induced superantigenic Th17 response. Furthermore, this Th17 response could not be suppressed by $Foxp3^+$ Tregs and IL-10, but were effectively controlled by exogenous IL-35, providing the rationale to further investigate the application of recombinant IL-35 in clinical diseases that are mediated by the pro-inflammatory Th17 responses.

Conclusion

My study highlights a critical cellular mechanism of Th17 activation in SAg-*Sau*-infected human nasopharynx, whereby IL-35 is identified as a key suppressive cytokine in controlling superantigen-driven Th17 responses. Foxp3$^+$ Tregs and IL-10 are known to play pivotal roles in suppressing CD4$^+$ T cell-mediated pro-inflammatory responses[114,146]. SAg-*Sau* was shown to induce Foxp3$^+$ Treg expansion and promote IL-10-producing CD4$^+$ T cells. SAg-*Sau*-expanded Tregs exhibited enhanced expression of IL-17A and defective suppressive function that may contribute to inflammatory pathologies. Whist SAg-*Sau*-activated Th1 responses can be suppressed by increased Treg and IL-10 levels, the Th17 responses were not affected. Instead, IL-35 expression in tonsillar CD4$^+$ T cells was markedly downregulated by SAg-*Sau* and addition of recombinant IL-35 suppressed highly activated Th17 responses. My data suggest that IL-10 and IL-35 have reciprocal regulatory effects on SAg-*Sau*-activated inflammatory Th1 and Th17 responses, thereby making them potential targets for therapy against inflammatory and autoimmune conditions.

References

1. Bogaert, D.*, et al.* Colonisation by Streptococcus pneumoniae and Staphylococcus aureus in healthy children. *The Lancet* **363**, 1871-1872 (2004).

2. Regev-Yochay, G.*, et al.* Association between carriage of Streptococcus pneumoniae and Staphylococcus aureus in Children. *JAMA* **292**, 716-720 (2004).

3. van den Bergh, M.R.*, et al.* Associations between pathogens in the upper respiratory tract of young children: interplay between viruses and bacteria. *PloS one* **7**, e47711 (2012).

4. McNally, L.M.*, et al.* Lack of association between the nasopharyngeal carriage of Streptococcus pneumoniae and Staphylococcus aureus in HIV-1-infected South African children. *The Journal of infectious diseases* **194**, 385-390 (2006).

5. Bogaert, D., Nouwen, J., Hermans, P.W. & Belkum, A. Lack of Interference between Streptococcus pneumoniae and Staphylococcus aureus in HIV-infected individuals? *The Journal of infectious diseases* **194**, 1617-1618; author reply 1618-1619 (2006).

6. Berger, S.*, et al.* Menstrual toxic shock syndrome: case report and systematic review of the literature. *The Lancet Infectious Diseases* **19**, e313-e321 (2019).

7. Kluytmans, J., van Belkum, A. & Verbrugh, H. Nasal carriage of Staphylococcus aureus: epidemiology, underlying mechanisms, and associated risks. *Clinical microbiology reviews* **10**, 505-520 (1997).

8. Ouedraogo, A.S.*, et al.* High Nasal Carriage Rate of Staphylococcus aureus Containing Panton-Valentine leukocidin- and EDIN-Encoding Genes in Community and Hospital Settings in Burkina Faso. *Front Microbiol* **7**, 1406 (2016).

9. Fijolek, J.*, et al.* The presence of staphylococcal superantigens in nasal swabs and correlation with activity of granulomatosis with polyangiitis in own material. *Clinical and experimental rheumatology* **36 Suppl 111**, 40-45 (2018).

10. Popa, E.R.*, et al.* Staphylococcal toxic-shock-syndrome-toxin-1 as a risk factor for disease relapse in Wegener's granulomatosis. *Rheumatology (Oxford)* **46**, 1029-1033 (2007).

11. Ben Zakour, N.L., Guinane, C.M. & Fitzgerald, J.R. Pathogenomics of the staphylococci: insights into niche adaptation and the emergence of new virulent strains. *FEMS Microbiology Letters* **289**, 1-12 (2008).

12. Wilson, G.J.*, et al.* A Novel Core Genome-Encoded Superantigen Contributes to Lethality of Community-Associated MRSA Necrotizing Pneumonia. *PLoS pathogens* **7**, e1002271 (2011).

13. Archer, N.K., Harro, J.M. & Shirtliff, M.E. Clearance of Staphylococcus aureus nasal carriage is T cell dependent and mediated through interleukin-17A expression and neutrophil influx. *Infection and immunity* **81**, 2070-2075 (2013).

14. Islander, U.*, et al.* Superantigenic Staphylococcus aureus stimulates production of interleukin-17 from memory but not naive T cells. *Infection and immunity* **78**, 381-386 (2010).

15. Stegeman, C.A.*, et al.* Association of chronic nasal carriage of Staphylococcus aureus and higher relapse rates in Wegener granulomatosis. *Ann. Intern. Med.* **120**, 12-17 (1994).

16. Blander, J.M., Torchinsky, M.B. & Campisi, L. Revisiting the old link between infection and autoimmune disease with commensals and T helper 17 cells. *Immunol. Res.* **54**, 50-68 (2012).

17. Christen, U. Editorial: pathogen infection and autoimmunity. *Int. Rev. Immunol.* **33**, 261-265 (2014).

18. Kallenberg, C.G.M. & Tadema, H. Vasculitis and infections: contribution to the issue of autoimmunity reviews devoted to "autoimmunity and infection". *Autoimmun Rev* **8**, 29-32 (2008).

19. Ruff, W.E. & Kriegel, M.A. Autoimmune host-microbiota interactions at barrier sites and beyond. *Trends in molecular medicine* **21**, 233-244 (2015).

20. Haidan, A.*, et al.* Pharyngeal carriage of group C and group G streptococci and acute rheumatic fever in an Aboriginal population. *Lancet (London, England)* **356**, 1167-1169 (2000).

21. Vanderlugt, C.L. & Miller, S.D. Epitope spreading in immune-mediated diseases: implications for immunotherapy. *Nature Reviews Immunology* **2**, 85 (2002).

22. Miller, S.D.*, et al.* Persistent infection with Theiler's virus leads to CNS autoimmunity via epitope spreading. *Nature medicine* **3**, 1133-1136 (1997).

23. Marrack, P. & Kappler, J. The staphylococcal enterotoxins and their relatives. *Science* **248**, 705-711 (1990).

24. Fraser, J.D. Clarifying the Mechanism of Superantigen Toxicity. *PLoS Biology* **9**, e1001145 (2011).

25. Schwab, J.H., Brown, R.R., Anderle, S.K. & Schlievert, P.M. Superantigen can reactivate bacterial cell wall-induced arthritis. *The Journal of Immunology* **150**, 4151 (1993).

26. Brocke, S.*, et al.* Induction of relapsing paralysis in experimental autoimmune encephalomyelitis by bacterial superantigen. *Nature* **365**, 642-644 (1993).

27. Schiffenbauer, J., Johnson, H.M., Butfiloski, E.J., Wegrzyn, L. & Soos, J.M. Staphylococcal enterotoxins can reactivate experimental allergic encephalomyelitis. *Proceedings of the National Academy of Sciences of the United States of America* **90**, 8543-8546 (1993).

28. Gaur, A., Fathman, C.G., Steinman, L. & Brocke, S. SEB induced anergy: modulation of immune response to T cell determinants of myoglobin and myelin basic protein. *The Journal of Immunology* **150**, 3062 (1993).

29. Kawabe, Y. & Ochi, A. Programmed cell death and extrathymic reduction of Vβ8+CD4+ T cells in mice tolerant to Staphylococcus aureus enterotoxin B. *Nature* **349**, 245-248 (1991).

30. Lussow, A.R. & MacDonald, H.R. Differential effects of superantigen-induced "anergy" on priming and effector stages of a T cell-dependent antibody response. *European journal of immunology* **24**, 445-449 (1994).

31. Soos, J.M., Hobeika, A.C., Butfiloski, E.J., Schiffenbauer, J. & Johnson, H.M. Accelerated induction of experimental allergic encephalomyelitis in PL/J mice by a non-V beta 8-specific superantigen. *Proceedings of the National Academy of Sciences of the United States of America* **92**, 6082-6086 (1995).

32. Pakbaz, Z., Sahraian, M.A., Sabzi, S., Mahmoodi, M. & Pourmand, M.R. Prevalence of sea, seb, sec, sed, and tsst-1 genes of Staphylococcus aureus in nasal carriage and their association with multiple sclerosis. *Germs* **7**, 171-177 (2017).

33. Lindberg, E., Nowrouzian, F., Adlerberth, I. & Wold, A.E. Long-time persistence of superantigen-producing Staphylococcus aureus strains in the intestinal microflora of healthy infants. *Pediatr Res* **48**, 741-747 (2000).

34. Kohno, H., Sakai, T., Tsuneoka, H., Imanishi, K.i. & Saito, S. Staphylococcal enterotoxin B is involved in aggravation and recurrence of murine experimental autoimmune uveoretinitis via Vbeta8+CD4+ T cells. *Exp. Eye Res.* **89**, 486-493 (2009).

35. Chowdhary, V.R., Tilahun, A.Y., Clark, C.R., Grande, J.P. & Rajagopalan, G. Chronic exposure to staphylococcal superantigen elicits a systemic inflammatory disease mimicking lupus. *J. Immunol.* **189**, 2054-2062 (2012).

36. Theofilopoulos, A.N., Kono, D.H. & Baccala, R. The multiple pathways to autoimmunity. *Nature immunology* **18**, 716-724 (2017).

37. Patel, D.D. & Kuchroo, V.K. Th17 Cell Pathway in Human Immunity: Lessons from Genetics and Therapeutic Interventions. *Immunity* **43**, 1040-1051 (2015).

38. Jackson, M.S., Bagg, J., Gupta, M.N. & Sturrock, R.D. Oral carriage of staphylococci in patients with rheumatoid arthritis. *Rheumatology (Oxford)* **38**, 572-575 (1999).

39. Mulvey, M.R*., et al.* Staphylococcus aureus harbouring Enterotoxin A as a possible risk factor for multiple sclerosis exacerbations. *Mult Scler* **17**, 397-403 (2011).

40. Tadema, H., Heeringa, P. & Kallenberg, C.G.M. Bacterial infections in Wegener's granulomatosis: mechanisms potentially involved in autoimmune pathogenesis. *Curr Opin Rheumatol* **23**, 366-371 (2011).

41. Leung, D.Y.*, et al.* Toxic shock syndrome toxin-secreting Staphylococcus aureus in Kawasaki syndrome. *Lancet (London, England)* **342**, 1385-1388 (1993).

42. Tabarya, D. & Hoffman, W.L. Staphylococcus aureus nasal carriage in rheumatoid arthritis: antibody response to toxic shock syndrome toxin-1. **55**, 823-828 (1996).

43. Laudien, M.*, et al.* Nasal carriage of Staphylococcus aureus and endonasal activity in Wegener s granulomatosis as compared to rheumatoid arthritis and chronic Rhinosinusitis with nasal polyps. *Clinical and experimental rheumatology* **28**, 51-55 (2010).

44. Popa, E.R. & Tervaert, J.W.C. The relation between Staphylococcus aureus and Wegener's granulomatosis: current knowledge and future directions. *Intern. Med.* **42**, 771-780 (2003).

45. Conti, F.*, et al.* Association between Staphylococcus aureus nasal carriage and disease phenotype in patients affected by systemic lupus erythematosus. *Arthritis Res. Ther.* **18**, 177 (2016).

46. Bassetti, S.*, et al.* Staphylococcus aureus in patients with rheumatoid arthritis under conventional and anti-tumor necrosis factor-alpha treatment. *The Journal of rheumatology* **32**, 2125-2129 (2005).

47. Wu, H.-J.*, et al.* Gut-Residing Segmented Filamentous Bacteria Drive Autoimmune Arthritis via T Helper 17 Cells. **32**, 815-827 (2010).

48. Lee, Y.K., Menezes, J.S., Umesaki, Y. & Mazmanian, S.K. Proinflammatory T-cell responses to gut microbiota promote experimental autoimmune encephalomyelitis. *Proceedings of the National Academy of Sciences* **108**, 4615-4622 (2011).

49. Ferber, I.A.*, et al.* Mice with a disrupted IFN-gamma gene are susceptible to the induction of experimental autoimmune encephalomyelitis (EAE). *J. Immunol.* **156**, 5-7 (1996).

50. Grifka-Walk, H.M., Lalor, S.J. & Segal, B.M. Highly polarized Th17 cells induce EAE via a T-bet independent mechanism. *European journal of immunology* **43**, 2824-2831 (2013).

51. Rangachari, M.*, et al.* T-bet negatively regulates autoimmune myocarditis by suppressing local production of interleukin 17. *J. Exp. Med.* **203**, 2009-2019 (2006).

52. Meller, S.*, et al.* T(H)17 cells promote microbial killing and innate immune sensing of DNA via interleukin 26. *Nature immunology* **16**, 970-979 (2015).

53. Zhang, Z., Clarke, T.B. & Weiser, J.N. Cellular effectors mediating Th17-dependent clearance of pneumococcal colonization in mice. *The Journal of clinical investigation* **119**, 1899-1909 (2009).

54. Ueno, A.*, et al.* Th17 plasticity and its relevance to inflammatory bowel disease. *Journal of autoimmunity* **87**, 38-49 (2018).

55. Lubberts, E.*, et al.* IL-1-independent role of IL-17 in synovial inflammation and joint destruction during collagen-induced arthritis. *Journal of immunology* **167**, 1004-1013 (2001).

56. Nakae, S., Nambu, A., Sudo, K. & Iwakura, Y. Suppression of Immune Induction of Collagen-Induced Arthritis in IL-17-Deficient Mice. *The Journal of Immunology* **171**, 6173-6177 (2003).

57. Komiyama, Y.*, et al.* IL-17 plays an important role in the development of experimental autoimmune encephalomyelitis. *Journal of immunology* **177**, 566-573 (2006).

58. Langrish, C.L.*, et al.* IL-23 drives a pathogenic T cell population that induces autoimmune inflammation. *J. Exp. Med.* **201**, 233-240 (2005).

59. Ivanov, II*, et al.* The orphan nuclear receptor RORgammat directs the differentiation program of proinflammatory IL-17+ T helper cells. *Cell* **126**, 1121-1133 (2006).

60. Cua, D.J.*, et al.* Interleukin-23 rather than interleukin-12 is the critical cytokine for autoimmune inflammation of the brain. *Nature* **421**, 744-748 (2003).

61. Weaver, C.T., Elson, C.O., Fouser, L.A. & Kolls, J.K. The Th17 Pathway and Inflammatory Diseases of the Intestines, Lungs, and Skin. *Annual Review of Pathology: Mechanisms of Disease* **8**, 477-512 (2013).

62. Choy, D.F.*, et al.* T H 2 and T H 17 inflammatory pathways are reciprocally regulated in asthma. *Science Translational Medicine* **7**, 301ra129-301ra301 (2015).

63. Noda, S.*, et al.* The Asian atopic dermatitis phenotype combines features of atopic dermatitis and psoriasis with increased TH17 polarization. *J Allergy Clin Immunol* **136**, 1254-1264 (2015).

64. Nakae, S.*, et al.* Antigen-Specific T Cell Sensitization Is Impaired in IL-17-Deficient Mice, Causing Suppression of Allergic Cellular and Humoral Responses. *Immunity* **17**, 375-387 (2002).

65. Joshi, A.D.*, et al.* Interleukin-17-mediated immunopathogenesis in experimental hypersensitivity pneumonitis. *Am J Respir Crit Care Med* **179**, 705-716 (2009).

66. Lambrecht, B.N. & Hammad, H. The immunology of asthma. *Nature immunology* **16**, 45-56 (2015).

67. Newcomb, D.C.*, et al.* Human TH17 cells express a functional IL-13 receptor and IL-13 attenuates IL-17A production. *J Allergy Clin Immunol* **127**, 1006-1013 e1001-1004 (2011).

68. Lee, Y.*, et al.* Induction and molecular signature of pathogenic TH17 cells. *Nature immunology* **13**, 991-999 (2012).

69. Reboldi, A.*, et al.* C-C chemokine receptor 6-regulated entry of TH-17 cells into the CNS through the choroid plexus is required for the initiation of EAE. *Nature immunology* **10**, 514-523 (2009).

70. El-Behi, M.*, et al.* The encephalitogenicity of T(H)17 cells is dependent on IL-1- and IL-23-induced production of the cytokine GM-CSF. *Nature immunology* **12**, 568-575 (2011).

71. Grumann, D.*, et al.* Immune Cell Activation by Enterotoxin Gene Cluster (egc)-Encoded and Non-egc Superantigens from Staphylococcus aureus. **181**, 5054-5061 (2008).

72. Abdulahad, W.H., Stegeman, C.A., Limburg, P.C. & Kallenberg, C.G.M. Skewed distribution of Th17 lymphocytes in patients with Wegener's granulomatosis in remission. *Arthritis Rheum.* **58**, 2196-2205 (2008).

73. Kim, J.M., Rasmussen, J.P. & Rudensky, A.Y. Regulatory T cells prevent catastrophic autoimmunity throughout the lifespan of mice. *Nature immunology* **8**, 191-197 (2007).

74. Roncarolo, M.G. & Battaglia, M. Regulatory T-cell immunotherapy for tolerance to self antigens and alloantigens in humans. *Nature reviews. Immunology* **7**, 585-598 (2007).

75. Stummvoll, G.H.*, et al.* Th1, Th2, and Th17 effector T cell-induced autoimmune gastritis differs in pathological pattern and in susceptibility to suppression by regulatory T cells. *Journal of immunology* **181**, 1908-1916 (2008).

76. Huter, E.N., Stummvoll, G.H., DiPaolo, R.J., Glass, D.D. & Shevach, E.M. Cutting edge: antigen-specific TGF beta-induced regulatory T cells suppress Th17-mediated autoimmune disease. *Journal of immunology* **181**, 8209-8213 (2008).

77. Chaudhry, A.*, et al.* CD4+ regulatory T cells control TH17 responses in a Stat3-dependent manner. *Science* **326**, 986-991 (2009).

78. Chaudhry, A.*, et al.* Interleukin-10 signaling in regulatory T cells is required for suppression of Th17 cell-mediated inflammation. *Immunity* **34**, 566-578 (2011).

79. Annunziato, F.*, et al.* Phenotypic and functional features of human Th17 cells. *J Exp Med* **204**, 1849-1861 (2007).

80. Evans, H.G., Suddason, T., Jackson, I., Taams, L.S. & Lord, G.M. Optimal induction of T helper 17 cells in humans requires T cell receptor ligation in the context of Toll-like receptor-activated monocytes. *Proceedings of the National Academy of Sciences of the United States of America* **104**, 17034-17039 (2007).

81. Fletcher, J.M.*, et al.* CD39+Foxp3+ regulatory T Cells suppress pathogenic Th17 cells and are impaired in multiple sclerosis. *J. Immunol.* **183**, 7602-7610 (2009).

82. Deaglio, S.*, et al.* Adenosine generation catalyzed by CD39 and CD73 expressed on regulatory T cells mediates immune suppression. *J Exp Med* **204**, 1257-1265 (2007).

83. Antonioli, L., Pacher, P., Vizi, E.S. & Haskó, G. CD39 and CD73 in immunity and inflammation. *Trends in molecular medicine* **19**, 355-367 (2013).

84. Borsellino, G.*, et al.* Expression of ectonucleotidase CD39 by Foxp3+ Treg cells: hydrolysis of extracellular ATP and immune suppression. *Blood* **110**, 1225-1232 (2007).

85. Huber, S.*, et al.* Th17 cells express interleukin-10 receptor and are controlled by Foxp3(-) and Foxp3+ regulatory CD4+ T cells in an interleukin-10-dependent manner. *Immunity* **34**, 554-565 (2011).

86. Aschenbrenner, D.*, et al.* An immunoregulatory and tissue-residency program modulated by c-MAF in human TH17 cells. *Nature immunology* **19**, 1126-1136 (2018).

87. Shouval, D.S.*, et al.* Interleukin-10 receptor signaling in innate immune cells regulates mucosal immune tolerance and anti-inflammatory macrophage function. *Immunity* **40**, 706-719 (2014).

88. Kotlarz, D.*, et al.* Loss of interleukin-10 signaling and infantile inflammatory bowel disease: implications for diagnosis and therapy. *Gastroenterology* **143**, 347-355 (2012).

89. Glocker, E.O.*, et al.* Inflammatory bowel disease and mutations affecting the interleukin-10 receptor. *The New England journal of medicine* **361**, 2033-2045 (2009).

90. Glocker, E.O.*, et al.* Infant colitis--it's in the genes. *Lancet (London, England)* **376**, 1272 (2010).

91. Saxena, A.*, et al.* Interleukin-10 paradox: A potent immunoregulatory cytokine that has been difficult to harness for immunotherapy. *Cytokine* **74**, 27-34 (2015).

92. Sanchez, M.*, et al.* O-Acetylation of Peptidoglycan Limits Helper T Cell Priming and Permits Staphylococcus aureus Reinfection. *Cell Host Microbe* **22**, 543-551 e544 (2017).

93. Choi, J., Leung, P.S., Bowlus, C. & Gershwin, M.E. IL-35 and Autoimmunity: a Comprehensive Perspective. *Clin Rev Allergy Immunol* **49**, 327-332 (2015).

94. Collison, L.W.*, et al.* IL-35-mediated induction of a potent regulatory T cell population. *Nature immunology* **11**, 1093-1101 (2010).

95. Niedbala, W.*, et al.* IL-35 is a novel cytokine with therapeutic effects against collagen-induced arthritis through the expansion of regulatory T cells and suppression of Th17 cells. *European journal of immunology* **37**, 3021-3029 (2007).

96. Whitehead, G.S.*, et al.* IL-35 production by inducible costimulator (ICOS)-positive regulatory T cells reverses established IL-17-dependent allergic airways disease. *J. Allergy Clin. Immunol.* **129**, 207-215.e201-205 (2012).

97. Collison, L.W.*, et al.* The inhibitory cytokine IL-35 contributes to regulatory T-cell function. *Nature* **450**, 566-569 (2007).

98. Dambuza, I.M.*, et al.* IL-12p35 induces expansion of IL-10 and IL-35-expressing regulatory B cells and ameliorates autoimmune disease. *Nature communications* **8**, 719 (2017).

99. Shen, P.*, et al.* IL-35-producing B cells are critical regulators of immunity during autoimmune and infectious diseases. *Nature* **507**, 366-370 (2014).

100. Wang, R.-X.*, et al.* Interleukin-35 induces regulatory B cells that suppress autoimmune disease. *Nature medicine* **20**, 633-641 (2014).

101. Bardel, E., Larousserie, F., Charlot-Rabiega, P., Coulomb-L'Herminé, A. & Devergne, O. Human CD4+ CD25+ Foxp3+ regulatory T cells do not constitutively express IL-35. *J. Immunol.* **181**, 6898-6905 (2008).

102. Sonmez, C.*, et al.* Correlation between IL-17A/F, IL-23, IL-35 and IL-12/-23 (p40) levels in peripheral blood lymphocyte cultures and disease activity in Behcet's patients. *Clinical Rheumatology* **37**, 2797-2804 (2018).

103. Fogel, O.*, et al.* Role of the IL-12/IL-35 balance in patients with Sjogren syndrome. *J Allergy Clin Immunol* **142**, 258-268.e255 (2018).

104. Nakano, S.*, et al.* Immunoregulatory role of IL-35 in T cells of patients with rheumatoid arthritis. *Rheumatology (Oxford)* **54**, 1498-1506 (2015).

105. Kiyono, H. & Fukuyama, S. NALT- versus PEYER'S-patch-mediated mucosal immunity. *Nature Reviews Immunology* **4**, 699-710 (2004).

106. Stanisce, L.*, et al.* Differential cellular composition of human palatine and pharyngeal tonsils. *Archives of Oral Biology* **96**, 80-86 (2018).

107. Geissler, K.*, et al.* Functional characterization of T-cells from palatine tonsils in patients with chronic tonsillitis. *PloS one* **12**, e0183214 (2017).

108. Bradley, C.P.*, et al.* Segmented Filamentous Bacteria Provoke Lung Autoimmunity by Inducing Gut-Lung Axis Th17 Cells Expressing Dual TCRs. *Cell Host & Microbe* **22**, 697-704.e694 (2017).

109. Eftimiadi, C., Eftimiadi, G. & Vinai, P. Staphylococcus aureus Colonization Modulates Tic Expression and the Host Immune Response in a Girl with Tourette Syndrome. *Front Psychiatry* **7**, 31 (2016).

110. Ou, L.S., Goleva, E., Hall, C. & Leung, D.Y. T regulatory cells in atopic dermatitis and subversion of their activity by superantigens. *J Allergy Clin Immunol* **113**, 756-763 (2004).

111. Taylor, A.L. & Llewelyn, M.J. Superantigen-induced proliferation of human CD4+CD25- T cells is followed by a switch to a functional regulatory phenotype. *J. Immunol.* **185**, 6591-6598 (2010).

112. Mubarak, A.*, et al.* A dynamic relationship between mucosal T helper type 17 and regulatory T-cell populations in nasopharynx evolves with age and associates with the clearance of pneumococcal carriage in humans. *Clinical Microbiology and Infection* **22**, 736.e731-736.e737 (2016).

113. Zeppa, J.J.*, et al.* Nasopharyngeal infection byStreptococcus pyogenesrequires superantigen-responsive Vβ-specific T cells. *Proceedings of the National Academy of Sciences* **114**, 10226-10231 (2017).

114. Josefowicz, S.Z., Lu, L.F. & Rudensky, A.Y. Regulatory T cells: mechanisms of differentiation and function. *Annual review of immunology* **30**, 531-564 (2012).

115. Lee, G.R. The Balance of Th17 versus Treg Cells in Autoimmunity. *Int J Mol Sci* **19**(2018).

116. Noack, M. & Miossec, P. Th17 and regulatory T cell balance in autoimmune and inflammatory diseases. *Autoimmun Rev* **13**, 668-677 (2014).

117. Zhang, Q.*, et al.* Characterisation of regulatory T cells in nasal associated lymphoid tissue in children: relationships with pneumococcal colonization. *PLoS pathogens* **7**, e1002175 (2011).

118. Voo, K.S.*, et al.* Identification of IL-17-producing FOXP3+ regulatory T cells in humans. *Proceedings of the National Academy of Sciences of the United States of America* **106**, 4793-4798 (2009).

119. Komatsu, N.*, et al.* Pathogenic conversion of Foxp3+ T cells into TH17 cells in autoimmune arthritis. *Nature medicine* **20**, 62-68 (2014).

120. Kleinewietfeld, M. & Hafler, D.A. The plasticity of human Treg and Th17 cells and its role in autoimmunity. *Semin. Immunol.* **25**, 305-312 (2013).

121. Worthington, J.J.*, et al.* Integrin αvβ8-Mediated TGF-β Activation by Effector Regulatory T Cells Is Essential for Suppression of T-Cell-Mediated Inflammation. *Immunity* **42**, 903-915 (2015).

122. Cuende, J.*, et al.* Monoclonal antibodies against GARP/TGF-beta1 complexes inhibit the immunosuppressive activity of human regulatory T cells in vivo. *Sci Transl Med* **7**, 284ra256 (2015).

123. Stockis, J., Colau, D., Coulie, P.G. & Lucas, S. Membrane protein GARP is a receptor for latent TGF-beta on the surface of activated human Treg. *European journal of immunology* **39**, 3315-3322 (2009).

124. Walker, L.S. Treg and CTLA-4: two intertwining pathways to immune tolerance. *Journal of autoimmunity* **45**, 49-57 (2013).

125. Qureshi, O.S.*, et al.* Trans-endocytosis of CD80 and CD86: a molecular basis for the cell-extrinsic function of CTLA-4. *Science* **332**, 600-603 (2011).

126. Rowshanravan, B., Halliday, N. & Sansom, D.M. CTLA-4: a moving target in immunotherapy. *Blood*, blood-2017-2006-2017 (2017).

127. Lo, B. & Abdel-Motal, U.M. Lessons from CTLA-4 deficiency and checkpoint inhibition. *Curr. Opin. Immunol.* **49**, 14-19 (2017).

128. Wing, K.*, et al.* CTLA-4 control over Foxp3+ regulatory T cell function. *Science* **322**, 271-275 (2008).

129. Watanabe, N., Kaminuma, O., Kitamura, N. & Hiroi, T. Induced Treg Cells Augment the Th17-Mediated Intestinal Inflammatory Response in a CTLA4-Dependent Manner. *PloS one* **11**, e0150244 (2016).

130. Allard, B., Longhi, M.S., Robson, S.C. & Stagg, J. The ectonucleotidases CD39 and CD73: Novel checkpoint inhibitor targets. *Immunological reviews* **276**, 121-144 (2017).

131. Magid-Bernstein, J.R. & Rohowsky-Kochan, C.M. Human CD39(+) Treg Cells Express Th17-Associated Surface Markers and Suppress IL-17 via a Stat3-Dependent Mechanism. *J. Interferon Cytokine Res.* **37**, 153-164 (2017).

132. Schenk, U.*, et al.* Purinergic control of T cell activation by ATP released through pannexin-1 hemichannels. *Sci Signal* **1**, ra6 (2008).

133. Schenk, U.*, et al.* ATP inhibits the generation and function of regulatory T cells through the activation of purinergic P2X receptors. *Sci Signal* **4**, ra12 (2011).

134. Maloy, K.J. & Powrie, F. Regulatory T cells in the control of immune pathology. *Nature immunology* **2**, 816-822 (2001).

135. Mason, D. & Powrie, F. Control of immune pathology by regulatory T cells. *Curr. Opin. Immunol.* **10**, 649-655 (1998).

136. Shevach, E.M. Regulatory T Cells in Autoimmmunity. *Annual review of immunology* **18**, 423-449 (2000).

137. Sakaguchi, S., Sakaguchi, N., Asano, M., Itoh, M. & Toda, M. Pillars article: immunologic self-tolerance maintained by activated T cells expressing IL-2 receptor alpha-chains (CD25). Breakdown of a single mechanism of self-tolerance causes various autoimmune diseases. J. Immunol. 1995. *Journal of immunology* **186**, 3808-3821 (2011).

138. Hori, S. Control of Regulatory T Cell Development by the Transcription Factor Foxp3. *Science* **299**, 1057-1061 (2003).

139. Fontenot, J.D., Gavin, M.A. & Rudensky, A.Y. Foxp3 programs the development and function of CD4+CD25+ regulatory T cells. *Nature immunology* **4**, 330-336 (2003).

140. Khattri, R., Cox, T., Yasayko, S.-A. & Ramsdell, F. An essential role for Scurfin in CD4+CD25+ T regulatory cells. *Nature immunology* **4**, 337-342 (2003).

141. Chatila, T.A.*, et al.* JM2, encoding a fork head-related protein, is mutated in X-linked autoimmunity-allergic disregulation syndrome. *The Journal of clinical investigation* **106**, R75-81 (2000).

142. Bennett, C.L.*, et al.* The immune dysregulation, polyendocrinopathy, enteropathy, X-linked syndrome (IPEX) is caused by mutations of FOXP3. *Nature Genetics* **27**, 20-21 (2001).

143. Wildin, R.S.*, et al.* X-linked neonatal diabetes mellitus, enteropathy and endocrinopathy syndrome is the human equivalent of mouse scurfy. *Nat Genet* **27**, 18-20 (2001).

144. Sakaguchi, S.*, et al.* Foxp3+CD25+CD4+ natural regulatory T cells in dominant self-tolerance and autoimmune disease. *Immunological reviews* **212**, 8-27 (2006).

145. Moore, K.W., De Waal Malefyt, R., Coffman, R.L. & O'Garra, A. INTERLEUKIN-10AND THEINTERLEUKIN-10 RECEPTOR. *Annual review of immunology* **19**, 683-765 (2001).

146. Ouyang, W., Rutz, S., Crellin, N.K., Valdez, P.A. & Hymowitz, S.G. Regulation and functions of the IL-10 family of cytokines in inflammation and disease. *Annual review of immunology* **29**, 71-109 (2011).

147. Fiorentino, D.F. Two types of mouse T helper cell. IV. Th2 clones secrete a factor that inhibits cytokine production by Th1 clones. *Journal of Experimental Medicine* **170**, 2081-2095 (1989).

148. Joss, A., Akdis, M., Faith, A., Blaser, K. & Akdis, C.A. IL-10 directly acts on T cells by specifically altering the CD28 co-stimulation pathway. *European journal of immunology* **30**, 1683-1690 (2000).

149. Fiorentino, D.F.*, et al.* IL-10 acts on the antigen-presenting cell to inhibit cytokine production by Th1 cells. *Journal of immunology* **146**, 3444-3451 (1991).

150. Bettelli, E.*, et al.* IL-10 is critical in the regulation of autoimmune encephalomyelitis as demonstrated by studies of IL-10- and IL-4-deficient and transgenic mice. *Journal of immunology* **161**, 3299-3306 (1998).

151. Létourneau, S., Krieg, C., Pantaleo, G. & Boyman, O. IL-2– and CD25-dependent immunoregulatory mechanisms in the homeostasis of T-cell subsets. *Journal of Allergy and Clinical Immunology* **123**, 758-762 (2009).

152. Pandiyan, P., Zheng, L., Ishihara, S., Reed, J. & Lenardo, M.J. CD4+CD25+Foxp3+ regulatory T cells induce cytokine deprivation-mediated apoptosis of effector CD4+ T cells. *Nature immunology* **8**, 1353-1362 (2007).

153. Laurence, A.*, et al.* Interleukin-2 signaling via STAT5 constrains T helper 17 cell generation. *Immunity* **26**, 371-381 (2007).

154. Fujimura, K., Oyamada, A., Iwamoto, Y., Yoshikai, Y. & Yamada, H. CD4 T cell-intrinsic IL-2 signaling differentially affects Th1 and Th17 development. *Journal of leukocyte biology* **94**, 271-279 (2013).

155. Cottrez, F. & Groux, H. Regulation of TGF-beta response during T cell activation is modulated by IL-10. *Journal of immunology* **167**, 773-778 (2001).

156. Stadhouders, R., Lubberts, E. & Hendriks, R.W. A cellular and molecular view of T helper 17 cell plasticity in autoimmunity. *Journal of autoimmunity* **87**, 1-15 (2018).

157. Codarri, L.*, et al.* RORgammat drives production of the cytokine GM-CSF in helper T cells, which is essential for the effector phase of autoimmune neuroinflammation. *Nature immunology* **12**, 560-567 (2011).

158. El-Behi, M.*, et al.* The encephalitogenicity of TH17 cells is dependent on IL-1- and IL-23-induced production of the cytokine GM-CSF. *Nature immunology* **12**, 568-575 (2011).

159. Hamilton, J.A. & Anderson, G.P. GM-CSF Biology. *Growth Factors* **22**, 225-231 (2004).

160. Becher, B., Tugues, S. & Greter, M. GM-CSF: From Growth Factor to Central Mediator of Tissue Inflammation. *Immunity* **45**, 963-973 (2016).

161. Gaffen, S.L., Jain, R., Garg, A.V. & Cua, D.J. The IL-23–IL-17 immune axis: from mechanisms to therapeutic testing. *Nature Reviews Immunology* **14**, 585-600 (2014).

162. McQualter, J.L.*, et al.* Granulocyte macrophage colony-stimulating factor: a new putative therapeutic target in multiple sclerosis. *J Exp Med* **194**, 873-882 (2001).

163. McGeachy, M.J.*, et al.* The interleukin 23 receptor is essential for the terminal differentiation of interleukin 17–producing effector T helper cells in vivo. *Nature immunology* **10**, 314-324 (2009).

164. Vignali, D.A. & Kuchroo, V.K. IL-12 family cytokines: immunological playmakers. *Nature immunology* **13**, 722-728 (2012).

165. Devergne, O., Birkenbach, M. & Kieff, E. Epstein-Barr virus-induced gene 3 and the p35 subunit of interleukin 12 form a novel heterodimeric hematopoietin. *Proceedings of the National Academy of Sciences* **94**, 12041-12046 (1997).

166. Devergne, O., Coulomb-L'Herminé, A., Capel, F., Moussa, M. & Capron, F. Expression of Epstein-Barr Virus-Induced Gene 3, an Interleukin-12 p40-Related Molecule, throughout Human Pregnancy. *The American Journal of Pathology* **159**, 1763-1776 (2001).

167. Seyerl, M.*, et al.* Human rhinoviruses induce IL-35-producing Treg via induction of B7-H1 (CD274) and sialoadhesin (CD169) on DC. *European journal of immunology* **40**, 321-329 (2010).

168. Wirtz, S., Billmeier, U., McHedlidze, T., Blumberg, R.S. & Neurath, M.F. Interleukin-35 mediates mucosal immune responses that protect against T-cell-dependent colitis. *Gastroenterology* **141**, 1875-1886 (2011).

169. Kochetkova, I., Golden, S., Holderness, K., Callis, G. & Pascual, D.W. IL-35 stimulation of CD39+ regulatory T cells confers protection against collagen II-induced arthritis via the production of IL-10. *J. Immunol.* **184**, 7144-7153 (2010).

170. Ouyang, H.*, et al.* Decreased interleukin 35 and CD4+EBI3+ T cells in patients with active systemic lupus erythematosus. *The American journal of the medical sciences* **348**, 156-161 (2014).

171. Wei, X.*, et al.* Reciprocal Expression of IL-35 and IL-10 Defines Two Distinct Effector Treg Subsets that Are Required for Maintenance of Immune Tolerance. *Cell reports* **21**, 1853-1869 (2017).

172. Sawant, D.V.*, et al.* Adaptive plasticity of IL-10+ and IL-35+ Treg cells cooperatively promotes tumor T cell exhaustion. *Nature immunology* (2019).

173. Dong, J.*, et al.* Amelioration of allergic airway inflammation in mice by regulatory IL-35 through dampening inflammatory dendritic cells. *Allergy* **70**, 921-932 (2015).

174. Lee, C.C.*, et al.* Macrophage-secreted interleukin-35 regulates cancer cell plasticity to facilitate metastatic colonization. *Nat Commun* **9**, 3763 (2018).

175. Collison, L.W.*, et al.* The composition and signaling of the IL-35 receptor are unconventional. *Nature immunology* **13**, 290-299 (2012).

176. Okada, K.*, et al.* Effect of interleukin (IL)-35 on IL-17 expression and production by human CD4(+) T cells. *PeerJ* **5**, e2999 (2017).

177. Korn, T. Disentangling the manifold functions of RORgammat. *Nature immunology* **18**, 1059-1060 (2017).

178. Newsom, S.W. Ogston's coccus. *J Hosp Infect* **70**, 369-372 (2008).

179. Brown, A.F., Leech, J.M., Rogers, T.R. & McLoughlin, R.M. Staphylococcus aureus Colonization: Modulation of Host Immune Response and Impact on Human Vaccine Design. *Frontiers in immunology* **4**, 507 (2014).

180. Muluk, N.B., Altın, F. & Cingi, C. Role of Superantigens in Allergic Inflammation: Their Relationship to Allergic Rhinitis, Chronic Rhinosinusitis, Asthma, and Atopic Dermatitis. *American Journal of Rhinology & Allergy* **32**, 502-517 (2018).

181. Stiles, B.G. & Krakauer, T. Staphylococcal enterotoxins: A purging experience in review, Part I. *Clinical Microbiology Newsletter* **27**, 179-186 (2005).

182. Fleischer, B.*, et al.* An evolutionary conserved mechanism of T cell activation by microbial toxins. Evidence for different affinities of T cell receptor-toxin interaction. *Journal of immunology* **146**, 11-17 (1991).

183. Sewell, A.K. Why must T cells be cross-reactive? *Nature reviews. Immunology* **12**, 669-677 (2012).

184. Chen, X., Poncette, L. & Blankenstein, T. Human TCR-MHC coevolution after divergence from mice includes increased nontemplate-encoded CDR3 diversity. *J Exp Med* **214**, 3417-3433 (2017).

185. Li, H., Llera, A., Malchiodi, E.L. & Mariuzza, R.A. The structural basis of T cell activation by superantigens. *Annual review of immunology* **17**, 435-466 (1999).

186. Choi, Y.W.*, et al.* Interaction of Staphylococcus aureus toxin "superantigens" with human T cells. *Proceedings of the National Academy of Sciences* **86**, 8941-8945 (1989).

187. Bretscher, P.A. A two-step, two-signal model for the primary activation of precursor helper T cells. *Proceedings of the National Academy of Sciences of the United States of America* **96**, 185-190 (1999).

188. Blum, J.S., Wearsch, P.A. & Cresswell, P. Pathways of Antigen Processing. *Annual review of immunology* **31**, 443-473 (2013).

189. Wing, J.B. & Sakaguchi, S. TCR diversity and Treg cells, sometimes more is more. *European journal of immunology* **41**, 3097-3100 (2011).

190. Takaba, H. & Takayanagi, H. The Mechanisms of T Cell Selection in the Thymus. *Trends in Immunology* **38**, 805-816 (2017).

191. Starr, T.K., Jameson, S.C. & Hogquist, K.A. Positive and negative selection of T cells. *Annual review of immunology* **21**, 139-176 (2003).

192. Malhotra, D.*, et al.* Tolerance is established in polyclonal CD4+ T cells by distinct mechanisms, according to self-peptide expression patterns. *Nature immunology* **17**, 187-195 (2016).

193. Legoux, F.P.*, et al.* CD4+ T Cell Tolerance to Tissue-Restricted Self Antigens Is Mediated by Antigen-Specific Regulatory T Cells Rather Than Deletion. *Immunity* **43**, 896-908 (2015).

194. Dieckmann, D., Plottner, H., Berchtold, S., Berger, T. & Schuler, G. Ex vivo isolation and characterization of CD4(+)CD25(+) T cells with regulatory properties from human blood. *J Exp Med* **193**, 1303-1310 (2001).

195. Jonuleit, H.*, et al.* Identification and functional characterization of human CD4(+)CD25(+) T cells with regulatory properties isolated from peripheral blood. *J Exp Med* **193**, 1285-1294 (2001).

196. Levings, M.K., Sangregorio, R. & Roncarolo, M.G. Human cd25(+)cd4(+) t regulatory cells suppress naive and memory T cell proliferation and can be expanded in vitro without loss of function. *J Exp Med* **193**, 1295-1302 (2001).

197. Lee, S.M., Gao, B. & Fang, D. FoxP3 maintains Treg unresponsiveness by selectively inhibiting the promoter DNA-binding activity of AP-1. *Blood* **111**, 3599-3606 (2008).

198. Hsieh, C.-S., Lee, H.-M. & Lio, C.-W.J. Selection of regulatory T cells in the thymus. *Nature Reviews Immunology* **12**, 157-167 (2012).

199. Malchow, S.*, et al.* Aire Enforces Immune Tolerance by Directing Autoreactive T Cells into the Regulatory T Cell Lineage. *Immunity* **44**, 1102-1113 (2016).

200. Kieback, E.*, et al.* Thymus-Derived Regulatory T Cells Are Positively Selected on Natural Self-Antigen through Cognate Interactions of High Functional Avidity. *Immunity* **44**, 1114-1126 (2016).

201. Chen, L. & Flies, D.B. Molecular mechanisms of T cell co-stimulation and co-inhibition. *Nature Reviews Immunology* **13**, 227-242 (2013).

202. Lenschow, D.J., Walunas, T.L. & Bluestone, J.A. CD28/B7 system of T cell costimulation. *Annual review of immunology* **14**, 233-258 (1996).

203. Lenschow, D.J.*, et al.* Expression and functional significance of an additional ligand for CTLA-4. *Proceedings of the National Academy of Sciences of the United States of America* **90**, 11054-11058 (1993).

204. Collins, A.V., *et al.* The interaction properties of costimulatory molecules revisited. *Immunity* **17**, 201-210 (2002).

205. Saha, B., Harlan, D.M., Lee, K.P., June, C.H. & Abe, R. Protection against lethal toxic shock by targeted disruption of the CD28 gene. *J Exp Med* **183**, 2675-2680 (1996).

206. Mittrucker, H.W., Shahinian, A., Bouchard, D., Kundig, T.M. & Mak, T.W. Induction of unresponsiveness and impaired T cell expansion by staphylococcal enterotoxin B in CD28-deficient mice. *J Exp Med* **183**, 2481-2488 (1996).

207. Muraille, E., De Smedt, T., Urbain, J., Moser, M. & Leo, O. B7.2 provides co-stimulatory functions in vivo in response to staphylococcal enterotoxin B. *European journal of immunology* **25**, 2111-2114 (1995).

208. Levy, R., *et al.* Superantigens hyperinduce inflammatory cytokines by enhancing the B7-2/CD28 costimulatory receptor interaction. *Proceedings of the National Academy of Sciences of the United States of America* **113**, E6437-E6446 (2016).

209. Popugailo, A., Rotfogel, Z., Supper, E., Hillman, D. & Kaempfer, R. Staphylococcal and Streptococcal Superantigens Trigger B7/CD28 Costimulatory Receptor Engagement to Hyperinduce Inflammatory Cytokines. *Frontiers in immunology* **10**, 942 (2019).

210. Arad, G., *et al.* Binding of superantigen toxins into the CD28 homodimer interface is essential for induction of cytokine genes that mediate lethal shock. *PLoS Biol* **9**, e1001149 (2011).

211. Bouguermouh, S., Fortin, G., Baba, N., Rubio, M. & Sarfati, M. CD28 co-stimulation down regulates Th17 development. *PloS one* **4**, e5087 (2009).

212. Revu, S., *et al.* IL-23 and IL-1beta Drive Human Th17 Cell Differentiation and Metabolic Reprogramming in Absence of CD28 Costimulation. *Cell reports* **22**, 2642-2653 (2018).

213. Paulos, C.M., *et al.* The inducible costimulator (ICOS) is critical for the development of human T(H)17 cells. *Sci Transl Med* **2**, 55ra78 (2010).

214. Xin, L., *et al.* Commensal microbes drive intestinal inflammation by IL-17-producing CD4+ T cells through ICOSL and OX40L costimulation in the absence of B7-1 and B7-

2. *Proceedings of the National Academy of Sciences of the United States of America* **111**, 10672-10677 (2014).

215. Mu, H.H., Nourian, M.M., Jiang, H.H., Tran, J.W. & Cole, B.C. Mycoplasma superantigen initiates a TLR4-dependent Th17 cascade that enhances arthritis after blocking B7-1 in Mycoplasma arthritidis-infected mice. *Cell Microbiol* **16**, 896-911 (2014).

216. Veldhoen, M., Hocking, R.J., Atkins, C.J., Locksley, R.M. & Stockinger, B. TGFβ in the Context of an Inflammatory Cytokine Milieu Supports De Novo Differentiation of IL-17-Producing T Cells. *Immunity* **24**, 179-189 (2006).

217. Bettelli, E*., et al.* Reciprocal developmental pathways for the generation of pathogenic effector TH17 and regulatory T cells. *Nature* **441**, 235-238 (2006).

218. Curotto de Lafaille, M.A. & Lafaille, J.J. Natural and adaptive foxp3+ regulatory T cells: more of the same or a division of labor? *Immunity* **30**, 626-635 (2009).

219. Zhou, L*., et al.* TGF-beta-induced Foxp3 inhibits T(H)17 cell differentiation by antagonizing RORgammat function. *Nature* **453**, 236-240 (2008).

220. Yang, X.O*., et al.* Molecular antagonism and plasticity of regulatory and inflammatory T cell programs. *Immunity* **29**, 44-56 (2008).

221. Xu, L., Kitani, A., Fuss, I. & Strober, W. Cutting edge: regulatory T cells induce CD4+CD25-Foxp3- T cells or are self-induced to become Th17 cells in the absence of exogenous TGF-beta. *Journal of immunology* **178**, 6725-6729 (2007).

222. Zhou, X*., et al.* Instability of the transcription factor Foxp3 leads to the generation of pathogenic memory T cells in vivo. *Nature immunology* **10**, 1000-1007 (2009).

223. Miyao, T*., et al.* Plasticity of Foxp3(+) T cells reflects promiscuous Foxp3 expression in conventional T cells but not reprogramming of regulatory T cells. *Immunity* **36**, 262-275 (2012).

224. Harrington, L.E*., et al.* Interleukin 17–producing CD4+ effector T cells develop via a lineage distinct from the T helper type 1 and 2 lineages. *Nature immunology* **6**, 1123-1132 (2005).

225. Park, H.*, et al.* A distinct lineage of CD4 T cells regulates tissue inflammation by producing interleukin 17. *Nature immunology* **6**, 1133-1141 (2005).

226. Schwartz, D.M., Bonelli, M., Gadina, M. & O'Shea, J.J. Type I/II cytokines, JAKs, and new strategies for treating autoimmune diseases. *Nature Reviews Rheumatology* **12**, 25-36 (2016).

227. Welsch, K., Holstein, J., Laurence, A. & Ghoreschi, K. Targeting JAK/STAT signalling in inflammatory skin diseases with small molecule inhibitors. *European journal of immunology* **47**, 1096-1107 (2017).

228. Zhou, L.*, et al.* IL-6 programs T(H)-17 cell differentiation by promoting sequential engagement of the IL-21 and IL-23 pathways. *Nature immunology* **8**, 967-974 (2007).

229. Willerslev-Olsen, A.*, et al.* Staphylococcal enterotoxin A (SEA) stimulates STAT3 activation and IL-17 expression in cutaneous T-cell lymphoma. *Blood* **127**, 1287-1296 (2016).

230. Schmetterer, K.G. & Pickl, W.F. The IL-10/STAT3 axis: Contributions to immune tolerance by thymus and peripherally derived regulatory T-cells. *European journal of immunology* **47**, 1256-1265 (2017).

231. Schmetterer, K.G.*, et al.* STAT3 governs hyporesponsiveness and granzyme B-dependent suppressive capacity in human CD4+ T cells. *Faseb j* **29**, 759-771 (2015).

232. Wei, L.*, et al.* Discrete Roles of STAT4 and STAT6 Transcription Factors in Tuning Epigenetic Modifications and Transcription during T Helper Cell Differentiation. *Immunity* **32**, 840-851 (2010).

233. Yang, X.P.*, et al.* Opposing regulation of the locus encoding IL-17 through direct, reciprocal actions of STAT3 and STAT5. *Nature immunology* **12**, 247-254 (2011).

234. Zheng, J.*, et al.* Gain-of-function STAT1 mutations impair STAT3 activity in patients with chronic mucocutaneous candidiasis (CMC). *European journal of immunology* **45**, 2834-2846 (2015).

235. Hiller, J.*, et al.* STAT1 Gain-of-Function and Dominant Negative STAT3 Mutations Impair IL-17 and IL-22 Immunity Associated with CMC. *Journal of Investigative Dermatology* **138**, 711-714 (2018).

236. Liu, L.*, et al.* Gain-of-function human STAT1 mutations impair IL-17 immunity and underlie chronic mucocutaneous candidiasis. *J Exp Med* **208**, 1635-1648 (2011).

237. Chen, Y.*, et al.* Anti-IL-23 therapy inhibits multiple inflammatory pathways and ameliorates autoimmune encephalomyelitis. *The Journal of clinical investigation* **116**, 1317-1326 (2006).

238. Basdeo, S.A.*, et al.* Ex-Th17 (Nonclassical Th1) Cells Are Functionally Distinct from Classical Th1 and Th17 Cells and Are Not Constrained by Regulatory T Cells. *Journal of immunology* **198**, 2249-2259 (2017).

239. Amadi-Obi, A.*, et al.* TH17 cells contribute to uveitis and scleritis and are expanded by IL-2 and inhibited by IL-27/STAT1. *Nature medicine* **13**, 711-718 (2007).

240. Stumhofer, J.S.*, et al.* Interleukin 27 negatively regulates the development of interleukin 17-producing T helper cells during chronic inflammation of the central nervous system. *Nature immunology* **7**, 937-945 (2006).

241. Gran, B.*, et al.* IL-12p35-deficient mice are susceptible to experimental autoimmune encephalomyelitis: evidence for redundancy in the IL-12 system in the induction of central nervous system autoimmune demyelination. *J. Immunol.* **169**, 7104-7110 (2002).

242. Willenborg, D.O., Fordham, S., Bernard, C.C., Cowden, W.B. & Ramshaw, I.A. IFN-gamma plays a critical down-regulatory role in the induction and effector phase of myelin oligodendrocyte glycoprotein-induced autoimmune encephalomyelitis. *Journal of immunology* **157**, 3223-3227 (1996).

243. Vermeire, K.*, et al.* Accelerated collagen-induced arthritis in IFN-gamma receptor-deficient mice. *Journal of immunology* **158**, 5507-5513 (1997).

244. Manoury-Schwartz, B.*, et al.* High susceptibility to collagen-induced arthritis in mice lacking IFN-gamma receptors. *Journal of immunology* **158**, 5501-5506 (1997).

245. O'Connor, R.A., Cambrook, H., Huettner, K. & Anderton, S.M. T-bet is essential for Th1-mediated, but not Th17-mediated, CNS autoimmune disease. *European journal of immunology* **43**, 2818-2823 (2013).

246. Jones, L.L. & Vignali, D.A. Molecular interactions within the IL-6/IL-12 cytokine/receptor superfamily. *Immunol Res* **51**, 5-14 (2011).

247. Kaplanski, G. Interleukin-18: Biological properties and role in disease pathogenesis. *Immunological reviews* **281**, 138-153 (2018).

248. Muller, J.R., Waldmann, T.A., Kruhlak, M.J. & Dubois, S. Paracrine and transpresentation functions of IL-15 are mediated by diverse splice versions of IL-15Ralpha in human monocytes and dendritic cells. *J Biol Chem* **287**, 40328-40338 (2012).

Appendix 1

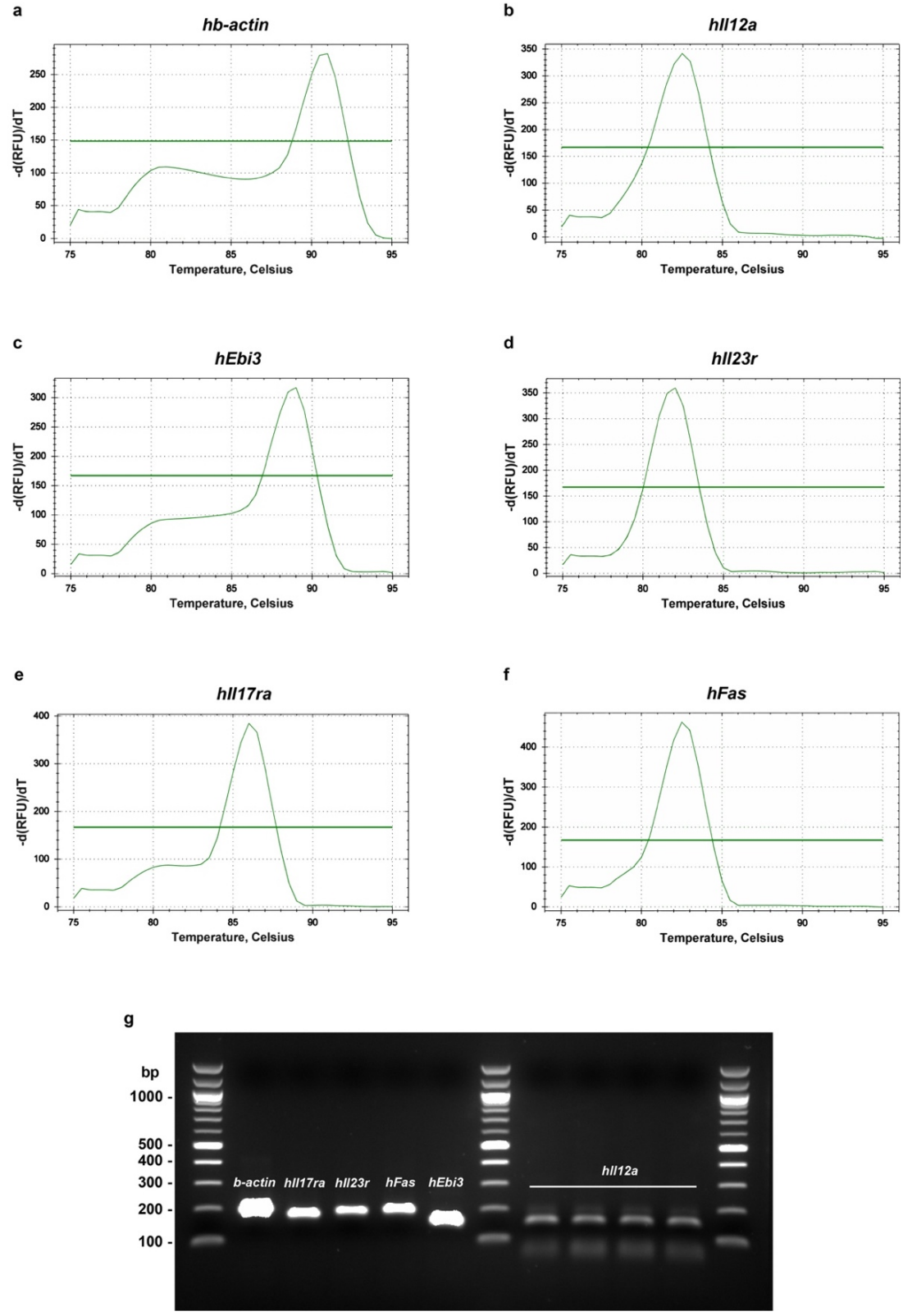

Figure 7.1 Melting curve and DNA gel image (human genes)

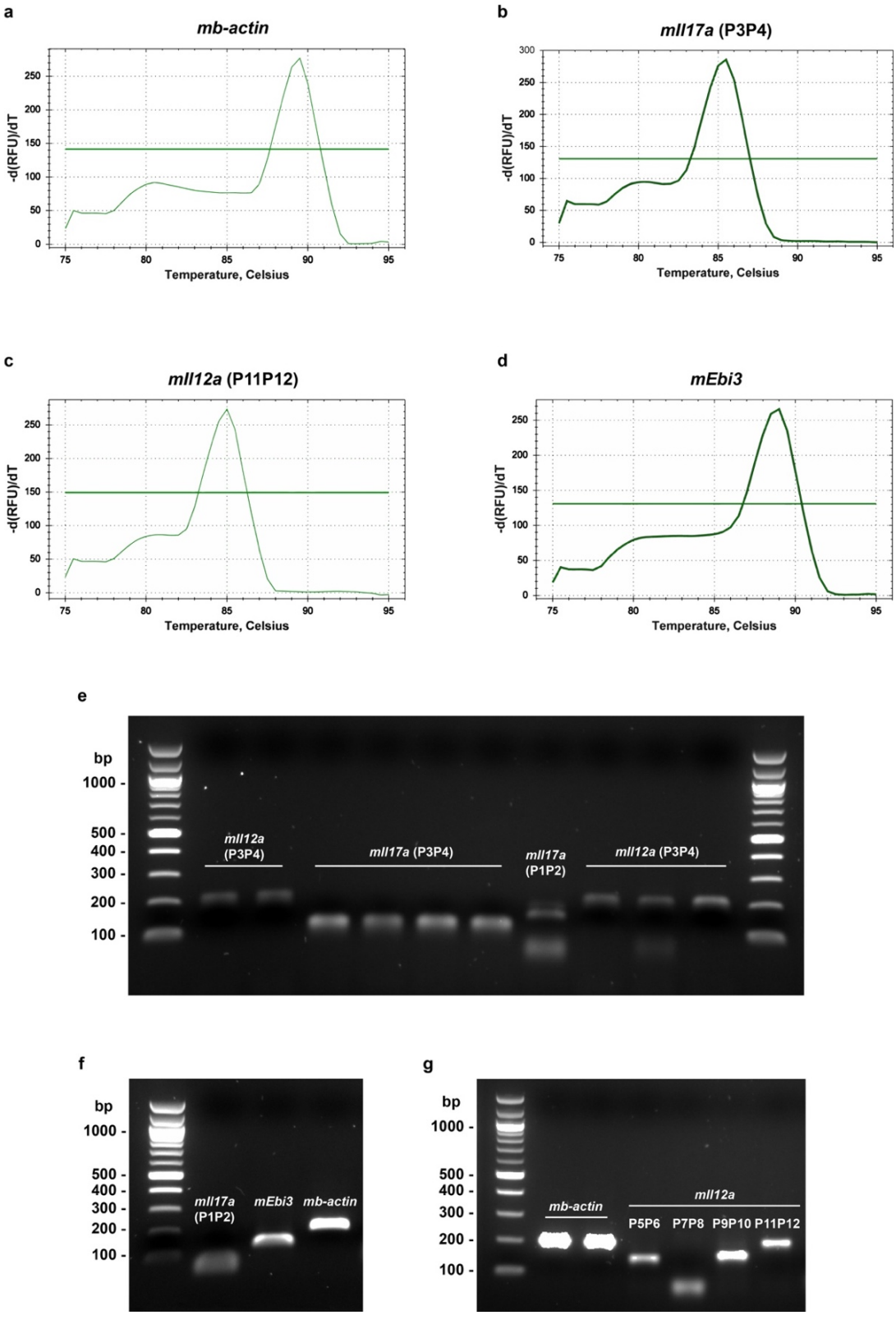

Figure 7.2 Melting curve and DNA gel image (mouse genes)

Multiple pairs of primers were tested to amplify gene *mll17a* and *mll12a* as shown in the DNA gel image **e-g**.

Appendix 2

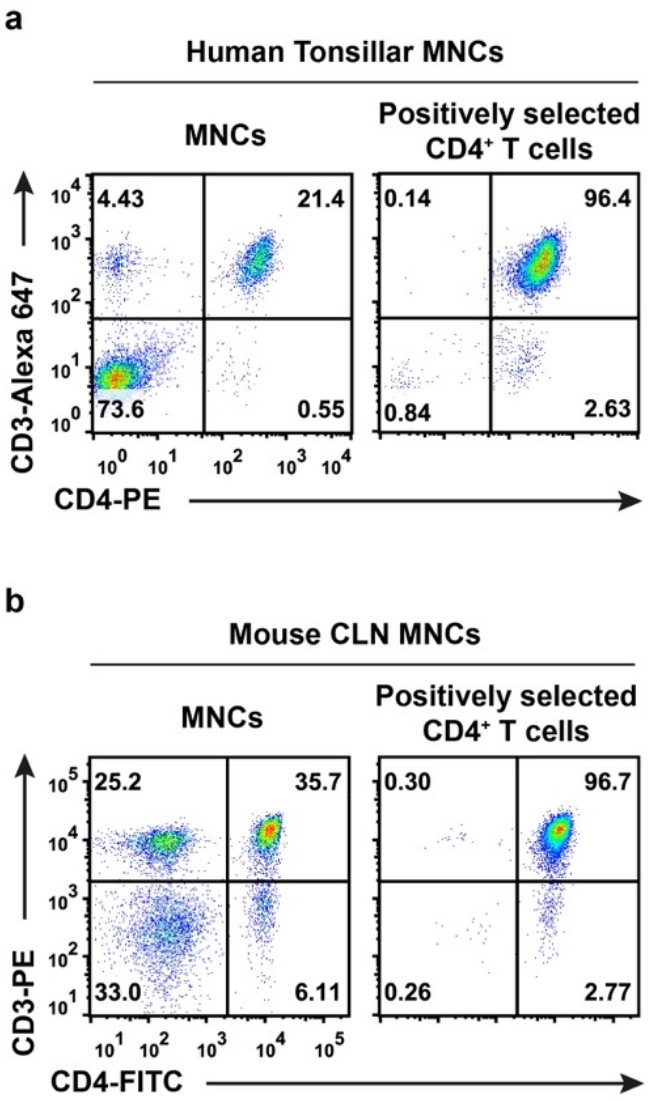

Figure 8 Purification of CD4⁺ T cells from human tonsillar MNCs and mouse CLN MNCs

CD4⁺ T cells were separated by magnetic cell sorting as described in the ***2.8***. Dot plots showing percentages of $CD3^+CD4^+$ cells (numbers in top right quadrants) in unfractionated MNCs and $CD4^+$ cell-depleted MNCs derived from the human tonsillar tissue (**a**) and mouse cervical lymph nodes (**b**) respectively.

Appendix 3

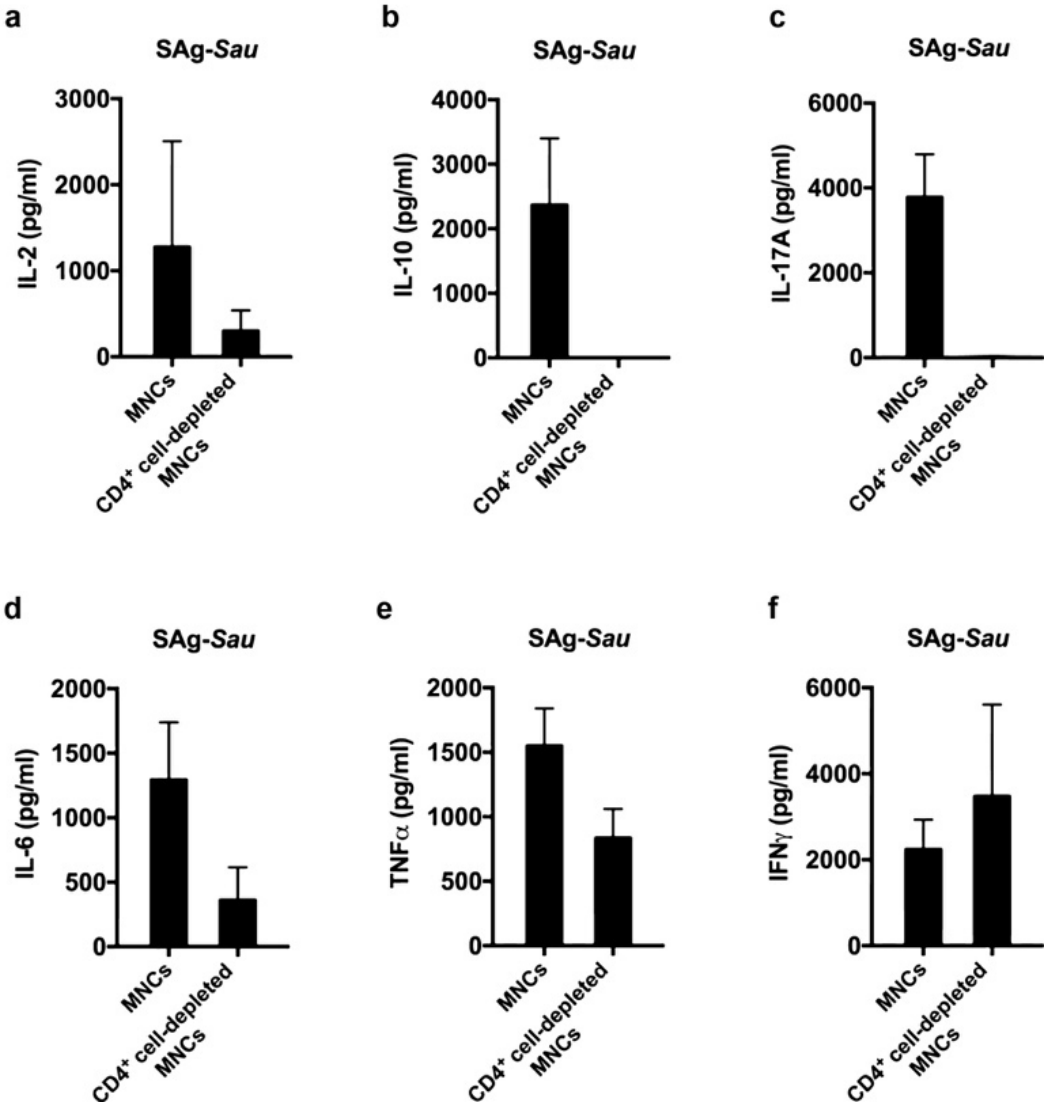

Figure 9 SAg-*Sau* stimulated cytokine production in unfractionated MNCs and $CD4^+$ T cell-depleted MNCs

Unfractionated MNCs and $CD4^+$ T cells-depleted MNCs were stimulated by 1 μg/ml of SAg-*Sau* for 48 hours. Cell culture supernatants were collected, and the cytokine production were detected by CBA.